U.S. Department of the Interior
U.S. Geological Survey

# Hydrology of the Bonneville Salt Flats, Northwestern Utah, and Simulation of Ground-Water Flow and Solute Transport in the Shallow-Brine Aquifer

U.S. Geological Survey Professional Paper 1585

Prepared in cooperation with the
Bureau of Land Management

USGS

# AVAILABILITY OF BOOKS AND MAPS OF THE U.S. GEOLOGICAL SURVEY

Instructions on ordering publications of the U.S. Geological Survey, along with prices of the last offerings, are given in the current-year issues of the monthly catalog "New Publications of the U.S. Geological Survey." Prices of available U.S. Geological Survey publications released prior to the current year are listed in the most recent annual "Price and Availability List." Publications that may be listed in various U.S. Geological Survey catalogs (**see back inside cover**) but not listed in the most recent annual "Price and Availability List" may be no longer available.

Order U.S. Geological Survey publications **by mail** or **over the counter** from the offices given below.

## BY MAIL

### Books

Professional Papers, Bulletins, Water-Supply Papers, Techniques of Water-Resources Investigations, Circulars, publications of general interest (such as leaflets, pamphlets, booklets), single copies of Preliminary Determination of Epicenters, and some miscellaneous reports, including some of the foregoing series that have gone out of print at the Superintendent of Documents, are obtainable by mail from

**U.S. Geological Survey, Information Services**
**Box 25286, Federal Center, Denver, CO 80225**

Subscriptions to Preliminary Determination of Epicenters can be obtained ONLY from the

**Superintendent of Documents**
**Government Printing Office**
**Washington, DC 20402**

(Check or money order must be payable to Superintendent of Documents.)

### Maps

For maps, address mail orders to

**U.S. Geological Survey, Information Services**
**Box 25286, Federal Center, Denver, CO 80225**

## OVER THE COUNTER

### Books and Maps

Books and maps of the U.S. Geological Survey are available over the counter at the following U.S. Geological Survey Earth Science Information Centers (ESIC's), all of which are authorized agents of the Superintendent of Documents:

- **ANCHORAGE, Alaska**—Rm. 101, 4230 University Dr.
- **LAKEWOOD, Colorado**—Federal Center, Bldg. 810
- **MENLO PARK, California**—Bldg. 3, Rm. 3128, 345 Middlefield Rd.
- **RESTON, Virginia**—USGS National Center, Rm. 1C402, 12201 Sunrise Valley Dr.
- **SALT LAKE CITY, Utah**—2222 West 2300 South
- **SPOKANE, Washington**—U.S. Post Office Bldg., Rm. 135, West 904 Riverside Ave.
- **WASHINGTON, D.C.**—Main Interior Bldg., Rm. 2650, 18th and C Sts., NW.

### Maps Only

Maps may be purchased over the counter at the following U.S. Geological Survey office:

- **ROLLA, Missouri**—1400 Independence Rd.

# Hydrology of the Bonneville Salt Flats, Northwestern Utah, and Simulation of Ground-Water Flow and Solute Transport in the Shallow-Brine Aquifer

*By* JAMES L. MASON and KENNETH L. KIPP, JR.

U.S. GEOLOGICAL SURVEY PROFESSIONAL PAPER 1585

Prepared in cooperation with the
Bureau of Land Management


1998

U.S. DEPARTMENT OF THE INTERIOR

BRUCE BABBITT, Secretary

U.S. GEOLOGICAL SURVEY

Mark Schaefer, Acting Director



**Library of Congress Cataloging in Publications Date**

Mason, James L.

Hydrology of the Bonneville Salt Flats, northwestern Utah, and simulation of ground-water flow and solute transport in the shallow-brine aquifer / by James L. Mason and Kenneth L. Kipp, Jr.

p. cm. — (U.S. Geological Survey Professional Paper ; 1585)

"Prepared in cooperation with the Bureau of Land Management."

Includes bibliographical references.

Supt. of Docs. no.: I 19. 16: 1585

1. Hydrology—Utah—Bonneville Salt Flats. 2. Groundwater flow—Utah—Bonneville Salt Flats. I. Kipp, Jr., Kenneth L. II. United States. Bureau of Land Management. III. Title. IV. Series.

GB1025.U8M38 1997

551.48'09792'43—dc21 97-34524

CIP

ISBN 0-607-88306-5

For sale by U.S. Geological Survey, Branch of Information Services
Box 25286, Federal Center
Denver, CO 80225

# CONTENTS

## FIGURES

## TABLES

## CONVERSION FACTORS, VERTICAL DATUM, AND ABBREVIATED WATER-QUALITY UNITS

| Multiply | By | To obtain |
|---|---|---|
| acre | 0.4047 | hectare |
| acre-foot (acre-ft) | 0.001233 | cubic hectometer |
| acre-foot per year (acre-ft/yr) | 0.001233 | cubic hectometer per year |
| cubic foot ($ft^3$) | 0.02832 | cubic meter |
| cubic foot per foot squared per day ($ft^3/ft^2/d$) | 0.3048 | cubic meter per meter squared per day |
| cubic foot per second ($ft^3/s$) | 0.02832 | cubic meter per second |
| cubic foot per day ($ft^3/d$) | 0.02832 | cubic meter per day |
| foot (ft) | 0.3048 | meter |
| foot per day (ft/d) | 0.3048 | meter per day |
| foot per mile (ft/mi) | 0.1894 | meter per kilometer |
| foot per second (ft/s) | 0.3048 | meter per second |
| foot per second squared ($ft/s^2$) | 0.3048 | meter per second squared |
| foot squared ($ft^2$) | 0.0929 | meter squared |
| foot squared per day ($ft^2/d$) | 0.0929 | meter squared per day |
| foot per year (ft/yr) | 0.3048 | meter per year |
| gallon per minute (gal/min) | 0.0631 | liter per second |
| inch (in.) | 25.4 | millimeter |
| inch per day (in/d) | 25.4 | millimeter per day |
| inch per year (in/yr) | 25.4 | millimeter per year |
| mile (mi) | 1.609 | kilometer |
| miles per hour (mi/hr) | 1.609 | kilometers per hour |
| mile squared ($mi^2$) | 2.590 | square kilometer |
| pound per cubic foot ($lbs/ft^3$) | 16.0185 | gram per liter |
| pound per inch squared ($lbs/in^2$) | 6.895 | Newton per meter squared |
| ton (short, 2,000 pounds) | 0.9072 | megagram |
| ton per year (ton/yr) | 0.9072 | megagram per year |

Degrees Celsius (°C) may be converted to degrees Fahrenheit (°F) by using the following equation:

$$°F = 9/5(°C)+32.$$

Degrees Fahrenheit (°F) may be converted to degrees Celsius (°C) by using the following equation:

$$°C = 5/9(°F-32).$$

**Sea level:** In this report, "sea level" refers to the National Geodetic Vertical Datum of 1929—a geodetic datum derived from a general adjustment of the first-order level nets of the United States and Canada, formerly called Sea Level Datum of 1929.

Solar radiation is reported in Langley (ly) units. One ly is equal to 1 calorie per centimeter squared and 3.6855 British Thermal Unit (BTU) per foot squared.

Chemical concentration and water temperature are reported only in metric units. Chemical concentration in water is reported in milligrams per liter (mg/L). Milligrams per liter is a unit expressing the solute per unit volume, liter (L), of water. One thousand milligrams per liter is equivalent to 1 gram per liter (g/L). For concentrations less than 7,000 milligrams per liter, the numerical value is about the same as for concentrations in parts per million. For concentrations much larger than 7,000 milligrams per liter, the concentration in milligrams per liter must be divided by water density to obtain the equivalent concentration in parts per million. Density of water in grams per cubic centimeter ($g/cm^3$) at 20°C is obtained by adjusting the specific-gravity measurement with the appropriate conversion factor that corresponds to temperature.

One tritium unit (TU), the more commonly used unit for tritium, is equivalent to 3.2 picocuries per liter (pCi/L). One picocurie is the amount of radioactive decay that produces 2.2 disintegrations per second in a unit volume (liter) of water.

Viscosity is reported in centipoise units. One centipoise is equal to 0.01 grams per centimeter-second.

The generic units of mass (*M*), length (*L*), and time (*T*) are used to define the units of variables in some equations presented in this report. The generic unit abbreviation for length (*L*) should not be confused with a unit volume, liter (L), of water and regular chemical concentrations (g/L) used in the text.

# Hydrology of the Bonneville Salt Flats, Northwestern Utah, and Simulation of Ground-Water Flow and Solute Transport in the Shallow-Brine Aquifer

By James L. Mason and Kenneth L. Kipp, Jr.

## ABSTRACT

The Bonneville Salt Flats is located in the western part of the Great Salt Lake Desert of northwestern Utah. The salt crust in the Bonneville Salt Flats covered an area of 43 square miles in September 1992, of which about 34 square miles consists of perennial salt more than 1 foot thick. The salt crust is the terminus for ground-water flow in the area except where this flow has been intercepted by brine-collection ditches used for mineral production.

For many years, the Bonneville Salt Flats has been used for high-speed automobile racing because of its uniquely flat surface and accessibility. Potash has been extracted from the underlying sodium-chloride-rich brines for commercial use since 1917. Three sets of salt-crust thickness measurements made during a 28-year period indicate a decrease in salt-crust volume and thickness. For these reasons, there appears to be a conflict between the primary uses of the playa.

Objectives of this investigation were to identify the natural and anthropogenic processes causing salt loss from the crust, and where feasible, to quantify these processes. Specific areas of study include the transport of salt in solution by ground-water flow and wind-driven ponds and the subsequent salt precipitation on the surface of the playa upon evaporation or seepage of brine into the subsurface. Data were collected to make conceptual estimates of these processes and to use in conjunction with variable-density, three-dimensional, solute-transport computer simulations.

The ground-water system in the Bonneville Salt Flats can be divided into three aquifers: (1) the shallow-brine aquifer that contains dense brines within the salt crust and underlying carbonate mud, (2) the alluvial-fan aquifer that yields water from coarse and fine-grained material at the flanks of the adjacent mountains, and (3) the basin-fill aquifer that is composed of a thick sequence of lacustrine sediment in the upper part and a conglomerate at depth. Brine is withdrawn for mineral production by seepage from the shallow-brine aquifer into brine-collection ditches and by pumping from the conglomerate in the lower part of the basin-fill aquifer. Because of possible effects of brine withdrawal on the salt crust, data were collected primarily from the shallow-brine aquifer.

Recharge to the shallow-brine aquifer is primarily by infiltration of precipitation that falls on the playa surface and dissolves salt from the crust, and by subsurface inflow from tne east and north that transports a small amount of salt into the shallow-brine aquifer. Evidence indicates that upward leakage might be a major source of recharge to the shallow-brine aquifer, but data were insufficient to quantify this source. Discharge from the shallow-brine aquifer is primarily by evaporation at the playa surface, seepage to the brine-collection ditch east of the salt crust, subsurface flow to the south where it mostly seeps into a brine-collection ditch, subsurface flow to the northwestern margin of the playa, and downward leakage to the underlying lacustrine sediment. Estimated fluid discharge was about 19,000 acre-feet in 1992, which was

substantially more than estimated recharge. Estimated net salt loss was more than 1.3 million tons.

Long-term water-level data indicate that the fluid phase of the shallow-brine aquifer appears to be in steady state despite seasonal fluctuations that can result in yearly fluid imbalances. A steady-state condition is defined as no change throughout time. Estimated recharge for 1992, therefore, was too small with respect to estimated discharge. Estimated recharge might be larger if a larger specific yield is assumed or if upward leakage could be quantified. Limited water-level data indicate that a small downward driving force exists between the shallow-brine aquifer and the underlying lacustrine sediment. Tritium values of essentially 0 tritium units at some locations in the shallow-brine aquifer can result only from upward leakage from the underlying lacustrine sediment. Discharge might be less than estimated. Removal of salt and compaction of underlying carbonate mud during highway construction might have constricted ground-water flow to the south.

Dissolved-solids and potassium concentrations in the brine within the shallow-brine aquifer have not changed over the long term. With an estimated net loss of salt from the shallow-brine aquifer, the dissolved-solids concentration must be maintained by dissolution of the salt crust. Potassium concentrations probably are maintained by diffusion from interstitial fluid within the shallow-brine aquifer and by upward leakage.

Deuterium and oxygen-18 isotope data indicate that there is possible brine movement from the shallow-brine aquifer and the underlying lacustrine sediment toward the alluvial-fan aquifer. Pumping from the alluvial-fan aquifer has resulted in a reversal of the natural hydraulic gradient toward the playa.

Extensive flooding of the Bonneville Salt Flats during the winter of 1992-93 dramatically changed the salt surface. Much of the near-surface salt was dissolved and remained in solution long into the summer of 1993. When salt was precipitated on the playa surface as the pond evaporated, a thin salt crust was deposited in areas beyond the usual areal extent of the crust. An estimated 10 to 14 million tons was dissolved and subsequently redeposited on the playa surface or infiltrated into the shallow-brine aquifer. Some surface salt might have been deposited beyond slight topographic divides where the salt might be lost from the crust.

A three-dimensional, ground-water flow and solute-transport model with variable density was developed for the shallow-brine aquifer in the Bonneville Salt Flats study area in order to (1) develop a fluid and solute balance, (2) evaluate the effect of the brine-collection ditches on the salt crust, and (3) identify the major and minor solute fluxes to and from the system. Preliminary simulations indicated that the ground-water flow system does not reach steady state during production or recovery seasons because the response time is longer than the seasonal duration of about 6 months. Because of the transient nature of the ground-water system, simulations were carried out to a periodic steady state with a repeated sequence of production and recovery seasons approximating a typical year rather than matching a specific period in time.

The conceptual understanding of the major flows to and from the shallow-brine aquifer was supported by the model. Simulation results indicate a net loss of solute of about 850,000 tons through subsurface outflow in a typical year, primarily through seepage to brine-collection ditches to the east of the salt crust and along the southern boundary. Simulated salt dissolution from recharge at the playa surface was almost 5 million tons, whereas simulated salt precipitation from evaporation was almost 4 million tons. In order to reasonably match measured heads along the southern part of the simulation region, permeability was decreased from original estimates. Simulated subsurface flow to the south was about one-third of the estimated value.

Simulations were made to test the sensitivity of the model to changes in permeability, specified water level in the brine-collection ditch, density of infiltrating fluid from the playa surface, evaporation, and effective porosity. The simulated solute transport was most sensitive to an increase in permeability along the southern boundary. All sensitivity simulations resulted in a net annual loss of solute.

## INTRODUCTION

The Bonneville Salt Flats is located in the western part of the Great Salt Desert of northwestern Utah (fig. 1). The salt crust on the Bonneville Salt Flats, which covered 43 $mi^2$ in late summer 1992, is unique for its size and accessibility.

The first documented non-Native American explorations of the area were instigated in the early 1830's by Captain Benjamin Louis Eulalie de Bonneville, for whom the area is named. Captain de Bonneville ordered Joseph Reddeford Walker to explore the region west of the Great Salt Lake in search of undiscovered areas with potential for fur trapping. During his explorations, Walker crossed the salt flats enroute to the Sierra Nevada Mountains. In 1835, Captain de Bonneville abandoned the area with very little success in acquiring furs. Because of the harsh conditions and remoteness of the area, the Bonneville Salt Flats was not surveyed until 1926, almost a hundred years later (Post, 1992, p. 30).

The salt crust has been used for high-speed automobile racing, and brine associated with the salt crust and surrounding playa has been used for mineral production for most of this century. More recently, the film-making industry has used this unique area because of the contrast of white salt against blue sky and vast horizons.

High-speed automobile racing on the Bonneville Salt Flats began in 1914. Over the years, the Bonneville Salt Flats has proven so desirable for racing that it has become one of the most preferred surfaces for speed enthusiasts from all over the world. A number of world speed records have been, and continue to be, set on the Bonneville Salt Flats. Each year, depending on salt-crust conditions, four separate racing events are scheduled. Speed Week, in August of each year, is the largest event, usually attracting more than 300 entries. A history of racing on the Bonneville Salt Flats is reported by Post (1992). Members of the racing community have been concerned about progressive deterioration of the quality of the racing surface, as well as the lateral extent and thickness of the salt crust. They have suggested that the cause of the deterioration of the salt crust is directly linked to brine withdrawal from the Bonneville Salt Flats for mineral production.

Mineral production on the Bonneville Salt Flats began in the early 1900's when halite (common salt) was extracted from the salt crust. Production of potash began in 1917 when supplies of potassium salts from Germany were interrupted during World War I. By 1920, most of the potassium salts produced in this country came from part of the Bonneville Salt Flats that passed into private ownership in 1917. Additional lands were passed into private ownership during 1933-35. Much of the private land is located south of the present Interstate Highway 80. When German potassium-salt supplies were available again in 1921, production from the Bonneville Salt Flats ceased until 1938. A more detailed description of the early history of potash production in this area is reported by Gwynn (1996). The area from which brine is withdrawn for potash production was expanded in 1963 when mineral leases on 25,000 acres of Federal land were issued. These Federal leases were renewed in 1983. Presently, the mineral company operates on private land (66 percent), Federal land (28 percent), and State land (6 percent). A description of the potash-extraction process has been written by Bingham (1980).

Other perennial salt crusts are present in remote regions of the world, but none match the mostly smooth, hard surface, size, and accessibility of the Bonneville Salt Flats. Because of these unique characteristics, in 1985 the Bureau of Land Management designated the Bonneville Salt Flats as an Area of Critical Environmental Concern. For such an area, management practices must reflect the need for preservation of the special feature and balance this preservation with the multiple-use concept that allows mineral extraction.

A decrease in thickness and areal extent of salt crust has been documented over a 28-year period, from 1960 to 1988, (Steven Brooks, Bureau of Land Management, written commun., 1989), but no definitive data have shown what processes are involved. The Bureau of Land Management needs to know the dynamics of the salt loss in order to make appropriate management decisions concerning the Bonneville Salt Flats. This hydrologic investigation was done by the U.S. Geological Survey, Water Resources Division, in cooperation with the Bureau of Land Management to provide them with data and interpretations concerning the present movement of salt through the hydrologic system. The study began in October 1991 and continued through September 1994.

### Purpose and Scope

This report describes the hydrologic system of the Bonneville Salt Flats with emphasis on the mechanisms of solute transport. Variable-density, three-

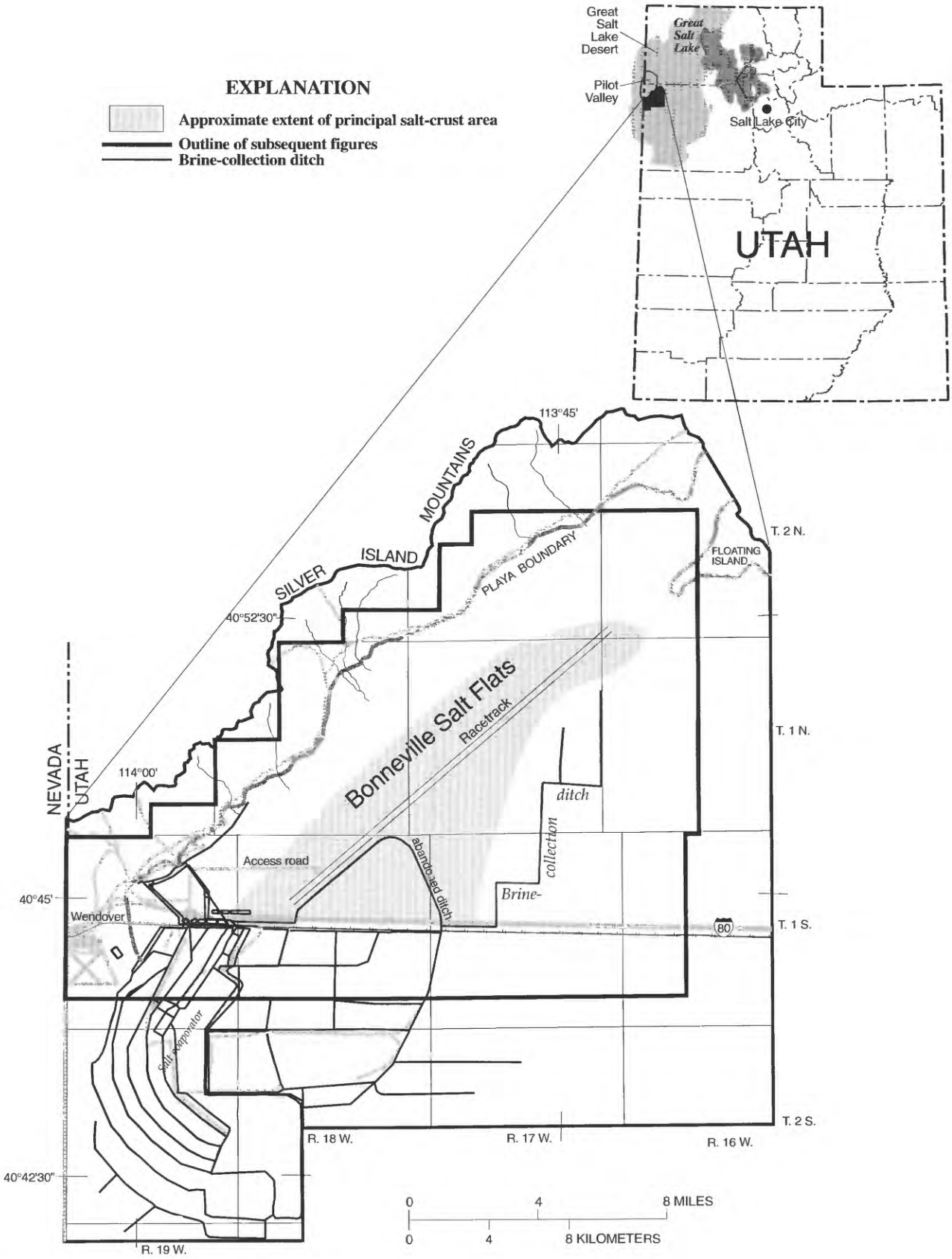


**Figure 1.** Location of the Bonneville Salt Flats study area, northwestern Utah.

dimensional computer simulations of the near-surface part of the ground-water system were done to quantify both the transport of salt dissolved in subsurface brine that leaves the salt-crust area and the salt dissolved and precipitated on the land surface.

The study was designed to define the hydrology of the brine ground-water system and the natural and anthropogenic processes causing salt loss, and where feasible, to quantify these processes. Specific areas of study include the transport of salt in solution by ground-water flow and the transport of salt in solution by wind-driven ponds and the subsequent salt precipitation on the surface of the playa upon evaporation or seepage into the subsurface. In addition, hydraulic and chemical changes in the hydrologic system since previous studies were documented. Data collected during this study were used in conjunction with variable-density, three-dimensional, solute-transport computer simulations to better understand and quantify the fluid- and salt-transport processes in the ground-water system of the Bonneville Salt Flats. Pilot Valley, located northwest of the Silver Island Mountains, contains a playa relatively undisturbed by human activities. An objective was to examine Pilot Valley as an analog to the Bonneville Salt Flats prior to mineral development; however, data were insufficient to make fluid and salt-budget comparisons between the Bonneville Salt Flats and Pilot Valley.

The ground-water system in the Bonneville Salt Flats study area consists of an alluvial-fan aquifer located along the playa margin on the southeast flank of the Silver Island Mountains, a deep basin-fill aquifer, and a shallow-brine aquifer. Brines that are of economic value are derived from the shallow-brine aquifer on the Bonneville Salt Flats. Evaporation of these brines contributes to the perennial salt crust on the Bonneville Salt Flats. Rainfall on the playa surface results in the dissolution of the salt and subsequent seepage into the subsurface. For these reasons, the primary emphasis of this study is the flow of brine in and out of the shallow-brine aquifer.

Data collected during this study are presented in a report by Mason and others (1995). Water-level and density data measured in wells located in the Bonneville Salt Flats were used to delineate potentiometric surfaces and areal distributions of dissolved solids within the shallow-brine aquifer. Data also were collected from wells in Pilot Valley and were presented by Mason and others (1995) but are not used in this report. The site-numbering system used in Utah to uniquely identify these wells and other hydrologic-data sites is described in figure 2.

## Previous Investigations

One of the first references to salt crusts in northwestern Utah was made by Gilbert (1890). While Gilbert was mapping the various shoreline features of Pleistocene-age Lake Bonneville, he perceived that these features did not represent level water surfaces. Many of the shoreline features west of the present Great Salt Lake were 180 ft higher than features on the east side. He inferred that these differences were the result of differential upward movement in response to the removal of lake water by evaporation.

Nolan (1928) did the first comprehensive study of shallow brines in the Great Salt Lake Desert. From data obtained from 405 shallow augured holes, Nolan mapped the extent of the salt crusts on the Bonneville Salt Flats and in Pilot Valley. On the basis of chemical analyses from brine samples collected in 1925, he delineated magnesium, potassium, and chloride concentrations. He suggested that differences in magnesium and potassium concentrations were the result of differences in the chemical composition of surface runoff at different locations in the desert.

Eardley (1962) used carbon-14 dating of the carbonate muds to develop the evaporative history of the Great Salt Lake Desert. Through this research, he believed that the present salt crust had migrated westward about 25 mi from its original site of deposition. The migration was attributed to the isostatic rebound of the center part of the basin.

Crittenden (1963) completed a detailed study of isostatic rebound resulting from the dwindling of Lake Bonneville. Maximum vertical displacement was at least 210 ft in the center of the basin. Crittenden estimated that isostatic recovery had reached at least 75 percent of the theoretical maximum.

Turk (1969) was the first to complete a detailed study of the hydrology of the Bonneville Salt Flats; however, much of the data collected were limited to areas adjacent to brine-collection ditches and evaporation ponds. Turk incorporated these data into a simple advective-flow and mixing model to estimate the potential for continued potash production. Turk (1970) reported the results of a field evaporation experiment during which the measured evaporation from surface brines decreased with increasing dissolved-solids concentration. Turk (1973) listed the results of aquifer tests

The system of numbering wells in Utah is based on the cadastral land-survey system of the U.S. Government. The number, in addition to designating the well, describes its position in the land net. The land-survey system divides the State into four quadrants separated by the Salt Lake Base Line and the Salt Lake Meridian. These quadrants are designated by the uppercase letters A, B, C, and D, indicating the northeast, northwest, southwest, and southeast quadrants, respectively. Numbers designating the township and range, in that order, follow the quadrant letter, and all three are enclosed in parentheses. The number after the parentheses indicates the section and is followed by three letters indicating the quarter section, the quarter-quarter section, and the quarter-quarter-quarter section—generally 10 acres for a regular section[1]. The lowercase letters a, b, c, and d indicate, respectively, the northeast, northwest, southwest, and southeast quarters of each subdivision. The number after the letters is the serial number of the well within the 10-acre tract. A number having all three quarter designations but no serial number indicates a miscellaneous data site other than a well, such as a location for a core sample. Thus, (C-1-17)18bbb-2 designates the second well constructed or visited in the northwest 1/4 of the northwest 1/4 of the northwest 1/4 of section 18, T. 1 S., R. 17 W.

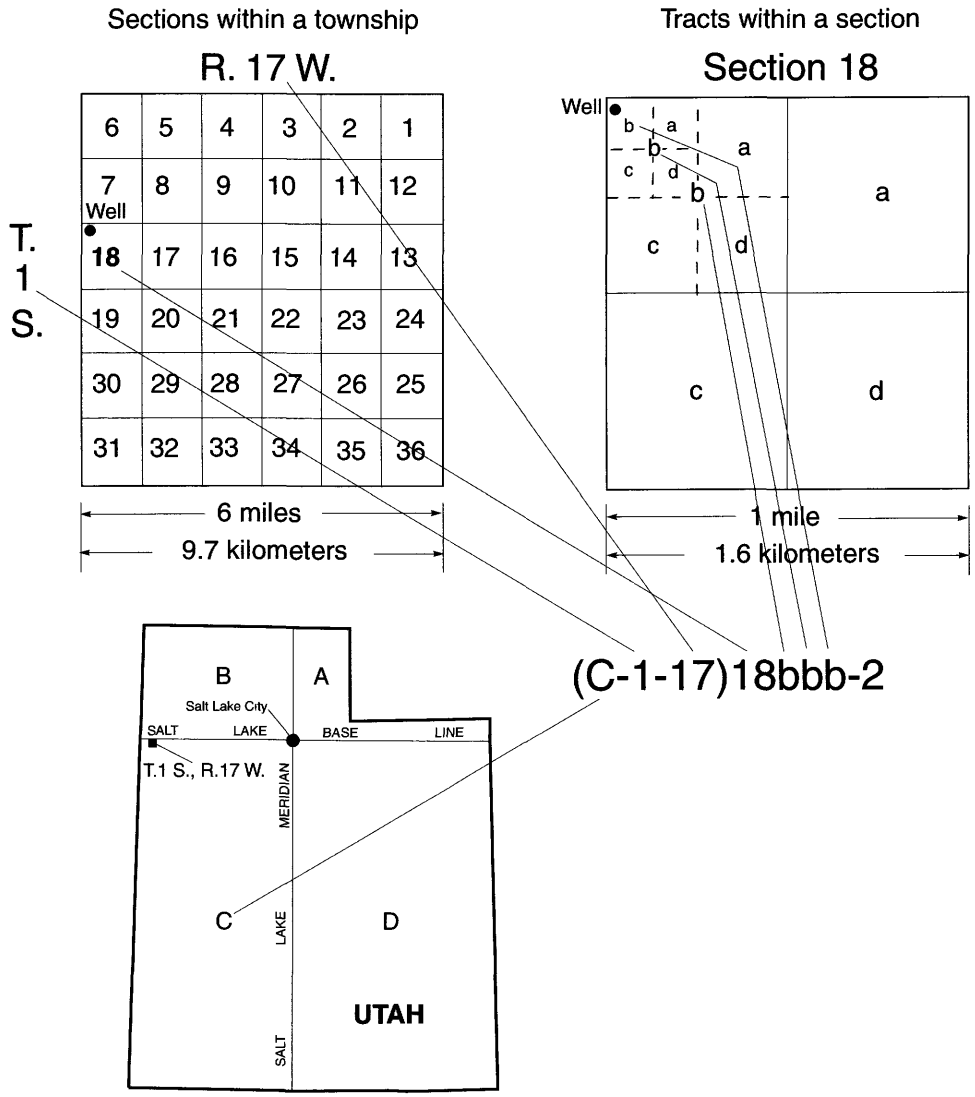


**Figure 2.** Numbering system used for hydrologic-data sites in Utah.

[1]Although the basic land unit, the section, is theoretically 1 square mile, many sections are irregular in size and shape. Such sections are subdivided into 10-acre tracts, generally beginning at the southeast corner, and the surplus or shortage is taken up in the tracts along the north and west sides of the section.

designed to determine the hydraulic properties of the shallow-brine aquifer and further elaborated on the results of the modeling for continued brine production. Turk and others (1973) describe the lithology of the sediments that comprise the shallow-brine aquifer and the implications on ground-water flow. Turk (1978) reported the use of satellite imagery in an attempt to determine the areal extent of the seasonal redistribution of salt on the playa surface. In this last report, Turk also described the use of a three-dimensional, advective, ground-water flow model to estimate the zone of influence resulting from brine withdrawal by brine-collection ditches within the shallow-brine aquifer.

Lines (1978 and 1979) completed two reports, the first listing data collected from July 1975 through June 1977, and the second containing the interpretations derived from those data. Lines described the morphology of the playa surface and its seasonal variation. Lines divided the playa surface into three separate zones, the outer carbonate zone composed mainly of clay-sized authigenic carbonate minerals, the sulfate zone composed mainly of authigenic gypsum, and the chloride zone composed of crystalline halite. More importantly, Lines was the first to estimate the hydrologic budget for the shallow-brine aquifer of the Bonneville Salt Flats. For 1976, he estimated that discharge exceeded recharge by about 2,000 acre-ft. Lines suggested that the difference between total recharge and total discharge resulted in a decrease in ground-water storage in the shallow-brine aquifer. Lines estimated that most of the recharge was derived from infiltration of precipitation directly on the playa surface or from winter surface ponds. The primary forms of discharge included evaporation from the playa surface and seepage to brine-collection ditches located east of the salt crust and south of Interstate Highway 80. Lines also made comparisons to Pilot Valley, a mostly undisturbed playa to the northwest.

## Field Work

Preliminary field work began in 1991. The primary data-collection period was the spring of 1992 through the fall of 1993. The study area is a unique hydrologic environment that poses many accessibility and logistical problems when the playa surface is wet. Field work on the Bonneville Salt Flats presented many problems with regard to travel on the playa surfaces and to data collection because of the corrosive nature of the brine. Travel on the playa surface was restricted during late fall through spring. Winter surface ponding and soft, muddy conditions on the remainder of the playa surface prevented normal travel. Generally, light all-terrain vehicles were used when feasible. Even during summer months, travel can be difficult. Newly formed deposits of thin salt concealed underlying soft mud that could easily entrap a 4-wheel drive truck. Time of year and selection of new well sites had to be chosen carefully when heavy equipment was used for drilling. Even with careful planning, deceptively soft surface conditions resulted in equipment becoming entrapped at times, with one drill rig stuck for 2 days.

In the initial phases of field work, existing monitoring wells were inventoried to determine which wells were suitable for continued monitoring. Forty-eight additional monitoring wells were completed in the shallow-brine aquifer where existing wells had been damaged or where additional data were needed. A trailer-mounted auger with hollow- or solid-stem capabilities was used to complete most of the shallow wells. Some shallow wells were hand augured when the playa surface would not support anything heavier than a light all-terrain vehicle. The completion of deep, nested piezometers and individual monitoring wells in the alluvial-fan and basin-fill aquifers required the use of larger drilling equipment with mud-rotary or hollow-stem auger capabilities. The network of monitoring wells on the Bonneville Salt Flats is shown in figure 3.

Water levels were measured in all monitoring wells for 2 years. After each water-level measurement was completed, brine was bailed from the well casing for temperature and specific-gravity (density) measurements. Ideally, water-level measurements were made every 3 months. Ponding during winter months and cold temperatures made travel on the playa extremely difficult and hazardous. During the winter of 1992-93, the areal extent of the surface pond was extensive and the depth was more than 1 ft in several places. Under these conditions, some monitoring wells were underwater or at the pond surface. For various other reasons, not all wells were measured during each measurement period. During the measurement periods in the spring of 1993, not all monitoring wells were accessible as would have been the case under normal conditions. During the summer measurement periods, some monitoring wells were inadvertently missed because of the difficulty in locating white well casing on the vast white salt crust.

In an attempt to quantify the amount of salt being redistributed during the winter months through dissolu-

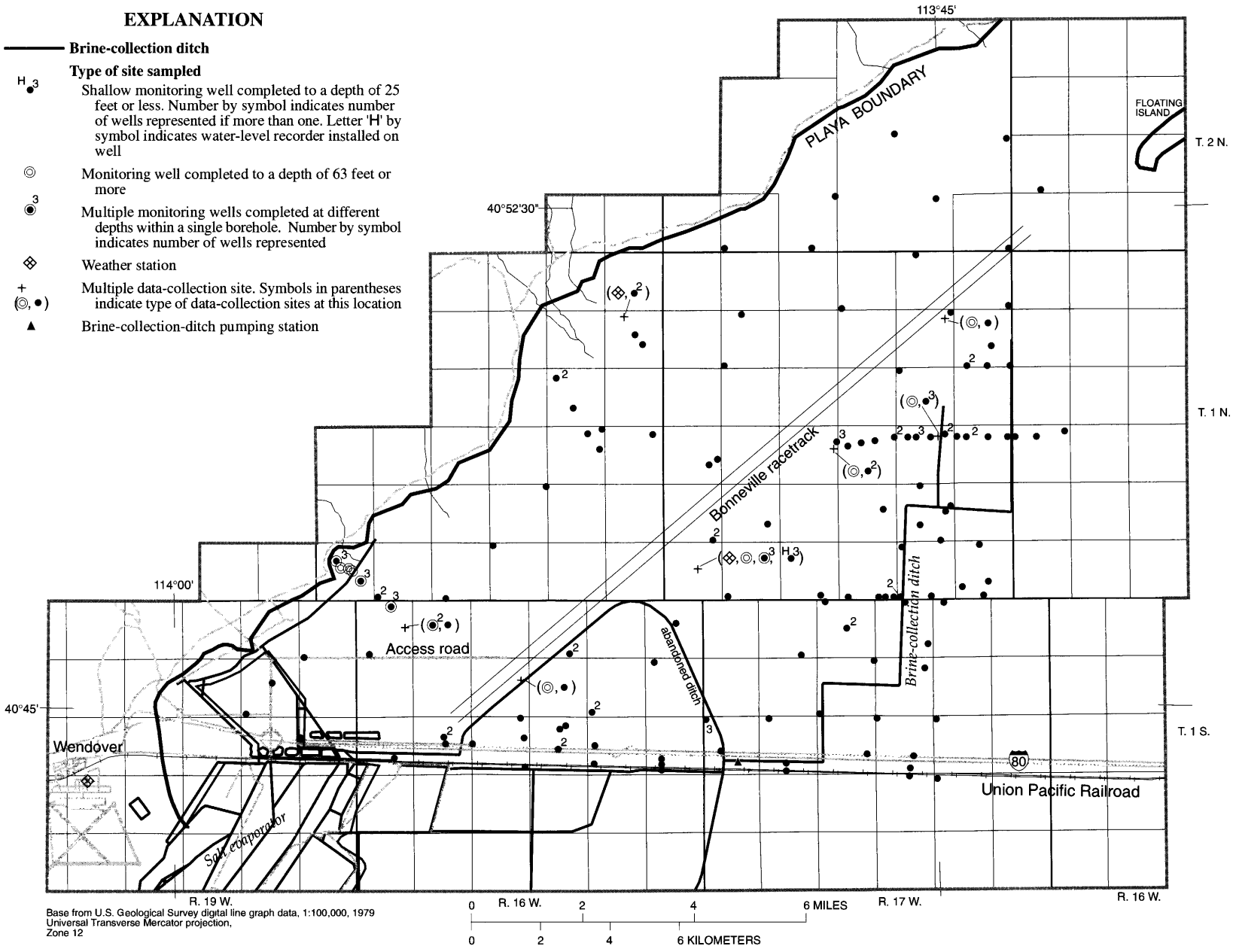


**Figure 3.** Location of weather stations and wells used for water-level measurements, Bonneville Salt Flats, Utah.

tion and precipitation, measurements from the top of the well casing to the salt crust were made at the same time as water-level measurements during 1993. From the differences in these measurements over time, the amount of salt dissolved in the winter of 1992-93 and precipitated in the summer of 1993 was estimated.

A continuous water-level recorder was installed and maintained on well (B-1-17)31acc-1, which was completed to a depth of 14 ft and located near the center of the salt crust. Six other wells completed at varying depths that ranged from 2.5 to 495 ft were also at this location. Two weather stations, installed and maintained by the Utah Climate Center, recorded data necessary to estimate actual evaporation from the playa surface.

Brine samples from wells on the Bonneville Salt Flats were collected for chemical and isotopic analysis. In most monitoring wells, yield was very low, thus preventing the withdrawal of three casing volumes. A minimum of one casing volume was pumped from each well before sampling and where feasible, three casing volumes were pumped. The distribution of samples was designed to examine the variation in chemical constituents areally, vertically within the ground-water system, and temporally. Twelve wells, originally sampled by Lines (1978, 1979), that were still usable were sampled again to determine any long-term variation. At most of the sampled wells completed in the shallow-brine aquifer, two samples were collected in early summer and fall. From these analyses, a seasonal variation for various constituents can be determined. All wells completed in the lacustrine sediment below the shallow-brine aquifer and at the northwest margin of the playa were sampled. Pore fluid from cores collected during drilling of some wells also was analyzed.

The quantity of brine obtained from land on Federal leases was estimated from data collected at the pumping station, which lifts the brine to a higher elevation in the collection ditch, south of Interstate Highway 80 (fig. 3). A continuous recorder was used to measure the brine level in the ditch upstream from the pumping station. Data from the recorder were used to determine the time the pump was in operation and the brine level at time of pumping. A vibration-time-totalizing meter was installed on the pump to monitor total length of time the pump was in operation. Instantaneous discharge, specific-gravity, and temperature measurements were made periodically. The instantaneous discharge measurements were compared to the level in the ditch from which the pump lifts the brine. Pump discharge is larger when the brine level in the ditch is high as compared to when the brine level in the ditch is low. From these data, a rating curve was developed that relates brine level to discharge when the pump is in operation.

The two weather stations that were installed by the Utah Climate Center are located at a multiple-well site near the center of the salt crust and to the northwest on the playa margin (fig. 3). These additional stations were designed to collect data necessary to determine precipitation, wind direction and velocity, air temperature, relative humidity, solar and net radiation, surface heat flux, and latent and sensible energy for the determination of actual and potential evaporation. The station on the playa margin northwest of the salt crust was put into service in November 1991. The weather station on the salt crust (fig. 4) was put into service in September 1992. These weather stations were serviced by personnel from the Utah State Climate Center.

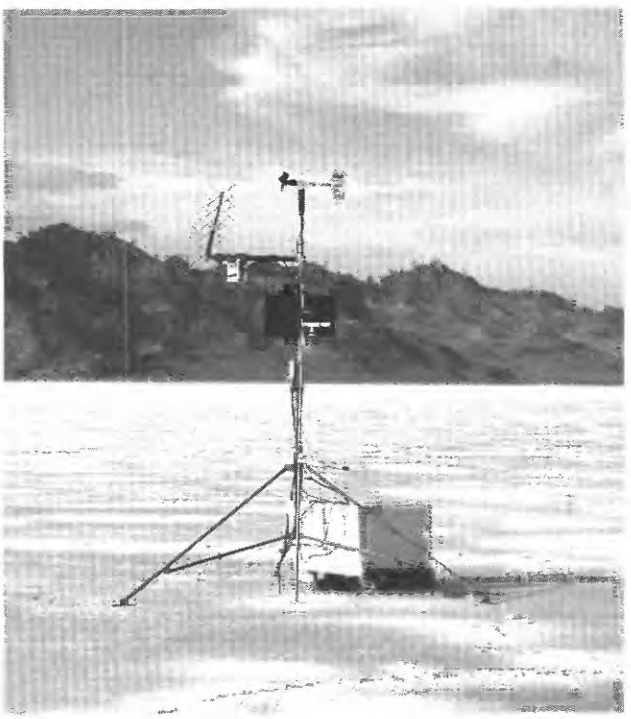

**Figure 4.** Weather station near the center of the salt crust, Bonneville Salt Flats, Utah.

## Acknowledgments

The authors express their appreciation to Reilly Wendover, a division of Reilly Industries. Reilly Wendover granted permission to drill monitoring wells on their property and allowed access to these wells and existing wells for water-level measurements and sampling for chemical analysis. Reilly Wendover granted permission to monitor their pumping station on the collection ditch and provided data.

Comments and suggestions provided by members of the technical review committee established by the Bureau of Land Management were greatly appreciated. Special appreciation goes to Blair F. Jones, U.S. Geological Survey, for numerous suggestions regarding the brine chemistry of the Bonneville Salt Flats, and to Brenda L. Coleman and Daniel M. Webster, U.S. Geological Survey, for x-ray diffraction identification of clay-size minerals and extraction and chemical analysis of pore fluid.

# DESCRIPTION OF STUDY AREA

## Physical Setting

The Bonneville Salt Flats study area is in the western part of the Great Salt Lake Desert, which is in the Great Basin part of the Basin and Range Physiographic Province (Fenneman, 1931, pl. 1). The Great Basin is a hydrologically closed region with no surface outlet. The only means for water to leave the Great Basin is by evaporation to the atmosphere. Typical topography of the Basin and Range Province consists of nearly north-trending mountain ranges separated by desert basins. The mountain ranges and separating basins are generally 5 to 15 mi wide and about 50 mi long, but the Bonneville Salt Flats is located in the western part of a basin that is more than twice as wide as a typical basin in the Basin and Range Province.

The Bonneville Salt Flats is bounded by the Silver Island Mountains to the northwest. The mountains rise abruptly from the playa floor to a maximum altitude of more than 7,500 ft. Paleozoic-age carbonate rocks and quartzites with some outcrops of Tertiary-age basaltic extrusive rocks are prominent. Several remnant Lake Bonneville shoreline features on the steep mountain flanks are visible from the Bonneville Salt Flats. Although sand and gravel are present in the subsurface, the surface features of alluvial-fan deposits are less prominent on the southeastern flank of the Silver Island Mountains, adjacent to the Bonneville Salt Flats, than on the northwestern flank.

Surface runoff, which generally results from intense summer thunderstorms, flows in distinct ephemeral stream channels from the mountains toward the playa. These channels cross the alluvial fans and continue toward the playa where most terminate in surface fractures before reaching the playa mud. Flow in some of the ephemeral stream channels might reach the playa beyond the vegetation at the playa margin and contributes to surface ponds. Surface flow reaching the playa, however, was not observed during this study.

On the northeast, east, and south margins of the Bonneville Salt Flats, the playa surface gradually slopes upward for several miles in each direction. The surface of the salt crust represents the lowest point of the basin, and surface-water flow generally moves toward the salt crust. Even slight changes in altitude of the land surface, such as less than 1 ft, can create small, closed basins that can accumulate water and salt, thus impeding flow toward the salt crust. These small, closed basins are easily breached when the water level rises as a result of precipitation and when strong winds move sheets of water across the playa surface. Surface-water flow that used to move toward the salt crust has been interrupted by man-made structures such as the brine-collection ditch and associated berm on the east side of the salt crust, and Interstate Highway 80 and the railroad to the south. Culverts were installed beneath Interstate Highway 80 to facilitate surface flow toward the salt crust. In 1983, additional culverts were installed beneath the roadbed to alleviate extensive flooding. A large amount of water again passed through these culverts in the spring of 1993 as a result of greater-than-normal precipitation in January and below-normal temperatures in January and February.

## Playa Morphology

The salt crust and associated near-surface deposits in the Bonneville Salt Flats playa are the result of desiccation of Lake Bonneville. As with other playas that formed by lake desiccation, evaporite mineral zonation, as described by Hunt and others (1966, p. B46-B48), can be divided into a carbonate zone, composed primarily of aragonite; a sulfate zone, composed primarily of gypsum; and a chloride zone, composed primarily of halite. As evaporation progresses, the dissolved-solids concentration of the evaporating fluid

increases. When the fluid reaches saturation with respect to a specific mineral, precipitation of that mineral progresses until the fluid is no longer at saturation with respect to that mineral, either due to dilution or depletion of one of the required ions. The carbonate minerals, which are the least soluble, will crystallize first, followed by sulfate minerals, and finally the most soluble, chloride minerals. In a simplified sense, the carbonate minerals will precipitate along the edges of the lake where they might interfinger with alluvial deposits and across the bottom where they overlie the lacustrine sediment. The sulfate minerals precipitate over the carbonate minerals and, likewise, the chloride minerals precipitate next and overlie the sulfate minerals. Each zone of minerals is transitional with adjacent zones and might be interfingered with adjoining zones as a result of erosional and mineral dissolution and precipitation processes. The volume of each zone will depend on the original composition of the evaporating fluid.

Because halite is the most soluble mineral and covers a large areal extent of the Bonneville Salt Flats, the chloride zone is most responsive to climatic changes. Through variability in rainfall on the playa, the salt crust can vary in surface texture and areal extent from 1 year to the next because of dissolution and precipitation of salt at the surface as described by Lines (1979, p. 42-56) and Turk (1978, p. 3-18). No attempt was made to delineate the seasonal variation in texture and areal extent of the various types of salt surfaces during this study.

Lines inventoried five different types of salt-crust surfaces: thin seasonal, pressure-ridge, sediment-covered, smooth perennial, and rough perennial, of which the rough perennial salt crust was not present during this study. The lack of rough perennial salt crust, which forms in areas where the salt crust does not become covered by water, is probably the result of more extensive ponding during the winter months of this study than was present during Lines' study. The more extensive ponding might be the result of increased winter precipitation and cool temperatures during the time of this study in combination with the elimination of surface drainage of brine into the collection ditch. The erosional channels on the west side of the brine-collection ditch, described by Lines (1979, p. 35), have been eliminated by subsequent dredging of the brine-collection ditch and building the resultant berm along the west side.

The extensive flooding of the Bonneville Salt Flats during the winter of 1992-93 dramatically changed the salt surface. Much of the near-surface salt was dissolved, especially in the southern part of the salt crust. When halite was dissolved, crystalline gypsum, which was not dissolved, and some insoluble silt interbedded within the salt crust became concentrated in a thin layer on the surface of the crust. At many locations, ripple marks were visible on this surface at the bottom of the pond. The Bonneville Salt Flats remained mostly flooded into the late summer of 1993 with the dissolved halite gradually precipitating on the playa surface as the pond evaporated. Much of the halite subsequently was deposited on the salt crust and smooth, thin seasonal halite crust also was deposited in areas beyond the usual areal extent of the salt crust.

A 30-in., vertical column of salt was removed from the salt crust by Bureau of Land Management personnel in August 1995. A 3-in. layer of crystalline salt was removed prior to extraction of the vertical column. This removal exposed the undulating, ripple-marked surface that was the result of salt dissolution and precipitation in 1993. Five additional, undulating surfaces could be delineated throughout the column. These surfaces indicate that salt dissolution and precipitation has occurred during the formation of the salt crust.

The pressure-ridge salt crust was prominent to the east of the Bonneville racetrack during late summer months of 1990-92. This type of salt surface generally forms where thin salt crust has precipitated over the carbonate mud. Additional accumulation of salt from evaporating subsurface brine causes lateral forces that rupture the thin crust. Subsequently, one section of the salt crust will thrust over an adjoining section of crust. Because of the short period of time in the summer of 1993 for evaporation from subsurface brine, the pressure-ridge salt crust did not develop where thin salt formed over the carbonate mud. Localized areas of pressure-ridge salt did develop, however, over the smooth perennial salt crust where gypsum or thin layers of sediment had accumulated at the bottom of the pond during the winter. Newly precipitated salt is susceptible to the formation of pressure ridges because of its lack of cohesion with the underlying gypsum or sediment.

## Climate

Climate plays an integral part in controlling the movement of water on the surface and within the ground-water system of the Bonneville Salt Flats. Pre-

cipitation, temperature, wind, and evaporation are all part of the mechanism that drives these hydrochemical systems. Climatic data have been collected from 1912 to 1994 at the U.S. National Weather Service station in Wendover, about 10 mi southwest of the center of the Bonneville Salt Flats. Data were collected at the playa-margin station from January 1992 through 1994 and at the salt-crust station from November 1992 through August 1994.

### Precipitation

Precipitation at the Wendover climatic station averaged 4.78 in/yr from 1912 through 1993, (data were incomplete in 1994) (U.S. Weather Bureau, 1936, 1957, 1961-66, and 1965; U.S. Environmental Science Services Administration, 1966-71; U.S. National Oceanic and Atmospheric Administration, 1971-94). Annual precipitation has varied from a minimum of 1.62 in. in 1992 to a maximum of 10.13 in. in 1941 (fig. 5). Lines (1979, p. 15) identified five wetter-than-normal and drier-than-normal periods from 1912 through 1973, ranging in length from 12 to 14 years. Precipitation records for 1974 through 1993, indicate the wetter-than-normal period beginning in 1962 lasted through 1983, with an average annual precipitation of 5.59 in. The period from 1984 to 1993 defines a drier-than-normal period, with an average annual precipitation of 3.64 in.

Lines (1979, p. 14) assumed that these wet and dry periods recorded at the Wendover station also occurred on the Bonneville Salt Flats on the basis of 15 months of concurrent record with temporary stations on the Bonneville Salt Flats and in Pilot Valley. The limited record from the playa-margin station on the southeast flank of the Silver Island Mountains indicates that area might receive more precipitation than the area near the Wendover station. In 1992, the playa-margin station recorded 3.05 in. of precipitation, and the Wendover station recorded 1.62 in. of precipitation. The greatest discrepancy was for January through May 1992 when 1.44 in. fell at the playa-margin station and only 0.31 in. fell at the Wendover station. During the 35 months for which concurrent record exists, the playa-margin station recorded greater monthly precipitation than the Wendover station during 24 months (fig. 6). The salt-crust station was not in service during much of 1992, but in 1993, 4.64 in. of precipitation were recorded, 1.41 in. more than at the Wendover station. Monthly precipitation at the three weather stations is listed in table 1, along with the monthly departures from the 1961-90 normals at Wendover, Utah.

### Wind

Wind is the primary mechanism for moving ponded water over the surface of the Bonneville Salt Flats. The two weather stations installed for this study were equipped with recording anemometers. For the period of record, the median of the average monthly wind directions at both sites was North 9° East (fig. 7). The median of the average monthly velocities was 6.5 mi/hr. During the spring and summer months (April through September) of 1992-94, the median of the average monthly wind directions was North 23° East. The median of the average monthly velocities for the spring and summer months was 7.8 mi/hr. The average monthly wind velocity ranged from 5.7 to 9.1 mi/hr from April through September. Maximum velocities recorded during spring and summer months generally exceeded 50 mi/hr during the period of record. In August and September 1993 and June 1994, maximum velocities exceeded 40 mi/hr.

### Temperature

Air and soil temperatures affect water evaporation from above and below land surface. Air temperature has been recorded at the Wendover weather station since 1921 (fig. 8). Not including 6 years of missing data, the average annual temperature at the Wendover weather station was 52.4°F. The average annual temperature has been as high as 56.3°F in 1934 and as low as 48°F in 1994. Typically, high average annual air temperatures occur during periods of less-than-normal precipitation, and low average annual air temperatures occur during periods of greater-than-normal precipitation.

Air and soil temperature were recorded at the two weather stations on the Bonneville Salt Flats in order to estimate evaporation. Monthly air and soil temperature at the playa-margin station were slightly higher than at the salt-crust station. Except in the fall, average monthly soil temperatures were always 2 to 10 degrees warmer than average monthly air temperature. The highest average monthly temperatures occurred during August (70° to 90°F), and the lowest average monthly temperatures occurred during January (15° to 25°F). Average monthly air temperature at the two stations was about the same as at the Wendover station for 1992-94 (table 1). Wet and dry bulb temperature also

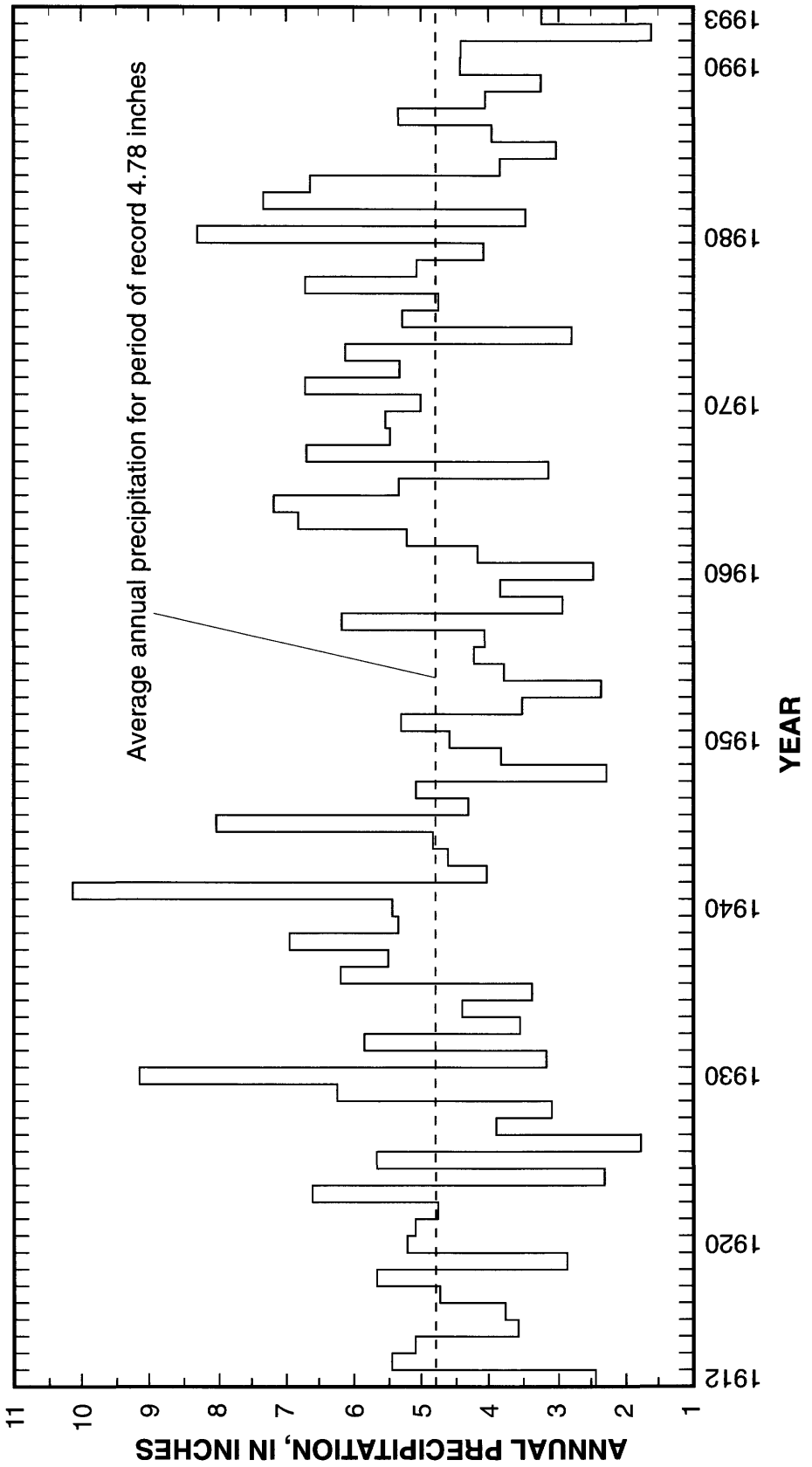


**Figure 5.** Annual precipitation at Wendover, Utah, 1912 through 1993.

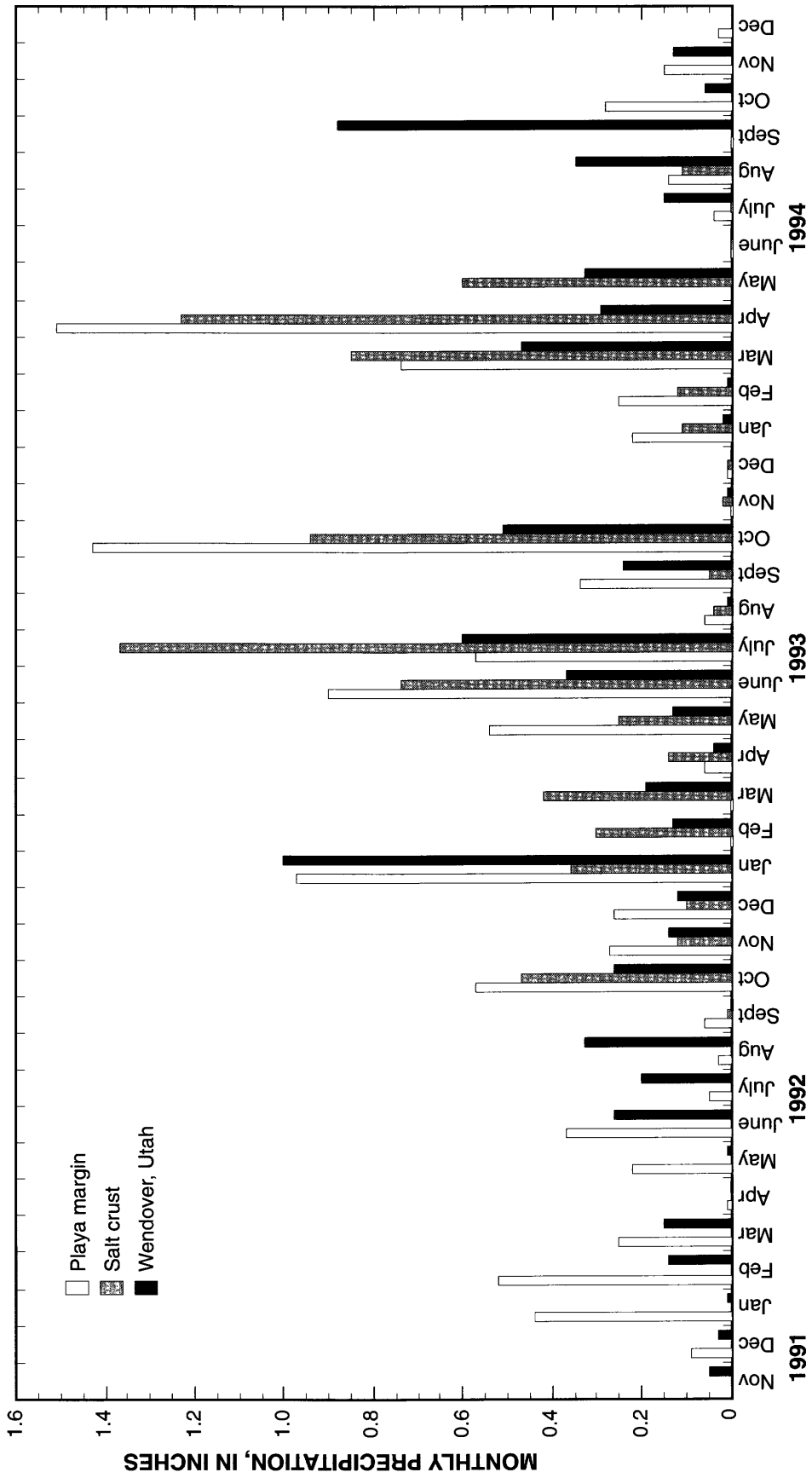


**Figure 6.** Monthly precipitation at the three weather stations on or near the Bonneville Salt Flats, Utah, November 1991 through December 1994.

**Table 1.** Monthly mean temperature and monthly precipitation and departures from 1961-90 normals at Wendover, Utah, compared to monthly mean temperature and monthly precipitation measured at two weather stations on the Bonneville Salt Flats, Utah, 1992-94.

[°F, degrees Fahrenheit; —, no data available; M, partial data missing; NA, departure not calculated because of missing data]

| | Wendover | | | | Playa margin | | Salt crust | |
|---|---|---|---|---|---|---|---|---|
| | Temperature (°F) | | Precipitation (inches) | | Temperature (°F) | Precipitation (inches) | Temperature (°F) | Precipitation (inches) |
| | Mean | Departure | Total | Departure | | | | |
| | | | | **1992** | | | | |
| January | 23.6 | -4.5 | .01 | -.33 | 22.8 | .44 | — | — |
| February | 37.7 | 3.3 | .14 | -.22 | 39 | .52 | — | — |
| March | 47.2 | 5.8 | .15 | -.27 | 49.1 | .25 | — | — |
| April | 57.5 | 7.0 | .0 | -.43 | 59.7 | .01 | — | — |
| May | 65.8 | 5.0 | .01 | -.84 | 68.2 | .22 | — | — |
| June | 71.1 | .7 | .26 | -.35 | 72.5 | .37 | — | — |
| July | 76.6 | -3.2 | .2 | -.05 | 78.7 | .05 | — | — |
| August | 77.1 | .4 | .33 | -.09 | 84.1 | .03 | — | — |
| September | 66.0 | .0 | .0 | -.23 | 65.5 | .06 | — | — |
| October | 55.2 | 2.8 | .26 | -.21 | 54.6 | .57 | 55.7 | .47 |
| November | 33.9 | -4.3 | .14 M | NA | 34.3 | .27 | 34.8 | .12 |
| December | 24.4 | -4.4 | .12 M | NA | 24.8 | .26 | 25.4 | .10 |
| | | | | **1993** | | | | |
| January | 15.4 | -11.4 | 1.0 | .76 | 17.6 | .97 | 19.5 | .36 |
| February | 24.5 | -9.2 | .13 M | NA | 25.0 | .0 | 27.6 | .3 |
| March | 42.5 | .3 | .19 M | NA | 42.5 | .0 | 44.9 | .42 |
| April | 48.6 | -2.1 | .04 | -.52 | 48.9 | .06 | 49.9 | .14 |
| May | 63.7 | 2.9 | .13 M | NA | 64.4 | .54 | 64.0 | .25 |
| June | 64.5 | -6.4 | .37 | -.28 | 65.2 | .9 | 64.4 | .74 |
| July | 71.3 | -8.4 | .6 | .29 | 71.6 | .57 | 69.5 | 1.37 |
| August | 73.0 | -3.7 | .01 | -.45 | 73.5 | .06 | 71.7 | .04 |
| September | 64.5 | -1.1 | .24 | -.14 | 64.9 | .34 | 62.9 | .05 |
| October | 50.7 | -1.3 | .51 | -.04 | 51.1 | 1.43 | 50.8 | .94 |
| November | 30.4 | -8.2 | .01 | -.37 | 30.7 | .01 | 30.2 | .02 |
| December | 21.5 | -1.1 | .0 | -.27 | 26.8 | .01 | 26.4 | .01 |
| | | | | **1994** | | | | |
| January | 30.7 | 3.9 | .02 | -.22 | 31.5 | .22 | 30.5 | .11 |
| February | 31.1 | -2.6 | .01 | -.31 | 31.9 | .25 | 32.0 | .12 |
| March | 44.8 | 2.6 | .47 | .02 | 45.3 | .74 | 44.8 | .85 |
| April | 52.4 | 1.7 | .29 M | NA | 52.5 | 1.51 | 52.1 | 1.23 |
| May | 64.4 | 3.6 | .33 | -.57 | — | — | 63.7 | .6 |
| June | 73.0 | 2.1 | .0 | -.65 | 74.1 | .0 | 72.7 | .0 |
| July | 79.4 | -.3 | .15 | -.16 | 80.8 | .04 | 79.7 | .0 |
| August | 78.4 | 1.7 | .35 | -.11 | 79.2 | .14 | 78.2 | .11 |
| September | 67.3 | 1.7 | .88 | .50 | 70.3 | .0 | — | — |
| October | 50.0 | -2.0 | .06 M | NA | 51.8 | .28 | — | — |
| November | 32.3 | -6.3 | .13 M | NA | 32.7 | .15 | — | — |
| December | 28.8 | 1.2 | — | NA | 29.9 | .03 | — | — |

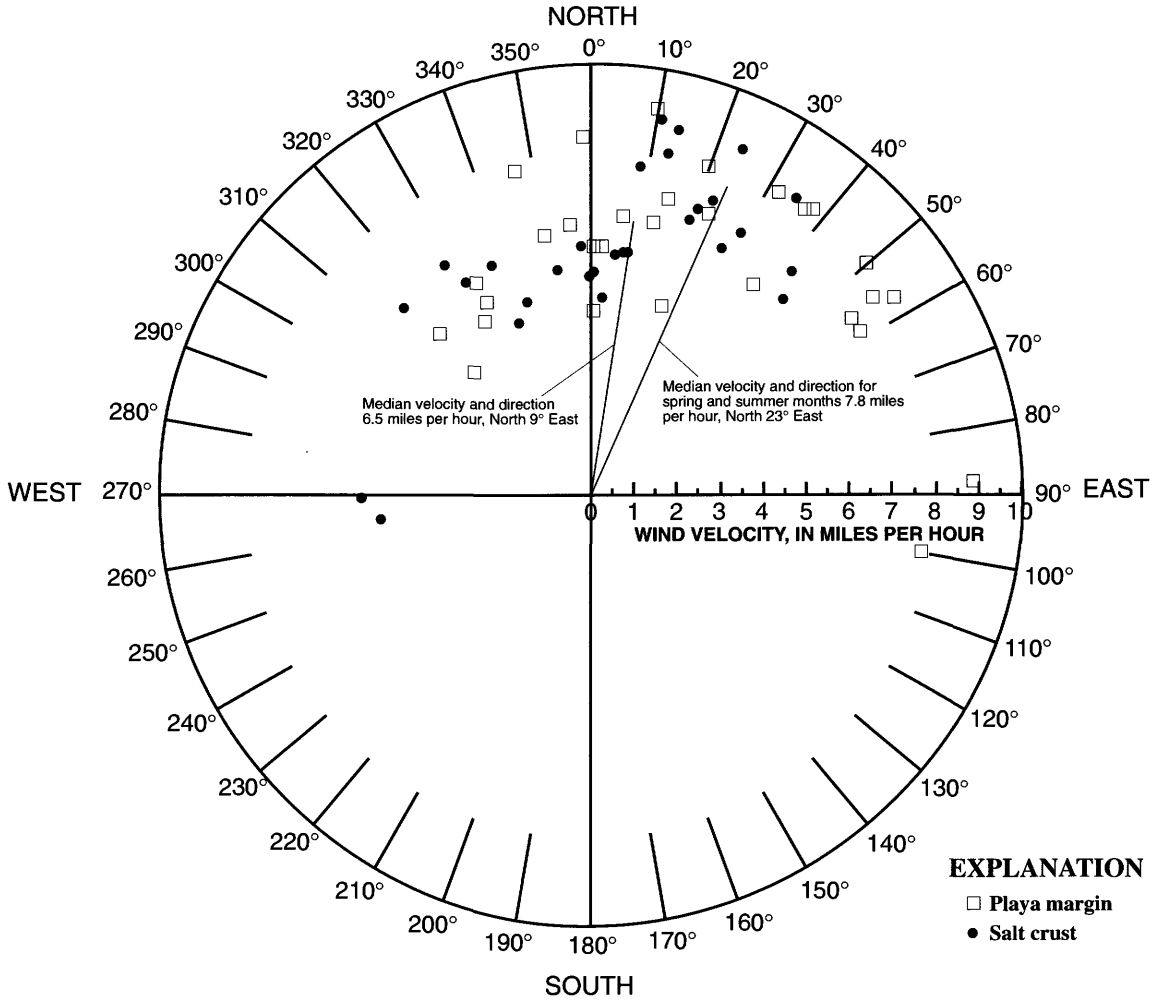


**Figure 7.** Average monthly wind direction and velocity for the two weather stations on the Bonneville Salt Flats, Utah, December 1991 through December 1993.

were recorded at the two weather stations on the Bonneville Salt Flats because they are needed for calculating actual evaporation by the Bowen-ratio method discussed later in this report.

## GROUND-WATER HYDROLOGY

### Description of Ground-Water System

In most of the western Great Salt Lake Desert, ground water is present in three distinct aquifers. The basin-fill aquifer generally is the largest in volume of the three aquifers. Because the alluvial-fan aquifer is in close proximity to sources of recharge, such as seepage through consolidated rock and infiltration of surface runoff, it generally is the source of the most usable water. The shallow-brine aquifer, where present, generally is in near-surface deposits and can have a thin ephemeral salt crust or a thick perennial salt crust, such as on the Bonneville Salt Flats. The spatial relation of these aquifers as they occur in the Bonneville Salt Flats is shown diagrammatically in figure 9.

The basin-fill aquifer generally is composed of several hundred feet of fine-grained, lacustrine sediment in the upper part and the underlying conglomerate yields brine to wells. These wells are completed to depths of more than 1,000 ft. The conglomerate is more than 800 ft thick (Lines, 1979, p. 57), and overlies Tertiary-age volcanic rocks or pre-Tertiary-age rocks. The

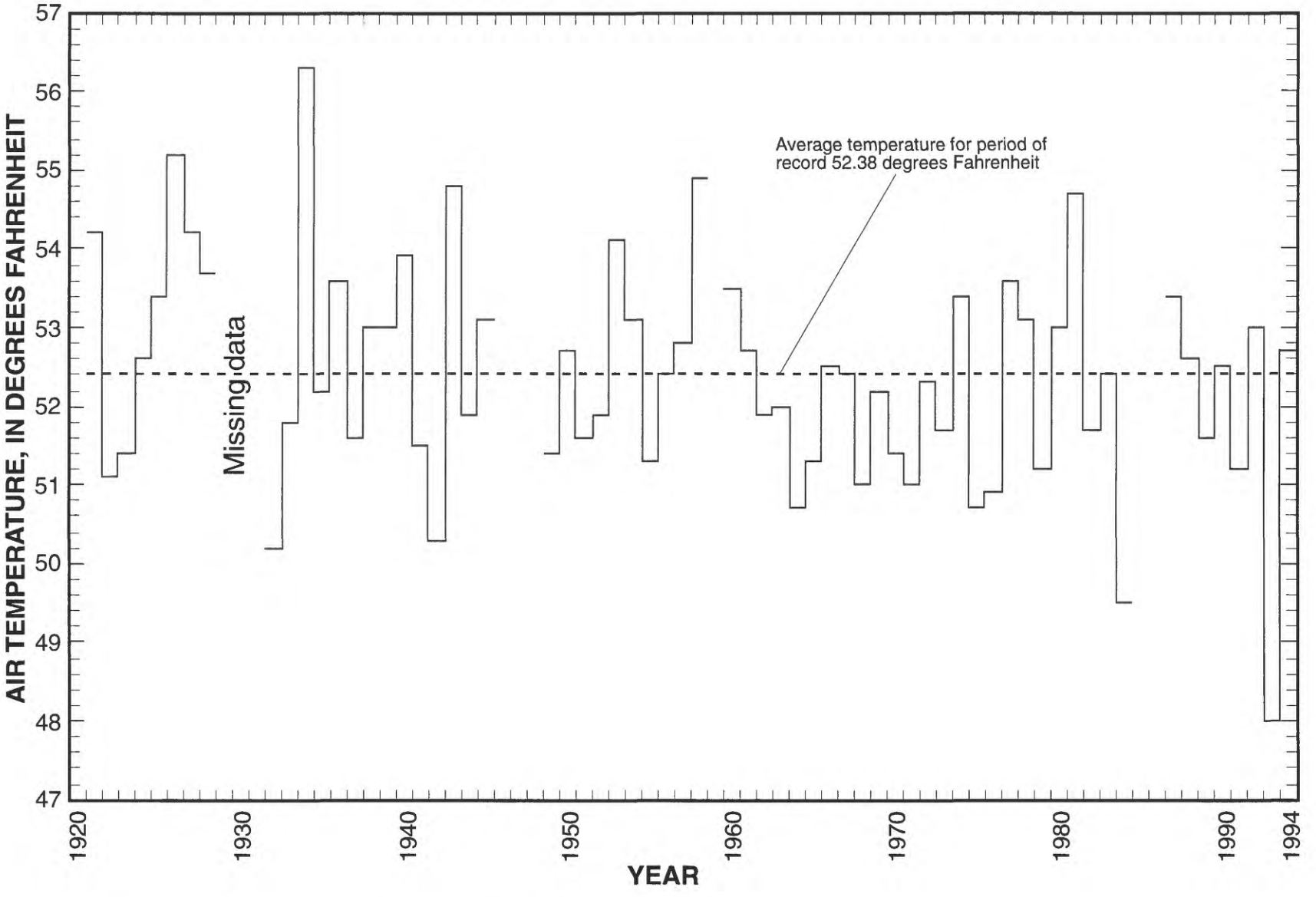


**Figure 8.** Average yearly air temperature at Wendover, Utah, 1921 through 1994.

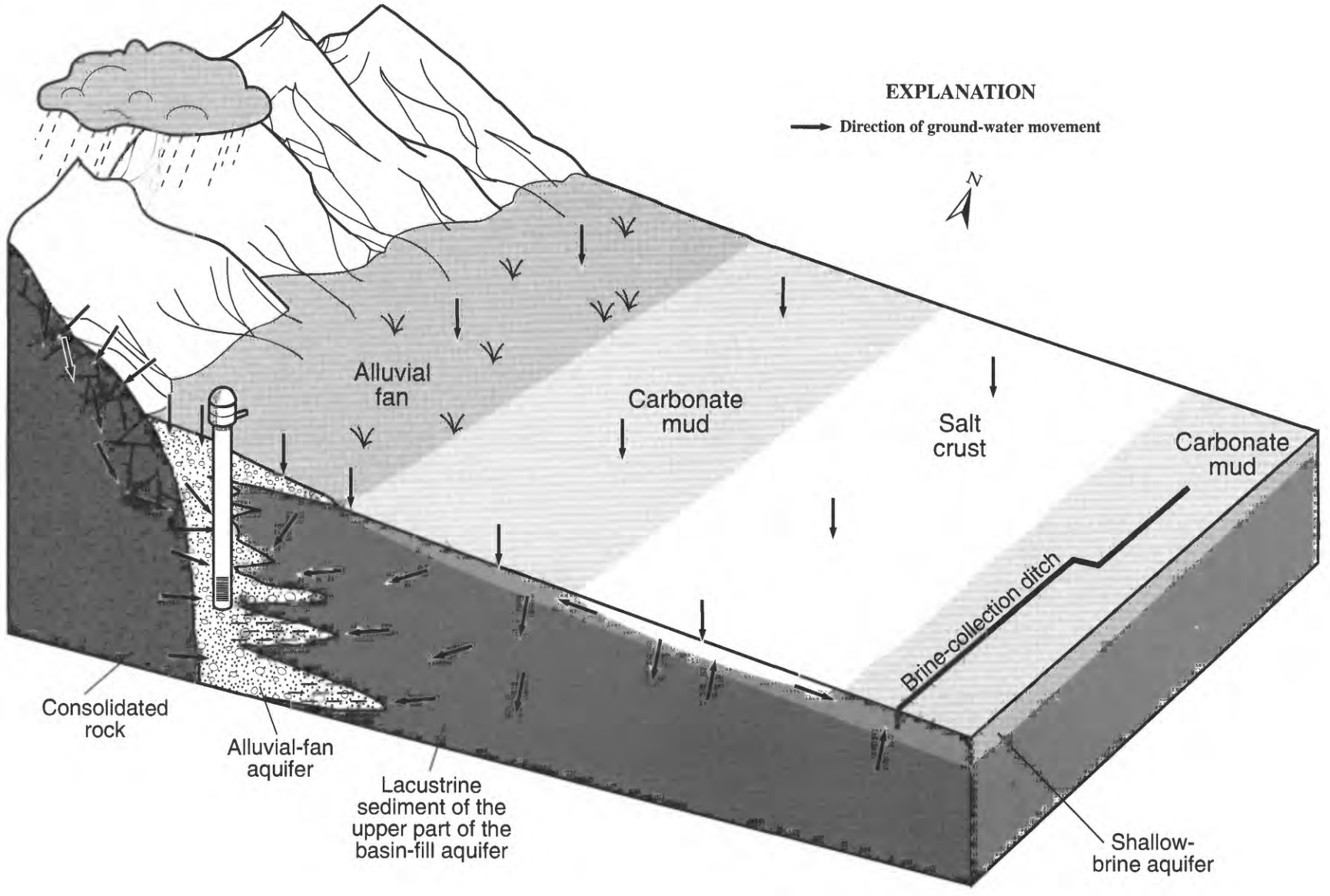


**Figure 9.** Generalized block diagram showing the relation of aquifers and direction of ground-water flow in the Bonneville Salt Flats, Utah.

thick lacustrine sediment between the conglomerate and the overlying shallow-brine aquifer previously was not considered part of the basin-fill aquifer. For the purposes of this report, the lacustrine sediment will be included as the upper part of the basin-fill aquifer.

Along the southeast flank of the Silver Island Mountains, the alluvial-fan aquifer in the Bonneville Salt Flats study area readily yields brackish water to wells. Sand and gravel of the alluvial-fan aquifer are interbedded with the carbonate mud of the shallow-brine aquifer and the lacustrine sediment of the upper part of the basin-fill aquifer. The vertical extent of these sands and gravels of the alluvial-fan aquifer is unknown; therefore, the degree of hydraulic connection with the conglomerate in the basin-fill aquifer at depth also is unknown. As the layers of the alluvial-fan aquifer extend toward the playa, the coarser material becomes intermixed with fine-grained sediment. Wells completed in these zones would be less likely to yield substantial amounts of water.

The shallow-brine aquifer is composed of a halite and gypsum crust at the surface and is surrounded by carbonate mud, both laterally and immediately beneath the salt crust. The transition zone between the shallow-brine aquifer and the alluvial-fan aquifer is difficult to identify at land surface, but the boundary between the aquifers is assumed to occur at the limit of vegetation or at a slight change in the slope of the land surface. On the basis of water levels in wells along the northwestern margin of the playa, the shallow-brine aquifer might be hydraulically connected to the alluvial-fan aquifer. The thick sequence of fine-grained, lacustrine sediment, generally several hundred feet thick, in the upper part of the basin-fill aquifer probably restricts the vertical movement of brine between the shallow-brine aquifer and the more porous conglomerate in the deeper part of the basin-fill aquifer.

Ground-water density in these three aquifers varies from less-dense brackish water in the alluvial-fan aquifer to dense brines in the shallow-brine aquifer. Ground-water density also can vary within an aquifer. Because of the widely varying ground-water density, additional features describing ground-water flow need to be considered in order to properly describe ground-water movement. Variable-density ground-water flow is somewhat more complicated than uniform-density flow because of buoyancy effects. For density variations caused by solute-concentration variations, quantification of ground-water flow is no longer obtainable from the gradient of a scalar potential field such as potentiometric head.

## Principles of Variable-Density Ground-Water Flow

Much of the following discussion of variable-density, ground-water flow is described in Hubbert (1953, 1956). These principles were originally used by Hubbert to describe the flow of petroleum under hydrodynamic conditions and later applied to ground-water flow.

The state of ground-water motion is a result of the energy conditions that prevail. A particle of water at any point possesses a potential energy per unit mass, more commonly known as potential, $\Phi$. If the potential field across a region is variable, work will be required to move an element of water from a point of lower potential to one of higher potential. In this case, an unbalanced force is exerted upon the fluid by its environment, driving it in the direction of the most rapid decrease of potential.

The potential at a given location is the amount of work that would be required to move a unit mass of water from a reference position and state to a position and state of the location considered. Total work consists of work against gravity and work against pressure. For the slow, creeping motion of ground-water flow, the kinetic-energy term can be neglected. Then the potential can be expressed by the following equation:

$$\Phi = g(z - z_0) + (p - p_0)/\rho \qquad (1)$$

where

$\Phi$ is the potential ($E/M$);
$g$ is the gravitational constant ($L/T^2$);
$z$ is altitude ($L$);
$z_0$ is the reference standard altitude ($L$);
$p$ is the fluid pressure ($F/L^2$);
$p_0$ is the fluid reference standard pressure ($F/L^2$); and
$\rho$ is the fluid density ($M/L^3$).

Because the choice of the reference state is arbitrary, sea level and atmospheric pressure can be selected. Thus, the potential depends on the altitude, pressure, and fluid density that can, in principle, be measured at any location in the subsurface. It can be determined at any point capable of being occupied by a fluid of given density, whether or not that fluid is actually present. Thus, freshwater potentials have values

not only in space saturated with freshwater, but also in space occupied by salt water and vice versa. The potential at a given point is related to the height above standard datum to which the fluid will rise in a manometer installed at that point. That is,

$$\Phi = gh \tag{2}$$

where

$h$ is the height of fluid above standard datum (potentiometric head) ($L$).

The value of potential is the amount of work required to lift a unit mass of fluid to the height, $h$, against the gravitational force.

The force exerted on a unit mass of fluid at any given point is related to the potential field. Specifically, the force is obtained from the gradient of the potential field by

$$\boldsymbol{E} = -\nabla\Phi = \boldsymbol{g} - \nabla p\rho^{-1} \tag{3}$$

where

$\boldsymbol{E}$ is the force vector on a unit mass of fluid ($F/M$);

$\nabla$ is the spatial gradient operator ($L^{-1}$); and

$\boldsymbol{g}$ is the gravitational vector ($L/T^2$).

The fluid is in a state of hydrostatic equilibrium when $\boldsymbol{E} = 0$, that is, $\Phi$ is a constant. The physical meaning of the force-intensity vector $\boldsymbol{E}$ comes from equation 3 that states at a given point, a unit mass of fluid will be acted upon by a force $\boldsymbol{E}$ that is the sum of a gravitational force $\boldsymbol{g}$ and a pressure-gradient force $\nabla p$ divided by the fluid density $\rho$. The force-intensity vector is obtained by vector addition shown in figure 10.

In ground-water flow, only rarely does $\boldsymbol{E}$ have a magnitude greater than a small fraction of the vector $\boldsymbol{g}$. When the pressure-gradient force is tilted somewhat from vertical, the force-intensity vector may point upward or downward, and the fluid will have a driving force in the direction of $\boldsymbol{E}$. The resulting fluid movement can be characterized by a specific discharge or volumetric fluid flux vector $\boldsymbol{q}$. For a homogeneous fluid in an isotropic porous media, $\boldsymbol{q}$ points in the direction of $\boldsymbol{E}$ with a scalar parameter of proportionality $K$ known as hydraulic conductivity. The relation is given by Darcy's law

$$\boldsymbol{q} = -K\nabla h \tag{4}$$

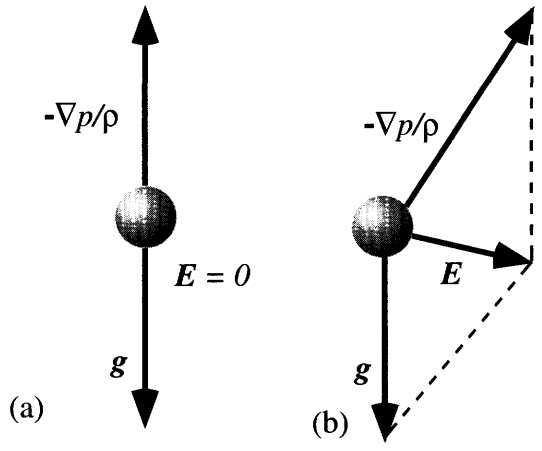


**Figure 10.** Force-intensity vector E for (a) hydrostatic conditions; and (b) hydrodynamic conditions.

where

$\boldsymbol{q}$ is the volumetric fluid-flux vector ($L^3/L^2$-$T$); and

$K$ is the hydraulic conductivity ($L/T$).

If a second fluid of density $\rho_2$, which is greater than that of our initial fluid, is considered, a similar force-vector diagram can be drawn as in figure 10. The resulting force-intensity vectors are shown for two fluids in the hydrodynamic case (fig. 11). Note that, for an isotropic porous medium, the denser fluid sinks relative to the less dense fluid.

Equation 3 can be written for each of the two fluids. Because the pressure field experienced by both fluids is the same, the force-intensity vector for fluid 2 then can be expressed in terms of that for fluid 1.

$$\boldsymbol{E}_2 = \boldsymbol{g} + \left(\frac{\rho_1}{\rho_2}\right)[\boldsymbol{E}_1 - \boldsymbol{g}] \tag{5}$$

A vector diagram (fig. 12) is useful to visualize this equation.

At a given point in space, the force per unit mass acting on fluid 2 depends on the density of fluid 2 and the force per unit mass that would act on fluid 1 if it were at that location. When $\boldsymbol{E}_1$ is neither zero nor vertical, $\boldsymbol{E}_2$ will be tilted from vertical in the direction of the horizontal component of $\boldsymbol{E}_1$. Fluid 2 will move in the same horizontal direction as fluid 1 but in a downward vertical direction relative to fluid 1.

If fluid 1 is freshwater and fluid 2 is saline water of a given density, the defining equation 1 for the force-

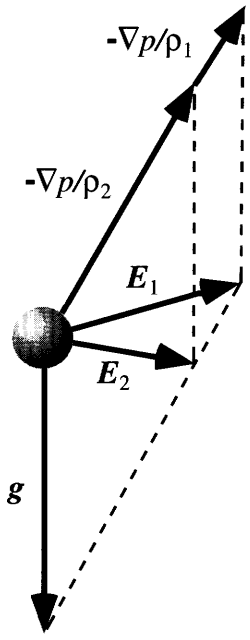


**Figure 11.** Force-intensity vectors for two fluids of different density acted upon by the same pressure and gravitational fields.

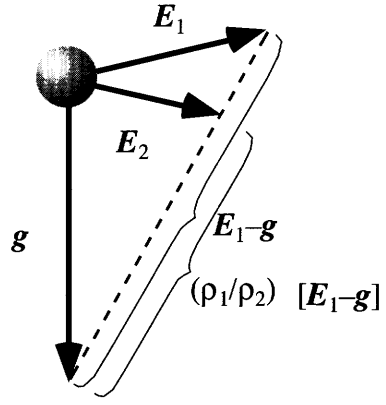


**Figure 12.** Forces acting on an element of fluid 1 and on an element of fluid 2 under hydrodynamic conditions.

intensity vector is substituted into equation 5, and a potentiometric head is defined as

$$h = \left(\frac{p}{\rho g}\right) + z \qquad (6)$$

then equation 7 relates the potentiometric head values for the two fluids.

$$h_1 = \frac{\rho_2}{\rho_1} h_2 - \frac{\rho_2 - \rho_1}{\rho_1} z \qquad (7)$$

This equation gives the equivalent freshwater head as a function of the in-place saline-water head. Note that the altitude of the measurement point must be known to make the conversion. The heads are the heights above datum that each of the two fluids would rise in a manometer installed at the measurement point.

By combining equations 3 and 6, an equation giving the force on a parcel of water as a function of potentiometric head is obtained as

$$\boldsymbol{E} = -g\nabla h \qquad (8)$$

Similarly, equations 5 and 7 can be combined to express the force on a parcel of saline water as a function of the potentiometric-head gradient for a parcel of freshwater. That is,

$$\boldsymbol{E}_2 = -g\frac{\rho_1}{\rho_2}\left[\nabla h_1 + \frac{\rho_2 - \rho_1}{\rho_1}\nabla z\right] \qquad (9)$$

The component of $\boldsymbol{E}_2$ in the vertical direction can be given by

$$\boldsymbol{E}_{2z} = -g\frac{\rho_1}{\rho_2}\left[\frac{\partial h_1}{\partial z} + \frac{\rho_2 - \rho_1}{\rho_1}\hat{e}_z\right] \qquad (10)$$

where

$\hat{e}_z$ is the unit vector in the vertical direction (-).

For simplicity, if an isotropic medium with equal viscosity of the fresh and saline water is assumed, Darcy's Law combined with equation 7 gives the velocity of the saline water as a function of the equivalent freshwater head.

$$v_2 = -\frac{k\rho_1 g}{\varepsilon\mu}\left[\nabla h_1 + \frac{\rho_2 - \rho_1}{\rho_1}\nabla z\right] \qquad (11)$$

where

$v_2$ is the interstitial velocity of the fluid ($L/T$);
$k$ is the permeability ($L^2$);
$\varepsilon$ is porosity (-); and
$\mu$ is the fluid viscosity ($F/L^2$ -$T$).

The vector diagram of equation 11 (fig. 13) shows that although the gradient of the equivalent freshwater-head field provides the horizontal orientation of the interstitial velocity vector, there is a vertical

component dependent on the density difference. This is why gradients of any given head field based upon any chosen reference density will not give the correct direction of flow. Because of the density variation from the reference value, the vertical component of the flow vector must be included to obtain the correct flow-velocity vector.

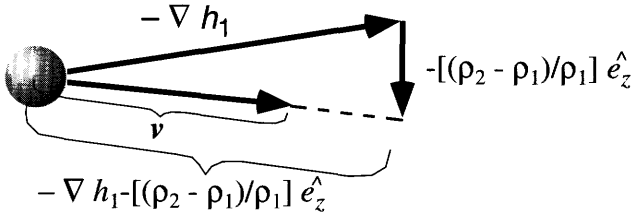


**Figure 13.** Interstitial velocity vector and the freshwater head and density-difference components.

Similar to the force-intensity vector, the component of the velocity vector in the vertical direction $z$ is given by

$$v_z = -\frac{k\rho_1 g}{\varepsilon\mu}\left[\frac{\partial h_1}{\partial z} + \frac{\rho_2 - \rho_1}{\rho_1}\hat{e_z}\right] \qquad (12)$$

where

$v_z$ is the vertical interstitial velocity of the fluid ($L/T$).

In a variable-density ground-water flow system, ground-water flow causes changes in the solute-concentration field, which also results in changes to the density field. This causes the ground-water flow field to change with time. The only practical way to account for the coupling between the ground-water flow field and the solute-concentration field is by use of numerical simulation. Evaluation of a ground-water system based on analysis of an approximate constant-density model will lead to erroneous flow rates and directions at locations where the driving forces, as a result of buoyancy effects, are large relative to the driving forces that result from hydraulic gradients based on a homogeneous fluid.

## Shallow-Brine Aquifer

The shallow-brine aquifer in the Bonneville Salt Flats has been defined by Turk (1973, p. 8) and Lines (1979, p. 65) as comprising a halite and gypsum crust that is surrounded by near-surface carbonate mud to a depth of 15-25 ft. Most of the brine withdrawn for potash production is derived from the shallow-brine aquifer. Precipitation of halite from evaporating brine sustains the salt crust that provides the racing surface. For these reasons, the water and salt budgets for the shallow-brine aquifer were examined in more detail than those of the other aquifers in the Bonneville Salt Flats.

The carbonate mud of the shallow-brine aquifer is composed primarily of aragonite, calcite, dolomite, quartz, feldspar, and clay. X-ray diffraction techniques were used to determine mineral composition of core samples. The most abundant clay minerals are the smectites, which expand as a result of hydration when in contact with water. The remaining clays are illites, which are non-expanding when in contact with water. Individual halite and gypsum crystals can occur within the carbonate mud at some locations where surface ponding readily occurs, and the infiltrating brine results in halite and gypsum crystallization under evaporating conditions. In the upper part of the carbonate mud, interbedded layers of oolitic sand are present. These layers vary in thickness and lateral extent and have the ability to transmit large amounts of brine, depending on the degree of connection between layers.

In areas of thick salt crust, the upper few inches are generally composed of tightly compacted crystalline halite. Ridges of soft, crystalline halite develop over fractures in the hard surface salt during the summer months when brine comes to the surface and evaporates. Beneath the hard, near-surface crust, halite crystals are large and well formed with little or no cohesion between the crystals. The large crystals are the result of slow growth in a stable environment. This zone in the halite crust is very porous and has the ability to readily transmit brine. Gypsum and insoluble clays may be interspersed throughout the halite crust. During winter months when extensive surface ponds are present, such as the winter of 1992-93, several inches of the upper halite crust can dissolve. Generally, the gypsum and insoluble clays concentrate on the submerged surface of the halite crust. In the summer months when evaporation occurs, halite precipitates over the gypsum and clay. Thus, depending on the history of salt dissolution and precipitation, the halite crust might contain thin, stratified layers of gypsum and insoluble clays. Beneath the halite crust, a gypsum layer generally separates the halite crust from the carbonate mud. This layer varies in thickness and in some

locations is difficult to distinguish from the loose halite and the underlying carbonate mud.

North of Interstate Highway 80, the salt crust on the Bonneville Salt Flats has a lense-shaped cross section in an east-west direction. On the margins, a thin crust of gypsum generally is present. This crust might be covered with clay, silt-sized material, or halite, if winter ponds cover the area and subsequently precipitate halite upon evaporation.

Vertical fractures in the carbonate mud can be seen readily along the exposed sides of brine-collection ditches. These fractures are assumed to be present throughout much of the shallow-brine aquifer. The fractures can be up to an inch wide, and the spacing between fractures is variable with 1 ft a common interval (Turk and others, 1973, p. 69). This report states that the fractures might have a hexagonal pattern in map view and probably coincide with the hexagonal pattern of the fractures on the surface of the salt crust. These fractures are probably the principal conduits by which brine is transmitted in the shallow-brine aquifer.

### Aquifer Properties

The transmissive properties of an aquifer generally depend on the type of porous material it contains, and can vary considerably throughout the aquifer. The porous material in the shallow-brine aquifer of the Bonneville Salt Flats varies from very transmissive crystalline halite and gypsum in the salt crust to poorly transmissive carbonate mud underlying the salt crust. Fractures and interbedded layers of oolitic sand within the carbonate mud, however, can result in areas of larger horizontal and vertical transmissivity, depending on the degree of connection between these fractures and oolitic sand layers.

During a period of several years, numerous aquifer tests were completed to determine the transmissive properties of the shallow-brine aquifer in the Bonneville Salt Flats. The first tests were completed in 1960 by personnel at the Utah State University Engineering Experiment Station, in cooperation with the Utah Department of Transportation, to determine aquifer properties in the area designated for construction of Interstate Highway 80 so that appropriate methods of construction could be determined. Twelve of the reported transmissivity values are included in a report by Turk (1973, table 9, fig. 13). About 70 aquifer tests were completed by personnel of Kaiser Aluminum Corporation and L. J. Turk during 1965-67, and the results are reported by Turk (1973, table 9). Lines completed four aquifer tests to determine the aquifer properties of the carbonate mud by excluding the influence of the very transmissive salt crust. The results of these tests, and those that Turk rated as "good" or better, were incorporated into the transmissivity map of Lines (1979, fig. 33). Lines (1979, p. 67) stated further that the transmissivity map was based on the results of aquifer tests that were completed during a 12-year period and therefore, transmissivity values mapped in some areas might not accurately represent those areas in 1976. Because no new aquifer tests were completed during this study with which to compare previous tests, Lines' statement is assumed to be true for this study.

The use of 2-in. casing in the shallow monitoring wells completed during this study precludes the use of any aquifer-test analysis that imposes a stress to the aquifer by pumping. Falling-head or slug tests easily could have been done, but the results would not be representative of the aquifer if the borehole did not intersect any fractures.

Turk (1973, p. 9) reported that transmissivity values increased from less than 100 $ft^2/d$ at the margin of the salt crust to more than 13,000 $ft^2/d$ near the center of the salt crust. The highest transmissivity value was determined for an area south of Interstate Highway 80, outside of the present study area. Transmissivity values reported by Turk that lie within the present study area generally do not exceed 5,000 $ft^2/d$. Turk noticed that the transmissivity values increased from the margin to the center of the salt crust, with the highest values coinciding with the highest concentrations of potassium and magnesium and the thickest part of the salt crust. He attributed the high transmissivity values to the permeable salt crust, fractures within the underlying carbonate mud, and thin layers of oolitic sand. In areas where the salt crust is thickest, transmissivity values are high because the permeable salt crust makes up a larger part of the shallow-brine aquifer.

Lines (1979, table 5) reported the results of four aquifer tests that were designed to stress the carbonate mud so that the effects in the overlying salt crust could be evaluated. Transmissivity values determined from these tests ranged from 490 to 8,100 $ft^2/d$ (Lines, 1979, p. 67). Data collected during the tests show that the salt crust and underlying carbonate mud are hydraulically connected and that the vertical hydraulic-conductivity values for the aquifer range from 30 to 140 ft/d (Lines, 1973, p. 70).

The porosity of the carbonate mud of the shallow-brine aquifer on the Bonneville Salt Flats has been

reported in previous studies for the mineral company. Turk (1969, p. 104) reported that porosity averaged 45 percent as determined from numerous wet and dry bulk-density measurements. This value fits into the normal range for clay of 40 to 70 percent (Freeze and Cherry, 1979, p. 37). During sample collection for this estimate, any fractures, if present, would not have been preserved. The estimate, therefore, is representative of only the intergranular pore spaces (primary porosity) and not the fractures (secondary porosity), which are the principal avenues for flow in the shallow-brine aquifer. Effective porosity, which is the amount of interconnected pore space or fractures available for fluid transmission, could not be determined accurately. Effective porosity derived from fractures, such as in fractured crystalline rock, is generally several orders of magnitude smaller than effective porosity derived from intragranular pore spaces (Domenico and Schwartz, 1990, p. 26). In the shallow-brine aquifer, however, with its large fracture apertures and relatively dense fracture spacing along with the porous salt crust and oolitic sand layers, effective porosity is probably in the same order of magnitude as the primary porosity value mentioned above.

An average specific-yield value of about 10 percent was reported by Turk and others (1973, p. 69). This estimate was derived from tests measuring gravity drainage of brine from saturated material obtained from the shallow-brine aquifer. Like the porosity estimate mentioned previously, if samples for the tests measuring specific yield did not include any fractures, then the estimate for specific yield might not be representative of the shallow-brine aquifer.

Values for storage coefficient determined from the results of aquifer tests in the shallow-brine aquifer varied from $1.2 \times 10^{-1}$ to $4 \times 10^{-5}$ (Turk, 1973, table 9). These values are indicative of both unconfined and confined conditions. Of the 22 storage-coefficient values reported by Turk, only 10 are representative of wells located in the present study area. Similar storage-coefficient values were determined from four aquifer tests completed by Lines (1979, p. 68) and ranged from $3.8 \times 10^{-3}$ to $4.1 \times 10^{-4}$. These values are indicative of semi-confined and confined conditions. Aquifer tests completed by Lines were designed to exclude pumping from the salt crust and, therefore, are representative of the carbonate mud.

Lines (1979, p. 70) attributed the larger storage-coefficient values reported by Turk to the large amount of brine pumped from the salt crust where the aquifer is under unconfined conditions and to flow in fractures and through the oolitic sand. Confined conditions are more prevalent where the salt crust is absent, fractures are less frequent, and the oolitic sand is absent. These conditions exist where shallow monitoring wells were hand augured along the north line of wells between the salt crust and the brine-collection ditch (fig. 3). The near-surface, carbonate-mud deposits were hard and dry. Brine encountered 2 to 3 ft below land surface rose in the borehole to within a few inches of the surface.

### Water-Level Fluctuation, Potentiometric Surface, and Ground-Water Movement

Water levels in wells fluctuate seasonally throughout the shallow-brine aquifer on the Bonneville Salt Flats as a result of variations in evaporation at the playa surface, precipitation on the playa surface, and brine withdrawal for mineral production. Water-level fluctuations in well (B-1-17)31acc-1, located at the center of the salt crust, are shown in figure 14. The overall water-level trend during late spring through early fall is downward with sharp variations that are the result of periods of very high temperatures and high evaporation or, conversely, intense thunderstorms. Water levels rose abruptly during October and November in both 1991 and 1992; the rise in October 1993 was not as abrupt. These rises were probably the result of drastically reduced evaporation that resulted from cooler temperatures combined with more precipitation. Data are insufficient to determine whether these rises can be attributed solely to decreased evaporation.

Temperature and specific gravity of the brine in each well casing were measured at the time of water-level measurement. From these data, density at 20°C was calculated. All water-level measurements were converted to a potentiometric head by using a reference density and equation 7 as described in the "Principles of Variable-Density Ground-Water Flow" section of this report. The reference density was the average density for the particular set of measurements. Instead of using the base of the shallow-brine aquifer to calculate the height of the water column in each well as was done by Lines (1979, p. 72), the altitude of the midpoint of the screened or perforated interval was used. This altitude was assumed to represent the measurement location for the water level. If the screened or perforated interval was unknown as for the wells completed by Turk (1969), the altitude of the midpoint of the drilled depth was used.

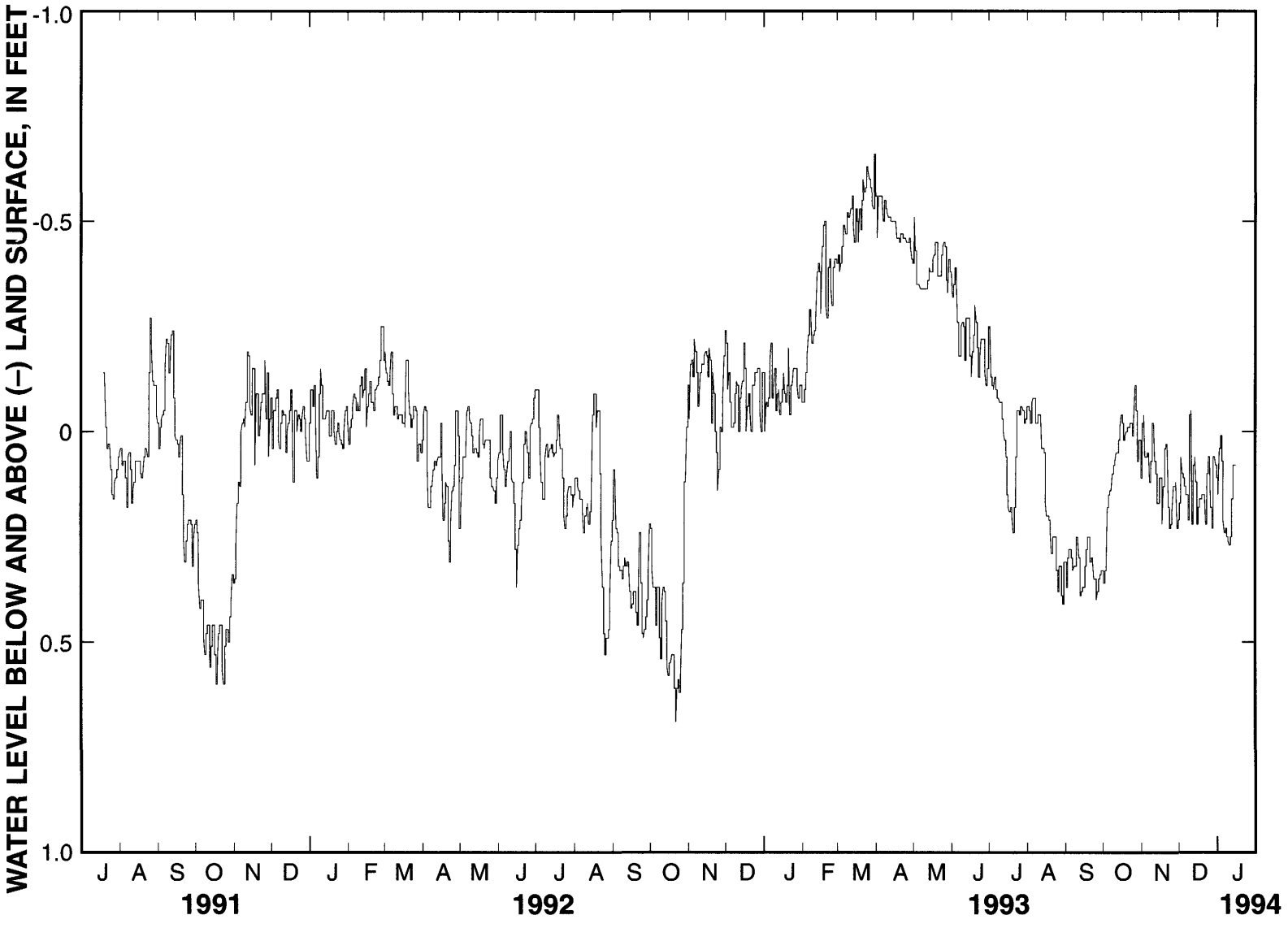


**Figure 14.** Water-level fluctuations in well (B-1-17)31acc-1, located near the center of the salt crust, Bonneville Salt Flats, Utah.

Average brine density was used as the reference density in equation 9 to minimize the magnitude of the gravitational term. This means that $\rho_2 - \rho_1$ was small throughout most of the region, and directions of ground-water flow are closely approximated using only the gradient of the reference potentiometric head. In addition, the areal potentiometric maps are based on projected head data from various elevations in the aquifer. Flow directions interpreted from these maps are correct for the horizontal components only. The maps provide no vertical flow information. In the shallow-brine aquifer, vertical flow components were calculated to be negligible at the few locations where vertical profiles of head and density data were obtained.

About 60 percent of the wells were completed in the upper third of the aquifer, 40 percent in the middle third, and only two wells in the lower third. The screened-interval length ranged from 2.5 ft to about 25 ft, with only a few wells having the smallest interval. Thus, it was not possible to obtain areally distributed data that would quantify any density profiles in the shallow-brine aquifer.

The potentiometric surface with respect to an average reference density of 1.171 g/cm$^3$ for the shallow-brine aquifer, shown in figure 15, was derived from water levels measured at the end of September 1992. This potentiometric surface is representative of conditions near the end of the evaporation season, after most of the brine has been withdrawn through the ditches. The general configuration and altitude of the contours are very similar to those mapped by Lines (1979, fig. 35) for the same time of year. This comparison indicates that there is no long-term change in transient storage in the shallow-brine aquifer. With no long-term change in storage, the shallow-brine aquifer appears to be in a fluid steady state despite seasonal and yearly fluctuations in fluid inflows and outflows.

The horizontal direction of ground-water movement is from a higher to a lower reference potential as described in the "Principles of variable-density ground-water flow" section of this report. At the end of the summer evaporation and brine-production season, the horizontal component of brine movement in the shallow-brine aquifer is from the ground-water divide, located along the approximate axis of the salt crust, to the northwestern margin of the playa, and to the brine-collection ditches on the east and south. The horizontal hydraulic gradient in the area of the salt crust and to the north is small. The horizontal hydraulic gradient toward the northwestern margin of the playa and toward the brine-collection ditches, in contrast, becomes relatively large near these boundaries as shown by the closeness of the contours (fig. 15).

The potentiometric surface with respect to an average reference density of 1.162 g/cm$^3$ for the shallow-brine aquifer in April 1993 (fig. 16) has a different configuration than it did in September 1992. The slightly lower average reference density is indicative of the infiltration of less-dense recharge water. Slight gradients toward the northwestern margin of the playa and the brine-collection ditch south of Interstate Highway 80 are discernible. Noticeable inflow is from the southeast. Much of the center of the playa has a flat potentiometric surface, resulting from the extensive surface ponding and lack of withdrawal at the brine-collection ditch east of the salt-crust area.

Because of the wet conditions on the playa in the summer of 1993 and the preceding winter months, the configuration of the potentiometric surface with respect to an average reference density of 1.161 g/cm$^3$ in October 1993 is not the same as in September 1992 (fig. 17). The influence of the brine-collection ditches is clearly visible, but water levels throughout the remainder of the playa are much higher. This indicates that less evaporation from the shallow-brine aquifer occurred during the summer of 1993. Similarly, the lower average reference density also is indicative of less evaporation.

Where a playa is part of a regional ground-water flow system, the playa generally is the terminus of that flow system. At the terminus, ground water converges from all directions, and the general direction of flow is upward where it discharges at the surface and evaporates. Because the Bonneville Salt Flats is the topographic low within the Great Salt Lake Desert, this salt-crust area probably represents the terminus for ground-water flow for this region. As suggested by Harrill and others (1988, sheet 2), the Great Salt Lake Desert and, ultimately, the Bonneville Salt Flats, is the terminus for regional ground-water flow from adjacent basins to the south and southwest. With the natural ground-water flow direction toward the basin fill beneath the Bonneville Salt Flats, ground-water movement should be upward from the basin-fill aquifer into the shallow-brine aquifer.

Water-level and density measurements from adjacent wells that were completed in the shallow-brine aquifer and the underlying lacustrine sediment of the upper basin-fill aquifer at five locations (fig. 3) were examined to determine vertical ground-water flow

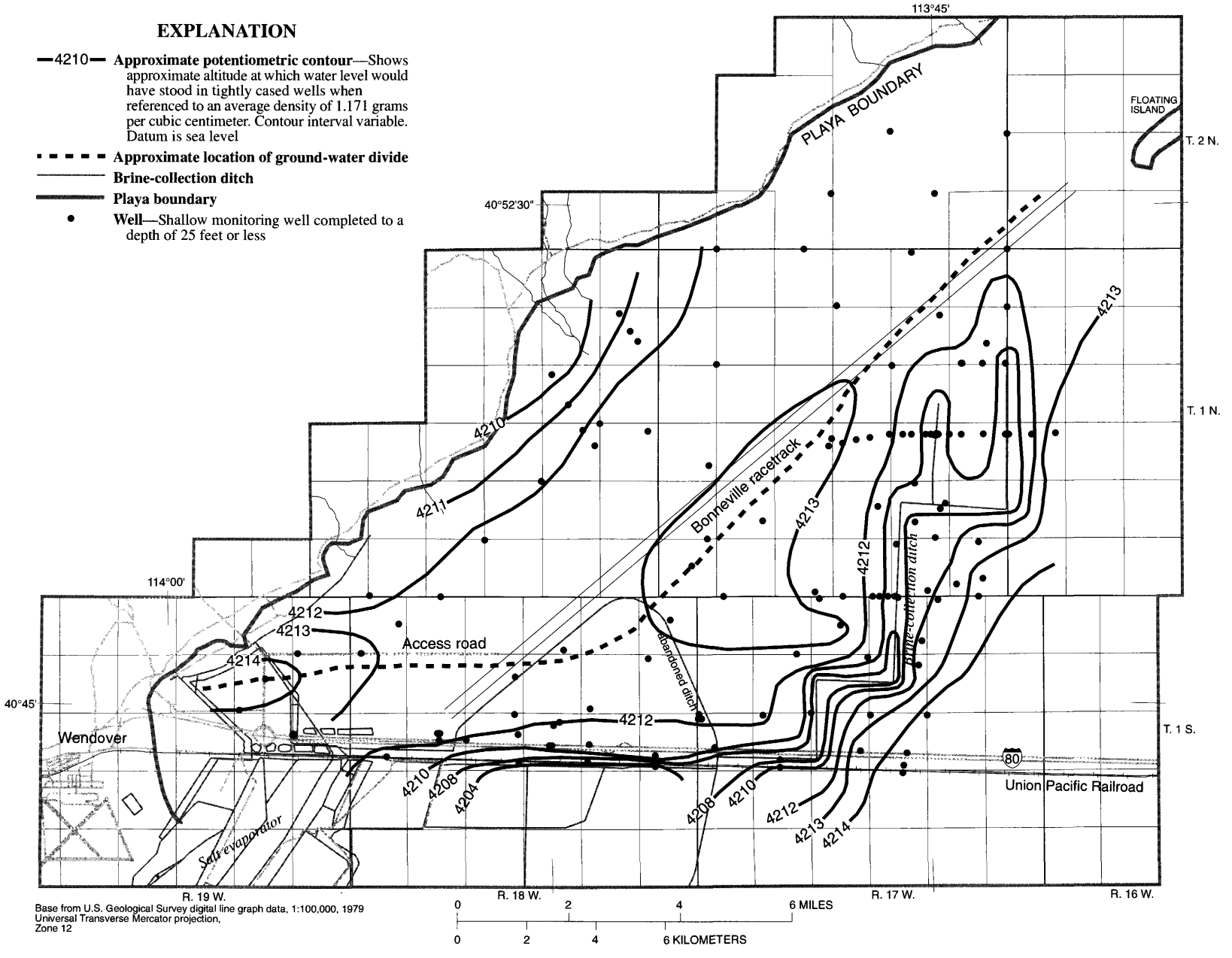


**Figure 15.** Approximate potentiometric surface, referenced to an average density, in the shallow-brine aquifer of the Bonneville Salt Flats, Utah, September 1992.

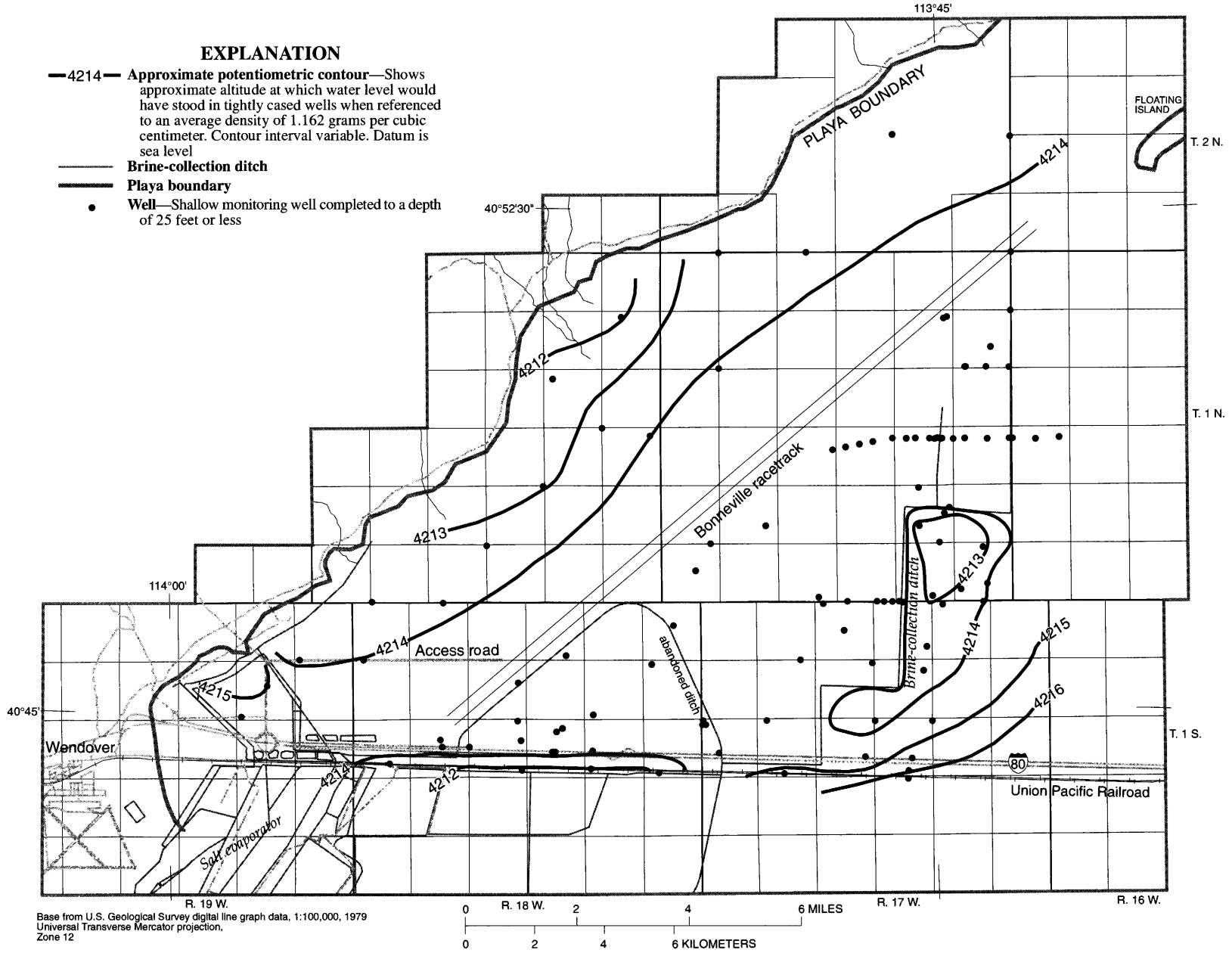


**Figure 16.** Approximate potentiometric surface, referenced to an average density, in the shallow-brine aquifer of the Bonneville Salt Flats, Utah, April 1993.

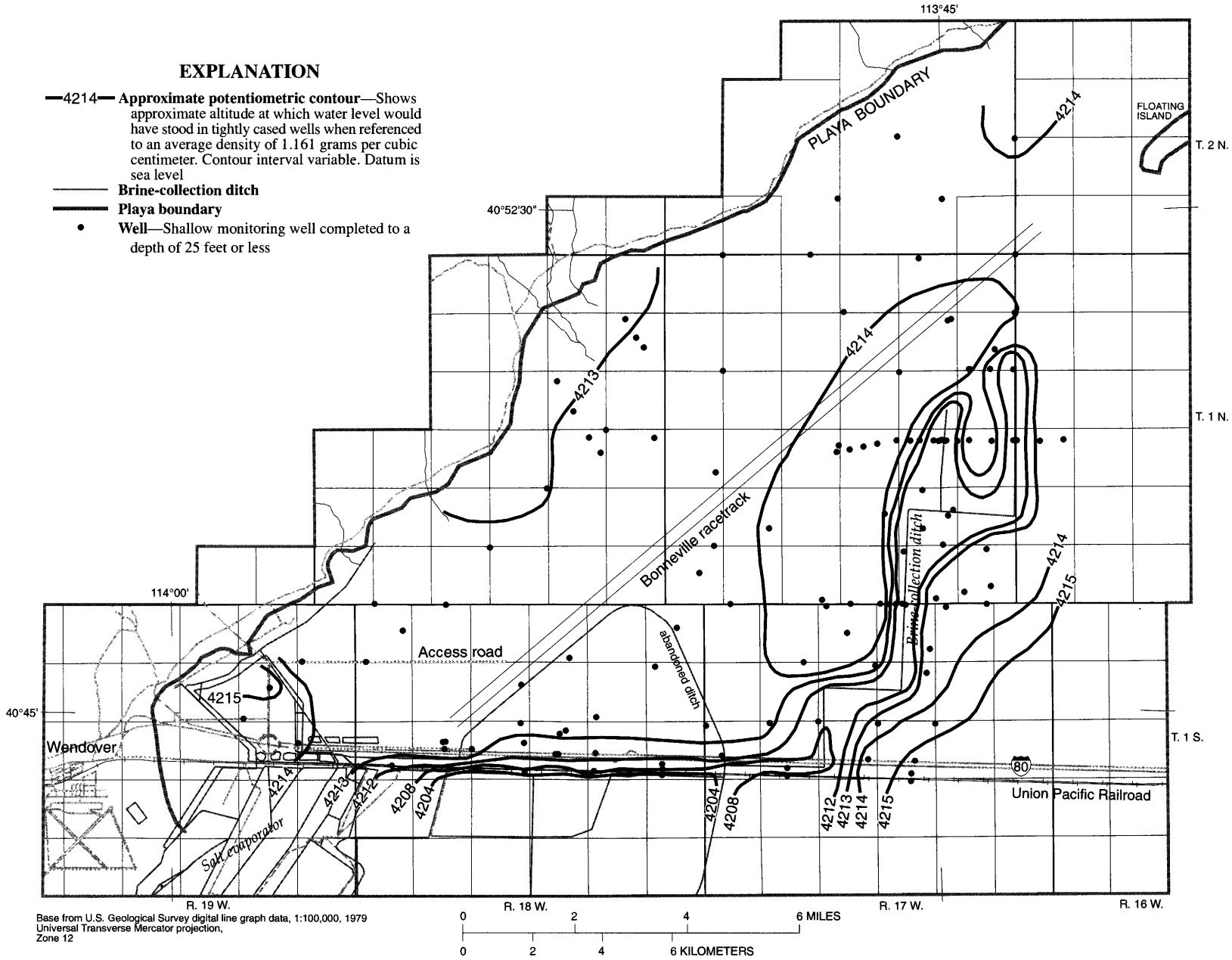


**Figure 17.** Approximate potentiometric surface, referenced to an average density, in the shallow-brine aquifer of the Bonneville Salt Flats, Utah, October 1993.

between the two aquifers. The reference heads were determined by converting the measured water levels to freshwater equivalent heads. The total vertical driving force is then calculated by adding the gradient of reference head with the gravitational force as shown by equation 10. The calculated total head gradient is assumed to give the direction of the driving force on a parcel of fluid located midway between the measurement points, even though the distance between the points is rather large. Calculated driving forces from limited data from 1993 show that downward movement might exist during most of that year. If the direction of vertical movement is determined only from the gradient of the reference head, then the direction would be upward. When the gravitational force was added, however, the resultant direction for the total driving force was generally downward in 1993 when conditions on the playa surface were wetter than normal.

When the water level in the brine-collection ditch is lowered during the summer, the water level in well (B-1-17)23abd-1 is lowered sufficiently so that the direction of the total driving force between the brine in this well and in the adjacent well, (B-1-17)23abd-2, completed in the underlying lacustrine sediment of the basin-fill aquifer, is upward. A similar condition occurred near the end of summer when the water level in well (B-1-17)31acc-1 was lowered by evaporation. The direction of the total vertical driving force on a parcel of fluid midway between the measurement point in well (B-1-17)31acc-1, completed in the shallow-brine aquifer, and well (B-1-17)31acc-7, completed in the lacustrine sediment of the basin-fill aquifer, was upward.

The calculated downward movement of brine from the shallow-brine aquifer into the lacustrine sediment of the upper basin-fill aquifer might be a pressure response to the withdrawal of brine from deep wells completed in the conglomerates at depth. Despite water-level measurements that indicate downward movement, additional evidence, presented later in this report, indicates that over the long term there might be considerable upward movement of brine from the lacustrine sediment of the upper basin-fill aquifer into the shallow-brine aquifer, particularly near the center of the salt-crust area.

The sensitivity of the calculated downward total driving force was analyzed with respect to density at the five locations. The calculated total driving force is dependent on both water-level and density measurements. To test for density, water-level measurements for the respective wells were not varied. Generally, the density of the brine in the wells completed in the shallow-brine aquifer would have to decrease by 0.02 to 0.05 g/cm$^3$ and likewise, the density of the brine in wells completed in the lacustrine sediment of the upper basin-fill aquifer would have to increase by 0.02 to 0.05 g/cm$^3$ in order to reverse the driving force. Density measurements of brine from the deeper wells do not vary as much as in the shallower wells. The calculated total driving force, therefore, is unlikely to reverse direction as a result of variability in density from the deeper zone. At times, density measurements of brine in wells completed in the shallow-brine aquifer have changed sufficiently to cause a reversal in the direction of the total driving force, but water-level measurements also have changed and thus canceled the density variation.

### Recharge

Sources of recharge to the shallow-brine aquifer include infiltration of precipitation on the playa surface, horizontal subsurface inflow, and possibly upward leakage from the underlying lacustrine sediment in the upper basin-fill aquifer. Recharge from infiltration of precipitation on the playa surface, which dissolves salt from the crust, is the largest source of recharge. Horizontal subsurface inflow contributes only a small amount of recharge and salt to the shallow-brine aquifer because of low permeabilities and small hydraulic gradients along the eastern and northern boundaries of the study area. Insufficient data were available to quantify upward leakage. Other possible sources of recharge to the shallow-brine aquifer include subsurface inflow from the alluvial fan along the northwestern margin of the playa and surface runoff that reaches the playa from the Silver Island Mountains. Because of the direction of ground-water flow and hydraulic gradients, recharge from these sources is considered to be insignificant compared to recharge from infiltration of precipitation.

From hydrographs of observation wells, Turk (1973, p. 13) suggested that rainfall in excess of 0.05 in. during winter and 0.1 in. during summer contributes to recharge in the area of the thick salt crust. Lines (1979, p. 85) suggested that minimal recharge occurred during winter months because the salt crust is often completely saturated and flooded on the surface. Additional winter precipitation was thought to accumulate at the surface until it evaporated or could infiltrate and replace brine that had moved laterally in the underlying

carbonate mud. Lines estimated recharge through the salt crust for 1976 by comparing precipitation to water-level changes for a monitoring well on the salt crust. Eighteen major recharge events were identified that resulted in a cumulative rise of 3.8 ft during the year. Lines assumed that this recharge occurred over the entire salt crust and that the specific yield of the aquifer was 10 percent, thus resulting in a total recharge of about 9,700 acre-ft.

Turk (1969, p. 146) states that lateral subsurface inflow adds some recharge to the system but is inconsequential compared to recharge from precipitation. Turk (1973) does not mention recharge other than from precipitation on the playa surface. Lines (1979, p. 84-86) stated that almost all recharge was from direct infiltration of precipitation with minor amounts coming from infiltration of runoff from the Silver Island Mountains and from subsurface inflow from beyond the limits of the study area. Lines attributed 40 acre-ft of recharge to subsurface inflow for 1976.

Subsurface lateral inflow is possible only from the east and from the northeast as shown by the potentiometric surfaces (figs. 15 and 17). During other seasons of the year when water levels in the shallow-brine aquifer are higher (fig. 16), hydraulic gradients along the northeastern and eastern margins of the study area were very small. Although water-level data from these margins are sparse, a maximum horizontal hydraulic gradient of 1 ft/mi could be assumed based on water levels measured in September 1992. When this hydraulic gradient was multiplied by a boundary length of 15 mi and a transmissivity value of 500 $ft^2/d$ (Lines, 1979, fig. 33), estimated subsurface lateral inflow was 60 acre-ft during 1992.

Observations during this study indicate that runoff from the Silver Island Mountains contributes to recharge along the northwestern margin of the playa. Although the amount of recharge is unknown, this source probably is not significant. The pH values of brine from several shallow wells along the northwestern margin of the playa are noticeably higher than the pH values of brine from wells that are on the playa or salt crust. This difference indicates that runoff from the Silver Island Mountains either infiltrates the alluvial sediments, similar to the probable recharge mechanism described for the alluvial-fan aquifer, or that it reaches the playa margin before infiltrating. Despite the horizontal hydraulic gradient toward the northwestern margin of the playa, recharge along this margin probably results in decreasing brine density and increasing pH values but probably does not contribute any substantial amount of recharge to the playa.

Recharge during this study was mostly from infiltration of water through the playa surface that resulted from intense thunderstorms during the summer months and rainfall and snowfall during the winter months, and is evident from the potentiometric surfaces as shown (figs. 15, 16, and 17). The location of the ground-water divide at the center of the salt crust during September 1992 (fig. 15) was the result of transient drawdown in the brine-collection ditches and of ground-water flow toward the northwest margin of the playa. Because ground-water flow was away from the center of the salt crust, recharge to this area of the shallow-brine aquifer during the summer months was possible only by direct infiltration from the surface or upward leakage from the underlying lacustrine sediment. As a result of these summer thunderstorms, water levels are increased temporarily, thus increasing evaporation until water levels return to previous levels. Water that has infiltrated into the shallow-brine aquifer from these thunderstorms, therefore, causes only a short-term change in storage that offsets the total amount of water removed by evaporation and seepage to brine-collection ditches.

The potentiometric surface in April 1993 (fig. 16) reflects the influence of recharge during the preceding winter months. Water levels are high throughout the center of the playa; only water levels in the southeastern corner of the study area are higher where the horizontal component of ground-water flow is toward the center of the playa. Along the southern and northwestern boundaries, the horizontal component of ground-water flow was away from the center of the playa. Although less obvious, the higher heads in the center of the playa are the result of infiltration from the playa surface, upward leakage, and possibly a small amount of subsurface inflow from the southeast. The potentiometric surface for August 1993 (fig. 17) also reflects the summer transient drawdown in the brine-collection ditches. The higher water levels in the central part of the playa were the result of infiltration of water on the playa surface from a large thunderstorm and diminished evaporation from the shallow-brine aquifer during the preceding months.

The bulk of recharge to the shallow-brine aquifer probably occurs from late autumn, when evaporation is negligible, to the following spring, when evaporation increases. Actual recharge or, more appropriately, actual change in storage in the shallow-brine aquifer

from any autumn to spring depends on the amount of brine removed through the brine-collection ditches or subsurface outflow, the amount of water removed by evaporation, and the amount of water available for infiltration from precipitation on the playa surface during the winter months.

An estimate for recharge was made by calculating the change in storage for the shallow-brine aquifer from September 1992 to late May 1993. This method for estimating recharge does not differentiate between recharge on the salt crust or carbonate mud, nor does it differentiate between surface and subsurface inflow. Subsurface inflow is assumed to be insignificant compared to infiltration from the playa surface. The change in storage was calculated by subtracting water-level measurements for September from those for May. Some of the May water levels were above land surface, thus indicating a fully saturated aquifer at that location and ponded water at the surface. These water levels were set to land surface for the change in storage calculation; otherwise, water on the surface would have been included. The differences between the two sets of water-level measurements were contoured. The area contoured was delineated by Interstate Highway 80 to the south, the 4,215-ft topographic contour along the northwestern margin of the playa, and an arbitrary north-south line 1 mi east of the easternmost part of the brine-collection ditch, east of the salt crust. This area is about 80 $mi^2$. The contoured volume is calculated to obtain the change in storage. The calculated volume was multiplied by a specific-yield value of 10 percent to obtain the estimated change in storage in the shallow-brine aquifer for September 1992 to the end of May 1993. The change in storage of 8,300 acre-ft was assumed to be equal to total recharge for that period. Most of this recharge probably occurs in the beginning of the 9-month period during which the two sets of water-level measurements were taken.

An areally averaged recharge rate of 0.16 ft/yr for this period was calculated by dividing the recharge, 8,300 acre-ft, by the area, 80 $mi^2$, about 30 $mi^2$ less than the area used by Lines. If average recharge is assumed to occur throughout the larger area, then total recharge would be 11,300 acre-ft. This is comparable to the 11,700 acre-ft estimated by Lines (1979, p. 85). Lines attributed 9,700 acre-ft to infiltration through the salt crust and 2,000 acre-ft to infiltration through the carbonate mud.

Infiltration of surface brine that is depleted in most chemical constituents other than sodium and chloride and the lack of evaporation during the winter months results in the dilution of the brine in the shallow-brine aquifer with respect to many chemical constituents, most notably magnesium and potassium. Recharge can be estimated by calculating the quantity of infiltrating brine necessary to dilute potassium concentrations in brine from wells sampled in the late summer of 1992 and June 1993. The mass-balance equation used to describe the mixing that occurred and to make the recharge estimates is

$$C_1Q_1 + C_2Q_2 = C_3(Q_1 + Q_2) \qquad (13)$$

where

$C_1$ is the concentration in August 1992 (mg/L);
$Q_1$ is the initial volume of brine with concentration
$C_1$ ($ft^3$);
$C_2$ is the concentration of infiltrating fluid in January 1993 (mg/L);
$Q_2$ is the volume of infiltrating fluid ($ft^3$); and
$C_3$ is the resultant concentration in June 1993 (mg/L).

Because the unknown is the volume of infiltrating fluid, the equation is rearranged to solve for $Q_2$:

$$Q_2 = Q_1(C_3\text{-}C_1)/(C_2\text{-}C_3) \qquad (14)$$

The initial volume of brine containing concentration $C_1$ was assumed to be the volume of fluid in a saturated column of aquifer material surrounding each well. This volume is calculated by multiplying the length of the column of water in each well, based on September 1992 water-level measurements, by 1 $ft^2$ representing the area of the surrounding aquifer material, and by a specific yield of 10 percent. This volume is substituted into equation 13 along with the appropriate concentrations (Mason and others, 1995, table 4) to determine the amount of fluid necessary for the measured dilution of potassium.

Within this method, estimates for recharge ranged from 0.01 to 1.6 ft for the 14 wells that show a dilution in potassium concentration. If the three extreme values are disregarded, the remaining 11 values range from 0.12 to 0.5 ft, with a median value of 0.25 ft, which equates to 12,800 acre-ft of recharge in 80 $mi^2$. This agrees favorably with the average value of 0.16 ft, 8,300 acre-ft, determined by the method that uses the change in storage of the shallow-brine aquifer. Recharge, therefore, ranged from 8,300 to 12,800 acre-ft for 1992. Both methods assume a specific yield of 10 percent in the shallow-brine aquifer. A larger value for

specific yield, which is quite possible, would increase both estimates accordingly.

Infiltration of brine from the winter surface pond is a dynamic process that is difficult to quantify. Data used in the estimates mentioned previously are localized, instantaneous measurements and might not reflect the constantly changing nature of the system. Water levels used in the estimate for change in storage might not represent the absolute minimum or maximum values. Similarly, chemical data from both sampling periods might not be representative of maximum and minimum potassium concentrations. Furthermore, the potassium concentration assumed to represent the infiltrating fluid (surface-pond sample, January 1993) might not be representative of the potassium concentration throughout the entire pond at the time of sampling or during the entire period in which most of the infiltration occurs.

### Discharge

Primary sources of discharge from the shallow-brine aquifer include evaporation from the playa surface, withdrawal from the brine-collection ditches, and lateral and vertical subsurface outflow. Evaporation, withdrawal from the brine-collection ditch located east of the salt crust, and subsurface outflow to the south are the largest sources of discharge; the last two components are the most controllable from a management perspective.

Evaporation generally is the largest source of discharge on any playa and is very difficult to quantify. Any estimated rate of evaporation determined at a specific site and then applied to the entire playa surface might result in substantial error if that rate is not truly representative of all types of surfaces on the playa. Evaporation depends on several factors including type of playa surface, depth to ground-water surface, density and temperature of evaporating water, atmospheric conditions, and solar radiation.

Numerous techniques for estimating evaporation have been developed and applied to playa surfaces in the past. Turk (1969, p. 180-196, and 1970, p. 1209-1215) studied the decrease in evaporation from a brine surface resulting from increasing brine density, but he did not correlate these results to evaporation of brine from beneath the playa surface. Lines (1979, p. 86-89) stated that the amount of halite on the playa surface is related directly to the delicate balance between recharge through the surface and discharge through the surface by evaporation. Lines observed that about 0.25 in. of halite built up over the thick salt crust during 1976 following evaporation of the flooded playa surface. This buildup of halite was considered to represent the amount of evaporation of brine from the shallow-brine aquifer (1,800 acre-ft) that exceeded recharge through the thick salt crust (4,900 acre-ft) during the summer months. Lines, therefore, estimated 6,700 acre-ft of brine evaporated from the area of thick salt crust during 1976.

Estimates for evapotranspiration made in earlier studies, or more appropriately evaporation because of the sparsity of vegetation on the Bonneville Salt Flats, were based on water-budget methods or simple meteorological techniques. With the development of sophisticated instrumentation since the previous studies, data that are necessary for evaporation estimates can now be collected using mass-transfer and energy-balance techniques. These techniques measure, either directly or indirectly, the transfer of water from the liquid to gaseous phase and are independent of fluid density. Evaporation is generally referred to in terms of actual and potential evaporation. Actual evaporation is the amount of water evaporated under any given conditions, whereas potential evaporation is the maximum amount of water that could be evaporated if water was given freely to the evaporating surface, such as evaporation from a pond. The Bowen ratio method, which was used to estimate actual evaporation on the Bonneville Salt Flats, is an energy-balance method that is dependent on measurements of temperature and humidity gradients. The Penman method was used to estimate potential evaporation and the Bowen ratio method was used to estimate actual evaporation. An explanation of both methods, the required instrumentation, and its application in Pilot Valley are presented in Malek and others (1990).

Much of the playa surface of the Bonneville Salt Flats remains flooded during the spring and possibly into the early summer months. Because an overall flow balance for the shallow-brine aquifer is an objective of this report, it is important to distinguish between evaporation from standing water and from playa surfaces. Evaporation from the playa surface would be included as discharge from the shallow-brine aquifer, whereas evaporation from a surface pond would not be included.

Actual and potential evaporation for 1993 and 1994 were determined from data collected at the two weather stations, located on the salt crust and playa margin (figs. 18 and 19). When the large surface pond

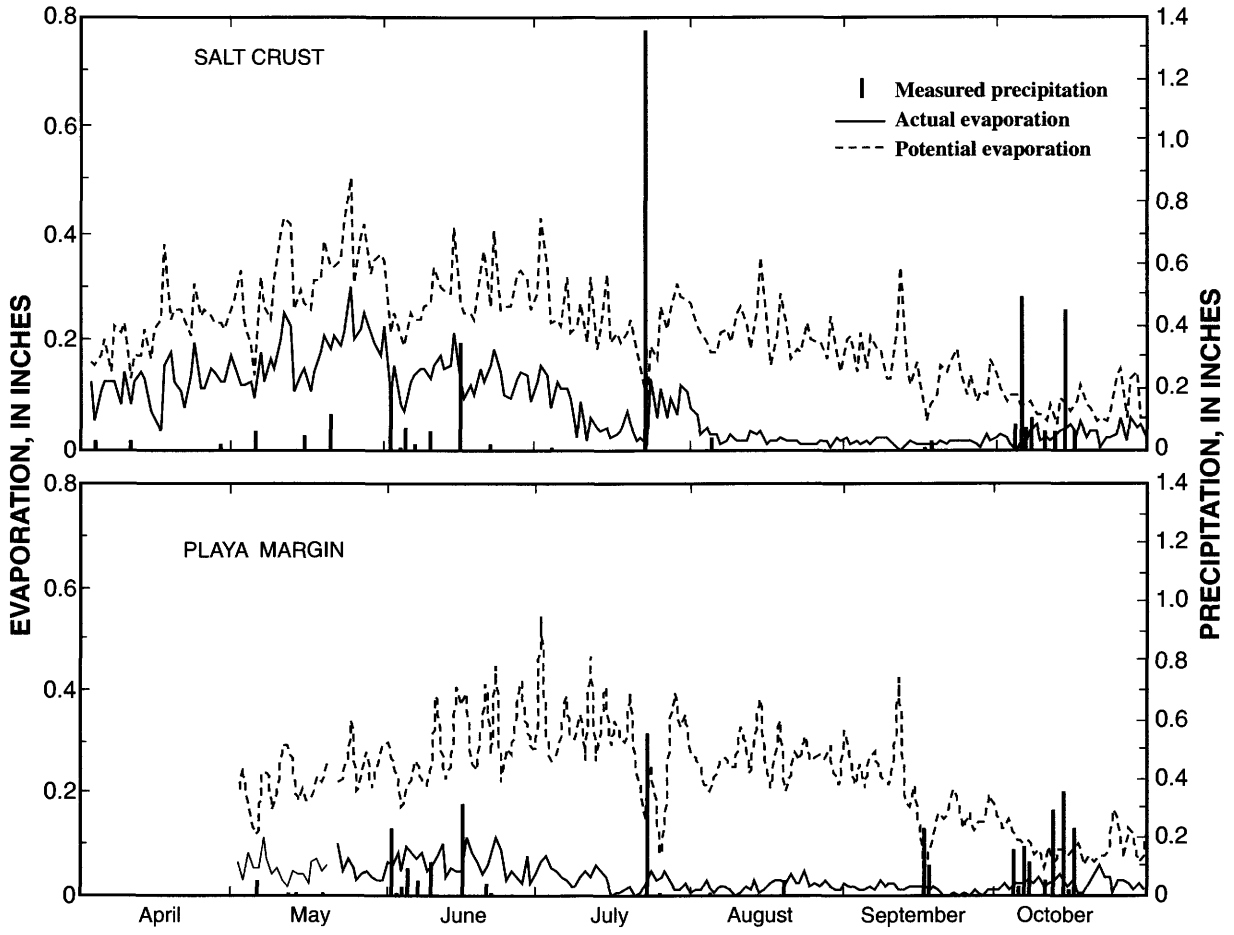


**Figure 18.** Estimated daily evaporation and precipitation for 1993, Bonneville Salt Flats, Utah.

was present through June of 1993, actual evaporation approached the potential evaporation rate at the station on the salt crust. Actual evaporation from a water surface is higher than from a bare land surface as can be seen by the difference in actual evaporation at the salt-crust station compared to the playa-margin station for the same period. Both actual and potential evaporation generally rise after precipitation has fallen on the playa surface (figs. 18 and 19). This is more noticeable in spring and early summer months when water remains on the surface from winter surface ponding or the near-surface material is still nearly saturated.

Total evaporation from the shallow-brine aquifer in the Bonneville Salt Flats was estimated from data collected at the two stations during 1993 and 1994. Estimated total evaporation for both years might be representative of minimum and maximum estimates for evaporation from the Bonneville Salt Flats. During the primary months for evaporation in 1993, monthly mean temperatures at both stations were 2 to 8° F below the 1961-90 normal mean monthly temperature at Wendover. Total precipitation for the same months in 1993 was virtually the same as the total 1961-90 normal monthly precipitation at Wendover. A large, single-day rainfall of more than 1.3 in. measured at the salt-crust station, however, was more than four times the normal monthly precipitation for July. This storm resulted in surface ponding shortly after the extensive surface pond remaining from winter had evaporated. Total evaporation from the shallow-brine aquifer in 1993, therefore, is smaller than in most years. Total evaporation from the shallow-brine aquifer in 1994, in contrast, is probably larger than in most years.

The area of the Bonneville Salt Flats from which total evaporation from the shallow-brine aquifer was estimated is larger than the area used in estimating recharge. Both areas are bounded on the south by Interstate Highway 80 and have the same arbitrary boundary to the east of the brine-collection ditch. The northwest

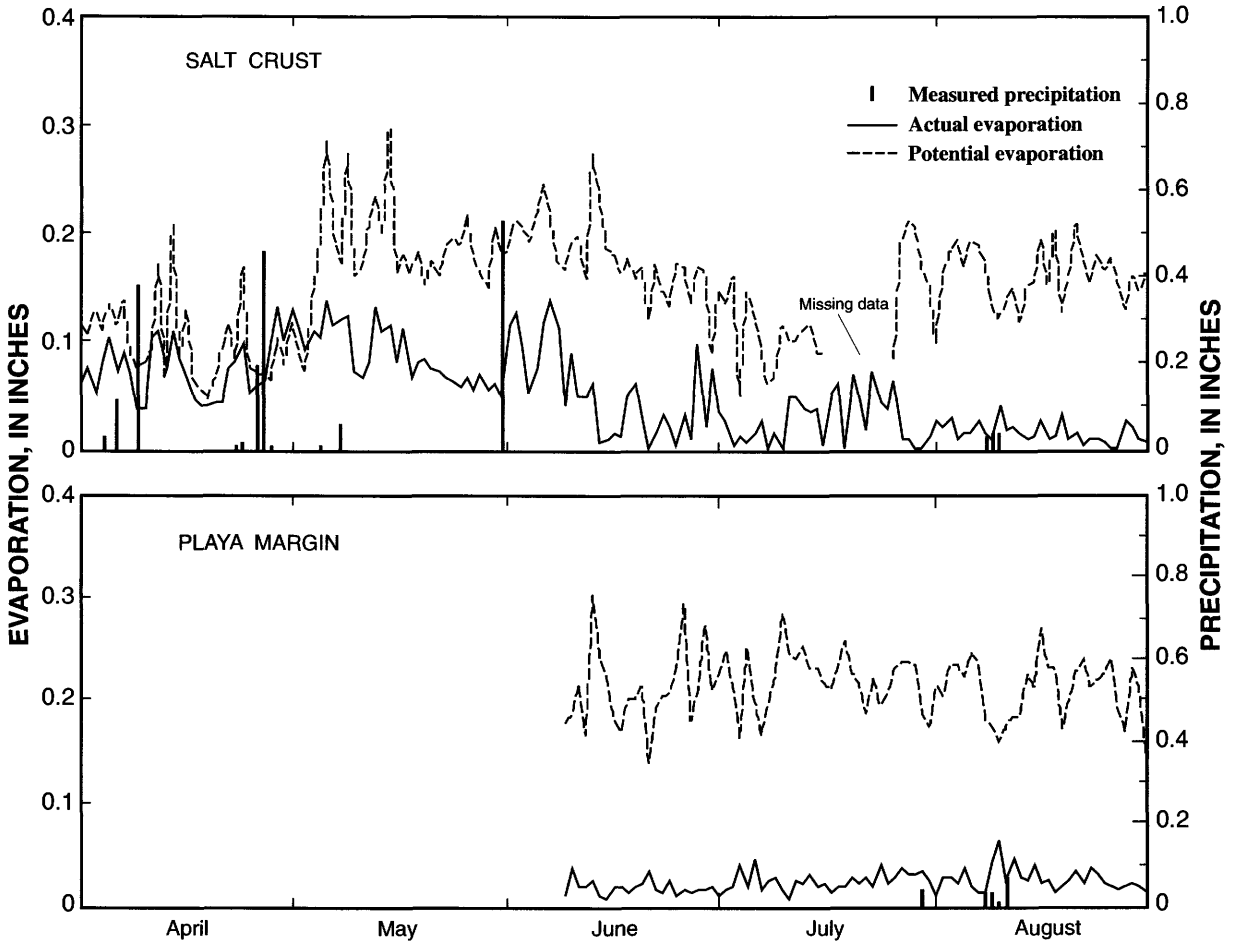


**Figure 19.** Estimated daily evaporation and precipitation for 1994, Bonneville Salt Flats, Utah.

boundary used for delineating evaporation is at the playa margin, whereas the boundary used in estimating recharge was limited to the area of measured seasonal change in storage in the shallow-brine aquifer. The area used for estimating evaporation was about 114 $mi^2$, and the area used for estimating recharge was about 80 $mi^2$. No water-level or chemical data were available to extend the area used in the recharge estimates to coincide with the area used in the evaporation estimate.

Net evaporation from the shallow-brine aquifer for each season was calculated at the two weather stations. The daily mean values for actual evaporation were totaled and total rainfall for the same period of time was subtracted. Evaporation of water on the playa surface from rainfall is subtracted from total evaporation because it is not part of the evaporation from the shallow-brine aquifer. If any rain falling on the playa surface does infiltrate into the subsurface, it is assumed to recirculate to the surface and evaporate in a short period of time. A net actual evaporation rate was then calculated by dividing the total net evaporation by the number of days in which data were collected during each year.

The number of days is critical for calculating a net actual evaporation rate from the shallow-brine aquifer at the salt-crust station. Because actual evaporation is higher when a surface pond is present on the playa surface than when a surface pond is not present, only those days after the surface pond has evaporated should be used in the calculation for total evaporation from the shallow-brine aquifer. Net actual evaporation rates at the salt-crust station for 1993 and 1994 were 0.0006 ft/d and 0.0018 ft/d, respectively. Net actual evaporation rates at the playa-margin station for 1993 and 1994 were 0.0013 ft/d and 0.0017 ft/d, respectively. Net actual evaporation rate for 1993 at the salt-crust station is considerably lower than at the playa-margin station, and both stations have a similar rate for 1994. The large difference in net actual evaporation rates is the result of

the large amount of rainfall on the salt crust in July 1993 (fig. 18) and lower-than-normal temperatures.

Net actual evaporation rates were not adjusted in response to varying depths to water. Net actual evaporation rates were assumed to apply to a uniform depth of water despite the fact that evaporation declines with increasing depth to water. At the salt-crust station, the ground-water level was close to land surface, whereas at the playa-margin station, the ground-water level can be several feet below land surface. In areas where the water beneath the carbonate mud is close to land surface, the evaporation rate from this surface could be much higher than the rate calculated at the playa-margin station. In areas where the depth to water was more than that at the two stations, such as near the brine-collection ditches, actual evaporation would be less than what was estimated. During the evaporation of the surface pond, no upward leakage of brine from the shallow-brine aquifer was assumed. If this movement occurs, estimated total evaporation is less than what actually occurs.

Total evaporation from the shallow-brine aquifer was estimated for each year by applying different net actual evaporation rates to the three different playa surfaces: thick salt, carbonate mud, and thin salt over carbonate mud. The area of thick salt is defined as the area where the salt-crust thickness is more than 1 ft (Steven Brooks, Bureau of Land Management, written commun., 1989). This area is assumed to remain constant for the years in which estimates were made and was calculated to be 34 $mi^2$. Because of the transient nature of thin salt precipitated on carbonate mud, the areas used to represent carbonate mud and thin salt over carbonate mud varied in each year. Carbonate mud and salt crust were delineated from satellite imagery for August 1993. The area of thick salt was subtracted from the total salt-crust area in 1993 to obtain the area of thin salt. The appropriate rates calculated previously were used where thick salt and carbonate mud are present.

In their study of evaporation in Pilot Valley, Utah, Malek, and others (1990, p. 23) suggest that where a thin salt crust is present there is a high resistance to water-vapor transfer; thus, evaporation is less than where a bare mud surface is present. This is especially true when the crust separates from the underlying mud surface upon drying and subsequent shrinkage. Because of the transient distribution of salt along the margins of the crust, a long-term data-collection station could not be established where a perennial layer of thin salt would form. A net actual evaporation rate, therefore, had to be assumed for each year and applied to the area where a thin salt crust was present.

Evaporation from the shallow-brine aquifer in the area of thick salt was estimated by multiplying 34 $mi^2$ by a rate of 0.0006 ft/d for 114 days. This number of days is the length of the evaporation season in which the area of thick salt was not covered by a pond. Evaporation from thick salt in 1993 was estimated to be 1,500 acre-ft. The area for carbonate mud in 1993 was 56 $mi^2$. This area was multiplied by a rate of 0.0013 ft/d for 185 days, the assumed duration of the evaporation season. Evaporation from the carbonate-mud surface was estimated to be 8,600 acre-ft. The area of thin salt was 24 $mi^2$, which was larger than in most years as a result of the extensive surface pond during the preceding winter months. An intermediate net actual evaporation rate of 0.0009 ft/d was assumed for the area of thin salt. This rate was deemed appropriate if rainfall was assumed to be between the amounts measured at the two weather stations. Evaporation from thin salt was estimated to be 2,100 acre-ft during 149 days of evaporation. Total evaporation for 1993 from the shallow-brine aquifer was estimated to be 12,200 acre-ft.

No satellite imagery data for 1994 were obtained; therefore, the area for carbonate mud and thin salt on the playa surface could not be delineated for that period. For the purpose of estimating total evaporation in 1994, the distribution of thin salt in September 1992, obtained from satellite imagery data for that period, was assumed to be more representative of 1994 conditions than the thin-salt distribution in 1993. Much of the thin salt that covered a large area in 1993 probably redissolved during the winter months and coalesced into a smaller salt-crust area by the summer of 1994, thus decreasing the area of thin salt.

The method used to estimate total evaporation from the shallow-brine aquifer in 1994 was the same as that used in 1993. The higher rate derived from data collected at the salt-crust station was used for 138 days of evaporation. Estimated evaporation from thick salt was 5,400 acre-ft. Evaporation from the carbonate-mud surface was calculated for an area of 71 $mi^2$ for 185 days. Evaporation from the carbonate mud was estimated to be 14,300 acre-ft. As mentioned previously, the actual evaporation rate from thin salt overlying the carbonate mud is probably lower than that for carbonate mud. A net actual evaporation rate of 0.0011 ft/d was assumed to be representative for 1994. This rate was multiplied by an area of 9 $mi^2$ for a period of 150

days, which was assumed to be an intermediate number of days for evaporation from thin salt. Evaporation from thin salt was estimated to be 1,000 acre-ft. Total evaporation from the shallow-brine aquifer in 1994 was estimated to be 20,700 acre-ft.

Withdrawal from the brine-collection ditch east of the salt crust is a major form of discharge from the shallow-brine aquifer as shown by the potentiometric contours in figure 16. Withdrawal from the brine-collection ditch was estimated to be about 1,500 acre-ft in 1992 and about 2,500 acre-ft in 1993. About 750 acre-ft of the amount estimated for 1993 were withdrawn during January through March, when more than the usual area of the Bonneville Salt Flats was flooded. Much of the estimated 750 acre-ft, therefore, could have been derived from surface drainage from the extensive surface pond south of Interstate Highway 80, where berms are less prominent, rather than from the shallow-brine aquifer. During 1993, this brine withdrawal from the shallow-brine aquifer probably was more than 1,750 acre-ft. The estimates for brine withdrawal in 1992 and 1993 are considerably more than the 680 acre-ft reported by Lines (1979, table 6).

Brine withdrawal from the brine-collection ditch was estimated by monitoring the pumping station located in the NW1/4, SW1/4, and SE1/4 of section 18, T. 1 S., R. 17 W. (fig. 3). Because of the lack of topographic relief on the Bonneville Salt Flats, canals do not have a natural slope and a head gradient is necessary in order to induce brine to flow to the primary evaporation ponds where the potash extraction process is begun. At the pumping station, the brine is pumped from a lower to a higher altitude, thus creating the artificial gradient. The level from which the brine was pumped was continuously recorded. Instantaneous discharge measurements were made periodically at the pump and correlated to the pumping level. From the relation of pump discharge to pumping level, the continuous record of pumping level, and hours of pump operation, an estimate of brine withdrawal can be obtained.

Lateral subsurface outflow from the shallow-brine aquifer to the south potentially might be another major cause of discharge. Lines (1979, p. 89) estimated that 2,000 acre-ft of brine migrated from the Bonneville Salt Flats north of Interstate Highway 80 to the collection ditch south of the highway in 1976. His estimate was made by using a form of Darcy's Law

$$Q = TiL \qquad (15)$$

where

$Q$ is the ground-water flow ($ft^3/d$);
$T$ is the transmissivity ($ft^2/d$);
$i$ is the horizontal hydraulic gradient (dimensionless);
and
$L$ is the length of cross section (ft).

The two components with the most uncertainty in this equation are transmissivity and horizontal hydraulic gradient. Transmissivity values are determined at specific sites and then extrapolated over a larger area. Similarly, horizontal hydraulic gradient might vary along the length of the cross section being considered. Lines used a transmissivity value of 6,000 $ft^2/d$ that was based on values determined from aquifer tests completed prior to construction of Interstate Highway 80 and an aquifer test completed just north of the highway after construction. Turk (1978, p. 75) has suggested that highway construction probably has reduced the transmissivity of the aquifer material in this area. During the construction, the salt crust was removed along the highway corridor and replaced with fill for a roadbed. Not only was the highly transmissive salt removed, but the use of heavy equipment might have compacted the underlying carbonate mud and thus destroyed much of the fracture permeability of the aquifer. No new aquifer-test data were collected along the Interstate Highway 80 corridor during this study because of possible uncertainty in test results. Pumping of brine in sufficient amounts necessary to obtain measurable effects in appropriately spaced observation wells was questionable. Furthermore, disposal of pumped brine at a sufficient distance necessary to prevent adverse effects in observation wells probably was not possible in this area because of the low topographic relief.

Subsurface outflow to the south was estimated where the hydraulic gradient indicated flow toward a brine-collection ditch located south of Interstate Highway 80. A vertical cross section oriented parallel to the brine-collection ditch was divided into three sections. This division allows the use of a spatial variation in transmissivity and a spatial and temporal variation in hydraulic gradient in the calculation of flow through the cross section. Transmissivity values presented by Lines (1979, fig. 33) were used in the calculations despite the questions presented previously. A hydraulic gradient was determined for each of the three cross sections from water-level data collected during this study and computed potentiometric heads referenced to an average fluid density for each measurement period. The

estimated subsurface outflow to the south for 1992 ranged from 1,800 to 2,300 acre-ft. A range is reported because of the variability in each hydraulic gradient used in the calculations. An estimate was not made for 1993 because the wet condition of the playa and high water levels are not representative of long-term ground-water flow. Any decrease in simulated transmissive properties of the shallow-brine aquifer in this area would decrease the amount of subsurface outflow. Seepage to the brine-collection ditch located south of Interstate Highway 80 is needed to obtain a better understanding of this component of subsurface outflow. Although this measurement would be difficult because of the dimensions of the ditch and the low flow velocity, the uncertainty in the measurement probably would be less than the uncertainty in the estimate given above. Flow in this brine-collection ditch, which is on private property, could not be measured because of its inaccessibility.

Lateral subsurface outflow to the northwest from the shallow-brine aquifer was estimated by Lines (1979, p. 90) to be 70 acre-ft in 1976. Lines made this estimate by using Darcy's Law and an estimated transmissivity value of 500 $ft^2/d$, a value that is representative of the area along the northwestern edge of the salt crust. Lines stated that recharge from precipitation balanced discharge from evaporation along this margin. Seepage from the shallow-brine aquifer toward the northwestern margin of the playa, and possibly to the alluvial-fan aquifer, therefore, was replaced by brine that had migrated through the aquifer from near the ground-water divide (fig. 15). Because the hydraulic gradient is small along this margin of the playa, the amount of subsurface outflow also is small. Water-level data collected during this study indicate that the hydraulic gradient is less than the value used by Lines in his estimate for seepage to the northwest. If the transmissivity value is assumed to be representative of this area, then seepage toward the northwestern margin of the playa was about 40 acre-ft for 1992.

Vertical leakage, upward or downward, between the shallow-brine aquifer and the underlying lacustrine sediment of the basin-fill aquifer had not been examined in any of the previous studies. The vertical-driving-force analysis, presented in the "Water-level fluctuation, potentiometric surface, and ground-water movement" section in this report for the shallow-brine aquifer, was extended to estimate vertical leakage through the bottom of the shallow-brine aquifer. Equation 12, which is described in the "Principles of variable-density ground-water flow" section of this report, was used to calculate the vertical interstitial velocity at five locations where head data were available in both the shallow-brine aquifer and the underlying lacustrine sediment of the basin-fill aquifer. An average vertical interstitial velocity was multiplied by the area where leakage was assumed to occur. The calculated vertical interstitial velocity at wells (B-1-17)23abd-1 and -2 was not included in the estimate for downward leakage because of the local bias from the influence of the ditch. Any estimate of total vertical leakage must be considered to be a crude approximation because of the simplifying assumptions necessary in making the calculations, discussed in the following paragraphs, and extrapolating these calculations over a large areal extent using data that are limited spatially and temporally.

Permeability in the vertical direction used in the calculation for interstitial velocity was the harmonic mean of estimated permeabilities for the shallow-brine aquifer and the underlying lacustrine sediment of the basin-fill aquifer because the vertical direction is generally perpendicular to stratification, and vertical movement will be controlled by the smallest permeability. Permeability for the shallow-brine aquifer at each site was calculated by converting the transmissivity reported by Lines (1979, fig. 33) to hydraulic conductivity and then permeability. Hydraulic conductivity, which was obtained by dividing the transmissivity by the aquifer thickness of 25 ft, was multiplied by viscosity and divided by density of the brine at each site and by the gravity constant. Viscosity was assumed to be equal to 1.4 centipoise for all calculations. No data were available for describing the permeability of the lacustrine sediment of the basin-fill aquifer. Permeability, therefore, was assumed to range from $1.0 \times 10^{-16}$ to $1.0 \times 10^{-14}$ $ft^2$, the upper range for unweathered marine clay and the lower range for silty sand (Freeze and Cherry, 1979, p. 29).

Vertical interstitial velocity was calculated for each set of measurements at the four well sites along the axis of the salt crust. Calculated interstitial velocities in a downward direction range from $3.0 \times 10^{-6}$ to $2.05 \times 10^{-5}$ ft/d when the permeability for the lacustrine sediment of the basin-fill aquifer was assumed to be $1.0 \times 10^{-16}$ $ft^2$. The average downward interstitial velocity is $7.32 \times 10^{-6}$ ft/d. If a permeability of $1.0 \times 10^{-14}$ $ft^2$ is assumed for the lacustrine sediment, the calculated interstitial velocities range from $3.0 \times 10^{-4}$ to $2.05 \times 10^{-3}$ ft/d, with an average velocity of $7.32 \times 10^{-4}$ ft/d. A linear relation clearly exists between assumed perme-

ability of the lacustrine sediment and the calculated interstitial velocities because the smallest permeability value predominates in the calculation of the harmonic mean. Total annual downward leakage was estimated by multiplying the average interstitial velocity by area and 365 days. The area of 34 $mi^2$ for which leakage might occur was assumed to be the area where the salt crust is more than 1 ft thick. Calculated annual leakage ranges from 58 to 5,800 acre-ft in the downward direction. The upper limit is probably too large when compared to other components of inflow and outflow for the shallow-brine aquifer. This is especially apparent when other evidence supporting upward leakage is presented later in the report. The estimated annual downward leakage, therefore, was assumed to range from 58 to 580 acre-ft.

## Alluvial-Fan Aquifer

The alluvial-fan aquifer in the Bonneville Salt Flats is composed of sand and gravel interbedded with the lacustrine sediment that underlies the playa. Specific layers of sand and gravel in the alluvial-fan aquifer gradually become mixed with silt and clay-sized particles as the fans extend into the lacustrine sediment. The alluvial fans generally are connected along the southeastern flank of the Silver Island Mountains. The extent of interbedding into the lacustrine sediment and the degree of connection within the alluvial-fan aquifer as distance increases from the mountains are unknown.

The alluvial-fan aquifer has been tapped by 27 wells that withdraw brackish water. This water is used in the production of potash. Not all the wells are in operation at present. In recent years, only four wells have been used. Drillers' logs, which are available for 12 of these production wells (Stephens, 1974, p. 46-47), indicate that sand and gravel layers compose from 12 to 52 percent of the material penetrated during drilling. This variation occurs in relatively short distances between wells. All wells were drilled about the same distance from the Silver Island Mountains along a line about 3 mi long.

Fourteen monitoring wells, of which 11 were nested in 4 boreholes, were completed during this study along a line perpendicular to the Silver Island Mountains and the playa margin (fig. 3). This line of wells includes an alluvial-fan production well, (B-1-18)31acc-1, that was drilled in 1947. The purposes of these monitoring wells were to analyze the effects of ground-water withdrawal from the alluvial-fan aquifer, monitor the water level in the alluvial-fan aquifer, and obtain water from the alluvial-fan aquifer for chemical analysis.

### Aquifer Properties

Results of aquifer tests at two wells completed in the alluvial-fan aquifer were reported by Turk (1969, p. 67, 1973, p. 3). Transmissivity values ranged from 24,000 to 52,000 $ft^2/d$, and storage-coefficient values ranged from $1.4 \times 10^{-4}$ to $3.4 \times 10^{-4}$. A longer test was completed in 1967. Data from this test indicated that leakage from confining layers yielded a substantial amount of water with time. Transmissivity values determined by using type curves for a leaky aquifer ranged from 21,000 to 55,000 $ft^2/d$. Storage-coefficient values ranged from $2 \times 10^{-4}$ to $5 \times 10^{-4}$. These storage-coefficient values are indicative of confined conditions.

Stephens (1974, p. 18) suggested that the ability of fractures and solution channels in the underlying carbonate rocks to transmit water to the alluvial-fan aquifer might be a contributing factor for these large transmissivity values. Brackish water is readily produced from the production wells completed in the coarse-grained zones of the alluvial-fan aquifer. A pumping rate of more than 1,500 gal/min from a single well is not unusual. Lines (1979, p. 76) attributed the hydraulic gradient from the center of the playa toward the Silver Island Mountains to pumping from the alluvial-fan aquifer. If withdrawal from the alluvial-fan aquifer is the cause of this hydraulic gradient, then the effects of this pumping extend a considerable distance beyond the pumping center to the northeast, along the playa margin (Lines, 1979, fig. 35). This suggests that the underlying carbonate rocks do not readily yield water to the alluvial-fan aquifer, as originally thought.

An aquifer test was done in an attempt to define further the aquifer properties of the alluvial-fan aquifer, determine the distance from the pumped well in which measurable effects could be observed in the lacustrine sediment that separates the shallow-brine and alluvial-fan aquifers, and determine the vertical hydraulic conductivity of the lacustrine sediment where such effects are measured. An unused alluvial-fan production well, well (B-1-18)31acc-1 (identified as FW-20 in earlier reports), was pumped for 72 hours at a rate of 1,500 gal/min. Water levels were measured in 14 monitoring wells prior to the test to determine pre-test trends, during the 72-hour pumping period, and for 72 hours after pumping had ceased.

Analysis of the data indicates that the discharge water in the vicinity of the pumped well had moved rapidly downward through probable fractures in the fine-grained sediment that overlies the coarse-grained material of the alluvial-fan aquifer. The artificial recharge created from the well discharge affected the water levels in two monitoring wells completed in or just above the production zone. Because of the interference from the discharge water, the transmissivity and storage-coefficient values calculated from the data are unreliable. These values, however, are in agreement with those determined from previous tests of the alluvial-fan aquifer. Aquifer properties determined from tests in earlier studies also might not be representative if the discharge water was not drained away from monitoring wells.

Water-level measurements in an adjacent monitoring well, completed in fine-grained lacustrine sediment almost 100 ft above the production zone, were analyzed by using the Neuman-Witherspoon ratio method (Neuman and Witherspoon, 1972). The value for vertical hydraulic conductivity determined from these data is almost five orders of magnitude larger than the value determined by laboratory analysis of a core sample collected during drilling operations. Because the laboratory value for vertical hydraulic conductivity was small and the time required for the water level in adjacent monitoring wells to be affected was short, the probable mechanism for transmitting the discharge water downward is through vertical fractures. Because of the rapid infiltration of discharge water, pumping from the production well was insufficient to affect the water level in the deep monitoring wells toward the playa.

### Water-Level Fluctuation and Ground-Water Movement

Water levels in wells completed in the alluvial-fan aquifer on the margin of the Bonneville Salt Flats were reported to be 10-20 ft above land surface when the production wells were drilled between 1946 and 1949 (Stephens, 1974, p. 44-45). At the end of 1965, Turk (1969, p. 74) reported that water levels had declined to 18-20 ft below land surface. Stephens (1974, p. 16) reported that at least one of the wells was again flowing in 1972. Water levels in two wells also were slightly above land surface in March 1985 (fig. 20). Present pumped water levels are generally more than 20 ft below land surface, and nonpumped water levels measured in the unused production wells northeast of the pumping area remain at about 20 ft below land surface. Long-term water-level fluctuations in the alluvial-fan aquifer are probably the result of the combined effects of reduced withdrawal and increased recharge during years of greater-than-normal precipitation.

Water levels in wells completed in the alluvial-fan aquifer were at or above land surface when the wells were drilled. The potentiometric surface, based on resident densities, sloped toward the playa. Because of continued withdrawal from the alluvial-fan aquifer, water levels have declined below land surface. During the present study, the potentiometric surface appears to be nearly level with the playa.

Water levels were measured in the line of nested monitoring wells, perpendicular to the northwestern margin of the playa (fig. 3). These water levels were converted to heads on the basis of resident densities in each well to determine horizontal and vertical driving forces. The upper monitoring wells in the three nests of wells, farthest from the playa boundary, are completed in the lacustrine sediment of the upper basin-fill aquifer. These wells are included in this discussion because they show effects on water levels that result from pumping from the alluvial-fan aquifer. Water-level measurements for wells at similar depths were referenced to an average density to determine reference potentiometric heads. The vertical driving forces were calculated using equation 10, described in the "Principles of variable-density ground-water flow" section in this report, and water-level and density data from each set of nested wells.

Based on the reference potentiometric head distribution, the direction of horizontal flow from the set of nested wells closest to the Silver Island Mountains, wells (B-1-18)31bda-1, -2, and -3, is toward the salt crust. Horizontal flow in the three sets of nested wells closest to the salt crust, wells (B-1-18)31dac-1, -2, -3, (C-1-18)6abb-1, -2, -3, and (C-1-18)6adc-1 and -2, is toward the Silver Island Mountains.

As would be expected in a recharge area, the calculated vertical driving forces are downward in the set of nested wells closest to the Silver Island Mountains. The calculated vertical driving forces also are mostly downward in the three sets of nested wells closest to the salt crust. The vertical driving force reverses periodically between the upper two wells of the nested set containing wells (B-1-18)31dac-1, -2, and -3. The reversal in the vertical driving force for these wells is the result of a change in density in water in well (B-1-18)31dac-

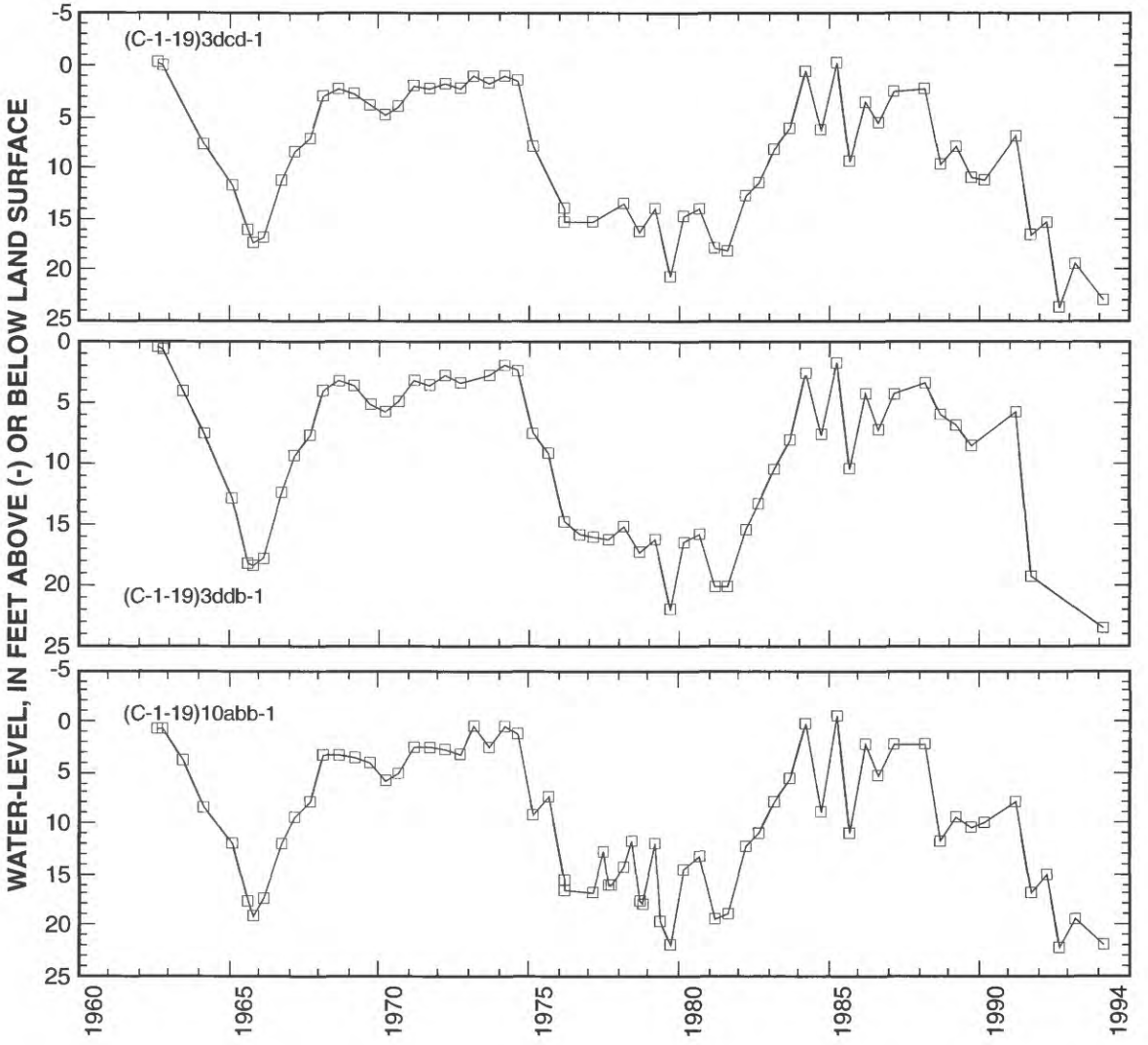


**Figure 20.** Water-level fluctuations in wells completed in the alluvial-fan aquifer, Bonneville Salt Flats, Utah.

2, which is completed at an intermediate depth in relation to the other two wells. The water in this well is more dense than water in either of the other two wells in this nest. Density in water from well (B-1-18)31dac-2 varies from 1.019 to 1.029 g/cm$^3$. Density in water from wells (B-1-18)31dac-1 and -3 was consistently 1.003 g/cm$^3$ (Mason and others, 1995, table 3). When the density of water in well (B-1-18)31dac-2 was about 1.027 g/cm$^3$ or more, the vertical driving force was upward between wells (B-1-18)31dac-1 and -2. The vertical driving force between wells (B-1-18)31dac-2 and -3, however, remains downward.

Sensitivity in the direction of the vertical driving force between wells (C-1-18)6abb-1, -2, and -3 varies with the density of water. The density of water in well (C-1-18)6abb-1 would have to decrease by more than 0.04 g/cm$^3$ to reverse the direction of the vertical driving force between wells (C-1-18)6abb-1 and -2. The density of water in well (C-1-18)6abb-2 would have to increase by more than 0.05 g/cm$^3$ to reverse the direction of the vertical driving force between wells (C-1-18)6abb-1 and -2, whereas a decrease of 0.008 g/cm$^3$ would reverse the direction of the vertical driving force between wells (C-1-18)6abb-2 and -3. The density of water in well (C-1-18)6abb-3 would have to increase by 0.01 g/cm$^3$ to reverse the direction of the vertical driving force between wells (C-1-18)6abb-2 and -3. Density values measured in water from these wells do not vary to this degree (Mason and others, 1995, table

3). The direction of the vertical driving force, therefore, is unlikely to change because of density.

Similar to the wells previously discussed, density of water from wells (C-1-18)6adc-1 and -2 would have to change considerably from measured values (Mason and others, 1995, table 3) to reverse the direction of the vertical driving force. The density of water in well (C-1-18)6adc-1 would have to decrease by more than 0.04 g/cm$^3$ and the density of water in well (C-1-18)6adc-2 would have to increase by more than 0.04 g/cm$^3$.

The horizontal and vertical driving forces toward the production zone of the alluvial-fan aquifer are the result of pumping and the induced drawdown in potentiometric head in the aquifer. Driving forces in the three nests of wells between the production well and the salt crust probably would be mostly toward the salt crust and upward if potentiometric head in the alluvial-fan aquifer were at the pre-development level. Groundwater flow toward the shallow-brine aquifer probably is minimal because of the low permeability of the lacustrine sediment that separates the coarse-grained material of the alluvial-fan aquifer from the shallow-brine aquifer and the small driving force.

### Recharge and Discharge

Probable sources of recharge to the alluvial-fan aquifer include surface runoff from the Silver Island Mountains and subsequent downward infiltration through fractures in the overlying lacustrine sediment, subsurface flow from the consolidated rocks in the Silver Island Mountains, and subsurface flow from the lacustrine sediment along the playa margin. Results of the aquifer tests mentioned in the previous section indicate that surface runoff and subsequent infiltration through fractures probably contributes more to the recharge of the alluvial-fan aquifer than thought previously. From field inspection of the alluvial-fan surface, numerous channels that provide avenues for surface runoff are visible. These channels terminate at pits that are the surface expression of the fractures (fig. 21). No data are available to quantify recharge by seepage through these fractures. If this is the principal form of recharge to the alluvial-fan aquifer, then the amount of recharge could be a large percentage of the precipitation from intense thunderstorms. This type of precipitation is most likely to produce surface runoff.

It is unknown whether this form of recharge to the alluvial-fan aquifer was ongoing prior to groundwater development or whether ground-water development with the declining water levels might have caused the fracturing of the lacustrine sediment. If these fractures had existed prior to development of the aquifer and if these fractures actually reach the coarser material of the alluvial fan, then the areas where the fractures are visible at the surface should have visible evidence of prior spring discharge. Dried organic material is present in one area, thus indicating prior surface discharge.

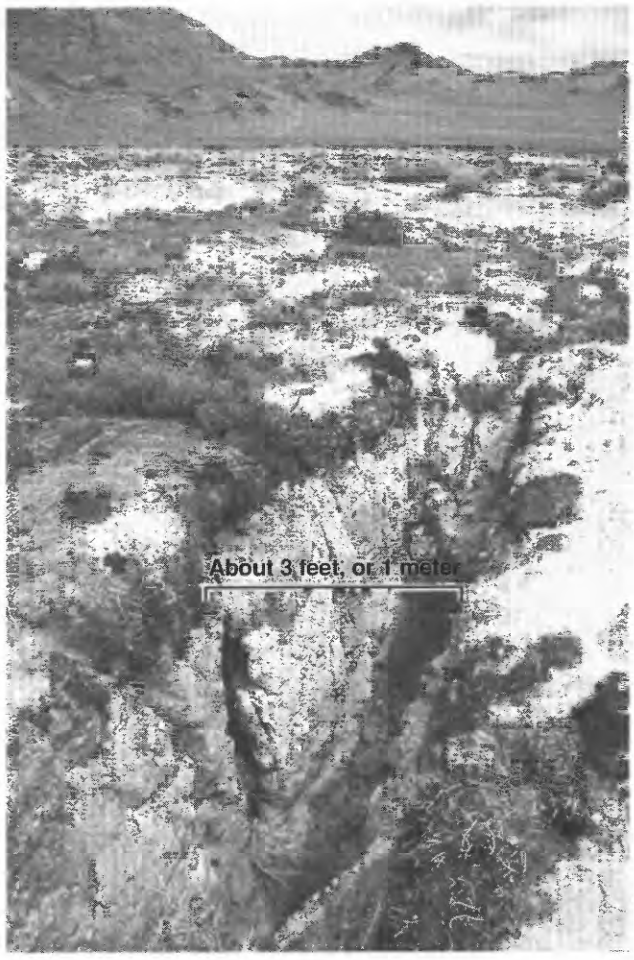


**Figure 21.** Large surface fracture in vegetation zone along northwestern margin of the playa, Bonneville Salt Flats, Utah.

Stephens (1974, p. 10) reported that about 800 acre-ft/yr recharges the alluvial-fan aquifer along the east flank of the Silver Island Mountains adjacent to the Bonneville Salt Flats. This estimate is derived by assuming that 8 percent of the average yearly precipitation that falls on the east flank of the Silver Island Mountains infiltrates into the consolidated rock and alluvium and eventually reaches the alluvial-fan aquifer. Turk (1973, p. 4) did not quantify recharge to the

alluvial-fan aquifer, but did suggest that small amounts of rainfall on the Silver Island Mountains preclude abundant recharge from precipitation. Turk suggested that other sources of recharge include lateral leakage of brine from the lacustrine sediment or upward leakage from Paleozoic carbonate rocks. Turk (1969, p. 76 and 1973, p. 4) cited increased dissolved-solids concentration as evidence to support leakage of brine from the lacustrine sediment. Elevated water temperature also was cited by Turk (1973, p. 4) as evidence to support upward leakage from a depth of 1,000 to 2,000 ft.

Stephens (1974, p. 19) estimated discharge by evapotranspiration from phreatophytes to be about 1,200 acre-ft/yr. Lines (1979, p. 63) reported that 800 acre-ft/yr of water was discharged by pumping. These two forms of discharge result in a considerable imbalance in the estimated inflows and outflows for the alluvial-fan aquifer. Lines suggested that the deficit between recharge and discharge was compensated by water being removed from storage in the aquifer and confining layers, leakage of brine from the lacustrine sediment resulting from the reversal of the hydraulic gradient, and by upward leakage from Paleozoic rocks. Although no data are available to quantify leakage from each source, Lines suggested that total leakage is less than the 800 acre-ft/yr of withdrawal.

Recent discharge from the alluvial-fan aquifer by pumping probably is much more than the 800 acre-ft/yr reported by Lines (1979, p. 63). Limited data collected during 1991-92 indicate that the present rate of withdrawal might be a few thousand acre-ft/yr. With discharge probably much more than previously reported and water levels not substantially lower than those of 30 years ago, recharge to the alluvial-fan aquifer must be larger than the 800 acre-ft/yr previously estimated (Stephens, 1974, table 3).

## Basin-Fill Aquifer

The basin-fill aquifer of the Bonneville Salt Flats has been defined in previous investigations as the conglomerate that overlies Tertiary-age volcanic rocks or pre-Tertiary-age rocks (Lines, 1979, p. 57). More than 800 ft of conglomerate has been logged during drilling of some deep brine wells used by the mineral company. The brine that is withdrawn by these deep wells is used mostly in ditches surrounding the evaporation ponds. A higher head is maintained in these ditches than in the evaporation ponds, which minimizes seepage losses of the valuable brine from the ponds (Turk, 1973, p. 5). A thick sequence of lacustrine sediment separates the shallow-brine aquifer from the conglomerate. Drillers' logs for the deep brine wells indicate that about 900 ft of mostly clay exists between the shallow-brine aquifer and the conglomerate of the lower part of the basin-fill aquifer (Turk, 1973, appendix B).

Few data are available that describe the hydrologic properties of conglomerate in the lower part of the basin-fill aquifer of the Bonneville Salt Flats. Most of the data available has been collected by the mineral company in the area south of Interstate Highway 80 and has been reported by Turk (1969 and 1973). More recent data, such as water levels and pumping rates, were not available. Data collected during this study from monitoring wells completed in the lacustrine sediment of the upper basin-fill aquifer are from a limited number of sites and are not necessarily representative of the lacustrine sediment in the upper basin-fill aquifer throughout the Bonneville Salt Flats.

### Aquifer Properties

The transmissivity of the conglomerate in the lower part of the basin-fill aquifer of the Bonneville Salt Flats has been determined from pumping data in the deep brine wells operated by the mineral company to average about 13,400 $ft^2/d$, and the storage coefficient is about $4 \times 10^{-4}$ (Stephens, 1974, p. 21). These values were provided by personnel of the mineral company. Turk (1969, p. 93) had suggested that the most likely range for transmissivity is 2,000 to 8,000 $ft^2/d$ and for storage coefficient is $2 \times 10^{-3}$ to $2 \times 10^{-4}$. A regional gravity survey by Cook and others (1964, pl. 1) indicates that the area where the deep brine wells are located coincides with the deepest part of the basin; therefore, thickness and transmissivity might not be as great in other parts of the basin.

During this study, monitoring wells were completed in the lacustrine sediment of the upper basin-fill aquifer in the Bonneville Salt Flats. No fracturing or layers of oolitic sand were encountered during drilling of completed wells. Cores were collected at depths from 48 to 63 ft at two locations on the Bonneville Salt Flats. The cores appear to be composed of blue-green clay that varied from being very stiff and dry to very plastic with interstitial fluid. No tests were done to estimate the permeability of the lacustrine sediment. For a discussion of assumed permeability, see "Discharge" section of the "Shallow-brine aquifer" section of this report, presented earlier. Samples from the cores were analyzed by x-ray diffraction techniques. The mineral-

ogic composition of the lacustrine sediment consists of clay, quartz, halite, aragonite, calcite, dolomite, and feldspar.

The upper monitoring wells in the three sets of nested wells, between the playa boundary and the salt crust, also were completed in lacustrine sediment of the upper part of the basin-fill aquifer. Because of the proximity to alluvial-fan deposits, the lacustrine sediment might have layers of slightly coarser material intermixed with the clay. In this area, the hydraulic properties of these deposits might be greater than those of the lacustrine sediment beneath the salt crust.

### Water-Level Fluctuation and Ground-Water Movement

Water-level data are lacking from wells completed in the conglomerate of the lower part of the basin-fill aquifer. Turk (1973, p. 8) reported that the water level in a deep well was about 25 ft below land surface in 1948. Measurements in two deep wells during 1966-67 varied from 44 to 50 ft below land surface (Turk, 1973, table 7). This change in water level equates to an average decline of about 1 ft/yr for that period of time. Lines (1979, p. 58) reported that water levels affected by pumping in nearby wells were lowered as much as 80 ft below land surface in 1976. Because of the limited water-level data, the potentiometric surface of the lower part of the basin-fill aquifer cannot be determined.

Water-level data are limited spatially for wells completed in the lacustrine sediment of the upper part of the basin-fill aquifer. Water levels were measured in wells (B-1-17)11aac-2, (B-1-17)21add-4, (B-1-17)23abd-2, (B-1-17)31acc-7, and (C-1-18)9adc-2, which are all completed to depths of 63 ft below land surface (Mason and others, 1995, table 3). The lowest water levels were measured in well (B-1-17)23abd-2, located adjacent to the brine-collection ditch. These data indicate that there is a horizontal gradient within the lacustrine sediment in the upper part of the basin-fill aquifer, from the salt crust toward the east. Data are insufficient to determine whether this direction of ground-water movement has been induced by withdrawals from the brine-collection ditch. Water levels in wells (B-1-17)11aac-2 and (B-1-17)21add-4, located near the northern end of the salt crust, are higher than those in wells (B-1-17)31acc-7 and (C-1-18)9adc-2, located near the center and southern end of the salt crust. These data indicate that the direction of ground-water movement within the lacustrine sediment beneath the shallow-brine aquifer is from the north toward the south, beneath the center of the salt crust.

Water levels were measured in nested wells, (B-1-17)31acc-4, -5, -6, and -7, located near the center of the salt crust. These wells were completed to depths of 63 to 495 ft below land surface, all within the lacustrine sediment of the upper basin-fill aquifer. These data were used to calculate the total driving force between wells for each measurement period. Although the calculated total driving force was small for each set of measurements, it was always downward. Because the Bonneville Salt Flats is the terminus for ground-water flow for most of the Great Salt Lake Desert, and probably the terminus for regional ground-water flow, ground-water movement within the basin-fill aquifer should be upward under undisturbed conditions.

### Recharge and Discharge

Possible sources of recharge to the conglomerate in the lower part of the basin-fill aquifer of the Bonneville Salt Flats include the alluvial-fan aquifer on the western margin of the playa and consolidated rock at depth as part of a much larger regional ground-water flow system. If ground-water withdrawals from the alluvial-fan aquifer were to increase, some of the water that might have been available for recharge to the lower part of the basin-fill aquifer could be intercepted. This would result in lower water levels in the basin-fill aquifer. The thick sequence and low permeability of the lacustrine sediment in the upper part of the basin-fill aquifer probably prohibits any substantial downward leakage from the overlying shallow-brine aquifer, even though the driving force is downward.

Discharge from the conglomerate in the lower part of the basin-fill aquifer is by pumping from deep brine wells and by upward leakage into the thick sequence of lacustrine sediment. Stephens (1974, p. 22) estimated that about 2,900 acre-ft/yr were withdrawn from October 1969 to September 1972. No data were available to estimate the present rate of withdrawal. Data also are insufficient to estimate any possible upward leakage.

Because of continued withdrawal from the alluvial-fan aquifer, ground water within the lacustrine sediment of the upper part of the basin-fill aquifer along the northwestern margin probably migrates into the alluvial-fan aquifer as discussed previously. Another form of discharge might be upward leakage into the shallow-brine aquifer.

## Brine Chemistry and Implications for Ground-Water Flow

The brine chemistry of the Bonneville Salt Flats is a consequence of the desiccation of ancient Lake Bonneville. The Bonneville Salt Flats subsequently became the natural terminus for ground-water discharge of much of the lake's area. The presence of the salt crust is an indicator of ground-water discharge by evaporation under these natural ground-water flow conditions. Under these conditions, the dissolved-solids concentration in the shallow-brine aquifer increases toward the salt crust where the brine comes to the surface and evaporates. Natural ground-water flow toward the salt crust on the Bonneville Salt Flats has been intercepted in recent decades as a result of anthropogenic causes as explained in previous sections of this report.

### Major Ion Chemistry

The brine chemistry of the shallow-brine aquifer in the Bonneville Salt Flats probably has not changed substantially since the Lines (1979) study. The dissolved-solids concentration of brine in the shallow-brine aquifer in the Bonneville Salt Flats ranges from about 65,000 mg/L along the northwestern margin of the playa to more than 325,000 mg/L in the salt-crust area (Mason and others, 1995, table 4). Dissolved-solids concentration in the Bonneville Salt Flats during 1992 (fig. 22) is virtually the same as that reported by Lines (1979, fig. 43). The ground-water flow regime in the shallow-brine aquifer has been changed because of brine withdrawal for mineral extraction. For the dissolved-solids concentration to remain unchanged, the concentration must be maintained by the dissolution of salt crust, upward leakage from the underlying lacustrine sediment of the upper part of the basin-fill aquifer, or a combination of both.

Because of the hydraulic gradient toward the northwestern margin of the Bonneville Salt Flats, Lines (1979, p. 91) suggested that the dissolved-solids concentration gradually increases with time along this margin. Data collected during this study, which included specific-gravity measurements and chemical analyses of brine from wells, indicate that seasonal influxes of more dilute recharge water from the east flank of the Silver Island Mountains have masked the proposed increase in dissolved-solids concentration. The pH in brine collected from shallow wells along the northwestern margin is consistently higher than in brine from wells closer to the salt crust. This suggests mixing of water from another source. The dissolved-solids concentration in the brine from some wells along the northwest margin decreased from the summer of 1992 to the spring of 1993 (Mason and others, 1995, table 3). This slight freshening of the brine can occur periodically when precipitation is sufficient to allow infiltration before evaporation.

Potassium concentrations in brine from wells completed in the shallow-brine aquifer (fig. 23) have a distribution similar to that reported by Lines (1979, fig. 46), with the highest concentrations in the general vicinity of the salt crust. Potassium and magnesium remain in solution because the density at which potassium chloride and magnesium chloride precipitate cannot be reached until sodium chloride has precipitated. The concentration of the potassium and magnesium cations becomes diluted as a result of infiltration of fresher water after a large thunderstorm during the summer months or rain and snow during the winter months when evaporation is minimal. The sodium chloride concentration, however, is maintained by dissolution of the salt crust. Because of dilution of some ions by the infiltration of fresher water, brine samples to be used for comparative purposes over a period of years must be collected during the same time each year. Lines collected samples during September 1976; the samples whose potassium concentrations are shown in figure 23 were collected during August and September 1992. Both data sets are representative of late summer conditions in which the potassium concentration probably has reached its maximum after several weeks of evaporation from the playa surface.

Prior to mineral development, the highest concentrations of potassium and magnesium coincided with the terminus of ground-water flow, generally in the center of the playa where topography is lowest, natural discharge is by evaporation, and the salt crust is thickest. This area coincides with the central part of the playa north of Interstate Highway 80 for about 2 mi and south of the highway for about 5 mi. Lines (1979, p. 91) suggested that brine withdrawal from the shallow-brine aquifer for mineral production has affected the areal distribution of potassium and magnesium in solution in the central part of the area just north of Interstate Highway 80 and along part of the brine-collection ditch east of the salt crust. The areas, depleted in potassium, remain evident (fig. 23). The percentage of potassium chloride by weight just north of Interstate Highway 80, however, is larger than the value shown by Lines (1979,

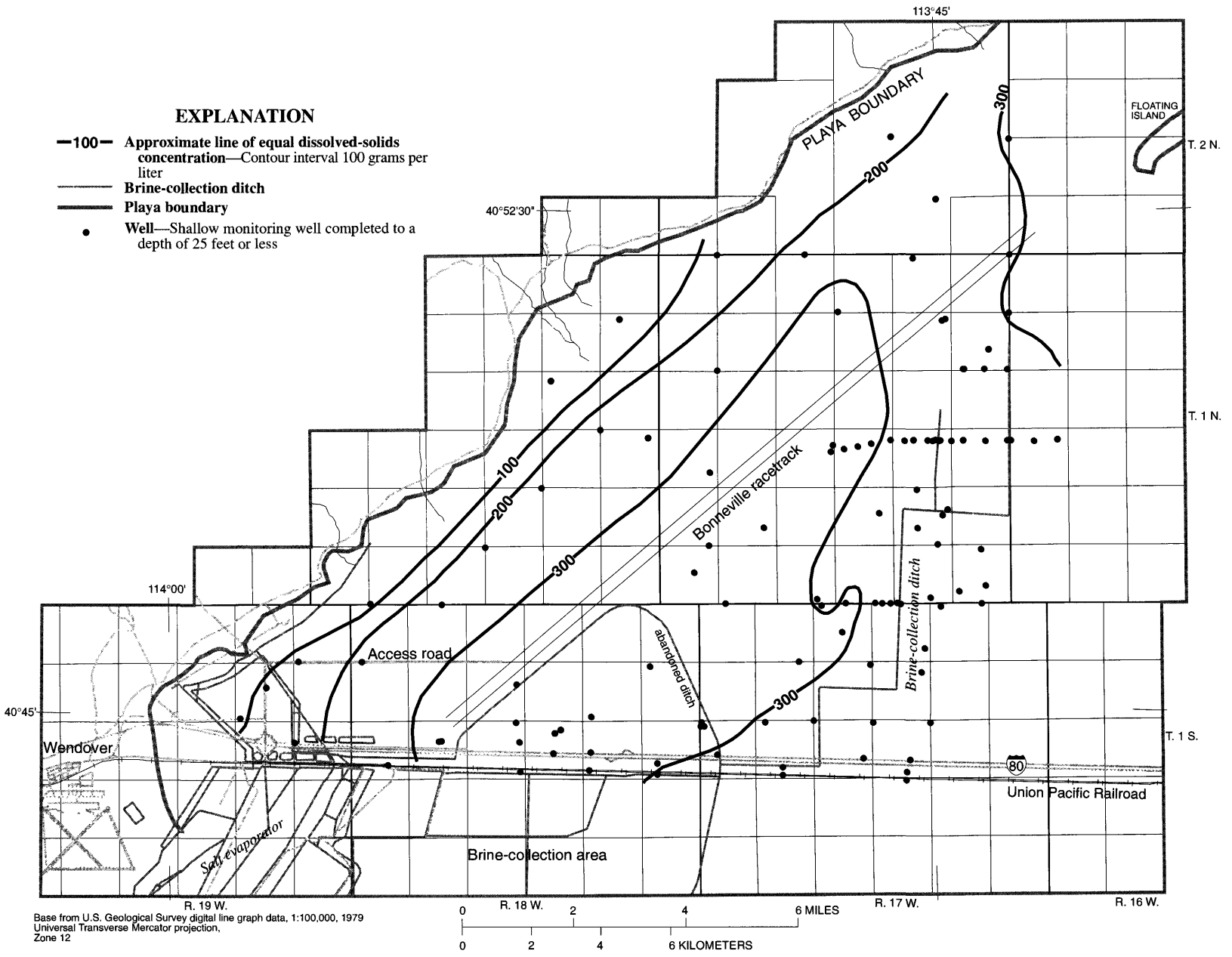


**Figure 22.** Dissolved-solids concentration in brine from the shallow-brine aquifer, Bonneville Salt Flats, Utah, September 1992.

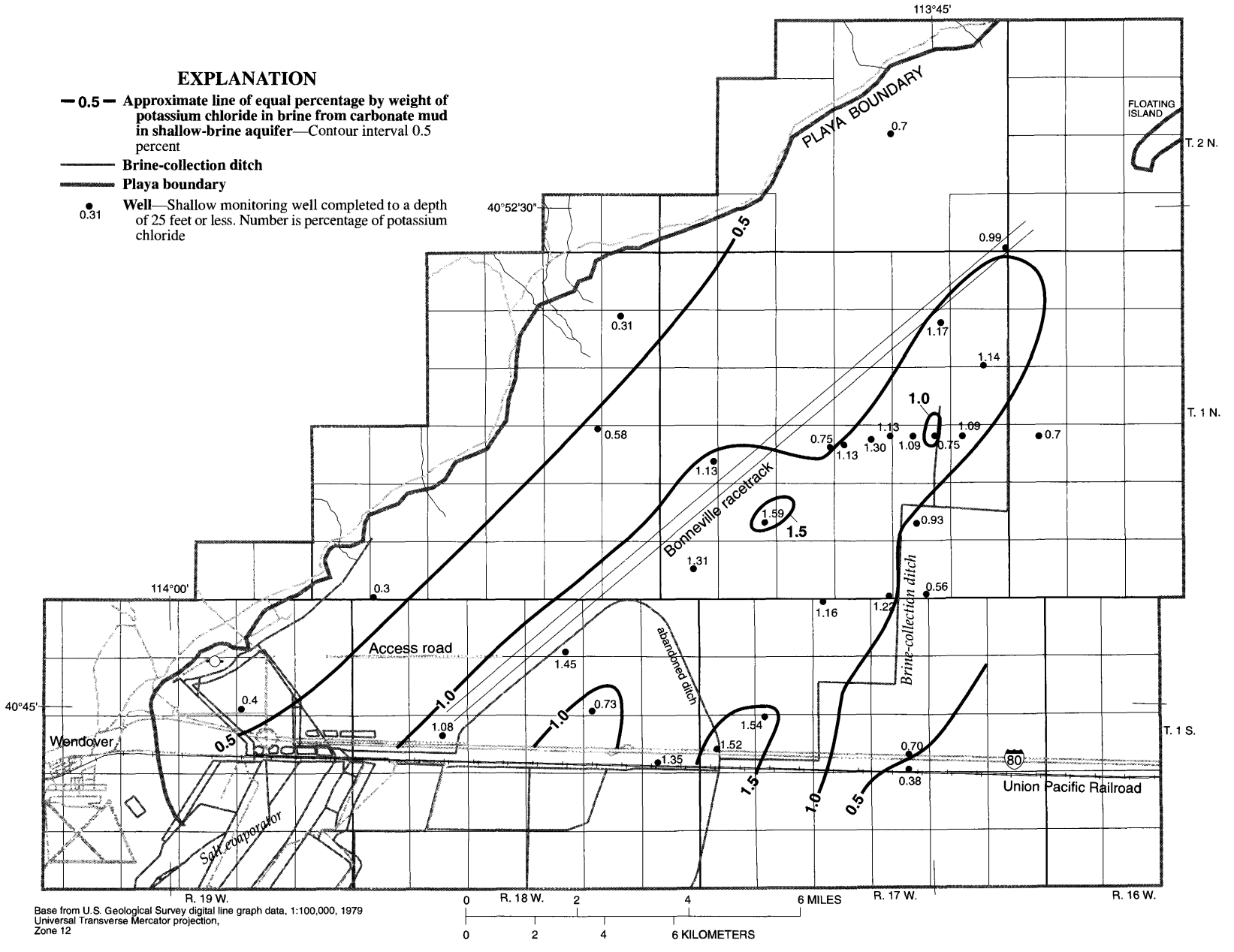


**Figure 23.** Approximate areal distribution of potassium chloride, percentage by weight, in brine from the carbonate mud of the shallow-brine aquifer, Bonneville Salt Flats, Utah, late summer, 1992.

fig. 46). It is uncertain whether the new value is indicative of a replenishment of potassium, or whether this is a seasonal effect in which the concentrating effect of evaporation at the salt surface was more prevalent in 1992 than in 1976. The lower percentages present to the east of the brine-collection ditch are representative of the brine migrating toward the ditch from east of the study area and should not change appreciably throughout time.

Evaporation from the playa surface has a concentrating effect on potassium and magnesium in the brine just below the playa surface because these cations will remain in solution as sodium chloride is precipitated. In contrast, Lines (1979, p. 94) reported that potassium and magnesium concentrations were less in brine from the salt crust than in the underlying carbonate mud at four of five locations where wells were completed in both zones. Lines suggested that the lower potassium concentrations in brine from the salt crust are the result of brine withdrawal for mineral production. He stated that where the lower potassium concentrations were present in the brine, the direction of vertical ground-water flow was downward throughout the year for water levels referenced to freshwater. If vertical driving forces are calculated using the same data, the direction of ground-water flow was upward during part of the summer at most of these sampling sites and downward at all sites during September 1976. These data suggest that seasonal effects might be a more plausible explanation for the lower potassium concentrations in brine from the salt crust.

Brine was collected for chemical analysis in May and September 1993, from three wells, (B-1-17)31acc-1, -2, and -3. These wells were completed at different depths in the shallow-brine aquifer. The percentage by weight for potassium chloride was similar for both samples in each of the three wells. The percentage potassium chloride in the brine from well (B-1-17)31acc-3, completed in the salt crust, was less than that in brine from well (B-1-17)31acc-1, completed in the carbonate mud immediately beneath the salt crust. This trend is the same as reported by Lines. The percent potassium chloride in the brine from the well completed in the salt crust, however, was similar to the value for brine from well (B-1-17)31acc-2, completed in the deepest part of the shallow-brine aquifer.

The vertical driving force for ground-water flow between the salt crust and the carbonate mud beneath the salt crust, wells (B-1-17)31acc-1 and -3, was upward during 1993. Climatic conditions at the Bonneville Salt Flats for the summer of 1993 were wetter and cooler than normal (table 1). The playa surface remained flooded for most of summer 1993, therefore, sufficient evaporation from the shallow-brine aquifer had not occurred by late summer to sufficiently lower the water level in the well completed in the salt crust to reverse the driving force.

Much of Lines' discussion concerning the percentage of potassium chloride in the shallow-brine aquifer pertains to the possible effects of brine withdrawal for mineral production. Turk (1969 and 1973), was concerned more with evaluating potassium inventory and producibility in the shallow-brine aquifer through the use of a simplified mixing model. Turk (1969, p. 179) suggested that the percentage of potassium chloride in brine from the shallow-brine aquifer would decline to about 0.5 percent in 30 to 40 years. As discussed previously, data collected during this study indicate that potassium is not being depleted. A possible explanation for the lack of potassium depletion throughout time might be the diffusion of potassium from pore fluid within the carbonate mud and clays into the brine that migrates through fractures within the shallow-brine aquifer to areas of discharge. Results of chemical analyses of pore fluid reported by Mason and others (1995, table 5) show that potassium concentrations in pore fluid are similar to those in samples from shallow wells. As brine is withdrawn from the fractures by the brine-collection ditch and subsequently replenished by infiltration from the playa surface, diffusion of interstitial potassium might occur as the brine migrates along its flow path. Another possible source for potassium is through upward leakage from the underlying lacustrine sediment of the basin-fill aquifer, despite the lack of measured water-level and density data to verify this movement. If these are the processes by which potassium might be replenished, then the potassium resource is unlikely to show any depletion in the next several years or possibly decades because of the large amount of interstitial fluid in storage within the carbonate mud and clays of the shallow-brine aquifer and the lacustrine sediment in the upper part of the basin-fill aquifer.

The chemical composition of brine from the lacustrine sediment in the upper part of the basin-fill aquifer appears to be basically the same as in the overlying shallow-brine aquifer, but the overall dissolved-solids concentration is considerably lower. Brine samples were collected from four wells at the center of the salt crust, wells (B-1-17)31acc-4, -5, -6, and -7, com-

pleted to depths of 95, 235, 495, and 63 ft, respectively. The highest dissolved-solids concentration is in brine from the well completed just beneath the shallow-brine aquifer. The concentration decreases and then increases again with depth (Mason and others, 1995, table 4). These data indicate that mixing with brine from the shallow-brine aquifer might be the cause of the increased dissolved-solids concentration in the lacustrine sediment of the upper part of the basin-fill aquifer, but that mixing probably has not affected the brine at depths of more than 63 ft. The apparent increase in dissolved-solids concentration in brine from the two deepest wells might be the result of incomplete well development after well completion. Brine collected from four additional wells, (B-1-17)11aac-2, (B-1-17)21add-4, (B-1-17)23abd-2, and (C-1-18)9adc-2, all completed to a depth of 63 ft, had similar concentrations as the brine from well (B-1-17)31acc-7.

Water from the production zone of the alluvial-fan aquifer along the northwest margin of the Bonneville Salt Flats has a dissolved-solids concentration that ranges from about 6,200 mg/L to more than 8,000 mg/L (Mason and others, 1995, table 4). The dissolved-solids concentration in the water from the nested wells located in a line perpendicular to the playa margin increases toward the playa. Results of chemical analyses of water from the alluvial-fan aquifer and the lacustrine sediment that separates the alluvial-fan and shallow-brine aquifers are listed in table 2.

Turk (1969, p. 76, and 1973, p. 4) and Lines (1979, p. 63) have indicated that the brackish water now present in the alluvial-fan aquifer has resulted from mixing of relatively freshwater with brine from the lacustrine sediment since pumping began in the late 1940's. As mentioned in the previous section, they attributed this increase to leakage of brine from the adjacent lacustrine sediment. Other probable sources for the dissolved-solids concentration in water from the alluvial-fan aquifer might include water leaking upward along fault zones, terminus of regional flow, surface runoff dissolving small amounts of salt deposited by wind on the surface of the alluvial fan prior to infiltration through surface fractures, or a combination of these possibilities. No data are available to provide a definitive answer as to which source is most probable. Chemical data that might have been collected when the production wells were drilled were not available. This type of data would have been useful for determining antecedent conditions. Results of chemical analyses of water from wells (C-1-19)10aba-1 and 10bac-1 (table 2) indicate that the water in the alluvial-fan aquifer in the pumping area might have become more saline during the 26-year period between samples. The sample collected in 1993 had about a 20-percent-higher concentration for all major constituents as compared to the sample collected in 1967. Unfortunately, these samples were not obtained from the same wells. The difference in chemical concentration, therefore, might result from a difference in well-completion depth.

On the basis of four pond samples collected and analyzed in January, May, June, and July 1993, the chemical evolution of the ponded water can be surmised. The analysis for the sample collected in January indicates the ponded water quickly attained a dissolved-solids concentration of 272,000 mg/L by dissolving salt from the salt crust (Mason and others, 1995, table 4). As evaporation of the pond progressed, the concentration of dissolved solids increased to more than 325,000 mg/L. After the total concentration exceeded 300,000 mg/L in May 1993, calcium, sodium, sulfate, and chloride concentrations increased by only a small percentage, but magnesium and potassium concentrations increased by 4 to 6 times as sodium chloride precipitated and evaporation decreased the volume of brine. Concentrations of bromide, boron, and strontium also increased as the size of the pond shrank from evaporation.

### Isotope Chemistry

In selected samples of brine from all aquifers in the Bonneville Salt Flats, the stable isotopes of hydrogen and oxygen were analyzed to help determine possible sources for the water within each aquifer. The stable isotopes are analyzed by measuring the ratios of hydrogen ($^2H/^1H$) and oxygen ($^{18}O/^{16}O$) in a sample of water. The $^2H/^1H$ isotope ratios of brackish water and brine samples were analyzed using the method described by Kendall and Coplen (1985). The $^{18}O/^{16}O$ isotope ratios of brackish water and brine samples were analyzed using a modification of the method described by Epstein and Mayeda (1953). The stable isotope of hydrogen ($^2H$) is commonly called deuterium (D). The isotope ratios are reported as differences from an arbitrary standard known as STANDARD MEAN OCEAN WATER (SMOW) and are expressed in $\delta$ units permil (parts per thousand or o/oo). The $\delta$ values are determined from the equation:

$$\delta = [(R\text{-}R_{standard})/R_{standard}] \times 1{,}000 \qquad (16)$$

**Table 2.** Results of chemical analyses of water from selected wells completed in the alluvial-fan aquifer

[°C, degrees Celsius; mg/L, milligrams per liter; —, no data; Location: See figure 2 for explanation of numbering system used for hydrologic-
in a standard referenced to Standard Mean Ocean Water (SMOW), calculated as: $[(({}^{2}H/{}^{1}H)_{sample} - {}^{2}H/{}^{1}H)_{standard})/({}^{2}H/{}^{1}H)_{standard}]$
ratio in a standard referenced to Standard Mean Ocean Water (SMOW), calculated as: $[(({}^{18}O/{}^{16}O)_{standard} -$

| Location | Date | Water temperature (°C) | Specific gravity, field | Solids, residue at 180°C, dissolved (mg/L) | pH, field (standard units) | Alkalinity, lab (mg/L as $CaCO_3$) | Calcium, dissolved (mg/L as Ca) | Magnesium, dissolved (mg/L as Mg) | Sodium, dissolved (mg/L as Na) |
|---|---|---|---|---|---|---|---|---|---|
| (B-1-18)29ccc-1 | 03-29-72 | 28.0 | — | 6,260 | 7.7 | — | 91 | 71 | 2,200 |
| (B-1-18)31acd-1 | 08-18-92 | 16.0 | 1.001 | 6,330 | 8.0 | 192 | 43 | 42 | 2,100 |
| (B-1-18)31bda-1 | 08-17-92 | 26.0 | 1.002 | 6,490 | 8.2 | 180 | 88 | 75 | 2,000 |
| | 09-07-93 | 20.0 | 1.002 | — | 7.6 | — | — | — | — |
| (B-1-18)31bda-2 | 08-17-92 | 21.0 | 1.000 | 6,360 | 8.2 | 172 | 71 | 69 | 2,000 |
| | 09-07-93 | 20.5 | 1.002 | — | 7.8 | — | — | — | — |
| (B-1-18)31bda-3 | 08-17-92 | — | 1.001 | 6,230 | 8.1 | 174 | 75 | 72 | 2,000 |
| | 09-07-93 | 23.5 | 1.002 | — | 7.7 | — | — | — | — |
| (B-1-18)31dac-1 | 08-18-92 | 18.0 | 1.004 | 11,600 | 8.1 | 317 | 91 | 94 | 3,700 |
| (B-1-18)31dac-2 | 08-18-92 | 19.0 | 1.004 | 37,000 | 8.1 | 262 | 310 | 410 | 12,000 |
| | 09-07-93 | 19.5 | 1.029 | — | 7.4 | — | — | — | — |
| (B-1-18)31dac-3 | 08-18-92 | 18.0 | 1.002 | 7,060 | 8.0 | 243 | 48 | 42 | 2,500 |
| | 09-07-93 | 15.0 | 1.002 | — | 7.8 | — | — | — | — |
| (C-1-18)6abb-1 | 08-19-92 | 17.0 | 1.068 | 100,000 | 7.2 | 297 | 990 | 1,700 | 31,000 |
| (C-1-18)6abb-2 | 08-19-92 | 20.0 | 1.066 | 101,000 | 7.5 | 224 | 1,100 | 1,500 | 30,000 |
| (C-1-18)6abb-3 | 08-18-92 | 17.0 | 1.060 | 87,800 | 7.5 | 152 | 1,200 | 1,200 | 27,000 |
| (C-1-18)6adc-1 | 08-19-92 | 22.0 | 1.062 | 97,600 | 7.5 | 249 | 1,100 | 1,600 | 31,000 |
| (C-1-18)6adc-2 | 08-19-92 | 16.0 | 1.083 | 98,300 | 7.4 | 316 | 1,200 | 1,400 | 39,000 |
| [1](C-1-19)2adb-1 | 03-29-72 | 24.5 | — | 5,700 | 7.5 | — | 79 | 63 | 2,000 |
| (C-1-19)10aba-1 | 02-05-93 | 30.0 | — | 8,310 | 7.8 | 154 | 130 | 95 | 2,600 |
| [2](C-1-19)10bac-1 | 08-04-67 | 31.0 | — | — | — | — | 100 | 80 | 2,100 |

[1] Reported by Lines, 1978, table 3.
[2] Reported by Turk, 1973, table 4b, as well FW-5.

where $R$ and $R_{standard}$ are the isotope ratios of sample and standard, respectively. A negative δ value indicates that the isotope ratio of the sample is depleted with respect to the heavy isotope in comparison to the heavy isotope in the standard, or conversely, a positive δ value indicates the sample is more enriched than the standard.

The relation between $\delta D$ and $\delta^{18}O$ is known as the meteoric water line and is determined by the equation:

$$\delta D = 8 \times \delta^{18}O + d \qquad (17)$$

where $d$ is the deuterium excess (Dansgaard, 1964, p. 456). The mean global value for $d$ in freshwater is 10 (Craig, 1961, p. 1702). The value for d may differ depending on location and geologic time. Any change in the value for $d$, whether larger or smaller, will merely shift the meteoric water line to either side of the mean global meteoric water line. The North American meteoric water line (fig. 24) has a $d$ value of 6 (Coplen, 1993, p. 235).

Evaporation from open-water bodies enriches D and $^{18}O$ in the remaining water so that the slope of the line for $\delta D/\delta^{18}O$ values is typically between 3 and 6 (Coplen, 1993, p. 235). In the evaporation trend for the Bonneville Salt Flats (fig. 24), the slope of the local evaporation line is slightly less than 5. This trend was determined from three pond samples collected during the winter through early summer of 1993 at varying

or overlying lacustrine sediment of the upper part of the basin-fill aquifer, Bonneville Salt Flats, Utah

data sites in Utah; $\delta^2H$: The relative difference in permil (parts per thousand) between the isotope ratio of $^2H$ to $^1H$ in a sample and the ratio x 1,000; $\delta^{18}O$: The relative difference in permil (parts per thousand) between the isotope ratio of $^{18}O$ to $^{16}O$ in a sample and the $(^{18}O/^{16}O)_{sample})/(^{18}O/^{16}O)_{standard}]$ x 1,000; Tritium, total: pCi/L, picocuries per liter detection limit, 5.7 pCi/L.

| Potassium, dissolved (mg/L as K) | Sulfate, dissolved (mg/L as $SO_4$) | Chloride, dissolved (mg/L as Cl) | Bromide, dissolved (mg/L as Br) | Boron, dissolved (mg/L as B) | Strontium, dissolved (mg/L as Sr) | $\delta^2H$ (permil) | $\delta^{18}O$ (permil) | Tritium, total (pCi/L) |
|---|---|---|---|---|---|---|---|---|
| 130 | 240 | 3,400 | — | 0.96 | — | — | — | — |
| 130 | 280 | 3,300 | 1.9 | 1.5 | 1.2 | -127.0 | -16.35 | — |
| 120 | 260 | 3,200 | 2.5 | 1.3 | 2.1 | -127.0 | -16.35 | — |
| — | — | — | — | — | — | — | — | <5.7 |
| 120 | 250 | 3,200 | 2.4 | 1.6 | 1.5 | -127.0 | -16.40 | — |
| — | — | — | — | — | — | — | — | <5.7 |
| 120 | 260 | 3,200 | 1.8 | 1.3 | 1.9 | -128.0 | -16.40 | — |
| — | — | — | — | — | — | — | — | <5.7 |
| 200 | 960 | 5,600 | 3.2 | 1.2 | 5.6 | -123.0 | -15.70 | — |
| 520 | 3,300 | 17,000 | 5.1 | 4.4 | 18 | — | — | — |
| — | — | — | — | — | — | -105.0 | -12.67 | <5.7 |
| 170 | 370 | 3,700 | 2.0 | 2.1 | 2.6 | -125.0 | -16.10 | — |
| — | — | — | — | — | — | -125.0 | -16.14 | <5.7 |
| 1,300 | 9,000 | 45,000 | 20 | 7.3 | 19 | -71.0 | -6.30 | — |
| 1,300 | 9,100 | 50,000 | 17 | 6.5 | 24 | -76.0 | -7.00 | — |
| 1,200 | 7,700 | 41,000 | 13 | 8.1 | 25 | -82.0 | -8.10 | — |
| 1,400 | 8,700 | 47,000 | 4.7 | 11 | 22 | -73.0 | -6.45 | — |
| 1,600 | 7,300 | 48,000 | 19 | 7.1 | 28 | -70.5 | -5.85 | — |
| 120 | 190 | 3,100 | — | — | — | — | — | — |
| 140 | 370 | 4,600 | 2.0 | 1.2 | 2.8 | -127.0 | -16.31 | — |
| 100 | 300 | 3,700 | — | — | — | — | — | — |

degrees of pond evaporation (Mason and others, 1995, table 4).

Brine from the shallow-brine aquifer on the Bonneville Salt Flats is the most enriched ground water from the study area and the δD and $\delta^{18}O$ values plot either very close to the local evaporation line or between the North American meteoric water line and the local evaporation line (fig. 24). The variation in δD and $\delta^{18}O$ values for these samples represent varying degrees of mixing with infiltrating water from precipitation on the playa surface and enrichment through evaporation. The least enriched (most negative) sample from the shallow-brine aquifer was collected from well (B-1-18)34bbb-1, located near the northwestern margin of the playa. These values are indicative of less evaporation than other samples from the shallow-brine aquifer because of the greater depth to water.

The δD and $\delta^{18}O$ values for brine from the lacustrine sediment of the upper part of the basin-fill aquifer beneath the salt crust are virtually the same as those in the overlying shallow-brine aquifer. These values support vertical mixing at the interface of these two aquifers.

The δD and $\delta^{18}O$ values for brackish water from the alluvial-fan aquifer and brine from the lacustrine sediment of the upper part of the basin-fill aquifer in the vicinity of the northwestern margin of the playa have a larger variation than samples from the shallow-brine aquifer and the underlying lacustrine sediment in the salt-crust area. These δD and $\delta^{18}O$ values form two dis-

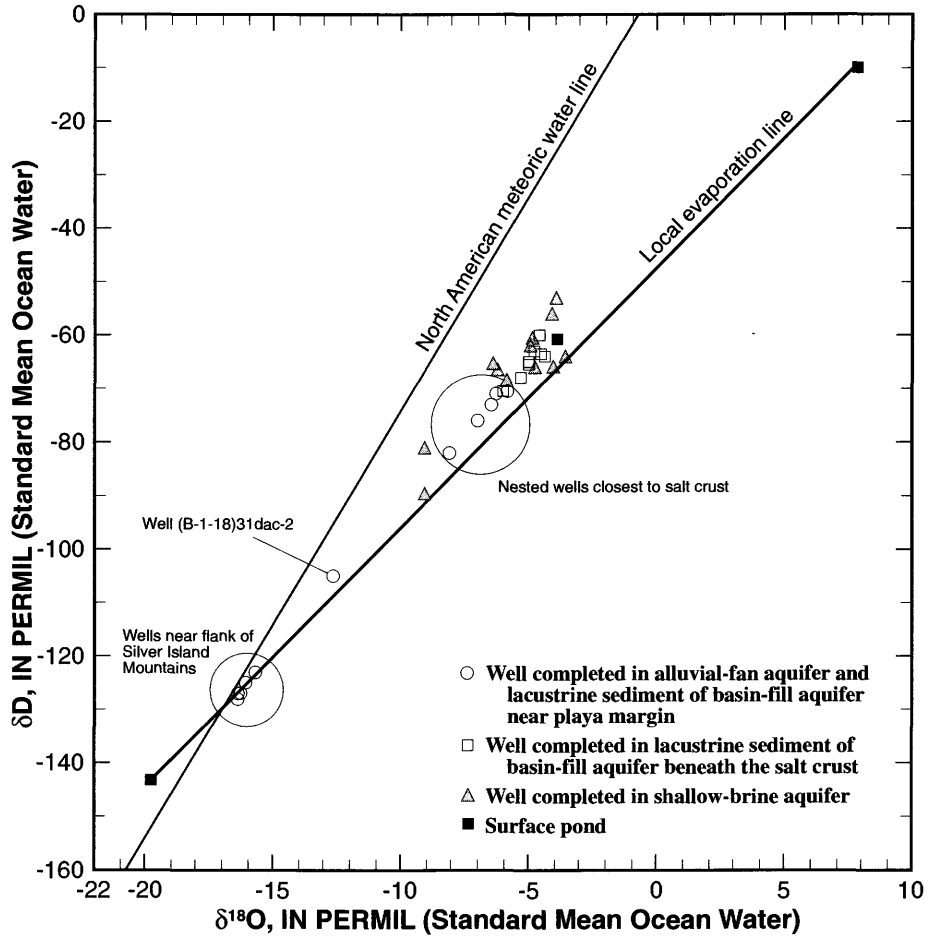


**Figure 24.** Relation of hydrogen and oxygen isotope ratios in ground water and surface pond, Bonneville Salt Flats, Utah.

tinct groups with a single intermediate value. The values that are the most depleted and coincide with the North American meteoric water line are from samples collected from wells (B-1-18)31acd-1, (B-1-18)31bda-1, -2, and -3, and (B-1-18)31dac-1and -3, all located very close to the flank of the Silver Island Mountains. These waters are indicative of recharge from precipitation, either directly on consolidated rock with rapid infiltration, or by runoff into open surface fractures with rapid infiltration, as discussed previously. If the dissolved-solids concentration, and more specifically the sodium and chloride concentrations, in water from these wells are the result of leakage from the lacustrine sediment, then the $\delta D$ and $\delta^{18}O$ values would have a more evaporative signature. The probable causes of the high dissolved-solids concentration in these waters are deep circulation of meteoric water through regional flow or along local faults or the dissolution of salt from the soil surface before the runoff enters surface fractures.

The single intermediate value was derived from water collected from well (B-1-18)31dac-2, which is completed to a depth of 149 ft. The dissolved-solids concentration is higher and the $\delta D$ and $\delta^{18}O$ values are more enriched in water from this well than from the other two wells in this nest of three wells, which are completed to depths of 74 and 245 ft. These values are indicative of mixing with brine from near the center of the playa. The chemically and isotopically distinct zones at this location are probably not indicative of a natural condition; rather, the tongue of higher dissolved-solids concentrations and more enriched isotope values are probably indicative of transient mixing, possibly induced by withdrawal by pumping from the alluvial-fan aquifer. The $\delta D$ and $\delta^{18}O$ values in brine from wells (C-1-18)6abb-1, -2, and -3, and (C-1-18)6adc-1 and -2, indicate varying degrees of enrich-

ment. These wells are located closer to the salt crust and therefore would allow more mixing with the concentrated brine.

In a more useful comparison of the different groups of water sampled for D and $^{18}O$ (fig. 25), the values for $\delta^{18}O$ are compared to dissolved-solids concentration. The trend toward higher dissolved-solids concentrations in water that has undergone more evaporation is evident. The sample from well (B-1-18)34bbb-1 is the outlier from the other groups.

Tritium ($^{3}H$) concentration also was determined in samples collected from the Bonneville Salt Flats. Tritium is a radioactive isotope of hydrogen and decays with a half-life of 12.43 years. It occurs naturally in the atmosphere by the interaction of cosmic rays with nitrogen and oxygen. More importantly, the largest source for $^{3}H$ was from above ground, thermonuclear weapons testing between 1952 and 1969. The natural level for $^{3}H$ in the atmosphere prior to weapons testing was 10 TU. During above-ground weapons testing, atmospheric levels were more than 10,000 TU (Drever, 1982, p. 347). At the present time (1996), $^{3}H$ concentrations are again approaching the natural (commonly called pre-bomb) level in the atmosphere.

Twenty-five samples were collected for $^{3}H$ analysis from wells completed in the shallow-brine and alluvial-fan aquifers and the lacustrine sediment of the upper part of the basin-fill aquifer. One sample, with a value of 10 TU, was collected from a winter surface pond to verify the $^{3}H$ concentration for infiltrating water. Other values ranged from less than detection limits (5.7 pCi/L) to 78 pCi/L (Mason and others, 1995, table 4). This range equates to less than 1.8 to 24 TU. For purposes of this report, any value below detection limits is considered equal to 0 TU. The samples with values of 0 TU are from waters that have infiltrated into the subsurface prior to the above-ground weapons testing. Samples with values above 10 TU are from water

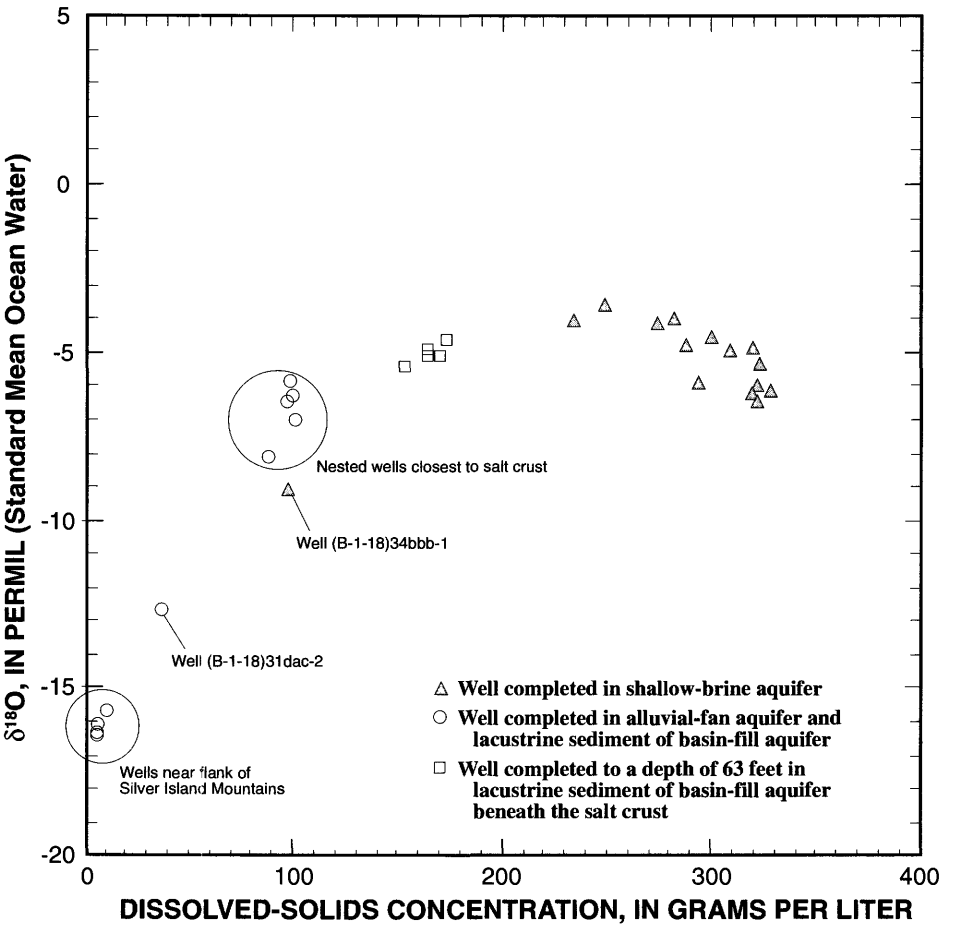


**Figure 25.** Relation of oxygen isotope ratio to dissolved-solids concentration in ground water, Bonneville Salt Flats, Utah.

that has infiltrated into the subsurface within a few years prior to sampling or has infiltrated after above-ground weapons testing and been diluted with pre-bomb water and possibly with recent water. A more precise date for infiltration is not possible because of uncertainty in knowing if and to what extent mixing has occurred.

Nineteen samples were collected from wells completed in the shallow-brine aquifer. A noticeable trend exists for these values. Generally, samples with the lower $^3H$ values, about 10 TU or less, are from the center of the salt-crust area, whereas samples with the higher values, from about 14 to 24 TU, are from the periphery. This distribution supports the concept that most of the infiltration from the surface occurs over the salt crust with brine migrating laterally to points of discharge. Wells from which samples having less than 10 TU were obtained are located along the axis of the salt crust. The sample from well (B-1-17)31acc-1 had a value of 0 TU. In order to have $^3H$ values of 0 to less than 10 TU, mixing with water from a source of pre-bomb water is necessary. The only probable source for this water entering the shallow-brine aquifer is through upward leakage from the lacustrine sediment of the upper part of the basin-fill aquifer. This is contradictory to water-level data and estimates for downward leakage discussed previously in this report. Upward leakage in the amount necessary to account for the low $^3H$ values is possible if water levels had been slightly lower than those measured in 1993 in shallow wells on the salt crust and if the permeability of the underlying lacustrine sediment of the upper part of basin-fill aquifer were two to four orders of magnitude greater than previously assumed. The required permeabilities are representative of silt rather than clay.

If surface runoff and infiltration through surface fractures are a relatively recent source of recharge to the alluvial-fan aquifer and to the lacustrine sediment of the upper part of the basin-fill aquifer, then traces of tritium are expected in these waters. Six samples were collected from the line of nested wells completed in these zones. None of the samples had a $^3H$ concentration above the detection level (table 2). The lack of $^3H$ in this water does not preclude surface runoff as a possible mechanism for the dissolved-solids concentration in the alluvial-fan aquifer; rather, it might indicate that post-bomb water has not had sufficient time to migrate to the sampling points.

## SALT-TRANSPORT MECHANISMS AND SALT BUDGET

An understanding of the amount of salt contained in the Bonneville Salt Flats is needed in order to place salt-budget and transport estimates in proper perspective. An estimate of total salt should be considered as a crude approximation because of sparse data and is only provided for a sense of scale.

The amount of salt contained in the crystalline salt crust north of Interstate Highway 80 was estimated from dry density and volume. The dry density of the crystalline salt near the surface of the salt crust ranges from 98.2 to 123.3 lbs/ft$^3$ (P. Allard, Bureau of Land Management, written commun., 1995). The average dry density from 30 measurements is 109.8 lbs/ft$^3$. If the average dry density is assumed to be representative of the entire salt crust, then the salt crust, as it existed north of the Interstate Highway 80 in 1988 (S. Brooks, Bureau of Land Management, written commun.,1988), contained more than 125 million tons of salt. The amount of salt dissolved in the brine that fills the pore space and fractures of the shallow-brine aquifer north of Interstate Highway 80 was estimated to exceed 175 million tons. This estimate is based on an average porosity of 0.45 (Turk, 1969, p. 104), an average aquifer thickness of 20 ft, an average dissolved-solids concentration of 286 g/L (17.85 lbs/ft$^3$), and an areal extent of 80 mi$^2$, the area where the brine is most concentrated. The amount of salt estimated to have been lost from the salt crust in the 28-year period, 1960-88, is more than 55 million tons. This estimate is based on the change in volume of the salt crust for the 28-year period (S. Brooks, Bureau of Land Management, written commun., 1988) and the average dry density.

For both principal mechanisms for transporting salt within the hydrologic system of the Bonneville Salt Flats, the salt is dissolved in water. The first mechanism transports salt by surface ponds blown by wind, or in some years, simply by the large areal extent of the surface pond. The second mechanism transmits salt by advective ground-water flow and associated dispersive transport, which can be the result of natural and (or) anthropogenic causes.

### Salt Transport by Surface Ponds

Precipitation on the Bonneville Salt Flats during the late fall, winter, and early spring generally undergoes little evaporation; thus, what does not infiltrate

into the subsurface accumulates at the lowest altitude in the basin and forms a shallow pond, generally a few inches deep but sometimes more than 1 ft deep in some areas. Ponds are most likely to be deeper, more extensive, and longer lasting when winter precipitation is normal or greater than normal and when temperatures are lower than normal. This relatively freshwater provides a mechanism by which salt can be dissolved and transported away from the normal bounds of the salt-crust area and deposited on the carbonate mud by evaporation.

As freshwater accumulates on the salt-crust surface, it dissolves underlying halite until the brine approaches saturation. Wind can easily move this brine over the virtually flat surface. Wind direction at the two weather stations was predominantly from the southwest to northeast during the winter months of 1992-94 when evaporation rates were the lowest. This wind moves surface brine from the salt-crust area northeastward toward Floating Island. If the water were to remain away from the center of the salt-crust area as it evaporated, then there would be a net loss of salt from the main body of the salt crust. This does not necessarily constitute a net loss of salt from or a gain to the basin, but only a temporary redistribution of salt. In the succeeding summer months, this salt can be redissolved by water from thunderstorms and then migrate back toward the salt crust.

During 1993, precipitation was greater than normal during January, and temperatures were much colder than normal for January and February. Because of these conditions, extensive flooding of the Bonneville Salt Flats dramatically changed the salt surface. A large amount of surface water, primarily from south and east of the study area, migrated toward the playa. The density of this inflow, as measured on March 26, 1993, ranged from 1.014 to 1.030 g/cm$^3$. By visual observations, the surface inflow was not turbid. Although this inflow added an unknown amount of salt to salt-crust area, the relatively freshwater dissolved salt from the southern part of the salt crust and transported it to the north. No data were collected from which to estimate total inflow. Much of the salt remained in solution into the summer of 1993, when the salt precipitated on the playa surface as the pond evaporated. Satellite imagery was used to determine the areal extent of the salt crust in September 1992 and August 1993 (fig. 26). The areal extent of the salt crust was 43 mi$^2$ in 1992 and 58 mi$^2$ in 1993. The newly redeposited salt extended to the west edge of the brine-collection ditch and to the northeast, about 3 mi beyond the brine-collection ditch. Measurements from the top of the well to the salt surface were used to estimate the thickness of salt dissolved and precipitated. The volume of salt that was dissolved and precipitated was estimated from these measurements. An estimated 10 to 14 million tons of salt were dissolved from the salt-crust area just north of Interstate Highway 80, with much of the salt redeposited to the north and east of the main body of salt.

The fate of the salt transported into the area north and east of the north ends of the brine-collection ditch is unknown. Much of this salt might have been redissolved and infiltrated into the subsurface where it could migrate to the brine-collection ditch, or this salt might have been deposited across a very subtle topographic rise where it would be unable to eventually migrate back to the salt crust by movement of small surface ponds that can form after thunderstorms. Some of the salt transported into the area that is influenced by the brine-collection ditch to the east of the salt crust might have redissolved, infiltrated into the subsurface, and migrated to the brine-collection ditch. No data were collected to quantify the amount of salt permanently removed from the salt-crust area.

## Salt Transport in Solution Through the Shallow-Brine Aquifer

The salt and fluid that circulate within the pore space of the salt crust and underlying carbonate mud are in a constant state of change. Freshwater from rainfall that infiltrates into the shallow-brine aquifer almost immediately dissolves salt in order to reach chemical equilibrium. Evaporation of the fluid during the summer months concentrates the dissolved salts in the remaining fluid until salt precipitates out of solution, forming new deposits.

From water levels measured in 1976, Lines (1979, p. 79) determined that brine in the shallow-brine aquifer moves from the main salt-crust area northwest toward the alluvial-fan aquifer, east toward the brine-collection ditches, and south under Interstate Highway 80 toward a network of brine-collection ditches. Brine flows into the study area through the subsurface from the east and northeast. In 1992, the same pattern of brine movement existed (fig. 15). The amount of brine moving across the study-area boundaries in 1992 was estimated from aquifer properties derived from tests (Turk, 1973, table 9; and Lines, 1979, table 5) and from

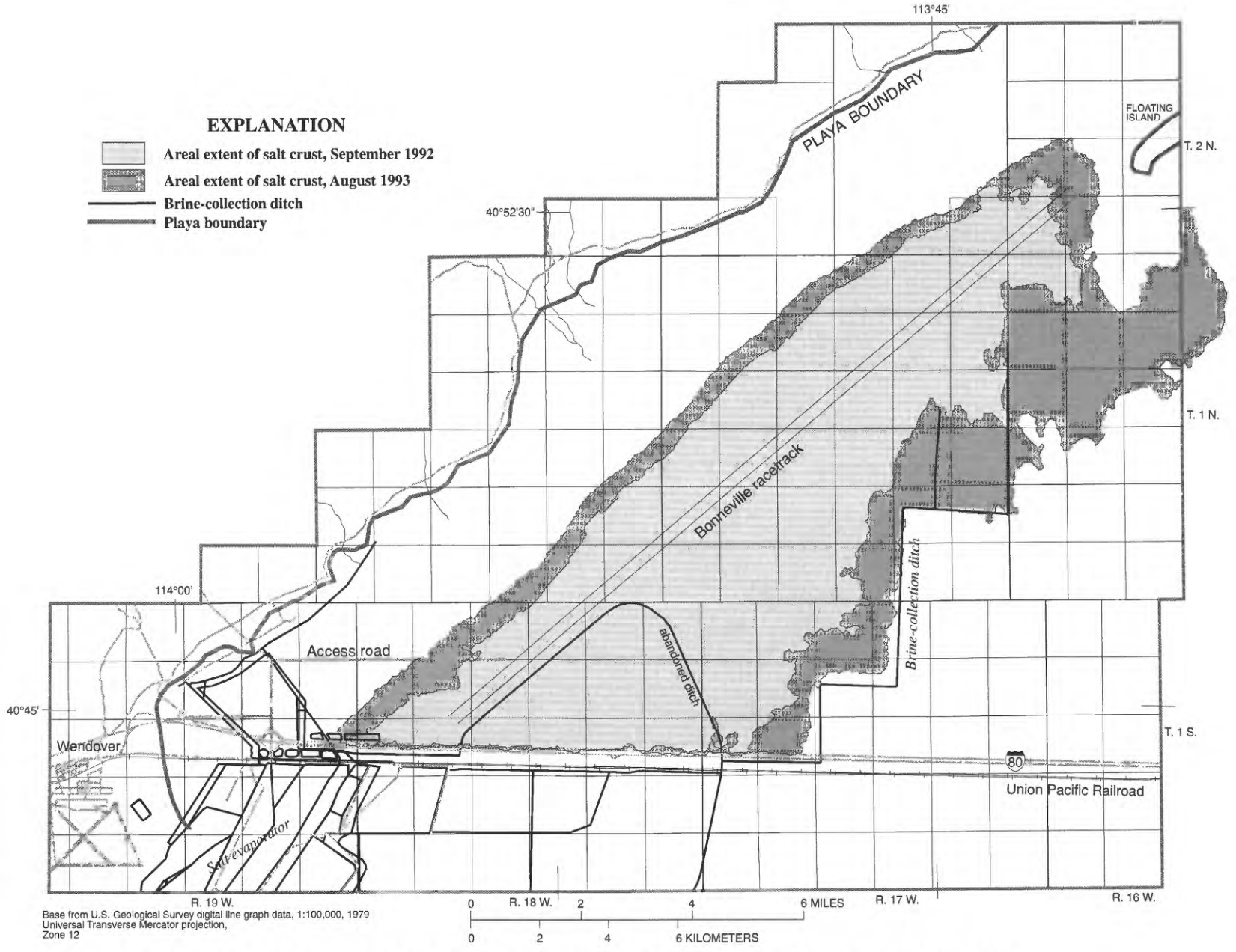


**Figure 26.** Increase in areal extent of the salt crust from September 1992 to August 1993, Bonneville Salt Flats, Utah.

**Table 3.** Estimated fluid flow and salt transport into and out of the shallow-brine aquifer, Bonneville Salt Flats, Utah

[—, no estimate]

| Component | 1976 (Lines, 1979) | | 1992 (this study) | |
|---|---|---|---|---|
| | Acre-feet | Tons of solute | Acre-feet | Tons of solute |
| **Recharge** | | | | |
| Subsurface inflow from east and northeast | 40 | 14,600 | 60 | 21,900 |
| Infiltration from playa surface | 11,740 | — | 8,300-12,800 | — |
| **Total** (rounded) | 11,800 | 14,600 | 8,400-12,900 | 21,900 |
| **Discharge** | | | | |
| Subsurface outflow to south | 2,000 | 780,000 | 1,800-2,300 | 700,000-895,000 |
| Subsurface outflow to brine-collection ditch | 680 | 264,000 | 1,500 | 580,000 |
| Subsurface outflow to northwest | 70 | 27,200 | 35 | 13,600 |
| Downward leakage | — | — | 58-580 | 22,600-226,000 |
| Evaporation | 10,900 | 0 | 15,000 | 0 |
| **Total** (rounded) | 13,600 | 1,071,000 | 18,400-19,400 | 1,316,000-1,715,000 |

horizontal hydraulic gradients derived from contours of reference potentiometric heads based on average density (fig. 15). These flow estimates are compared to those made by Lines (table 3). Differences in these estimates result from the different method used by Lines to calculate reference potentiometric heads and temporal variations in recharge from precipitation and evaporation. Variations in precipitation and evaporation occur on a seasonal and annual basis, but the long-term conditions have remained virtually unchanged during the past 20 years.

No evaporation data were collected for the summer of 1992. As discussed previously, the estimate for evaporation from the shallow-brine aquifer of 12,200 acre-ft in 1993 is probably less than the usual amount that occurs on the Bonneville Salt Flats because of cooler-than-normal temperature and larger-than-normal precipitation in June and July. The estimate for 1994 of 20,700 acre-ft is probably more than the typical amount because of hotter-than-normal temperature and less-than-normal precipitation. An intermediate value of about 15,000 acre-ft might be more representative of evaporation from the playa surface in 1992.

In both estimates, total discharge is more than total recharge. Lines (1979, table 6) attributed the difference to a decrease in ground water stored within the shallow-brine aquifer. The difference in the estimate from this study is considerably larger than the difference stated by Lines, and yet, no long-term decline in storage has been observed because the shallow-brine aquifer appears to be in a fluid steady state. No long-term change in storage would dictate that fluid recharge would have to be about the same as fluid discharge. As suggested previously, subsurface flow to the south might be less than estimated because of compaction or removal of porous material during construction of Interstate Highway 80, and downward leakage might be offset by upward leakage at the center of the salt crust. Even if subsurface flow to the south was assumed to be a fraction of the estimate stated in table 3, total discharge would remain considerably larger than the estimated total recharge. No substantial changes in water levels have occurred within the shallow-brine aquifer; therefore, more fluid must be entering the aquifer than previously estimated by Lines (1979, table 6). On the basis of the ground-water flow directions (fig. 15), the probable source of fluid in a large enough amount to compensate for discharge would be upward leakage.

Previous and current estimates of recharge into and discharge from the shallow-brine aquifer can be used to estimate the amount of salt entering and leaving the Bonneville Salt Flats study area (table 3). Subsurface inflow from the northeast and east was estimated to be 60 acre-ft in 1992. On the basis of an average dissolved-solids concentration of 268,500 mg/L (16.75

lbs/ft$^3$) from four wells on the northeastern and eastern boundaries, an estimated 21,900 tons of salt per year are transported into the study area at these boundaries, a small amount of the total salt budget.

An average brine density of 1.18 g/cm$^3$, which equates to a dissolved-solids concentration of 286,200 mg/L (17.86 lbs/ft$^3$), was assumed to be representative for all fluid exiting the shallow-brine aquifer. This dissolved-solids concentration was used to convert all subsurface outflow (table 3) to tons of salt. An estimated 700,000 to 895,000 tons of salt were transported out of the study area along the south boundary in 1992. The amount of salt that was transported into the brine-collection ditch in 1992 was estimated to be 580,000 tons. The amount of salt transported from the shallow-brine aquifer into the alluvial-fan aquifer in 1992 was estimated to be 13,600 tons.

On the basis of limited data indicating downward leakage, the amount of salt that might be transported downward to the lacustrine sediment that underlies the shallow-brine aquifer is estimated to range from 22,600 to 226,000 tons. If upward leakage occurs, then the estimated net loss of salt would be less because of the transport of salt into the shallow-brine aquifer.

Total inflow of salt to the shallow-brine aquifer system in 1992 was estimated to be about 22,000 tons, but total outflow of salt from the same system was about 1.3 million to 1.7 million tons. Lines (1979) estimated that in 1976, total inflow of salt was about 14,600 tons and total outflow of salt was about 1 million tons.

## SIMULATION OF VARIABLE-DENSITY GROUND-WATER FLOW AND SOLUTE TRANSPORT IN THE SHALLOW-BRINE AQUIFER

### Modeling Approach

A model is a representation of some, but not necessarily all, features of an actual system (Foley and others, 1990, p. 286). The purpose of a model is to enhance visualization and understanding of the structure and behavior of the actual system, and to provide a convenient means of experimentation and prediction of the effects of various changes to the model parameters. Computer models in the physical sciences, such as ground-water flow and solute-transport models, are typically expressed as systems of mathematical equations, and the modeler learns by experimenting with different values of independent variables and parameters.

Any numerical simulation of ground-water flow and solute transport is necessarily limited in its ability to realistically portray hydrologic interactions in the field. If, however, a sufficient amount of parameter information is available, numerical simulation can be useful in quantifying and testing hypotheses of the mechanisms and relations in the simulation region. This was the role of the numerical simulation of the shallow-brine aquifer in the Bonneville Salt Flats study area.

Numerical simulation was used as a tool to aid in the understanding of the hydrologic environment and solute transport in the study area. It helped to quantify transport mechanisms, integrate field information, and test hypotheses. It also was used to evaluate sensitivity of the system to boundary-condition and parameter values and to address the following questions:

1. What quantitative effects does withdrawal of brine for mineral production have on the salt crust?
2. What quantitative effects do annual evaporation and precipitation have on the salt crust?

To answer these questions, a three-dimensional, ground-water flow and solute-transport model was developed for the Bonneville Salt Flats study area. Calculation of an overall ground-water flow and solute-transport balance was a major objective. The mass balance on the salt crust itself would be a consequence of the cumulative transport amount at the land-surface boundary of the model.

The primary goals of the combined ground-water flow and solute-transport modeling are to (1) develop a fluid and solute balance for the ground-water system in the simulation region, (2) evaluate the effect of the brine production from the ditches on the salt crust, and (3) identify the major and minor solute fluxes to and from the system.

#### Description of the Simulator of Ground-Water Flow and Solute Transport

Simulator refers to the computer code that simulates ground-water flow and solute transport. Model refers to the application of the simulator to represent the shallow-brine aquifer underlying the study area. Solute refers to the dissolved constituents in the ground water and is equivalent to dissolved solids. Salt refers

to the solid-phase mixture of salt minerals, primarily halite and gypsum. Salt crust refers to the perennial salt deposit on a large part of the playa surface.

The numerical simulation of ground-water flow and solute transport for this study area consisted of the computation of numerical solutions to the equation of saturated ground-water flow coupled with the equation for solute transport. For an assumed isothermal situation of variable fluid density, the saturated ground-water flow equation is formed from the combination of the conservation of total fluid mass and Darcy's Law for flow in porous media. The solute-transport equation is formed from the conservation of mass for a single solute species.

The three-dimensional Heat and Solute Transport (HST3D) computer code (Kipp, in press) of the U.S. Geological Survey was the simulator used to model the shallow-brine aquifer underlying the Bonneville Salt Flats. This simulator was chosen because of its ability to model variable-density flow and solute-transport in three dimensions. Although this simulator can calculate heat and solute transport simultaneously, effects of temperature variation on the density of the brine were assumed to be negligible for the purposes of this study. Therefore, only ground-water flow and associated solute transport were simulated. The flow and transport equations are coupled through the interstitial pore velocity and the dependence of the fluid density and viscosity on pressure and solute-mass fraction.

The HST3D simulator uses some different variables and parameters than are used for ground-water flow and solute transport for constant-density fluids. They include (1) pressure instead of potentiometric head as the dependent variable of flow, (2) mass fraction instead of volumetric concentration as the dependent variable of solute, (3) porosity instead of specific yield for storage in unconfined flow systems, (4) conservation of mass rather than conservation of volume for the flow equation, (5) permeability instead of hydraulic conductivity in Darcy's Law, and (6) energy per unit mass instead of potentiometric head at the external surface of a leakage boundary.

Pressure is chosen as the dependent variable for fluid flow because no potentiometric-head function exists for density fields that depend on temperature and solute concentration. All pressures are expressed relative to atmospheric pressure.

The partial-differential equation of ground-water flow is based on the following assumptions and limitations:

1. Ground water fully saturates the porous medium below the water table.
2. Ground-water flow is described by Darcy's Law.
3. The coordinate system is chosen to be aligned with the directions of the permeability tensor so that this tensor is diagonal for anisotropic media.
4. Diffusive fluxes of the bulk fluid caused by density gradients are neglected relative to advective-mass fluxes.
5. Osmotic potential driving forces are neglected.
6. Dispersive-mass fluxes of the bulk fluid from spatial-velocity fluctuations are not included.

Although Hassanizadeh and Leijnse (1988) show that in high-concentration solutions, fluid motion is dependent on solute concentration gradients, and they present a formulation of Darcy's and Fick's Laws that contains density flow and pressure diffusion, their equation formulations are not implemented in the HST3D simulator. The flow equation is based on the conservation of total fluid mass in a volume element, coupled with Darcy's Law for flow through a porous medium. Thus,

$$\frac{\partial(\varepsilon\rho)}{\partial t} = \nabla \cdot \rho\frac{\boldsymbol{k}}{\mu}(\nabla p + \rho g \hat{e_z}) \qquad (18)$$

where:

$\varepsilon$ is the effective porosity (-);
$\rho$ is the fluid density ($M/L^3$);
$t$ is the time ($T$);
$\boldsymbol{k}$ is the porous-medium permeability tensor ($L^2$);
$\mu$ is the fluid viscosity ($F\text{-}T/L^2$);
$p$ is the fluid pressure ($F/L^2$);
$g$ is the gravitational constant ($L/T^2$); and
$\hat{e}_z$ is the unit vector in the z-direction (-).

Equation 18 relates the rate of change of total mass in the fluid phase to net fluid-inflow rate. The fluid consists of pure water plus the dissolved solids. Capacitance is described by effective porosity rather than specific yield. In this report, effective porosity simply will be called porosity.

The interstitial or pore velocity, $\boldsymbol{v}$, is obtained from Darcy's Law as:

$$\boldsymbol{v} = -\frac{\boldsymbol{k}}{\varepsilon\mu}(\nabla p + \rho g \hat{e_z}) \qquad (19)$$

where:

$\boldsymbol{v}$ is the interstitial-velocity vector ($L/T$).

The equation for conservation of a single solute species is based on the following assumptions and limitations:

1. Solute transport by local, interstitial, and velocity-field fluctuations and mixing at pore junctions is described by a hydrodynamic-dispersion coefficient.
2. Thermal and pressure diffusion are neglected.
3. Forced diffusion by gravitational, electrical, and other fields is neglected.

The mass fraction of solute is considered to be the dependent variable for solute transport. It is the mass of dissolved solids per mass of solution (solute plus water), that is, a mass-based concentration. The more widely used concentration term is an amount per unit volume of fluid, that is, a volume-based concentration. But volume-based concentration is not conserved in a variable-density system. The term "solute concentration" refers to the mass-based concentration or mass fraction. In the simulator, the density field is derived from the mass fraction. The conservation equation for the solute in the fluid phase can be written:

$$\frac{\partial(\varepsilon\rho w)}{\partial t} = \nabla \cdot \varepsilon\rho \boldsymbol{D}_S \nabla w + \nabla \cdot \varepsilon\rho D_m \boldsymbol{I} \nabla w - \nabla \cdot \varepsilon\rho \boldsymbol{v} w \quad (20)$$

where

$w$ is the mass fraction of solute in the fluid phase (-);
$\boldsymbol{D}_S$ is the mechanical-dispersion-coefficient tensor ($L^2/T$);
$D_m$ is the effective-molecular diffusivity of the solute ($L^2/T$); and
$\boldsymbol{I}$ is the identity matrix of rank 3 (-).

Equation 20 relates the rate-of-change of solute in the fluid phase to the net dispersive and diffusive flux, and the net advective flux. The equation is written for a unit volume of saturated porous medium.

The conservation equations for ground-water flow and solute transport are based upon the conservation of mass, not conservation of volume as in a constant-density flow system. A change in volume occurs when fluids containing different amounts of salt are mixed. For example, mixing 1 L of freshwater (density 1 g/cm$^3$) with 1 L of brine (density 1.2 g/cm$^3$) yields a total mass of 2.2 kg of salt water, but the volume is 2.075 L, not 2.000 L, which is about a 4-percent difference.

Before the two conservation equations can be solved, information about the fluid properties, aquifer properties, and transport coefficients needs to be obtained. The fluid properties are density and viscosity. The porous-matrix properties are porosity and permeability. The transport coefficients are solute-dispersion tensors and the effective molecular diffusivity of the solute. In the HST3D simulator for the present model application, density and viscosity are functions of the solute-mass fraction. The solute-dispersion tensors are functions of the interstitial velocity. The other parameters are either uniform or functions of space within the simulation region.

For fluids such as water, a linear-density function is typically adequate for the ranges of pressures and solute concentrations encountered. Fluid viscosity is strongly dependent on temperature, less dependent on solute concentration, and least dependent on pressure. The fluid-density function in the simulator is linear in pressure, temperature, and solute concentration (Kipp, in press).

The HST3D simulator uses an empirical equation for viscosity of brines as a function of pressure, temperature, and solute concentration. Moderate curvature can be seen in a plot of fluid viscosity as a function of solute-mass fraction at 20°C (fig. 27).

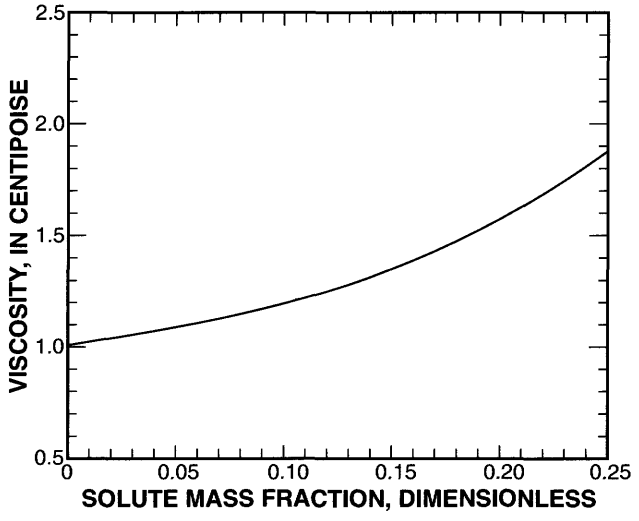


**Figure 27.** Fluid viscosity as a function of solute mass fraction at 20 degrees Celsius.

In the HST3D simulator, the mechanical-dispersion coefficient is taken from the work of Scheidegger (1961) as presented by Bear (1972, chap. 10). For an isotropic porous medium, two parameters describe the

mechanical-dispersion tensor: the longitudinal dispersivity, $\alpha_L(L)$, and the transverse dispersivity, $\alpha_T(L)$. Field data have shown that longitudinal dispersivity typically is 3 to 10 times larger than transverse dispersivity (Freeze and Cherry, 1979, p. 396; Anderson, 1979) and that their magnitudes are dependent on the scale of observation distance over which the solute is transported in a system. The dispersivities are affected by the heterogeneity of the permeability distribution for the aquifer.

Discretization of the ground-water flow and solute-transport equations and boundary conditions in space and time was done using finite-difference techniques (Kipp, in press). This converted the equations into sets of simultaneous linear equations at the node points in space that are solved numerically for each time step.

This flow and transport simulator is based on a finite-difference approximation of the partial-differential equations derived by the subdomain collocation method described by Cooley (1974), Varga (1962), and Patankar (1980). The grid of node points can have variable node spacing, and a point-distributed grid is used as opposed to a cell-centered grid (Kipp, 1987). Aquifer properties are specified by zones that are subregions bounded by planes of nodes. This means that properties change values at planes of nodes rather than at cell boundaries. Any full cell may have up to eight subdomains with different aquifer properties. The resultant cell property is a volume-weighted average of the subdomain values. A conductance property is an area-weighted average of up to four subdomain values, for a full cell, over the relevant cell face. An element is a volume with a node at each of the eight corners. A node with its associated cell and one of its subdomains and associated element is shown in figure 28.

Aquifer properties are uniform over an element. Thus, an element is the smallest zone possible for variation of aquifer properties.

The boundary conditions were discretized on a nodal or cell basis. For the specified-pressure boundaries, entire cells have the specified value. For flux and leakage boundaries, the face to which the flux or leakage is applied is the entire cell face. Spatial changes in flux values or leakage parameters occur at cell boundaries, not at nodes.

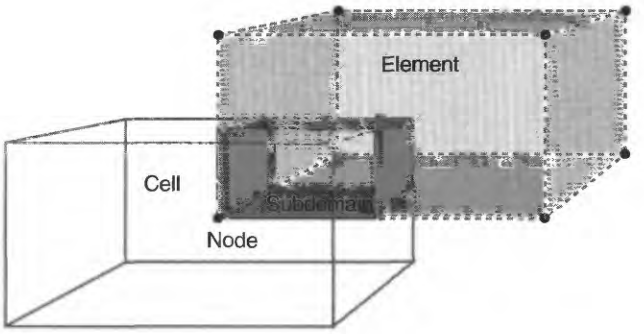


**Figure 28.** Diagram of a model cell with associated node, one subdomain, and the associated element.

### Application to Study Area

For the Bonneville Salt Flats, the equation of ground-water flow had the following additional assumptions specific for this application:

1. Ground-water flow is described by Darcy's Law, although this is a fractured-clay and fractured-salt medium.
2. The porous medium and fluid are incompressible for this unconfined system.
3. The storage coefficient representing elastic storage effects from fluid and porous-matrix compressibilities is negligible for this unconfined system.
4. The fluid viscosity is a function of space and time through dependence primarily on solute concentration.
5. Contributions to the total fluid mass from pure solute-mass sources within the region are not included.

The first assumption was adopted, although it is known that the shallow-brine aquifer underlying the Bonneville Salt Flats is a fractured medium of carbonate mud and salt crust. There is a slight dependence of viscosity on pressure in the function employed, but the effect is negligible for the pressures encountered in the shallow-brine aquifer.

The ground-water system simulated for the Bonneville Salt Flats is assumed to be isothermal at 20°C, so no heat-transport equation is needed. Examination of water density as a function of temperature (Weast and others, 1964, p. F-4) shows that a 10°C temperature change causes a density change of about 0.002 g/cm$^3$, which is within measurement error. On this basis, temperature effects on density were neglected.

Consideration of viscosity changes as a function of temperature for a brine with a mass fraction of 0.22 has about a 20-percent viscosity change for a 10°C change in temperature from 15 to 25°C. This means that seasonal changes in aquifer temperature do not produce major changes in hydraulic conductivity. Minor changes in hydraulic conductivity, therefore, would be masked by the uncertainty in the hydraulic-conductivity distribution. Neglecting temperature effects on viscosity does not compromise the realism of the simulations.

An evaluation of the potential for induced buoyant thermal convection can be made by evaluating the dimensionless Rayleigh number (Ra) for typical aquifer parameters (Nield and Bejan, 1992, p. 147). A stability analysis shows that a Rayleigh number of more than about 27 is needed to induce thermal convection for an unconfined ground-water system. Using typical thermal and hydraulic parameters for the shallow-brine aquifer, the flow system is stable under a temperature difference of 10°C from the bottom to the top of the aquifer (Ra = 10). This condition might be possible when winter cooling causes a temperature profile that increases from top to bottom of the aquifer, assuming uniform salinity. The thermal conduction mechanism is sufficient to stabilize the adverse density gradient caused by the temperature profile.

A similar analysis can be done to evaluate the potential for convective circulation resulting from an unstable density or solute-concentration gradient with the denser brine within the salt crust overlying the slightly less dense brine in the carbonate mud. The critical Rayleigh number is also about 27. An unstable density gradient condition occurs when summer evaporation causes a denser brine to form at the top of the aquifer. Assuming an isothermal system, for a density difference of 0.02 g/cm$^3$ between the top and the bottom of the shallow-brine aquifer, static brine is always unstable when the denser fluid is on top (Ra = 30,000). This is because the molecular diffusivity for the dissolved salt is so small that diffusive transport cannot overcome forces for convective transport to stabilize the adverse density gradient.

For brine moving near the brine-collection ditches and the water-table surface where evaporative discharge and precipitation recharge occur, dispersive mixing maintains a stable configuration (Ra = 0.05 to 25) with denser brine on top. In other parts of the aquifer where interstitial velocities are less than about $10^{-3}$ ft/d, convective circulation would be expected when the denser brine overlies the less dense brine (Ra = 30 to 800). These results are based on an estimated dispersivity of 1,000 ft, which is characteristic of the flowpath length under the salt crust.

For the Bonneville Salt Flats, the equation of solute transport had the following additional assumptions specific for this application:

1. The salt mixture is considered to be a single solute species.
2. No mechanisms for solute precipitation or dissolution are included.
3. No pure solute sources occur in the fluid or solid phases.

The solutes being transported in the Bonneville Salt Flats shallow-brine aquifer include several types of salt, of which about 90 percent is sodium chloride. For modeling purposes, assumption 1 is made. Assumption 2 means that the simulator does not contain a mechanism for precipitation of salt when brine evaporates, nor a mechanism for dissolution of salt when undersaturated water moves through crystalline salt. The lack of these mechanisms in the simulator means that when formulating a calculation for the amount of crystalline salt, it is assumed that brine precipitates salt at a rate given by the solute concentration of the evaporating fluid at the boundary face, and the infiltration of rain and snowfall advects dissolved salt into the aquifer at a specified concentration.

The HST3D simulator uses the SI metric system internally but accepts input and provides output data in English units. The units used for the modeling of the Bonneville Salt Flats study area were time in days, length in feet, mass in pounds, volumetric flow rate in cubic feet per day, mass flow rate in pounds per cubic foot per day, and pressure in pounds per inch squared.

Boundary-condition types employed include specified pressure, specified solute mass-fraction, specified fluid flux, evaporation, leakage, and a free surface or water table. All boundary conditions can be functions of time.

Certain additions and modifications were made to the HST3D simulator for application to the Bonneville Salt Flats simulation region. These modifications are described by Kipp (in press). They include:

1. Addition of an evapotranspiration boundary condition.
2. Modification of the algorithm for location of the free surface or water table.
3. Addition of the ability to input data as a linear distribution over a boundary segment.
4. Addition of the ability to input data node-by-node and element-by-element from gridded data prepared by a geographical information system.
5. Elimination of the partial Gauss reduction used for numerical coupling of the difference equations for flow and transport.
6. Computation of data for postprocessing of flow rates and cumulative flow amounts.
7. Addition of output of water-table altitude and density field for postprocess contour plotting.

The evaporation boundary condition has a piecewise linear function of evaporation flux with depth to the water table. The function is non-linear because of the sharp breaks in function slope at the land surface and at the extinction depth. Evaporation flux decreases as the water table drops until it becomes zero at the extinction depth.

The fifth item was necessary to prevent simulation failure due to instability of the original partially reduced difference-equation system when a cell went dry. It also corrected a major mass-balance problem associated with cells going dry.

Postprocessing programs were written for the totalization of boundary flow rates and individual cumulative flows by boundary faces at selected locations, and for the computation of pond volumes and fluid mass at the end of each simulated season. The simulator calculates cell flow rates and cumulative amounts at each cell for each type of boundary condition. These values are written to a file for postprocessing so that total flow rates and cumulative amounts can be calculated for any desired part of a boundary face. The trapezoidal rule is used for temporal integration of the flow rates to obtain the cumulative amounts. The volume of the pond that appears during the recovery season is calculated by adding the volume of fluid between the water table and the altitude of the pond bottom over the pond area on a cell-by-cell basis. The mass of brine in the pond is calculated by adding the density-weighted pond volume using the density of the bottom layer of cells in the pond.

The finite-difference approximations to the advective-transport terms were chosen to be upstream in space. The temporal finite-difference approximations were chosen to be backward in time or fully implicit. These choices mean that a certain amount of artificial numerical dispersion is introduced into the solutions calculated by the simulator. This numerical dispersion is a function of the time-step size and the mesh spacing (Kipp, in press), and it prevents nonphysical oscillations in the solute-concentration field at the cost of artificial smoothing or dispersion of concentration gradients.

The simulation region in the Bonneville Salt Flats study area focused on the shallow-brine aquifer. The areal extent of the simulation region is shown in figure 29.

The simulation region contains the entire area of thick perennial salt crust north of Interstate Highway 80 that is known as the Bonneville Salt Flats. Carbonate mud surrounds the salt crust and extends toward the northwest to the Silver Island Mountains and to the east into the Great Salt Lake Desert. A thinner, ephemeral salt crust forms seasonally on the surface of the carbonate mud. Also, evaporation from the water table precipitates salt in the fractures of the carbonate mud and the existing salt crust. For modeling purposes, the term "salt crust" will be used to refer to the perennial salt deposit encompassing the area where the salt crust is at least 1 ft thick. The salt crust plus the thin, ephemeral salt deposits make up the total crystalline salt deposit at any given time.

The vertical extent of the simulation region represents the thickness of the shallow-brine aquifer from the water table at or near the land surface down to the contact with the lacustrine sediment of the upper part of the basin-fill aquifer. The areal extent of the simulation region represents the study area from the alluvial-fan aquifer along the flank of the Silver Island Mountains on the northwestern and northern boundaries to the brine-collection ditch along Interstate Highway 80 on the south, and from the alluvial-fan aquifer on the west to the limit of available data east of the brine-collection ditch, which is located east of the salt crust.

Previous work (Lines, 1979) indicates that the shallow-brine aquifer in the Bonneville Salt Flats study area was of large areal extent (125 $mi^2$) and rather thin vertically (25 ft). However, the large fluid-density variation between the northwestern boundary with the alluvial-fan aquifer (1.04 $g/cm^3$) and the shallow-brine aquifer (as much as 1.21 $g/cm^3$) raises the potential for density-induced flow. Thus, a variable-density flow and solute-transport simulator was needed. The model has to be three-dimensional to allow for buoyant effects from density contrasts and to include the areal features

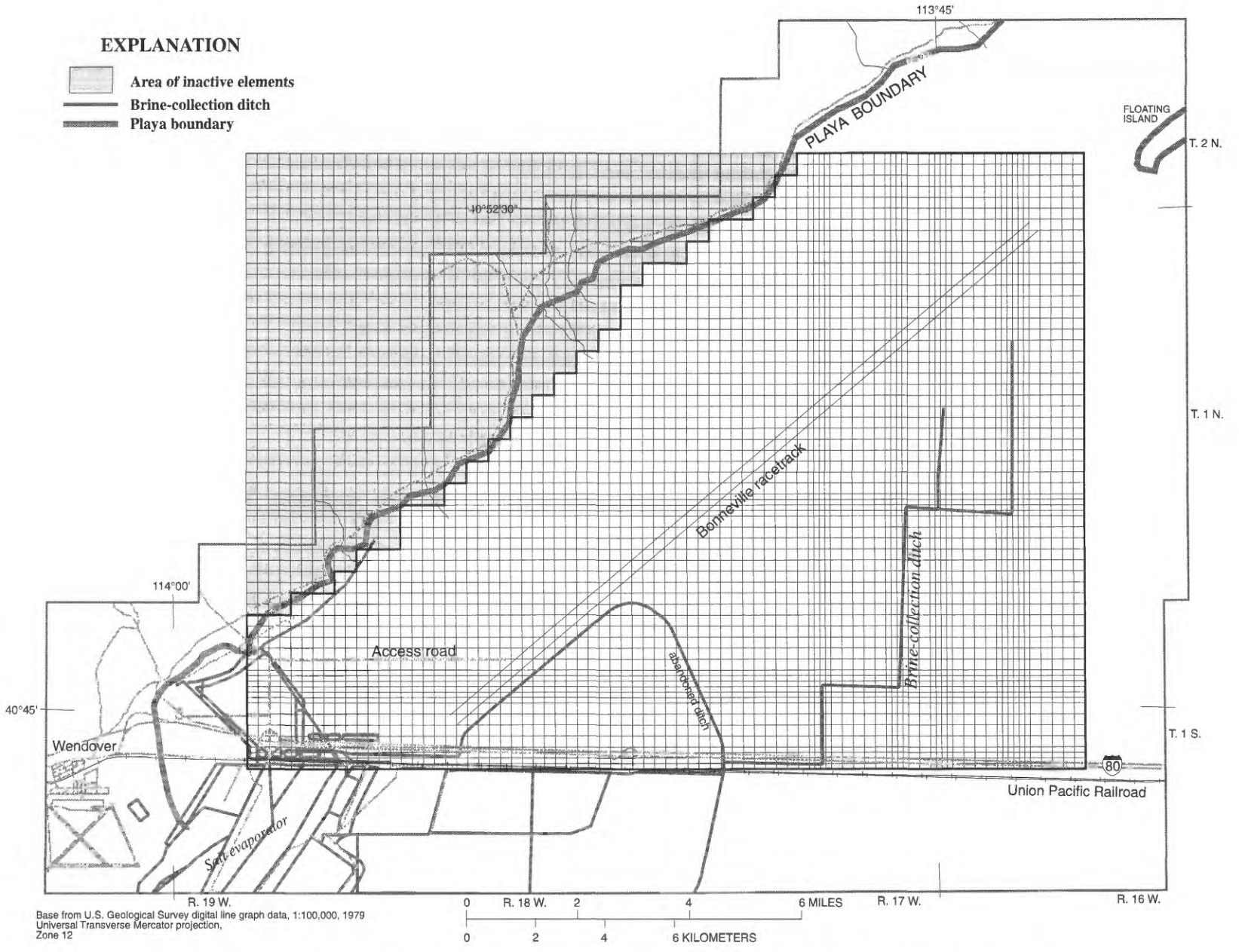


**Figure 29.** Location of model grid and inactive elements for the model of the shallow-brine aquifer, Bonneville Salt Flats, Utah.

of the brine-collection ditch and aquifer boundaries. Although some density variation was measured between brine from the salt crust and brine from the underlying carbonate mud, vertical profiles of density variation throughout the thickness of the shallow-brine aquifer were not obtainable.

The shallow-brine aquifer consists of carbonate mud, oolitic sand, gypsum, and halite, and is fractured with fissures up to 1 in. in width extending down to 25 ft with fissure spacing of about 1 ft being common. Although the aquifer is fractured, the well known assumption of an equivalent porous medium was made. This was necessary because data to characterize the fracture distribution were insufficient. Also, the density of fractures was believed to be high enough to be represented as a distributed porosity and permeability for the purposes of this model.

Inflow to and outflow from the simulation region were identified as follows. Water and brine enters the simulation region by (1) infiltration of precipitation and (2) ground-water inflow from the north, east, and west, and a small segment at the west end of the southern boundary (fig. 15). Brine leaves the simulation region by (1) evaporation, which precipitates crystalline salt on the playa surface, (2) ground-water outflow to a brine-collection ditch along the southern boundary, south of Interstate Highway 80, (3) ground-water seepage into the brine-collection ditch east of the salt crust, (4) ground-water outflow to the adjacent alluvial-fan aquifer along the northwestern margin of the playa, and (5) leakage to the underlying basin-fill aquifer. Ponding occurs over the lower areas of the salt crust in response to seasonal precipitation and reduction in evaporation rate during the winter months.

Review of several years of available data shows considerable annual variation of precipitation, evaporation, production from brine-collection ditches, and other hydrologic conditions. Model calibration by historically matching periods of actual site conditions was not done for the following reasons:

1. Insufficient data were available to define initial conditions, for an undisturbed state or for a period of current brine production.
2. Boundary conditions show transient variations on the time scale of days to weeks.
3. Purposes of modeling this study area involve a time scale of years to decades.

Preliminary simulations show that the ground-water flow system does not reach a steady state during the production or recovery seasons because the response time is longer than a seasonal duration of about 6 months. For simulation purposes, a synthetic seasonal sequence was formulated representing a typical year split into a 6-month summer-fall season of production and evaporation followed by a 6-month winter-spring season of recovery and recharge. For purposes of this report, the former season will be denoted as the production season and the latter season as the recovery season. An average brine-production volume, estimated during this study, was used for the production season. The goal was to simulate a periodic steady state representing a typical climatic year with average brine production from the brine-collection ditch east of the salt crust. Then the fluid and solute balances could be evaluated to help answer the key questions pertaining to model simulations in this study as presented in the "Modeling approach" section of this report.

The simulation region was contained in a rectangular parallelepiped of dimensions 76,000 ft by 56,000 ft by 26 ft in the east-west, north-south, and vertical directions, respectively. The land surface is flat to within 2 ft over the Bonneville Salt Flats. To simplify the geometry, an altitude of 4,215 ft was assumed for the carbonate-mud surface and 4,214 ft was assumed for the salt-crust surface.The contact with the underlying basin-fill aquifer was assumed to be a horizontal plane at an altitude of 4,189 ft.

The mesh or grid was constructed with variable node spacing. The horizontal spacing varied from 500 to 1,000 ft, and the finer divisions were made in the vicinity of the brine-collection ditch. One reason for the 1,000-ft spacing was to be able to define the permeability, pond area, salt-crust area, recharge flux, evaporation flux, and porosity distribution with realistic geometric structure. Altitudes of the node layers were 4,189, 4,194, 4,199, 4,204, 4,209, 4,214, 4,214.5, and 4,215 ft. The finer mesh near the top was to accommodate the ponding representation. The total number of nodes in the simulation region was 44,032; however, only about 36,000 nodes were active. The nodes are located at the intersection of the model-grid mesh lines. Thus, the mesh lines delineate element boundaries, not cell boundaries.

The ground-water flow and solute-transport simulator requires specification of boundary conditions to determine the numerical solutions for the dependent variables of pressure and solute concentration. The boundary conditions for the simulation region include specified pressure, specified recharge flux for the infiltration of precipitation, evaporation, and leakage from

an adjacent aquifer or outer aquifer region. The leakage boundary condition was chosen for those boundaries along which water-level distributions in space are known only at a few locations. The location of the different boundary-condition types is shown in figure 30.

At all flux and pressure boundaries, associated solute-mass fractions were specified for possible advective inflow. Fluid flowing into the simulation region advects solute at the specified mass fraction. Solute is advected by fluid flowing from the simulation region at the current solute concentration at a given location on the boundary. For model simulations, no boundaries had a specified solute concentration because this would have constrained the simulated solute-concentration distribution unrealistically.

The boundary conditions (fig. 30) were specified as follows by locations and types: (1) along the south and west boundaries, specified pressure; (2) along the east, north, northwest, and bottom boundaries, leakage; (3) along the top (free-surface) boundary, evaporation flux during the production season and specified recharge flux from the infiltration of precipitation during the recovery season; and (4) specified pressure along the brine-collection ditch boundary east of the salt crust and interior to the simulation region. Equations defining the boundary-condition types are described by Kipp (in press). Actual values associated with the various boundary conditions were assigned by a variety of methods to be described in the "Parameter estimation and available data" section of this report.

A leakage boundary condition was chosen along those boundaries where water levels are known only at a few locations. This boundary condition does not specify water levels, but allows the simulated water levels to rise and fall in response to inflow and outflow across these boundaries. Thus, neither fluxes nor water levels are specified at the leakage boundaries; therefore, they are suitable in regions in which information is sparse. Interpolated water levels were used to set the driving forces at leakage boundaries by specifying the potential energy per unit mass of fluid at the exterior surface of the leaky layer.

A limitation of the simulator is that, although cells at edges and corners of the active simulation region may have two or three boundary faces, only one flux or leakage boundary condition can be specified for a given cell. For example, along edges where a lateral leakage-boundary face may meet a vertical leakage-boundary face, one of those faces must be pulled back from that edge so that there are not two leakage faces for that cell. This is inconvenient, but not a serious problem for regions with a high density of cells because the lost-leakage area would be a small fraction of the total-leakage area along that boundary. The boundary face chosen to be pulled back from the edge was the one containing the greater number of cells, so that the lost fraction is minimized.

The brine-collection ditch, located east of the salt crust, in the interior of the simulation region is represented as a specified-pressure boundary. It penetrates two-thirds of the thickness of the shallow-brine aquifer. The areal location of the ditch is a sequence of line segments joining node points. The ditch was located approximately to align the segments with the north-south and east-west axes of the model grid. During the recovery season, the brine-collection ditch boundary was removed from the simulator. This allowed the water table to rise in response to the changes in the other boundary conditions, such as at the land surface and along the south and east boundaries. To keep a specified-pressure boundary for the brine-collection ditch would have provided an artificial instant recovery of the ditch water level, and it would have become a false source of recharge to the shallow-brine aquifer.

The shallow-brine aquifer, simulated as an unconfined aquifer, has a free-surface boundary condition at the water table. The free surface is allowed to move to any cell in a vertical column of cells. Recharge from precipitation across the free-surface boundary was represented by an areally distributed flux over the top surface of the simulation region. This flux was applied to the cell containing the water table at each areal location. Evaporation also was represented by an areally distributed flux applied to the cell containing the water table. As explained earlier, this flux depends on the water-table depth below land surface.

A transient pond forms seasonally on the Bonneville Salt Flats during the winter months, when the water table rises above the land surface in areas where the altitude of the land surface is lowest. During model development and calibration, an approximate representation of this ponding was incorporated by defining an area with a land surface uniformly 1 ft lower than the general land surface altitude of 4,215 ft. This pond area consists of 36 percent of the land surface of the simulation region. It also approximates the area overlain by 1 ft or more of perennial salt crust. The lower land surface created a zone in the model representing the seasonal pond. Porosity in this zone was set to unity and permeability to four orders of magnitude greater than

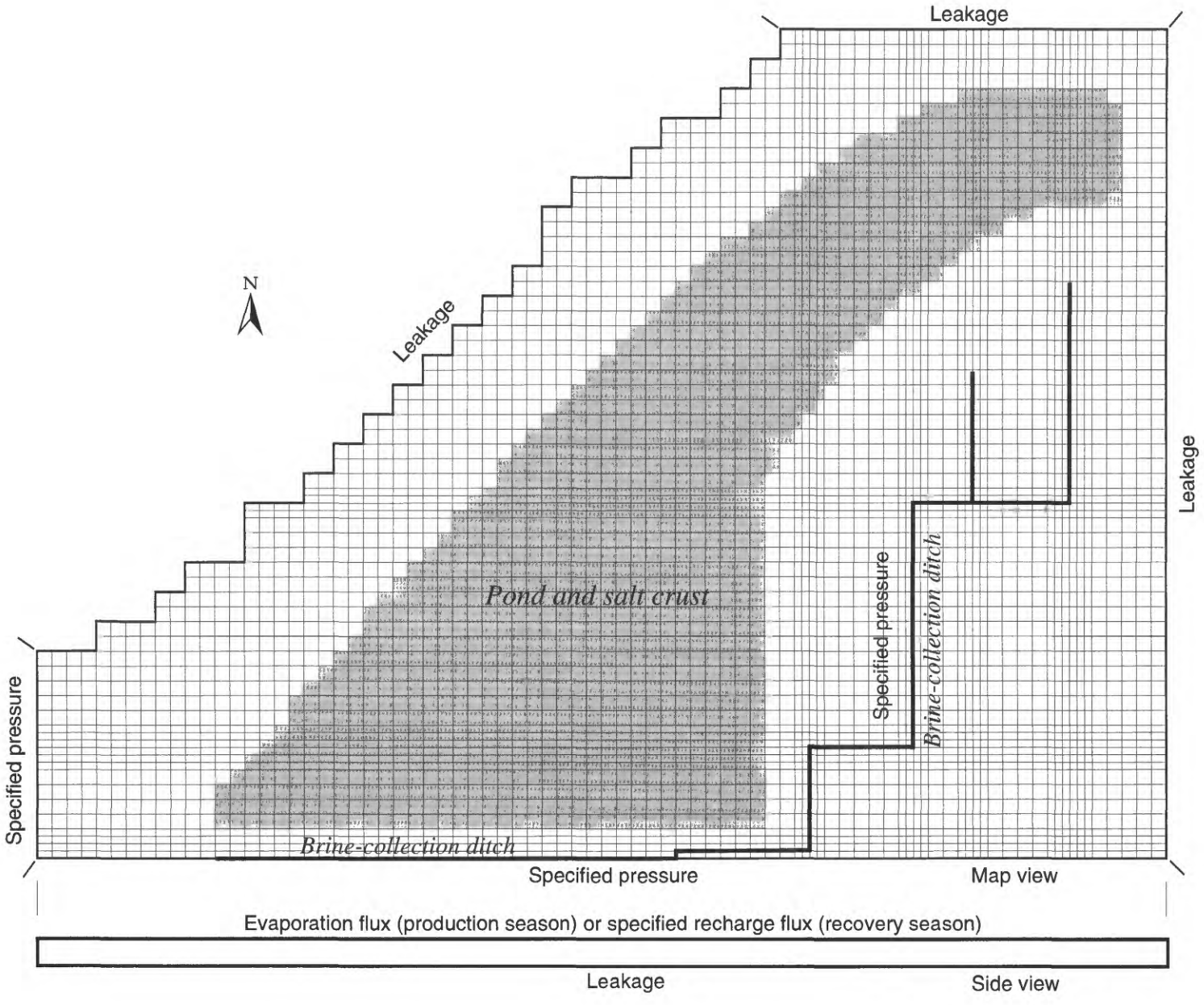


**Figure 30.** Simulation region for the shallow-brine aquifer with boundary-condition types and locations, Bonneville Salt Flats, Utah.

for the shallow-brine aquifer. This approximated an open body of water when the water table rose into this zone and provided additional fluid storage for the overall simulation region. Because aquifer properties are defined on an element basis, the cells spanning the pond-bottom altitude of 4,214 ft have an effective average porosity of about 20 percent. Thus the effective pond bottom could be regarded as the cell boundary of the lowest cell with porosity of 100 percent. This bottom surface was located at an altitude of 4,214.25 ft. It would have been desirable to represent the pond by an open body of water whose level responded to net inflow through the pond bottom as described by Cheng and Anderson (1993). The same approach could also have been used to model the brine-collection ditches. However, development of such a fully coupled model for open bodies of water with variable-density flow and transport was beyond the scope of the study.

Alternatively, representation of the brine-collection ditch, interior to the simulation region, as a leakage boundary was not feasible because it penetrated six of the nodal layers of the model. The brine-collection ditch was assumed to be 17 ft deep, which located the ditch bottom at an altitude of 4,198 ft, and corresponds to the sixth nodal layer down from the top of the model grid.

At the beginning of the study, it was believed that the fluid system was at periodic steady state for several decades but that the solute in the system could be in transient evolution. The salt crust was regarded as not in periodic steady state, based on the long-term decline in area and thickness. Data obtained later in the study show that the solute content of brine in the shallow-brine aquifer also was in a periodic steady state for more than 20 years. The model was calibrated to achieve this condition.

Simulations were carried out to a periodic steady state with a repeated sequence of production and recovery seasonal periods with their associated boundary conditions, approximating a typical year. Seasonal average values for boundary pressures, recharge flux, leakage parameters, and evaporation flux were used. This removed the dependence of the results on the initial pressure distribution, and, to a lesser extent, on the initial solute-concentration distribution. The initial conditions of the water-table configuration and the density distribution were quite uncertain because of the lack of data for a typical year or set of years from which to obtain an average representative of initial conditions. The alternative approach of using a pre-development initial condition also was discarded because of the lack of data to quantify this condition.

A periodic steady state for the flow system implies the following at the end of two successive production or two successive recovery seasons:

1. The water-table configuration is the same.
2. The boundary fluid volumetric flow rates are the same.
3. The volume of fluid in the system is the same.

A periodic steady state for solute transport also implies the following:

1. The density and solute-mass-fraction fields are the same.
2. The mass of fluid and solute in and out of the system has a net value of zero for a year of simulation.

The durations of seasonal simulations were 180 days for the production season and 185 days for the recovery season. An automatic time-step control was used for each simulation starting at 0.01 days. The main control was on the pressure change per time step, which was limited to 0.01 lbs/in$^2$, corresponding to about 0.025 ft of change in altitude of the water table. Although almost never invoked, the secondary control was to limit the concentration change per time step to 0.01 in solute-mass fraction.

Because the flow simulation was run to obtain a periodic steady state, the pressure-field results are independent of the initial-condition pressure distribution. Therefore, for simplicity, a hydrostatic pressure with a flat water table was chosen as the initial condition for the ground-water flow equation. The initial condition for the solute-transport equation was a mass-fraction distribution derived from a cubic trend surface fit to density data (see "Parameter estimation and available data" section of this report).

Output files were postprocessed to compute flow rates and cumulative flow amounts for each boundary segment. Trapezoidal integration in time was used to compute cumulative flow amounts from the boundary-cell data.

Seasonal evaporation from the shallow-brine aquifer was computed as total evaporation for the simulation region less the initial amount stored in the seasonal pond. The pond was totally evaporated during the production season so there was no residual pond to include in the computation for this season. Similarly, seasonal recharge to the shallow-brine aquifer was calculated as the total recharge amount less accumulation in the seasonal pond during the recovery season. The

pond volumes were calculated by numerical integration of the volume of water contained in each cell within the pond volume. The pond depth at each node within the pond area was the height of the free surface above the effective pond-bottom altitude of 4,214.25 ft.

The volume of brine stored in the pond at the end of the previous recovery season was subtracted from total evaporation at the end of the production season just completed to get actual evaporation from the shallow-brine aquifer. Similarly, the volume of brine stored in the pond at the end of the recovery season just completed was subtracted from total recharge for this recovery season to get actual recharge to the shallow-brine aquifer. The mass of solute in the pond at the beginning of the production season was subtracted from the mass of solute removed from the simulation region to obtain the net mass of solute removed from the shallow-brine aquifer during this season. Similarly, the mass of solute in the pond at the end of the recovery season was subtracted from the mass of solute added to the simulation region by recharge from infiltration of precipitation to obtain the net mass of solute added to the shallow-brine aquifer during this season. These methods account for the solute in storage in the seasonal pond.

The budget for the crystalline salt was calculated from the cumulative-amount results. At the end of the production season, the total amount of salt precipitated through evaporation was assumed to be the total amount of solute advected out through the top boundary of the model by evaporative flow, less the amount of salt contained in the seasonal pond at the beginning of the production season. This calculation neglects any concentrating mechanism occurring in the actual system, so the simulated outgoing solute concentration is not necessarily at halite saturation. At the end of the recovery season, the total amount of salt dissolved and recharged to the shallow-brine aquifer was assumed to be the amount advected in through the top boundary of the model by the recharge flux less the solute in storage in the pond at the end of the season. Because there was no salt dissolution mechanism in the simulator, the density or solute concentration of the recharge flux was specified. The difference between solute outflow and inflow was calculated as the net gain or loss of crystalline salt during the year.

## Parameter Estimation and Available Data

For the purposes of this report, parameter estimation refers to the process of selecting values for the various model parameters estimated without the use of computer simulations. These parameters were not adjusted during the subsequent model-calibration procedure. The initial estimates of parameter values adjusted during model calibration also are described here. Data from previous studies of the Bonneville Salt Flats, data collected during this study, and general hydrologic information from similar settings were used to estimate model parameters. Parameters estimated at the beginning of model development define (1) geometry of the aquifer, (2) geometry of the salt crust and pond area, (3) aquifer elastic-storage properties, (4) heads used to set the specified-pressure boundaries (except at the brine-collection ditch), (5) external potentials for the leakage boundaries, (6) leakage-boundary flow properties and geometry, (7) evaporation extinction depth, (8) densities used to set the associated solute concentrations at the boundaries, and (9) aquifer dispersivities. The remaining model parameters were established during the model calibration and are described in the next section. They include: (1) aquifer-permeability distribution, (2) aquifer-porosity distribution, (3) maximum evaporation-flux distribution, (4) precipitation-recharge flux distribution, and (5) brine-collection ditch water levels.

### Aquifer and Fluid Properties

All aquifer properties were assumed to be uniform throughout the aquifer thickness because of a lack of data indicating otherwise. The aquifer properties for conductance (permeability) and storage (porosity) were calibration variables. Initial estimates of permeability distribution were based on a contour map of transmissivity values by Lines (1979, fig. 33). This transmissivity map was digitized into piecewise constant bands of transmissivity, and interpolated bands of permeability values were generated for the elements formed by the areal nodal mesh by geographical-information-system computer software. Zonation by element was used in the horizontal planes of nodes, with each element extending from the land surface to the aquifer bottom. This gave the finest possible horizontal resolution for permeability at the given mesh definition. The permeability values were set to be uniform throughout the thickness of the shallow-brine aquifer because no data were available on vertical variation.

Conversion of transmissivity to permeability was done by the following equation:

$$k = 7.37 \times 10^{-11} \frac{T\mu}{\rho g b} \quad (21)$$

where

$k$ is the permeability ($ft^2$);
$T$ is the transmissivity ($ft^2/d$);
$\mu$ is the fluid viscosity (centipoise);
$\rho$ is the fluid density ($lbs/ft^3$);
$g$ is the gravitational acceleration ($ft/s^2$); and
$b$ is the aquifer thickness (ft).

The density and viscosity distributions used in this conversion were calculated from the density distribution used for initial conditions. This density-distribution contour map also was digitized into piecewise constant bands. An associated piecewise constant-viscosity distribution was calculated from the bands of constant density by converting the density to solute-mass fraction, then using the viscosity equation from the HST3D simulator to obtain the viscosity value for each band. The proper densities and viscosities to use in the conversion would be those measured during each aquifer test; however, these data were not available. The initial horizontal permeability distribution ranged from $1.29 \times 10^{-10}$ $ft^2$ to $1.15 \times 10^{-9} ft^2$. Lines (1979, p. 70) reported that the vertical hydraulic conductivity for his aquifer tests on the shallow-brine aquifer ranged from 30 to 140 ft/d. The ratio of vertical to horizontal hydraulic conductivity for these tests ranged from about 0.6 to 0.9 based on an anisotropic hydraulic conductivity aquifer-test analysis. On the basis of these tests and the vertical fractures penetrating most, if not all, of the thickness of the shallow-brine aquifer, the vertical permeability of the equivalent porous media was assumed to be 0.8 of the horizontal value for each zone.

Storage of the flow system was characterized by porosity. Because this aquifer is being simulated as an unconfined flow system, fluid and porous-matrix compressibility were assumed to be negligible. A uniform effective porosity of 10 percent was used initially. Specific yield for this unconfined aquifer is assumed equal to the effective porosity of 10 percent, however, this parameter is not used in the simulator.

The solute-dispersivity values were somewhat arbitrarily selected to be 500 ft in both longitudinal and transverse directions because no data were available to estimate the field values for the study area. The amount of numerical dispersion contributed by the mesh spacing used is equivalent to a dispersivity of up to 500 ft for flow along a horizontal coordinate direction, and up to 2.5 ft for flow in the vertical coordinate direction. Estimating the numerical dispersion for oblique flow is beyond the scope of this report but probably falls within the above limits. The total effective longitudinal and transverse dispersivities range from about 500 to 1,000 ft, which may be unrealistically large for simulating vertical mixing. Longitudinal-dispersivity values from field-scale tracer experiments tend to be one-tenth or less of the length scale of the flowpath (Gelhar and others, 1992). The transverse dispersivity was set equal to the longitudinal to represent the hydrodynamic mixing effects of the predominantly vertical fractures that are the major flow conduits. A high transverse dispersivity results in a great deal of vertical mixing with flow that is predominantly horizontal. For flow that is vertical, the large longitudinal dispersivity also results in vertical mixing. The amount of numerical dispersion contributed by the largest time-step length used is equivalent to a dispersivity value of as much as about 50 ft, clearly less significant than that caused by the mesh spacing.

The fluid-density and viscosity functions are described in the "Modeling approach" section of this report. For modeling purposes, the system was treated as isothermal at 20°C. The range of measured fluid density in the shallow-brine aquifer in the Bonneville Salt Flats was 1.04 to 1.2 $g/cm^3$. The calculated brine viscosity from this density range extends from 1.25 to 1.99 centipoise. The latter value is more than twice that of freshwater. No laboratory measurements of viscosity of the brine were made.

### Boundary-Condition Parameters

General methods used for quantifying all boundary conditions of the several types used in the model are as follows. The specified-pressure boundary conditions were assigned to segments of the boundaries by extrapolation from maps of the measured seasonal water tables (figs. 15 and 16) and by using the initial-condition density distribution to calculate pressure variation with depth to the aquifer bottom. Hydrostatic conditions were assumed to apply throughout each specified-pressure boundary segment.

A leakage boundary needs an energy per unit mass specified at its external surface. This energy was calculated from extrapolation of measured water levels near the relevant boundary locations (figs. 15 and 16). The lateral thicknesses were chosen to place the exter-

nal potentials sufficiently far away from the simulation region to lessen their effect on the water-table configuration. Also, the lateral thicknesses were chosen to place the outer boundary of the leaky layer at a horizontal location where there were at least a few wells to provide external potential and density data. The permeability of the lateral leakage boundaries was taken to be a smooth approximation of the horizontal permeability for the shallow-brine aquifer in the vicinity of the respective boundary. It was assumed that all properties and potentials were uniform over the vertical extent of each boundary segment.

The head distributions specified for the various boundary segments in the production and recovery seasons, respectively, are shown in figures 31 and 32. The head distributions along leakage boundaries were used to set the external boundary potentials. The boundary-density values used for head-to-pressure conversion and for specification of boundary-solute concentrations are shown in figure 33. Associated solute-mass fraction for possible inflow was calculated from the initial-condition density distribution along that boundary. Some of the boundary-condition pressure and energy values changed from production season to recovery season. The following sections describe the various boundary conditions by geometric location around the model region.

The boundary on the north, located just south of the northeastern end of the Silver Island Mountains, was defined as leakage. The western half of this boundary is the north edge of the shallow-brine aquifer, possibly near a connection to the alluvial-fan aquifer if it exists in this area. North of the eastern half of this boundary is the extension of the shallow-brine aquifer through the pass between Floating Island and the Silver Island Mountains. The northern boundary of the model has ground-water flow to or from the northeast and also receives runoff from the Silver Island Mountains to the north and northwest. The horizontal thickness of this leakage boundary was set at 100 ft. The use of such a thin leakage layer effectively makes this boundary a specified-pressure boundary. Permeability was set at $1.8 \times 10^{-10}$ ft$^2$.

The shallow-brine aquifer was assumed to be in direct contact with the alluvial-fan aquifer along the northwestern boundary of the simulation region. A leakage boundary was used here. Water-table maps have shown a depression over part of the alluvial-fan aquifer, perhaps caused by pumpage of process water for the mineral-extraction plant operation. This implies that ground water flows out from the shallow-brine aquifer to the northwest and west. Water levels from the few wells in this boundary area were used to set the external potentials for the leakage-boundary segments. The horizontal thickness of the leakage boundary was set at 100 ft. This boundary is also effectively a specified-pressure boundary because of the thin leakage layer. Permeability was set at $1.4 \times 10^{-10}$ ft$^2$.

The shallow-brine aquifer also was assumed to be in contact with the alluvial-fan aquifer along the western boundary of the simulation region. A specified-pressure condition was used along this boundary. Water levels from the wells in this area and a linear density variation in the horizontal direction were used to set the pressure distribution.

The southern boundary, south of Interstate Highway 80, was simulated as a specified-pressure boundary. The middle half of the south boundary is a length of brine-collection ditch (fig. 30), whereas the east and west parts have no hydrologic or topographic features. More wells are present at this boundary, relative to the other boundaries, from which to establish heads for the pressure distribution.

The water level in the brine-collection ditch at the south boundary was not measured during the study because this ditch, which is on private property, was inaccessible. For the production season, the altitude of the head in the brine-collection ditch along the south boundary was estimated to be 4,200 ft based on water levels in wells to the north. During the recovery season, the water level was assumed to be 4,208 ft. The western and eastern parts of the south boundary were assigned piecewise linear or piecewise constant pressure distributions based on heads (figs. 31 and 32) and densities (fig. 33).

The eastern boundary has no hydrologic features, but represents the eastern limit of available data from the shallow-brine aquifer. The shallow-brine aquifer continues to the east, outside the area of primary interest and where data were not available. The connection of the simulation region with the outer basin region to the east was represented by a leakage boundary. This leakage boundary, with a 2,000-ft horizontal thickness, was used to insulate the simulation region from the uncertain spatial distribution of exterior potential. The permeability of this leakage boundary was set at $2.0 \times 10^{-10}$ ft$^2$.

The brine-collection ditch, east of the salt crust and internal to the simulation region (fig. 30), was represented as a specified-pressure boundary. The areal

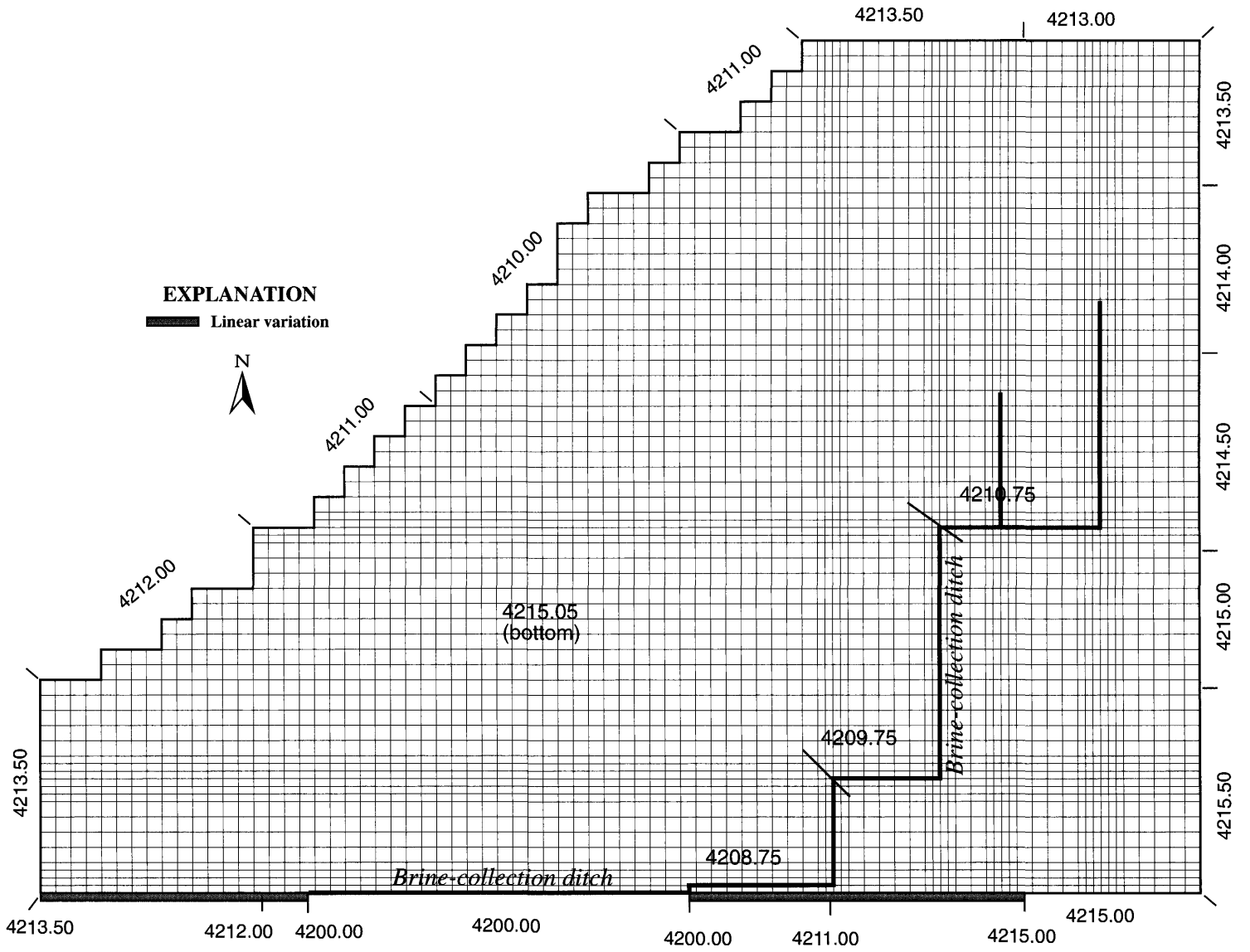


**Figure 31.** Head distribution specified along the boundaries of the simulation region for the shallow-brine aquifer during the production season, Bonneville Salt Flats, Utah.

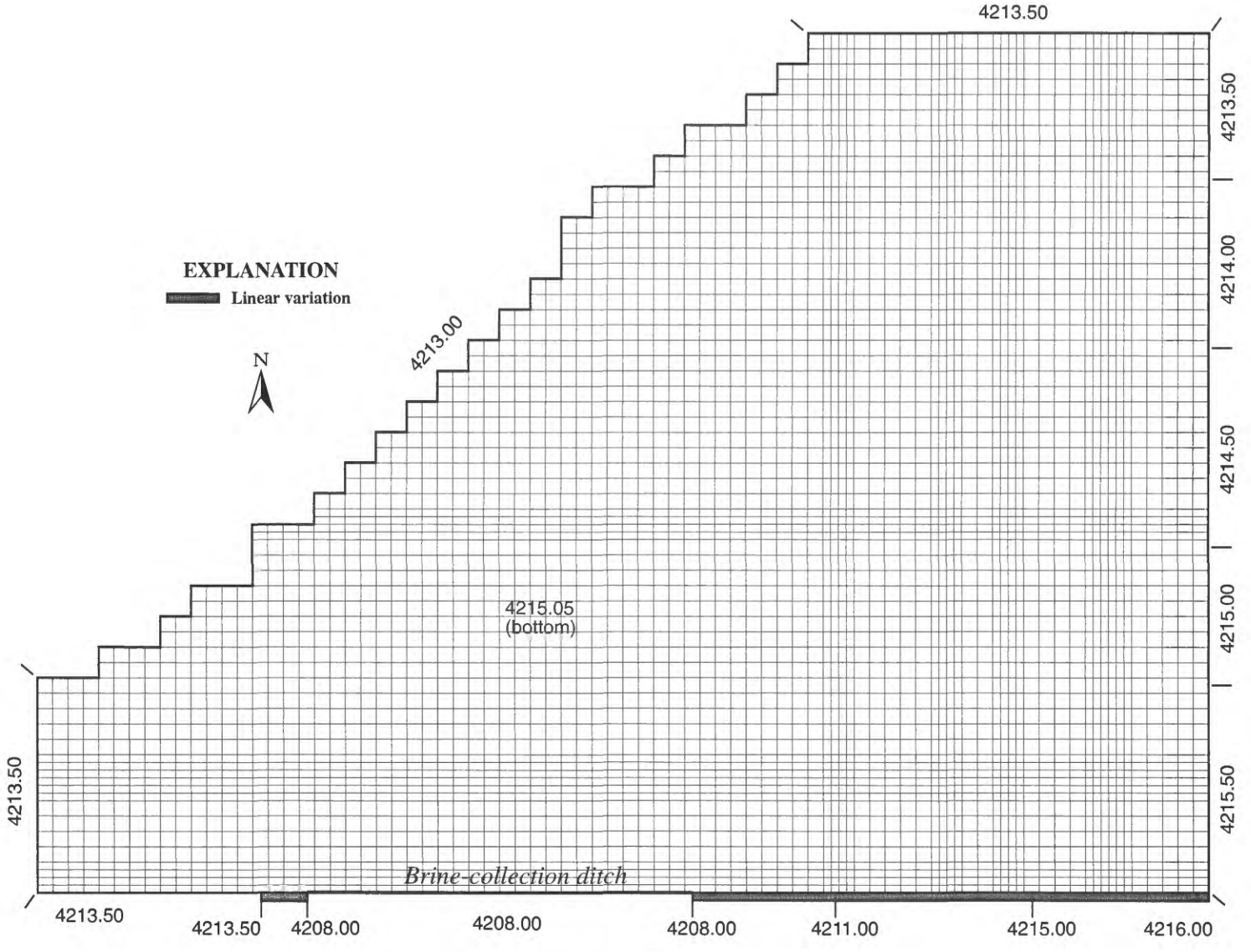


**Figure 32.** Head distribution specified along the boundaries of the simulation region for the shallow-brine aquifer during the recovery season, Bonneville Salt Flats, Utah.

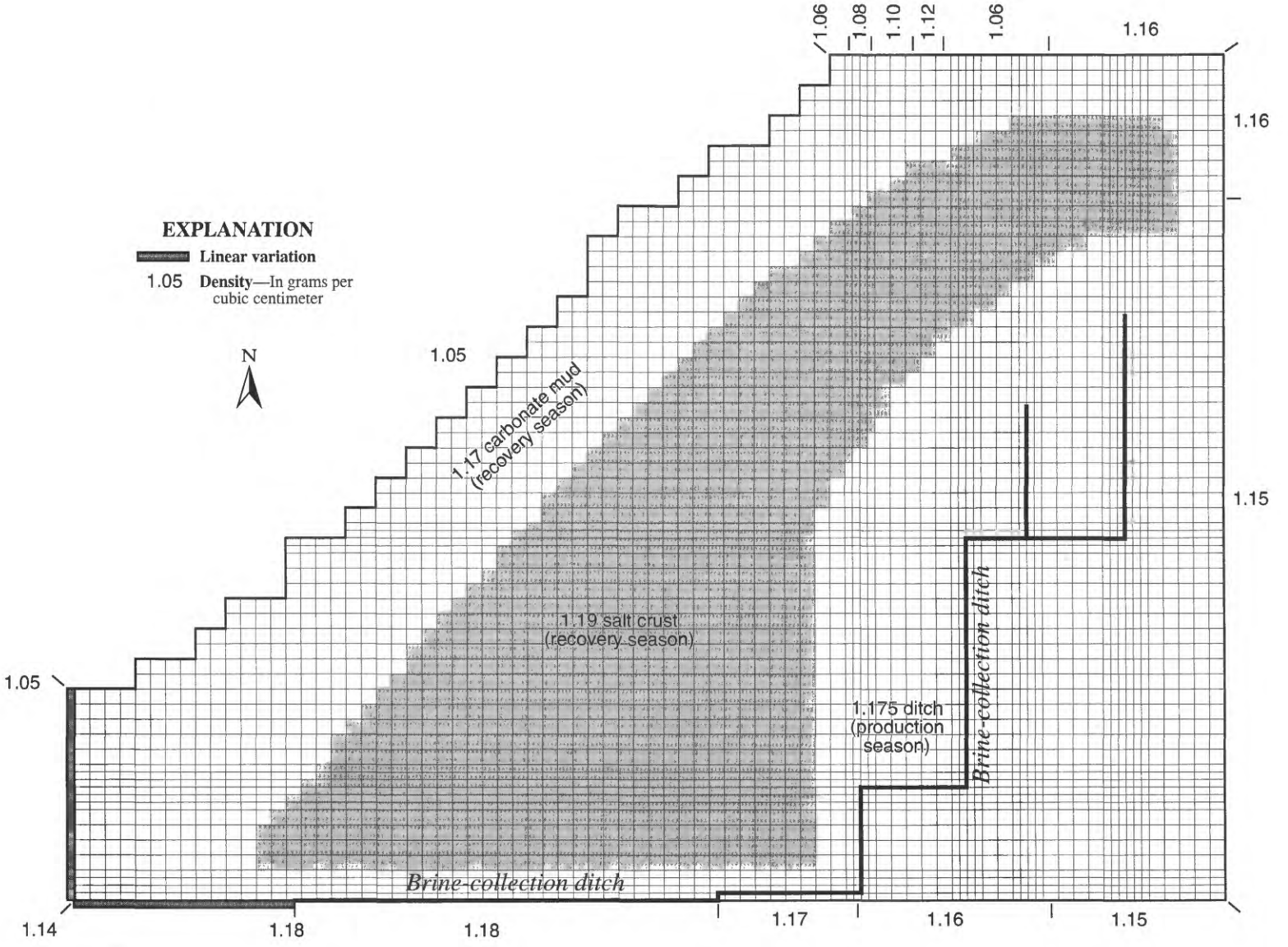


**Figure 33.** Density distribution specified along the boundaries of the simulation region for the shallow-brine aquifer during both seasons, Bonneville Salt Flats, Utah.

location of the brine-collection ditch was taken from 1:24,000-scale quadrangle maps. In the model, the areal representation of the brine-collection ditch was a sequence of line segments joining node points. Some approximations to the location of the ditch were made to align the segments with the north-south orientation of the model grid. The width of the ditch was estimated to vary from 28 ft at the land surface to 15 ft at the bottom. Actual ditch width is not represented in the model. The depth was estimated to be 16 ft, which places the ditch bottom at an altitude of 4,198 ft. Thus, it penetrates two-thirds of the thickness of the shallow-brine aquifer.

In the model, the brine-collection ditch is one cell wide, which is 500 ft at the mesh spacing employed in its vicinity. Computational limitations prevented using a finer mesh at the brine-collection ditch. The specified water level or pressure means that the ditch has instant drawdown at the beginning of the production season, which is somewhat artificial. Analytical solutions show that it takes a few days for the water level in the ditch to decline to its specified altitude. The gradually sloping water surface in the brine-collection ditch is of unknown profile. For simulation purposes, the brine-collection ditch in the model was divided into three reaches of nearly equal length, and estimates of water levels were made to approximate the sloping water surface. The initial water-level altitudes were 4,206.5, 4,207.5, and 4,208.5 ft; and these values were adjusted during the calibration process. The pressure distribution was assumed to be hydrostatic with depth, based on the average density of 1.175 g/cm$^3$ observed in the actual brine-collection ditch. The boundary condition at the brine-collection ditch east of the salt crust was removed to allow the water table to rise during the recovery season. This is clearly more realistic than imposing a pressure in the ditch during the recovery season.

The bottom boundary is at the contact between the shallow-brine aquifer and the lacustrine sediment in the upper part of the basin-fill aquifer. A leakage condition was assigned to this boundary. The shallow-brine aquifer bottom was assumed to be a horizontal plane set at 4,189 ft, which corresponds to an average shallow-brine aquifer thickness of 25 ft. Well data, locating the material contrast between the shallow-brine aquifer and the underlying lacustrine sediment of the upper part of the basin-fill aquifer, show virtually no variation of the aquifer bottom throughout most of the shallow-brine aquifer. However, along parts of the northwestern margin of the playa, the lacustrine sediment of the upper part of the basin-fill aquifer was encountered about 9 ft below land surface.

A uniform thickness of 38 ft for the semiconfining layer was chosen based on the distance between the altitude of the bottom of the shallow-brine aquifer, 4,189 ft, and the depth of the monitoring wells completed in the lacustrine sediment of the upper part of the basin-fill aquifer. The uppermost well drilled into the basin-fill aquifer at each of five locations was 63 ft below land surface. Thus, the leaky-layer thickness does not represent the actual thickness of a semiconfining layer, but, rather, a part of the upper part of the basin-fill aquifer. The exterior energy potential was determined as a spatial average from data available from four wells in the fall of 1992. Wells (B-1-17)23abd-1, -2, and -3, near the brine-collection ditch, were not used because they are influenced by ditch water levels. Data were insufficient to determine a spatial distribution of basin-fill aquifer energy potential. A uniform value was based on a water level of 4,215.05 ft and a fluid density of 1.11 g/cm$^3$. As described previously in the "Principles of variable-density groundwater flow" section of this report, the net driving force on fluid in the shallow-brine aquifer provides a calculated downward leakage into the lacustrine sediment of the upper part of the basin-fill aquifer at the five piezometer nest sites at most times of measurement. However, geochemical and isotopic data suggest upward leakage has occurred historically, as discussed previously in the "Brine chemistry and implications for ground-water flow" section of this report.

The permeability of the leaky boundary in the model at the bottom of the shallow-brine aquifer was chosen to be representative of unweathered clays, which is the type of material found in the upper part of the basin-fill aquifer. The permeability of these clays was estimated to range from $1 \times 10^{-16}$ to $1 \times 10^{-14}$ ft$^2$, and a permeability of $1.1 \times 10^{-16}$ ft$^2$ was chosen.

A water table forms the upper boundary of the shallow-brine aquifer. Its position varies in space and time in response to the dewatering and rewetting of the porous medium. Evaporation and recharge fluxes were applied to cells containing the water table or the pond surface in the model.

As described previously, a seasonal pond was simulated by using a porosity value of 1.0 and a very large permeability value that is four orders of magnitude larger than that of the underlying aquifer material. Use of any greater value of permeability in the pond

resulted in numerical instability. The longitudinal and transverse dispersivity values used for the pond were 2 x $10^5$ ft to allow salt mixing to a nearly uniform concentration.

Evaporation occurs at the land surface and from the surface pond during the summer months. Maximum evaporation flux from the land surface was estimated on the basis of the average of values calculated as net actual evaporation after subtracting rainfall. A value of 0.019 in/d (1.6 x $10^{-3}$ $ft^3/ft^2/d$) was applied over the entire upper surface of the simulation region. The evaporation rate from the seasonal pond was set at 0.10 in/d (8.0 x $10^{-3}$ $ft^3/ ft^2/d$), which was five times the maximum evaporation rate from the land surface. This higher rate is justified because over open water, the actual evaporation rate approaches the potential evaporation rate (figs. 18 and 19). Use of a higher evaporation rate over the pond increases the nonlinearity of the evaporation function by adding a discontinuity at the land surface (pond bottom). An extinction depth of 3 ft was chosen on the basis of curves from Ripple and others (1975, p. A-18) for evaporation from bare soils. The effective land-surface altitude beneath the pond was set at 4,214.25 ft for evaporation calculations. This altitude also was used for all calculations of volume of brine in the pond.

Recharge at the land surface and from the surface pond during the recovery season is assumed to be from infiltration of water that is from direct precipitation on the playa surface. Precipitation during the summer months evaporates either before or soon after infiltrating into the subsurface and therefore is not considered to be a substantial component of recharge to the shallow-brine aquifer. Winter precipitation is subject to less evaporation and provides substantial recharge. At the weather station in Wendover, the 1961-90 normal monthly precipitation during the 6 months of winter is 2.25 in. As mentioned in the "Climate" section of this report, there appears to be more precipitation at the Bonneville Salt Flats weather stations than at the Wendover weather station; however, the period of record is too short to know if this is representative over the long term. The 2.25 in. of precipitation, when applied to the playa, is more than the amount needed for recharge to the shallow-brine aquifer; the excess contributes to the formation of a surface pond. This amount of precipitation was converted into a seasonal volume of water applied to the simulation region. Initially, this recharge volume of water was apportioned between two areal zones. The corresponding precipitation rates for the 185-day recovery period were 0.034 in/d (2.8 x $10^{-3}$ $ft^3/ft^2/d$) for the salt crust and 0.0036 in/d (3.0 x $10^{-4}$ $ft^3/ ft^2/d$) for the carbonate-mud surface. This apportionment was based on Lines' (1979, p. 85) estimated ratio of 80 percent of recharge occurring on the salt crust and 20 percent on the carbonate mud.

The associated density of the recharge fluid initially was assumed to be 1.19 $g/cm^3$ for the salt crust and 1.17 $g/cm^3$ for the carbonate-mud surface. These values were assumed to approximate the density for the brine infiltrating the aquifer. Water infiltrating through the salt crust will approach halite saturation more quickly than water infiltrating through the carbonate mud, where halite crystals are not as prevalent.

### Initial Conditions for Dependent Variables

Because the ground-water system was simulated as being in a periodic steady state, the simulation results will be independent of the initial condition for the pressure field. Thus, for simplicity, a hydrostatic pressure distribution based on a flat water table at an altitude of 4,214.5 ft was used as the initial condition.

The initial condition for the solute-transport equation was a concentration distribution derived from brine-density data. The initial density distribution was developed by fitting a cubic trend surface to measured density data. The contoured cubic trend surface for the density of brine in the shallow-brine aquifer, in grams per cubic centimeter, is shown in figure 34. Density data were measured primarily in wells completed in the carbonate mud of the shallow-brine aquifer. Some density data were measured in wells completed in the perennial salt crust. Brine-density values from the salt crust were near halite saturation and those from the carbonate mud were typically below saturation. Other than the density variation mentioned previously, the amount of density profile data available was limited and failed to define a density variation with depth. Furthermore, the vertical fractures were presumed to cause vertical mixing of brine. Therefore, the initial-condition density distribution was assumed to be uniform throughout the aquifer thickness.

To obtain an initial condition for the solute-concentration field, the measured density field was transformed using the equation from Lines (1979, p. 94, fig. 45) and the definition of solute-mass fraction. Thus, the concentration is given by

$$c = 1590(\rho - 1.000) \qquad (22)$$

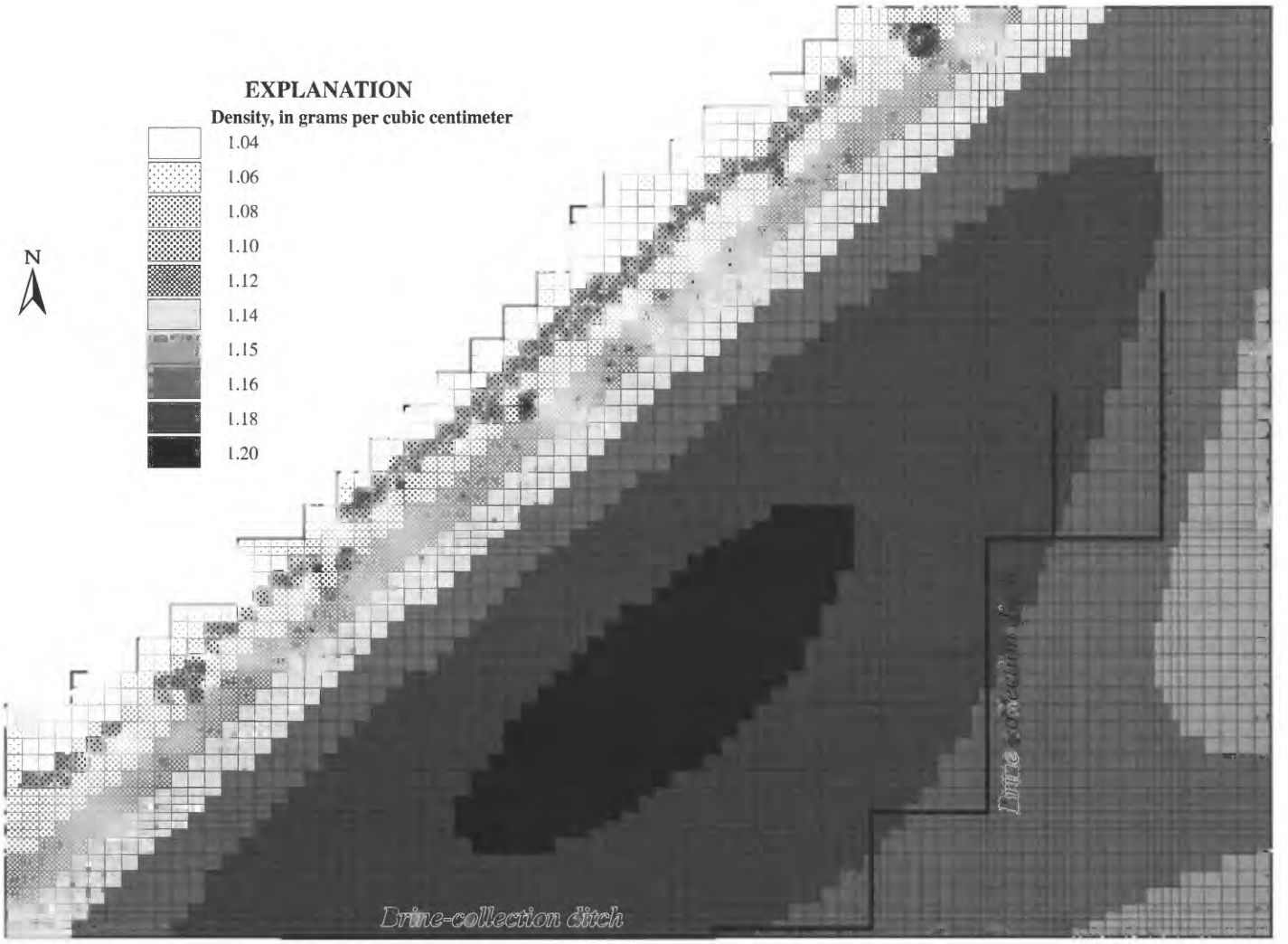


**Figure 34.** Initial-condition density field used in the model of the shallow-brine aquifer and represented by cubic trend surface, Bonneville Salt Flats, Utah

and the mass fraction is obtained from

$$w = \frac{c}{0.99823 + c} \qquad (23)$$

where

$c$ is the solute concentration (g/L);
$\rho$ is the fluid density at 20°C (g/cm$^3$);
$w$ is the solute-mass fraction (-); and
0.99823 is the density of pure water at 20°C (g/cm$^3$).

The resulting solute-concentration field is very similar in pattern to figure 34 and will not be shown here.

## Model Calibration

Model calibration refers to the procedure whereby a set of the model parameters, and possibly their distributions, are adjusted to obtain an optimal match between a set of model-output values and those observed in the actual system being simulated. The first step in model calibration is to select the set of parameters that are to be adjusted to their optimal values. Ranges are then estimated for each selected parameter, within which the search for optimal values is carried out. Some parameters are distributed in space, so the possibility of searching for the optimal spatial distribution arises. Clearly, the multitude of possible spatial distributions makes all but a limited trial of a few distributions impractical in the absence of automated parameter-estimation techniques.

Model calibration was done in the classical method of sequential parameter adjustment, by using a series of simulations in the search for optimal parameter values and distributions. It would have been more objective to use a numerical optimization procedure on a computer for model calibration, but this was beyond the scope of the study.

Model calibration consisted of seasonal transient simulations run to periodic steady state. A synthetic steady-state simulation representing average conditions for a typical year was attempted, but that approach was abandoned because of the inability to apportion the annual average boundary-condition values to uniquely represent the production and recovery seasons. Simulations to periodic steady state were run for seven annual cycles.

### Calibration Criteria

Comparisons were made between observed and model-computed results at the end of the two seasons once periodic steady state was obtained. The following criteria were chosen to evaluate the quality of the model:

1. Match the brine-production volume from the brine-collection ditch to within 10 percent of the estimated annual production volume of 1,500 acre-ft.
2. Balance the outflow volume of fluid during the production season with the inflow volume of fluid during the recovery season to within the global volumetric balance error of the simulation.
3. Obtain a reasonable match between contour patterns of the simulated water-table surface and contour patterns of measured water-level data at the end of the production season and at the end of the recovery season.
4. Create a pond with water depth of a few tenths of a foot at the end of the recovery season.

### Parameter Value and Distribution Adjustments

Several parameter values and distribution patterns were adjusted to obtain a calibrated model of the shallow-brine aquifer under the Bonneville Salt Flats. The model parameters that were selected to be adjustable for calibration were (1) aquifer permeability and porosity values and distributions; (2) water levels in the brine-collection ditch; (3) evaporation-flux values and distribution; and (4) precipitation-recharge flux values and distribution.

Permeability in the vicinity of the south boundary was lowered by modifying the digitized transmissivity distribution from Lines (1979, fig. 33) and then recalculating permeability using the density and viscosity distributions as described in the "Parameter estimation and available data" section in this report. The initial transmissivity distribution was modified only within its original range of 500 ft$^2$/d to 6,000 ft$^2$/d. During initial simulations, the computed hydraulic gradient toward the south boundary was less and extended farther north of Interstate Highway 80 than shown by measured water-level data. The transmissivity was decreased to one-sixth of its initial value in four rows of cells just north of the brine-collection ditch along the south boundary and the porosity was decreased from 0.10 to 0.07 in the same area. By decreasing both

parameters, the hydraulic gradients from the simulation more closely matched gradients calculated from measured water-level values during both the production and the recovery seasons. The reduction of these parameters is justified as a result of construction of Interstate Highway 80 as discussed previously in the "Discharge" section for the shallow-brine aquifer.

Porosity was increased from 0.10 to 0.20 in the area of the salt crust and the area between the salt crust and the brine-collection ditch to the east. This increase was to reduce an excessive rise in water levels during the recovery season and is believed to be within conceptual limits because of the large number of fractures in this area. Permeability for the shallow-brine aquifer in these areas was not changed from the initial distribution.

Permeability values were adjusted by a factor of two and porosity values by a factor of 1.5 along the northwestern margin of the playa to better match the hydraulic gradient based on measured water levels in this area. The initial simulations gave a hydraulic gradient that was too steep in the vicinity of this boundary. With the initial porosity value, simulated water levels were too high during the recovery season. Seasonally changing potentiometric heads were specified on the external boundary of the leakage layer along this boundary (figs. 31 and 32). The contour map of horizontal permeability distribution for the calibrated model after all of these adjustments is shown in figure 35. Vertical permeability was set at 0.8 of the horizontal value, as mentioned previously. The final porosity distribution included values of 0.20, 0.15, 0.10, and 0.07 and assigned to the salt crust, northwest carbonate mud, east carbonate mud, and south carbonate mud, respectively (fig. 36).

The brine-collection ditch levels were estimated to vary more than 4 ft during a typical year. Water levels measured near the booster pump south of Interstate Highway 80 ranged in altitude from 4,206 to 4,211 ft during the summer of 1992. The initial set of three water-stage levels was adjusted through this range to obtain the target brine-production volume previously reported. For the calibrated model, the brine-collection ditch water levels were 4,208.75, 4,209.75, and 4,210.75 ft.

During the model-calibration phase, maximum evaporation flux was divided into two zones (fig. 37), one for the pond/salt-crust area and one for the surrounding carbonate-mud surface. During calibration, maximum evaporation rates of 0.019 in/d (0.0016 $ft^3/ft^2/d$) from the salt crust and 0.016 in/d (0.0013 $ft^3/ft^2/d$) from the carbonate-mud surface were determined. This distribution represents a reduction from the initial uniform maximum evaporation flux. The total seasonal volume of precipitation recharge was reapportioned among four zones shown in figure 38.

Recharge rates of 0.025 in/d ($2.075 \times 10^{-3}$ $ft^3/ft^2/d$) for the salt crust, 0.012 in/d ($1.01 \times 10^{-3}$ $ft^3/ft^2/d$) for the carbonate-mud surface between the salt crust and the brine-collection ditch, 0.0078 in/d ($6.5 \times 10^{-4}$ $ft^3/ft^2/d$) for the carbonate-mud surface east of the brine-collection ditch, and 0.0050 in/d ($4.18 \times 10^{-4}$ $ft^3/ft^2/d$) for the remaining carbonate-mud surface to the northwest and north were determined as optimal. The higher recharge rates occur for the salt crust and the area between the salt crust and the brine-collection ditch. This is supported by the more fractured nature of the salt crust and the carbonate mud in this area where crystalline halite has precipitated within the carbonate-mud matrix. In addition, ponding on the carbonate-mud surface in this area increases the net recharge to more than that which applies to carbonate-mud surfaces that do not experience ponding. This four-zone distribution gave a better match of the simulated water-table configuration to measured water-table values in the vicinity of the brine-collection ditch during the recovery season and provided sufficient water for ponding in the area of the salt crust. Recall that the initial recharge distribution was over two zones with a somewhat larger value over the salt crust.

### Results of Calibration

After seven annual cycles of simulation, the maximum absolute water-table configuration changes were less than 0.06 ft for two successive production periods and less than 0.09 ft for two successive recovery periods. The volume of fluid in the system was the same as at the end of the previous cycle to within 0.3 percent of the change in volume for 1 year. Because the mass balance on the simulated system had errors of about 1.5 percent, these results were deemed accurate enough to assume that periodic steady state had been achieved for the ground-water flow system. The simulated seasonal volume of the brine-collection ditch was 1,451 acre-ft ($6.32 \times 10^7$ $ft^3$), which was well within the calibration criterion of plus or minus 10 percent of the estimated volume.

A periodic steady state for the flow system was attained after seven cycles of simulation, or 7 years. The length of time required to achieve periodic steady

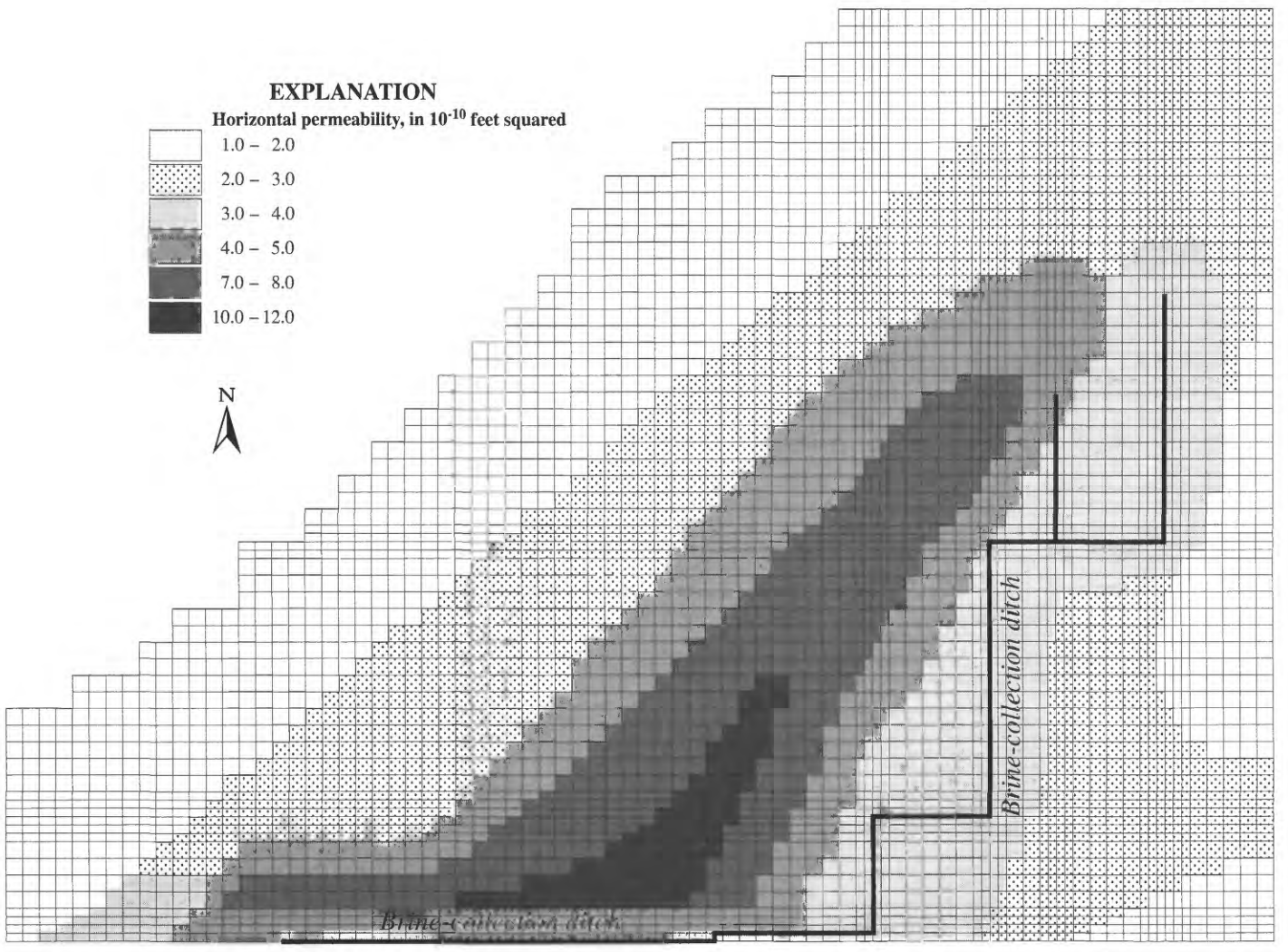


**Figure 35.** Final distribution of horizontal permeability used in the calibrated model of the shallow-brine aquifer, Bonneville Salt Flats, Utah.

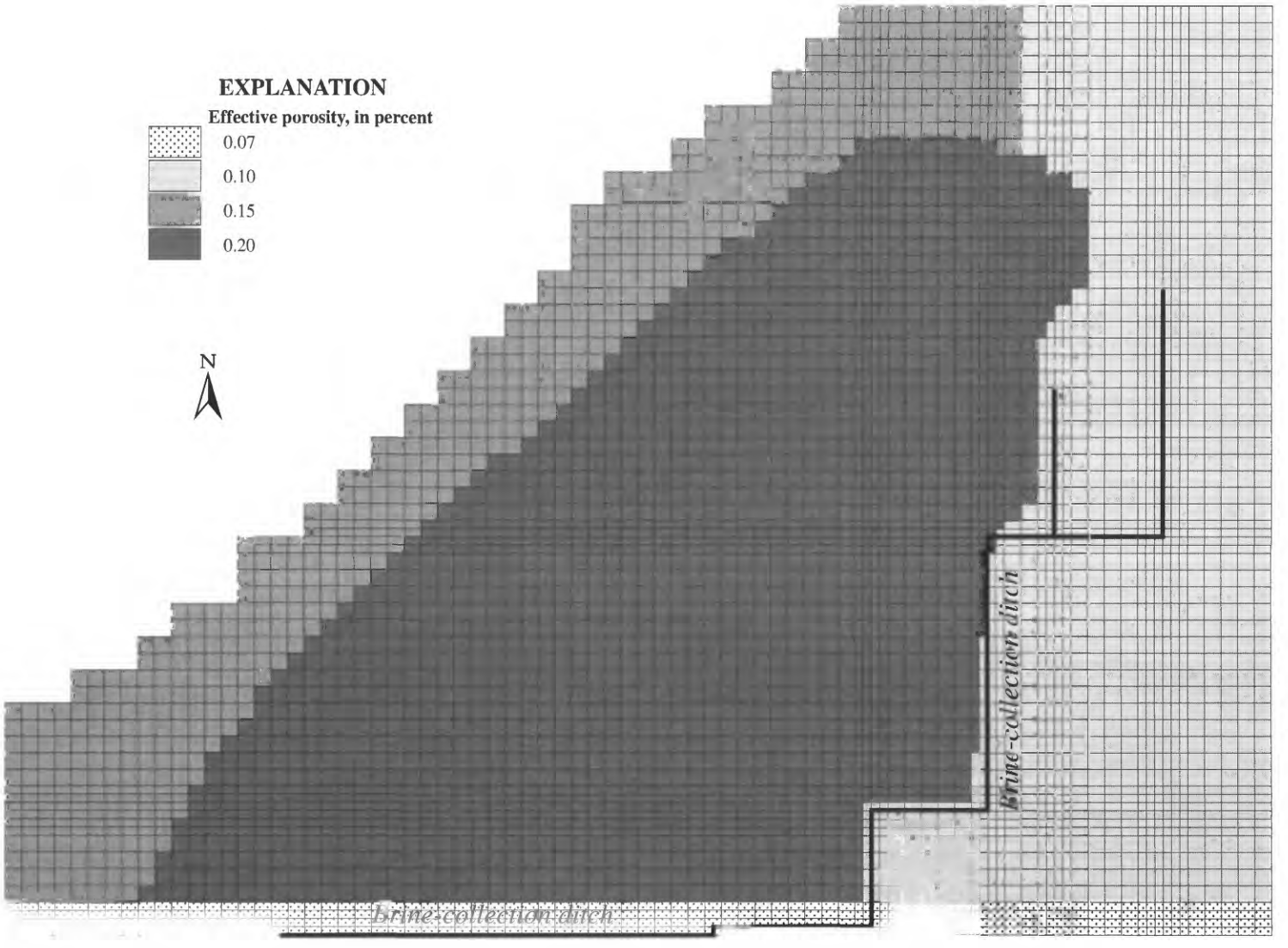


**Figure 36.** Final distribution of effective porosity used in the calibrated model of the shallow-brine aquifer, Bonneville Salt Flats, Utah.

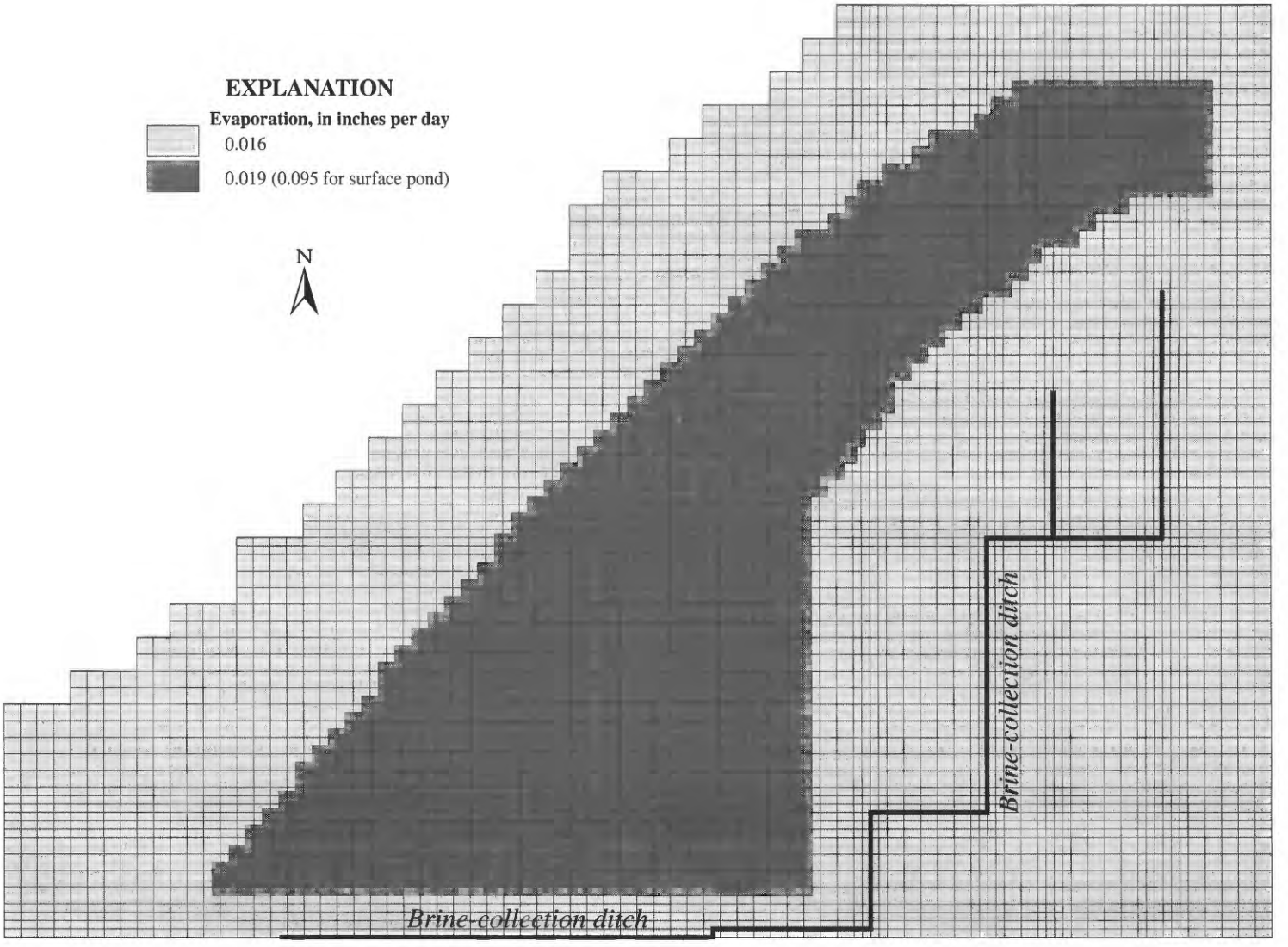


**Figure 37.** Final distribution of maximum evaporation rates used in the calibrated model of the shallow-brine aquifer during the production season, Bonneville Salt Flats, Utah.

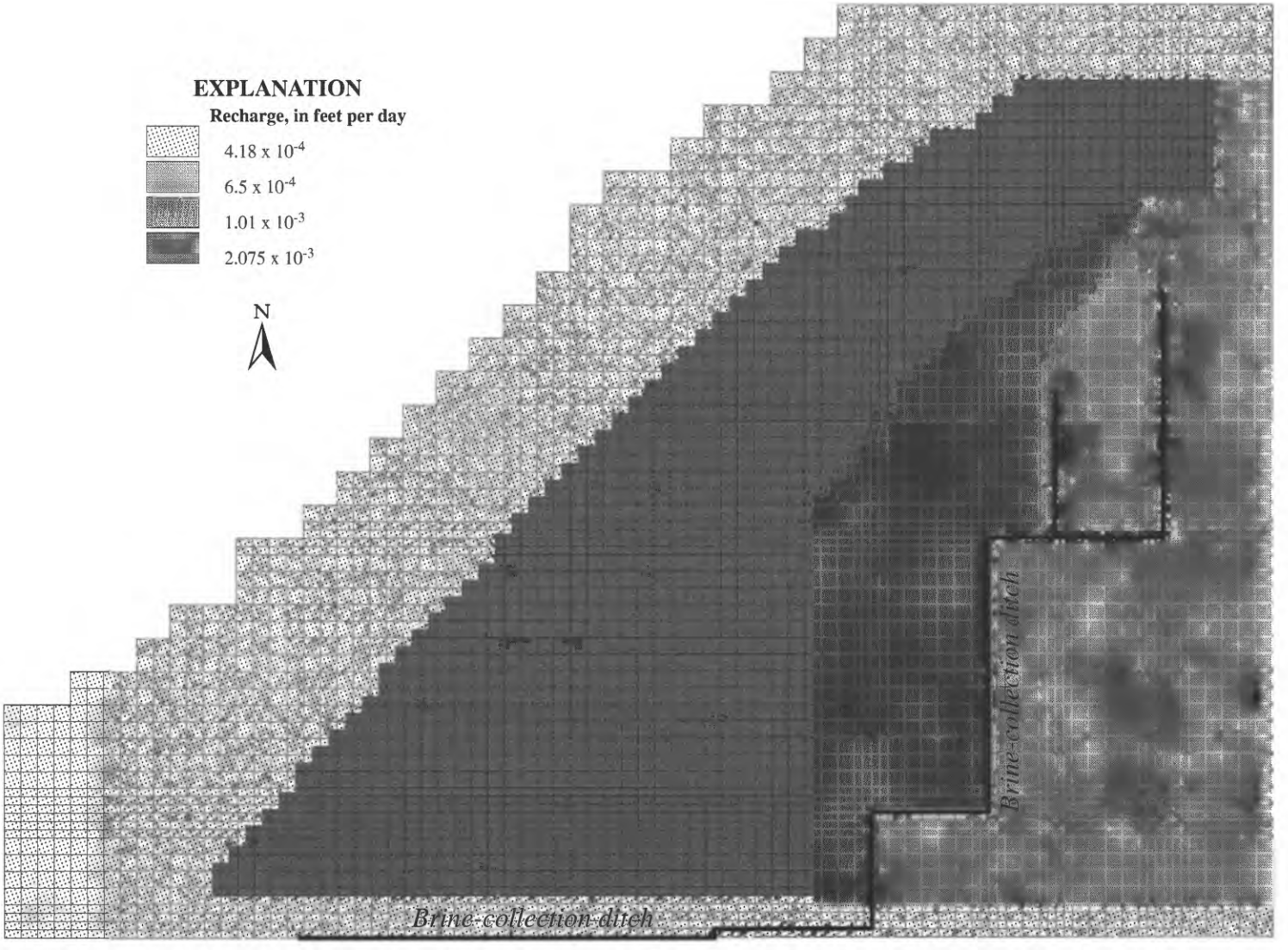


**Figure 38.** Final distribution of recharge rates used in the calibrated model of the shallow-brine aquifer during the recovery season, Bonneville Salt Flats, Utah.

state implies that the response time for the flow system is on the order of a decade. Changes in boundary-condition pressures, fluxes, or leakage parameters can be expected to affect the flow system for time on the order of a decade provided that these changes are not far from the calibrated model values. The response time for the solute-transport system is longer than for the flow system. Simulations were not run for a sufficient number of cycles to achieve periodic steady state with respect to solute concentration. The average residence time within the shallow-brine aquifer, however, was estimated to be about 120 years. This was calculated as the quotient of the maximum ground-water volume divided by the through-flow rate. The through-flow rate is the annual inflow rate or the annual outflow rate, because both must balance at periodic steady state for an annual cycle.

The periodic change in fluid volume for the calibrated model (fig. 39) includes the pond. The approach to periodic steady state is clearly seen. The net volume change over a year is a loss of 39 acre-ft. But the volumetric balance error of the simulator in the seventh year of simulation was 650 acre-ft. Therefore, the deviation from an exact steady-state volumetric balance is well within the balance error of the simulator. Thus, the second calibration criterion was met to within the accuracy of the simulation.

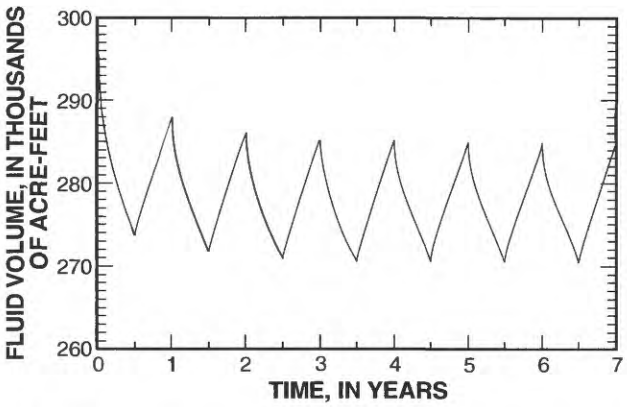


**Figure 39.** Change in total volume of fluid in the simulation region for the calibrated model of the shallow-brine aquifer during seven annual cycles, Bonneville Salt Flats, Utah.

A general increase with time can be seen in the periodic change in solute content of the ground water in the calibrated model (fig. 40). The total increase during the 7-year simulation, however, is only 1.25 percent of the solute mass in the simulation region, which is within the mass-balance error of each year of the simulation. Therefore, no further calibration was done to remove this upward trend.

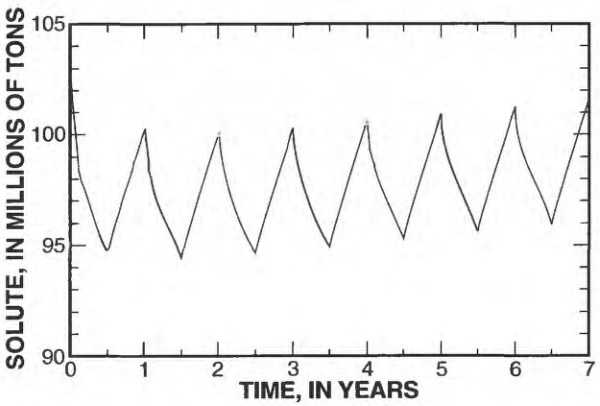


**Figure 40.** Change in total mass of solute in the simulation region for the calibrated model of the shallow-brine aquifer during seven annual cycles, Bonneville Salt Flats, Utah.

No statistical measurements were made that describe the quality of the match between the simulated water-table surface and the measured water-level data. This was because only a small set of seasonal measurements were made during a 2-year period. One of those years was much cooler and wetter than normal, which resulted in unusual conditions on the Bonneville Salt Flats. The amount and duration of ponding increased dramatically. A semi-quantitative assessment of the water-table patterns and water levels shows that the simulated water-table surfaces match the measured water-level data satisfactorily for the representative steady-state conditions and meet the third calibration criterion.

The pond at the end of the recovery season covers more than 90 percent of the pond area with a depth of more than 0.2 ft and a maximum depth near 0.4 ft. The southwestern and southeastern corners of the pond area have water depths as shallow as 0.05 ft because of boundary-condition influences. Thus the fourth calibration criterion, that of pond formation, is satisfied.

## Simulation Results

Results of the simulations from the calibrated model include water-table altitudes, density fields, and cumulative fluid volume and solute-mass amounts through the boundary surfaces. As described in the

"Modeling approach" section of this report, the goals of simulating the solute transport in the shallow-brine aquifer under the Bonneville Salt Flats were: (1) develop a fluid and solute balance for the shallow-brine aquifer in the study region, (2) evaluate the effect of brine production from the ditches on the salt crust, and (3) identify the major and minor solute fluxes to and from the shallow-brine aquifer. The first two goals are met by computing (1) a flow balance on the shallow-brine aquifer beneath the Bonneville Salt Flats, (2) a solute balance for the simulation region, and (3) a mass balance on the total crystalline salt deposit. These quantitative balances help to understand how the brine production affects the gradual disappearance of the salt crust. The third goal is achieved by examination of the cumulative flow and transport amounts calculated for each boundary face.

The set of seasonal simulations leading to a periodic steady state began with the production season. An automatic time-step control was used by the simulator starting at 0.01 days and increased to about 20 days during the simulation seasons. The main control was on the pressure change per time step, which was limited to 0.01 lbs/in$^2$ and corresponds to about 0.025 ft of water-table altitude change. The secondary control, almost never invoked, was to limit the concentration change per time step to 0.01 in solute-mass fraction. With these time-step control parameters, the overall mass-balance error for the brine was within 1.5 percent for production seasons and 0.6 percent for recovery seasons. Similar errors were obtained for the solute balance. These errors are presented as percentages of the net outflow of brine and net outflow of solute from the simulation region. Most of the errors occurred because cells became dry or rewetted and because of the nonlinearity (piecewise linearity) and explicit treatment of the evaporation boundary condition. To reduce the mass-balance error through use of shorter time steps by imposing more restrictive pressure change and solute-concentration change limits would have made simulation times excessively long.

### Dependent Variables

The dependent variables from the simulations were fluid pressure and solute-mass fraction. The pressures at the uppermost saturated cells were used to calculate a water-table altitude distribution for comparison with measured water levels. The solute-mass-fraction field was used to calculate the density distribution for the aquifer and pond brine. Other simulator outputs of primary interest were the flow rates and cumulative amounts of brine and solute that moved through the boundary surfaces of the simulation region and the mass-balance calculations for the region.

The water-table configurations at the end of the production and recovery seasons are shown in figures 41 and 42. At the end of the production season, the drawdown in the vicinity of the brine-collection ditch and along the southern boundary can be seen. Also, the gradient toward the northwest with flow to the alluvial-fan aquifer is apparent. At the end of the recovery season, the water-table drawdown in the vicinity of the brine-collection ditch has not recovered completely. Setting the water level in the brine-collection ditch along the south boundary at 4,200 ft during production and 4,208 ft during recovery has maintained a water-table slope to the south along the southern boundary. One significant result of calibration is that the high transmissivity values at the southern boundary interpreted by Lines (1979, fig. 33) appear inconsistent with the calibrated permeability values converted to equivalent transmissivity. To match the measured water levels and obtain similar head gradients along the south-ditch boundary, the transmissivity had to be reduced by a factor of one-sixth.

Net cumulative flow through the northwestern boundary reverses during the recovery season and enters the shallow-brine aquifer. The approximation for a seasonal pond, which is described in the "Model approach" section of this report, does result in the formation of a pond at the end of the recovery season with a water depth of as much as 0.4 ft as mentioned in the "Model calibration" section of this report.

At the end of both seasons, a comparison was made between the simulated vertical leakage through the bottom boundary at the five nested-well locations and the vertical leakage calculated from observed water levels and brine densities (see "Discharge" section of the "Shallow-brine aquifer" section of this report). In general, all the calculated specific-discharge fluxes were downward. The simulated specific-discharge fluxes agreed with the calculated fluxes to within factors of 1.2 to 3 for both seasons at all but one location. At wells (B-1-17)23abd-1, -2, and -3, the simulated flux was greater than the calculated flux by a factor of 7 during the recovery season. That is the only site with an observed hydraulic gradient that was sometimes in the upward direction. The simulated specific-discharge flux at the bottom boundary at the four other locations was always downward at the end of the seasons.

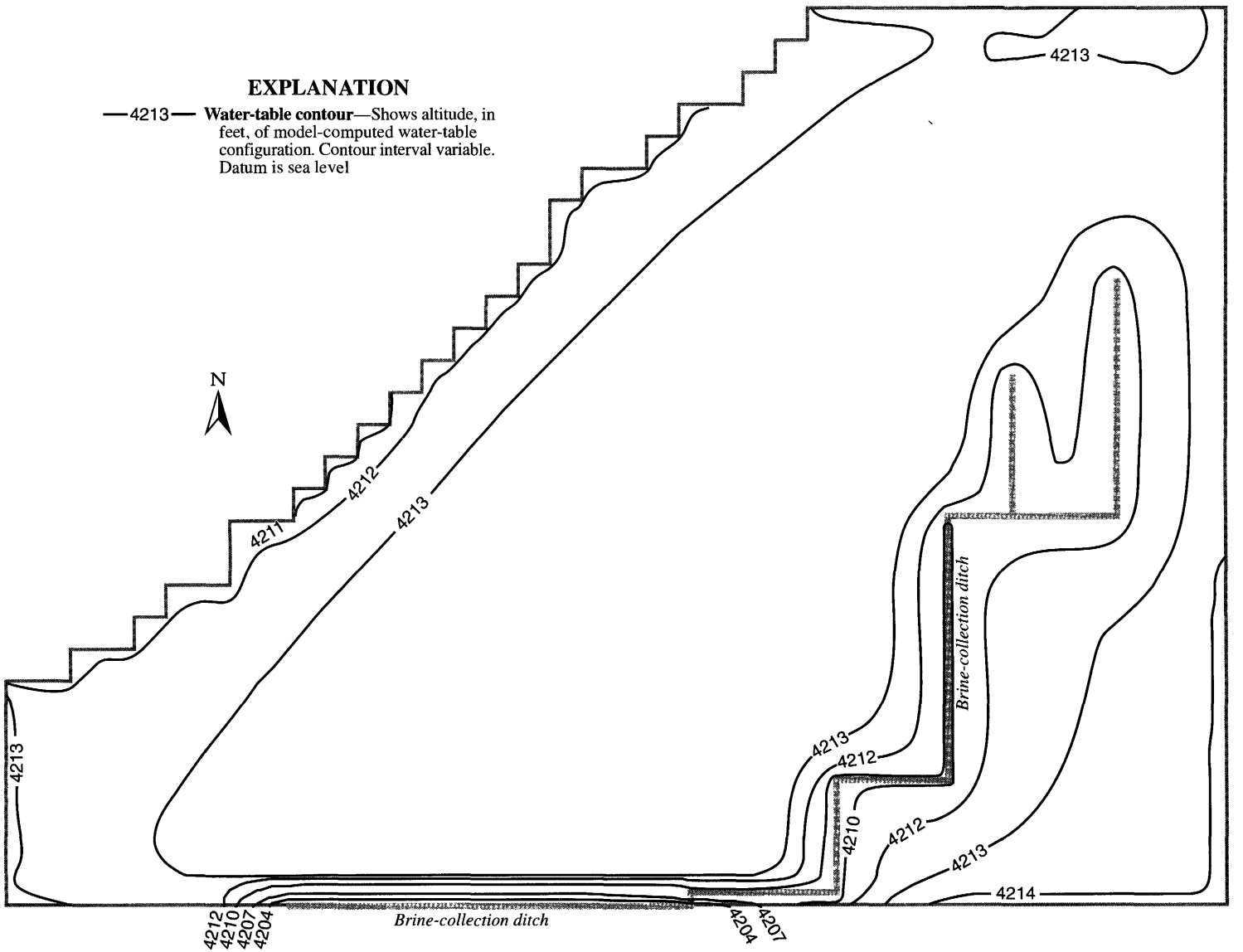


**Figure 41.** Water-table configuration at the end of the last simulated production season for the calibrated model of the shallow-brine aquifer, Bonneville Salt Flats, Utah.

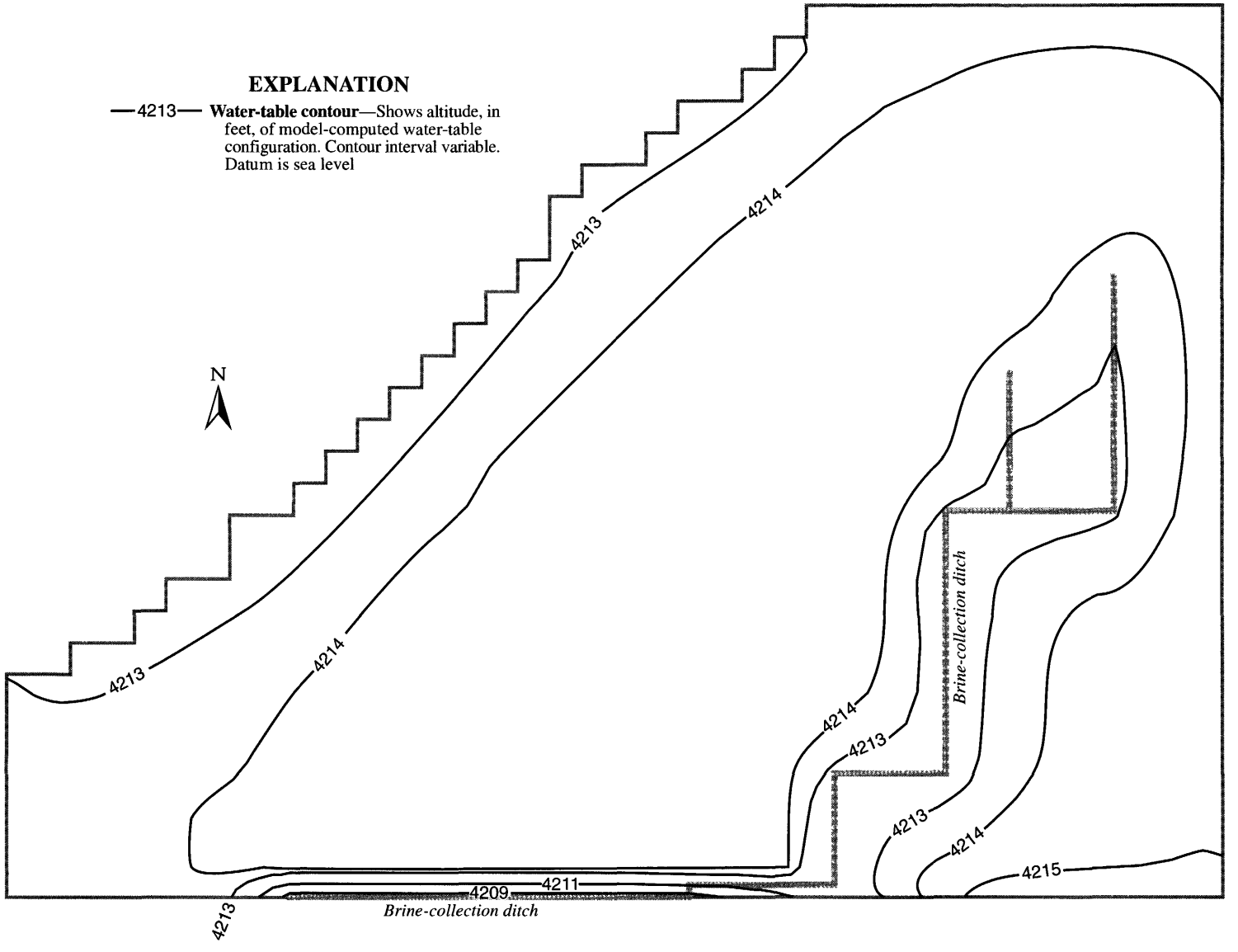


**Figure 42.** Water-table configuration at the end of the last simulated recovery season for the calibrated model of the shallow-brine aquifer, Bonneville Salt Flats, Utah.

The simulated vertical interstitial velocity above the aquifer bottom at the five nested-well locations was variable with depth. At the end of the production season there was upward flow between all cell layers at three locations, where wells (B-1-17)11aaa-1 and -2, (B-1-17)21add-3 and -4, and (C-1-18)9adc-1 and -2 are located. At the location for wells (B-1-17)23abd-1, -2, and -3, there was downward flow between all cell layers. These wells are located adjacent to the brine-collection ditch, which is probably influencing the flow direction. At the location for wells (B-1-17)31acc-1 and -7, the flow was downward from cell layers 4 to 1 and upward from cell layers 4 to 6. The reason for the split-flow directions at this location is unknown. At the end of the recovery season there was downward flow at only two locations, where wells (B-1-17)11aaa-1 and -2 and (B-1-17)31acc-1 and -7 are located. At the location for wells (C-1-18)9adc-1 and -2, there was upward flow from cell layers 1 to 4 and downward flow from cell layers 7 to 4. This location is at the southwestern end of the salt-crust/pond area, but there are no known hydrologic features to account for the split flow here.

An inspection of the simulated velocity fields at the end of each season revealed no ground-water interstitial velocities that were unusually large. Maximum interstitial velocities were less than 2 ft/d except within the pond and through the pond bottom. Interstitial velocities ranged from $10^{-4}$ to $10^{-2}$ ft/d throughout most of the simulation region.

Density fields are calculated by the HST3D simulator (Kipp, 1987) from the solute-mass-fraction fields using the linear relation of density as a function of solute-mass fraction. Because the simulated density field had only minor variation throughout the thickness of the shallow-brine aquifer (less than 0.001 g/cm$^3$), results for the density fields are presented as averages throughout the aquifer thickness. The vertically averaged density fields at the end of the last simulated production and recovery seasons are shown in figures 43 and 44. The essentially uniform density with depth is mostly caused by the large amount of vertical mixing that occurs from using a high transverse dispersivity (500 ft), which enhances vertical transport by the mostly horizontal flow in the system. In areas where vertical flow was large, there was also a large amount of vertical mixing because the longitudinal dispersivity also was 500 ft.

The density field appears to be nearly the same at the end of the production and recovery seasons. The only difference was a slightly larger mound with density greater than 1.18 g/cm$^3$ near the east-central edge of the salt crust at the end of the final production season as compared to the recovery season. The decrease of density toward the northwest is about the same as the initial condition and is maintained by runoff of fresher water from the Silver Island Mountains that provides recharge through the alluvial-fan aquifer, especially in the recovery season. The initial zone of density greater than 1.19 g/cm$^3$ has disappeared and the zone of density greater than 1.17 g/cm$^3$ has enlarged to approximately the outline of the pond and salt crust. The density contours from the initial condition in the vicinity of the brine-collection ditch have moved to reflect the influence of the ditch. A zone of density greater than 1.17 g/cm$^3$ in the southeastern corner of the simulation region is a remnant of the initial-condition density distribution and is probably not realistic. Few data were available in this area to constrain the least-squares cubic trend surface. This remnant also indicates that the solute distribution has not reached periodic steady state to the same degree as the flow system at the end of seven annual cycles.

### Cumulative Amounts

In order to present the simulated cumulative amounts of fluid and solute that flowed into and out of the shallow-brine aquifer, the volume of the region being considered needs to be defined. For accounting purposes, this volume is called the control volume. For flow and transport budget purposes, the control volume is defined as being bounded by the land surface, the bottom of the shallow-brine aquifer, and the northern, northwestern, western, southern, and eastern boundaries used in the formulation of the simulation region (fig. 30). The control volume includes the crystalline salt crust on the land surface and interbedded crystalline salt within the carbonate mud above the water table and the brine in the simulated pond. Water in the brine-collection ditch in the interior of the simulation region is excluded. The transfer of salt between the solid and liquid phase within the shallow-brine aquifer is enclosed with parentheses and not included in the totals for fluid and solute entering and leaving the control volume.

The estimated and simulated cumulative amounts of fluid and solute that passed through each boundary of the shallow-brine aquifer during a year are listed in table 4. During a typical year, most of the ground-water flow leaves the simulation region through evaporation and enters by infiltration from the playa

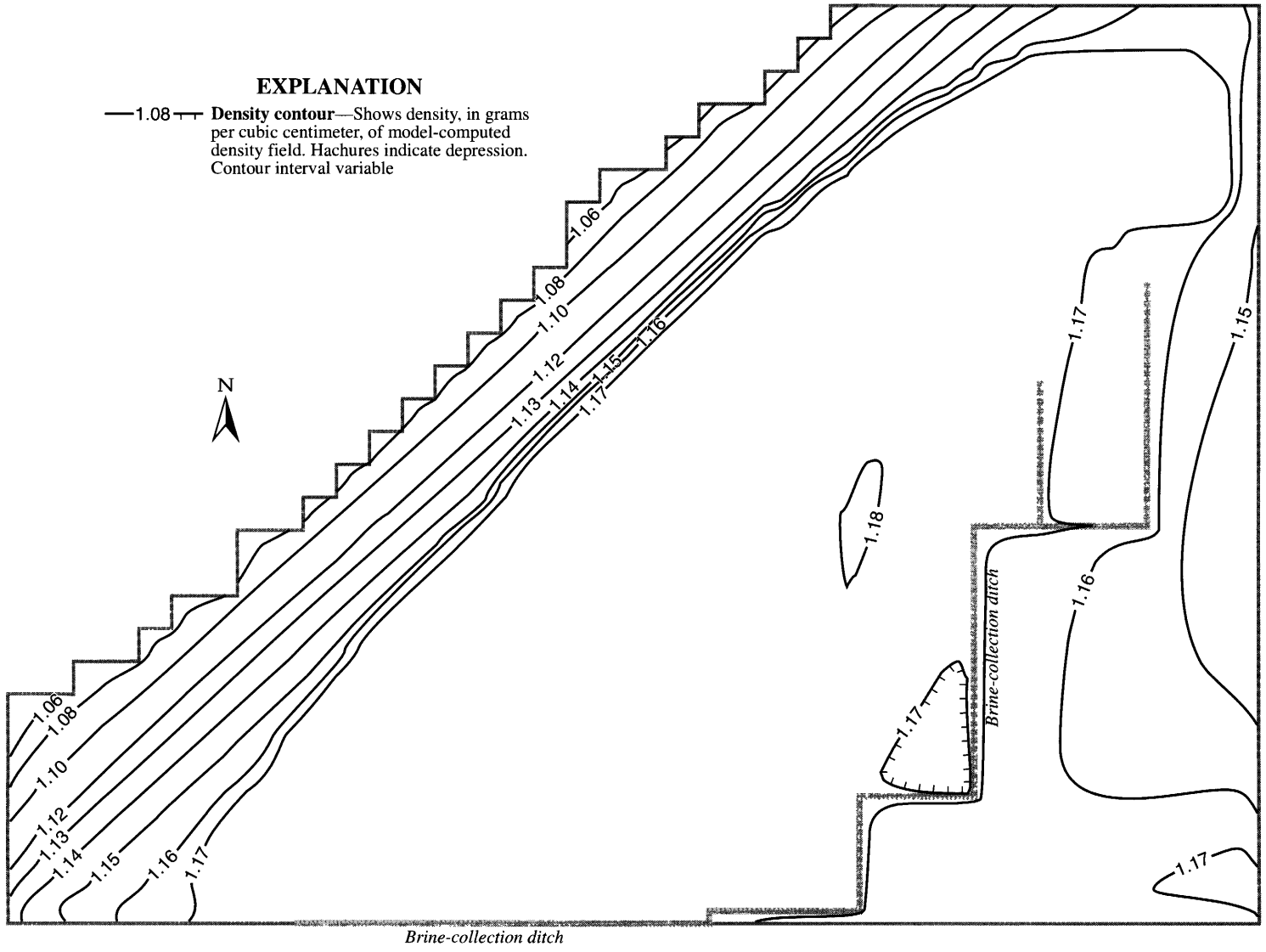


**Figure 43.** Vertically averaged density field at the end of the last simulated production season for the calibrated model of the shallow-brine aquifer, Bonneville Salt Flats, Utah.

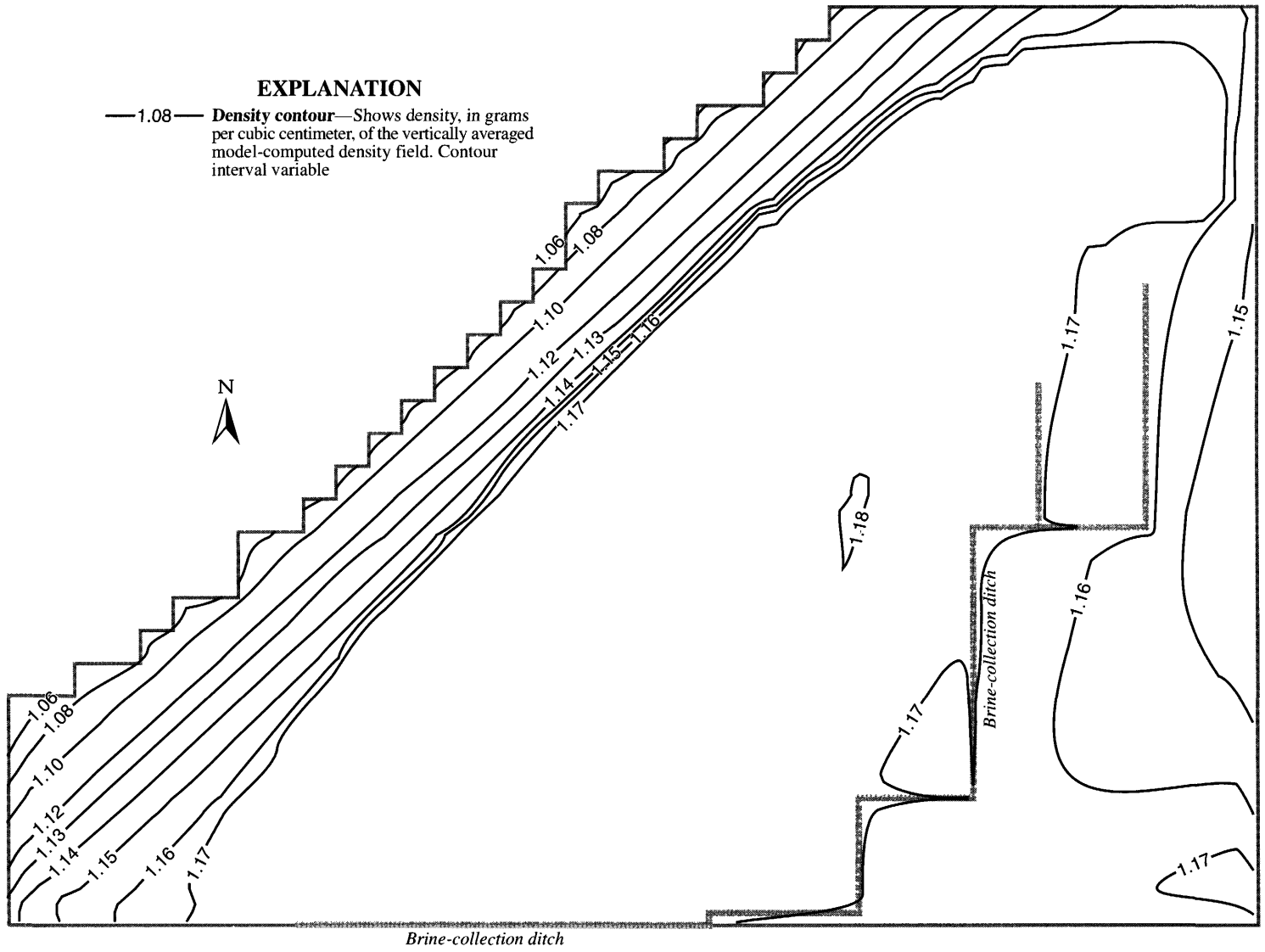


**Figure 44.** Vertically averaged density field at the end of the last simulated recovery season for the calibrated model of the shallow-brine aquifer, Bonneville Salt Flats, Utah.

**Table 4.** Estimated and simulated annual fluid flow and solute transport into and out of the shallow-brine aquifer, Bonneville Salt Flats, Utah

[—, no estimate; -, indicates direction of movement is opposite of designated category; NA, not applicable because salt not leaving shallow-brine aquifer; (), indicates value not added to total]

| Components | Current study | | Calibrated simulation | |
|---|---|---|---|---|
| | Acre-feet | Tons of solute | Acre-feet | Tons of solute |
| **Recharge** | | | | |
| Subsurface inflow from east and northeast | 60 | 21,900 | 88 | 27,750 |
| Subsurface inflow from west | — | — | 9 | -750 |
| Infiltration from playa surface | 8,300-12,800 | NA | 11,830 | (4,712,000) |
| **Total** (rounded) | 8,400-12,900 | 21,900 | 11,930 | 27,000 |
| **Discharge** | | | | |
| Subsurface outflow to south | 1,800-2,300 | 700,000-895,000 | 705 | 285,100 |
| Subsurface outflow to brine-collection ditch | 1,500 | 580,000 | 1,450 | 525,000 |
| Subsurface outflow to northwest | 35 | 13,600 | 315 | 50,590 |
| Downward leakage | 58-580 | 22,600-226,000 | 27 | 11,000 |
| Evaporation | 15,000 | NA | 10,050 | (3,742,000) |
| **Total** (rounded) | 18,400-19,400 | 1,316,000-1,715,000 | 12,550 | 872,000 |

surface. Significant amounts of brine are removed by the brine-collection ditch, located east of the salt crust, and net outflow through the southern boundary. Most of the outflow along the south boundary was toward the brine-collection ditch located south of Interstate Highway 80. There is net subsurface outflow of brine through the northwestern boundary. The remaining boundaries have minor amounts of subsurface flow. The sum of the minor inflow amounts is about 1.2 percent of the total annual inflow amount for the shallow-brine aquifer, and the sum of the minor outflow amounts is about 0.2 percent of the total annual outflow amount. The boundary-flow amounts for brine entering and leaving the simulation region are shown in a generalized block diagram (fig. 45). Note that along the western boundary, the net flow is into the shallow-brine aquifer during the recovery season, and the net solute flow is out.This is because the average density of the outflow is greater than that of the inflow.

For the calibrated model, the change in fluid volume between the end of the production season and the end of the recovery season was 14,500 acre-ft (6.3 x $10^8$ $ft^3$) or about 5 percent of the volume in the simulation region at the end of the recovery season. The pond volume at the end of the recovery season was 2,440 acre-ft (1.07 x $10^8$ $ft^3$), which is about 17 percent of the annual volumetric change of brine in the simulation region. The amount of water that evaporates from and recharges to the seasonal pond is listed in table 5 and shown in figure 45. The net flow of brine is nearly zero (4 percent of the average through flow, and 0.2 percent of the peak volumetric inventory) because the groundwater system is in periodic steady state.

The cumulative solute-mass amounts that passed through each boundary during the production and recovery seasons are listed in table 5. An imbalance of 125,000 tons/yr of solute, which represents about 0.1 percent of the peak inventory during the year, is lost from the shallow-brine aquifer. More solute is transported into and out of the seasonal pond than the sum of solute produced by the brine-collection ditch and that which is transported through the southern boundary. The boundary-flow amounts for solute also are shown in figure 45.

## Balances

For a discussion of simulation balances, amounts of fluid flow and solute transport are listed for the production and recovery seasons. The control volume for accounting purposes, however, is slightly different than the one defined previously. Because the model simulates primarily advective fluid flow and associated sol-

**Table 5.** Simulated fluid and solute inflow to and outflow from the shallow-brine aquifer and pond for the production and recovery seasons in the final year

[-, indicates direction of movement is out of shallow-brine aquifer; (), indicates value not added to total]

| Component | Production season | | Recovery season | |
|---|---|---|---|---|
| | Acre-feet | Tons of solute | Acre-feet | Tons of solute |
| South | -650 | -264,500 | -53 | -20,550 |
| Ditch | -1,450 | -525,000 | 0 | 0 |
| Northwest | -380 | -52,500 | 64 | 1,910 |
| Bottom | -13 | -5,250 | -14 | -5,750 |
| Evaporation (pond) | (-2,440) | (-933,500) | (0) | (0) |
| Evaporation (aquifer) | -10,050 | -3,742,000 | 0 | 0 |
| West | 8 | 270 | 1 | -1,020 |
| North | 17 | 4,050 | -9 | -2,450 |
| East | 35 | 11,400 | 45 | 14,750 |
| Recharge (pond) | (0) | (0) | (2,440) | (938,300) |
| Recharge (aquifer) | 0 | 0 | 11,830 | 4,712,000 |
| **Total** (rounded) | -12,500 | -4,574,000 | 11,860 | 4,699,000 |
| Subsurface outflow | 2,490 | 847,000 | 76 | 29,800 |
| Subsurface inflow | 60 | 15,700 | 111 | 16,700 |

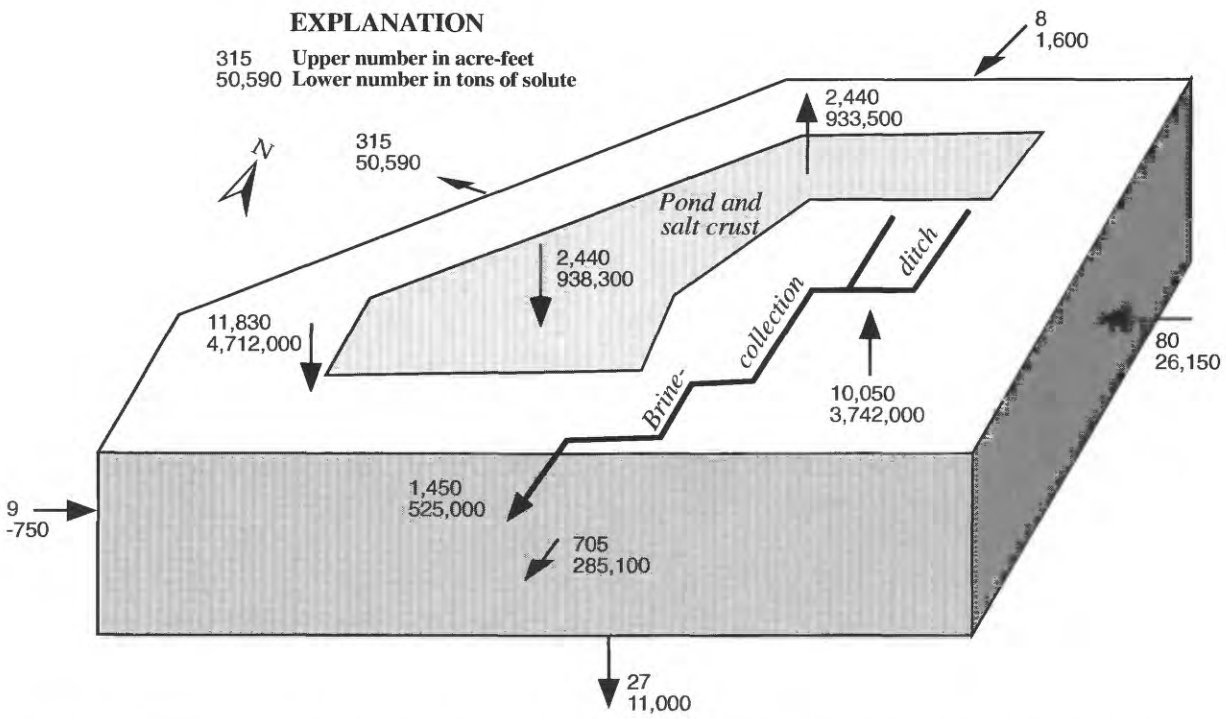


**Figure 45.** Generalized block diagram showing the direction of annual inflows and outflows of fluid and solute for the calibrated model of the shallow-brine aquifer, Bonneville Salt Flats, Utah.

ute transport into and out of the shallow-brine aquifer, the simulated seasonal pond, although part of the simulation region, is defined as a separate volume, external to the control volume. Transfers of fluid and solute to and from the simulated pond are not included in the totals that apply to the control volume and therefore are enclosed in parentheses.

As mentioned previously, global balance errors for cumulative flow and solute-transport amounts for the simulation region were 1.5 percent for the production season and 0.6 percent for the recovery season. This gives an annual balance error of about 2 percent. Because the aquifer system is in periodic steady state, net brine outflow during the production season is replenished by an excess of precipitation that recharges the aquifer during the recovery season in the winter and spring. A volumetric imbalance of about 5 percent for the shallow-brine aquifer exclusive of the seasonal pond is shown by the difference in totals for the two seasons listed in table 5. This represents the degree to which periodic steady state was not achieved.

The net subsurface outflow of solute is mostly replenished by dissolution of crystalline salt, both from the crust on the playa surface and from crystalline salt within the carbonate mud. This gives a solute inventory for the shallow-brine aquifer that is nearly in periodic steady state. A solute-mass imbalance of about 3 percent can be seen in table 5.

In all simulations (including the sensitivity cases discussed later in this report), the amount of solute entering the shallow-brine aquifer through recharge is slightly more than the amount leaving by solute transport in the subsurface. Thus, the average brine density (solute in storage) is slowly increasing during the cycles of simulation. This indicates that the specified densities of the recharging precipitation are slightly too high. An adjustment could have been made, but the drift in density is within the solute-balance error of the model. In fact, the drift in density could be considered to be a result of cumulative model error.

The evaporating brine precipitates salt at the playa surface and within interstitial pore space and small fractures above the water table within the carbonate mud and in the salt crust. The simulator calculates seasonal solute-flow amounts, which can be translated to changes in the total crystalline-salt deposit due to evaporation and precipitation fluxes during the year. Although the simulator has no salt-precipitation mechanism, the amount of salt accumulated as precipitate can be approximated by totaling the solute removed from the saturated ground-water region by the evaporation flux. This approximation neglects any effects of concentrating the brine near the water table as evaporation occurs.

Recharge by precipitation (rainfall and snowfall) dissolves salt from the crust and crystalline halite within the carbonate mud as it infiltrates down to the water table. Although the simulator lacks a salt-crust dissolution mechanism, a solute-recharge amount equal to a salt-dissolution amount for the recovery season was approximated by specifying the fluid density (solute concentration) of the recharging precipitation. This concentration must be estimated from density measurements of brine samples from the wells near the salt-crust surface. The recharging fluid is not necessarily at halite saturation and concentrations range from 1.15 to 1.20 g/cm$^3$. This gives a significant degree of uncertainty for estimating average incoming density.

The difference between the solute entering the shallow-brine aquifer and the seasonal pond through dissolution of crystalline salt during recharge in the recovery season and the solute leaving through salt precipitation upon evaporation during the production season at periodic steady state represents the crystalline-salt budget primarily for the salt crust overlying the simulation region. The crystalline-salt budget (table 5) indicates that for the calibrated model there is a net loss of crystalline salt of almost 975,000 tons during an average year of which 850,000 tons are by subsurface outflow. From model output, the global solute mass-balance error during the year is about one-quarter of this amount, so the loss of crystalline salt is partially masked by the simulator balance error.

The model adequately simulates the effects of brine withdrawal for mineral production on the solute and salt-crust balance of the system. Model simulations, which use the average rate of withdrawal from the brine-collection ditch estimated during this study, do not refute the conceptual understanding that brine withdrawal is a major cause to the loss of salt from the playa surface. Other than the cycling of fluid and solute through the playa surface with each season, subsurface fluid flow and solute transport to the south boundary and to the brine-collection ditch east of the salt crust are the largest losses of salt from the simulation region (tables 4 and 5).

## Sensitivity Analysis

A sensitivity analysis is an evaluation of the effects of changes in individual model parameters on simulation results, including specific values and distribution patterns. In principle, the pattern of distributed parameters could be varied, but sensitivity to variation of distribution patterns, and to distribution patterns themselves, can be difficult to quantify. A sensitivity analysis provides an indication of the uncertainty of the calibrated model as a function of the uncertainty of estimation of the parameters. Observations of the sensitivity of the model to variations in parameters were made throughout the calibration process. A more methodical analysis was done at the end of model calibration for selected parameters.

### Sensitivity to Model Parameter Values and Distributions

The following parameters were selected from those with greater uncertainty in estimation, or with higher observed sensitivity during the calibration process. The set of parameters for sensitivity evaluation included:

- permeability near south boundary;
- south-boundary ditch water level;
- density of infiltrating precipitation;
- evaporation rates; and
- porosity values.

The response of the simulations to the parameter variations was evaluated relative to the results obtained for the calibrated model. Because the calibration simulations were run for seven annual cycles to reach a periodic steady state, the sensitivity simulations also were run for seven cycles. In some cases, this was not long enough to reach periodic steady state for the solute distribution; however, a periodic steady state for brine flow was reached for all simulations.

The seasonal simulations for sensitivity were combined into total annual results for comparison and evaluation of the cumulative flow and solute-transport amounts. In the following discussion of sensitivity results, percentage changes in annual flow amounts and annual solute-transport amounts will be highlighted. Each percentage change will be expressed relative to the corresponding flow or solute-transport amount for the calibrated model. The minor boundary flows and solute transport will not be discussed, although on a percentage basis some of them exhibited large changes. Results are compared to those for the calibrated model and appear in a separate table for each sensitivity simulation.

#### Permeability Near South Boundary

Permeability near the south boundary was increased by a factor of 2. The water-table surface dropped at least 0.1 ft within about 10,000 ft of the brine-collection ditch along the south boundary during both seasons. The maximum drop was about 0.6 ft during the production season and 0.4 ft during the recovery season. There was an associated reduction in water-table gradient. Subsurface outflow at the southern boundary increased about 110 percent for the year (table 6). Solute production from the brine-collection ditch east of the salt crust decreased by about 6 percent. Pond volume at the end of the recovery season decreased to 1,960 acre-ft ($8.54 \times 10^7$ ft$^3$) or about 7 percent. Crystalline-salt accumulation from evaporation of seasonal ponds and from the shallow-brine aquifer during the production season decreased about 7 percent, and crystalline-salt dissolution from recharge decreased 0.3 percent. Total net annual loss of crystalline salt increased 33 percent and total net subsurface outflow of solute increased 24 percent. The change in solute inventory in the ground water at the end of the recovery season was less than 1 percent. Net subsurface outflow of fluid increased 22 percent for the simulation region.

#### Water Level in South-Boundary Ditch

The water level in the south-boundary ditch was raised to 4,203 ft during the production season and to 4,210 ft during the recovery season. The resulting water-table rise of 1 ft or more was restricted to within 1,000 ft of the brine-collection ditch along the south boundary for both seasons. The flow amount and solute-transport amount through the south boundary decreased 27 percent during the year (table 7). Solute production from the brine-collection ditch east of the salt crust increased by about 3 percent. The volume of the pond at the end of the recovery season increased about 5 percent. Total net annual loss of crystalline salt decreased about 6 percent. The change in solute inventory in the ground water at the end of the recovery season was less than 1 percent. Net subsurface outflow for the simulation region decreased 6 percent.

**Table 6.** Relation of fluid and solute components for calibrated simulation and sensitivity simulation when permeability was doubled along south boundary

[-, indicates direction of movement is opposite of designated category; (), indicates value not added to total]

| Component | Calibrated simulation | | Sensitivity simulation | |
|---|---|---|---|---|
| | Acre-feet | Tons of solute | Acre-feet | Tons of solute |
| **Recharge** | | | | |
| West | 9 | -750 | 9 | -750 |
| North | 8 | 1,600 | 8 | 1,540 |
| East | 80 | 26,150 | 80 | 25,960 |
| Recharge (pond) | (2,440) | (938,300) | (1,960) | (749,100) |
| Recharge (aquifer) | 11,830 | 4,712,000 | 12,330 | 4,883,000 |
| **Total** (rounded) | 11,930 | 4,739,000 | 12,430 | 4,910,000 |
| **Discharge** | | | | |
| South | 705 | 285,100 | 1,460 | 584,000 |
| Ditch | 1,450 | 525,000 | 1,360 | 491,200 |
| Northwest | 315 | 50,590 | 315 | 50,850 |
| Bottom | 27 | 11,000 | 26 | 10,780 |
| Evaporation (pond) | (2,440 ) | (933,500) | (1,960) | (745,900) |
| Evaporation (aquifer) | 10,050 | 3,742,000 | 9,780 | 3,629,000 |
| **Total** (rounded) | 12,550 | 4,614,000 | 12,940 | 4,766,000 |
| Total net subsurface outflow | 2,400 | 844,700 | 3,060 | 1,110,000 |
| Total net loss to crystalline salt | | 974,800 | | 1,257,000 |

### Density of Recharge Flux

Because of the uncertainty associated with the solute concentration of the infiltrating precipitation, the density associated with the precipitation-recharge flux applied to the salt crust was varied from the calibrated-model value of 1.185 g/cm$^3$. The density was increased to 1.21 g/cm$^3$ for the salt crust, but held at the calibrated value of 1.17 g/cm$^3$ for the carbonate-mud surface. The water-table configuration remained essentially the same as for the calibrated model with maximum changes of less than 0.02 ft. Recharge of dissolved solute to the shallow-brine aquifer increased 9 percent (table 8). Crystalline-salt accumulation from evaporation increased 4 percent. Ditch-production volume was virtually unchanged. Net subsurface outflow for the simulation region was unchanged, but there was a 1-percent increase in net outflow of solute. The total net annual loss of crystalline salt increased 25 percent; however, the solute mass in the ground-water system gradually increased 3 percent, which is somewhat more than a single season mass-balance error but within seven times the seasonal error. This means that the gradual increase in solute mass during the simulation was within the overall mass-balance accuracy.

The density of the recharge flux was decreased from 1.17 to 1.15 g/cm$^3$ for the carbonate-mud surface, while the density for the salt crust was held at the calibrated value of 1.185 g/cm$^3$. Again, the water-table configuration remained essentially the same. Solute production from the brine-collection ditch east of the salt crust decreased 5 percent (table 9). Recharge of solute to the shallow-brine aquifer decreased 5 percent. The amount of solute transported out through the southern boundary decreased less than 1 percent for the year. Net subsurface outflow for the simulation region was virtually unchanged, but there was a 4-percent decrease in net transport of solute out of the system. The annual net loss of crystalline salt decreased 21 percent, and the solute mass in the ground-water system decreased 1 percent.

### Maximum Rate of Evaporation

Maximum evaporation flux was increased by 20 percent of the calibrated rates throughout the simulation region. Water levels during the production season

**Table 7.** Relation of fluid and solute components for calibrated simulation and sensitivity simulation when specified level in brine-collection ditch along south boundary was raised during production and recovery seasons

[-, indicates direction of movement is opposite of designated category; (), indicates value not added to total]

| Component | Calibrated simulation | | Sensitivity simulation | |
|---|---|---|---|---|
| | Acre-feet | Tons of solute | Acre-feet | Tons of solute |
| **Recharge** | | | | |
| West | 9 | -750 | 9 | -750 |
| North | 8 | 1,600 | 8 | 1,560 |
| East | 80 | 26,150 | 80 | 26,030 |
| Recharge (pond) | (2,440) | (938,300) | (2,580) | (991,100) |
| Recharge (aquifer) | 11,830 | 4,712,000 | 11,700 | 4,639,000 |
| **Total** (rounded) | 11,930 | 4,739,000 | 11,800 | 4,666,000 |
| **Discharge** | | | | |
| South | 705 | 285,100 | 518 | 211,900 |
| Ditch | 1,450 | 525,000 | 1,500 | 545,500 |
| Northwest | 315 | 50,590 | 315 | 50,860 |
| Bottom | 27 | 11,000 | 27 | 10,560 |
| Evaporation (pond) | (2,440) | (933,500) | (2,580) | (985,700) |
| Evaporation (aquifer) | 10,050 | 3,742,000 | 10,010 | 3,723,800 |
| **Total** (rounded) | 12,550 | 4,614,000 | 12,370 | 4,543,000 |
| Total net subsurface outflow | 2,400 | 844,700 | 2,260 | 792,000 |
| Total net loss to crystalline salt | | 974,800 | | 920,600 |

dropped more than 0.1 ft for most of the region and more than 0.2 ft to the southwest, southeast, and west of the brine-collection ditch east of the salt crust. During the recovery season, water levels did not recover as much as in the calibrated model and were more than 0.1 ft lower in the pond area and more than 0.2 ft lower in the three areas listed previously. Pond volume at the end of the recovery season decreased 46 percent (table 10). Flow and solute-transport amounts through the south boundary decreased about 7 percent. Removal of solute from the shallow-brine aquifer by evaporation increased 12 percent. Production brine volume and solute mass from the brine-collection ditch decreased 3 percent. Total net annual loss of crystalline salt decreased by about 3 percent, and total net outflow of solute decreased 6 percent. The change in solute inventory in the ground water at the end of the recovery season was a decrease of 1 percent. The net subsurface outflow for the simulation region decreased 7 percent.

Maximum evaporation flux was decreased by 20 percent of the calibrated rates throughout the simulation region. The water table rose more than 0.1 ft throughout the region during the production season and rose more than 0.2 ft in the area of the salt crust. There was about a 0.3-ft rise in the southeastern area. During the recovery season, the water table in the pond area was within 0.1 ft of that of the calibrated model. The water table was more than 0.2 ft higher outside the northwestern margin of the pond and west of the brine-collection ditch and was more than 0.3 ft higher in the southeastern area. Pond volume at the end of the recovery season increased about 54 percent (table 11). Flow of brine and associated solute transport through the south boundary increased 8 percent for the year. Evaporation amounts from the shallow-brine aquifer decreased 18 percent for the brine and 14 percent for the associated solute transport. Solute production from the brine-collection ditch east of the salt crust increased 4 percent. Recharge to the shallow-brine aquifer decreased 11 percent. Total net annual loss of crystalline salt increased 2 percent, and net subsurface outflow of solute increased 7 percent. Solute inventory in the ground water at the end of the recovery season was increased by 1 percent. Net subsurface outflow for the simulation region increased 8 percent. Clearly, there is a high sensitivity to evaporation rate.

**Table 8.** Relation of fluid and solute components for calibrated simulation and sensitivity simulation when density of infiltrating fluid over salt crust was increased from 1.185 to 1.21 grams per cubic centimeter

[-, indicates direction of movement is opposite of designated category; (), indicates value not added to total]

| Component | Calibrated simulation | | Sensitivity simulation | |
|---|---|---|---|---|
| | Acre-feet | Tons of solute | Acre-feet | Tons of solute |
| **Recharge** | | | | |
| West | 9 | -750 | 9 | -745 |
| North | 8 | 1,600 | 7 | 1,400 |
| East | 80 | 26,150 | 80 | 26,000 |
| Recharge (pond) | (2,440) | (938,300) | (2,460) | (982,900) |
| Recharge (aquifer) | 11,830 | 4,712,000 | 11,830 | 5,167,000 |
| **Total** (rounded) | 11,930 | 4,739,000 | 11,930 | 5,194,000 |
| **Discharge** | | | | |
| South | 705 | 285,100 | 695 | 292,100 |
| Ditch | 1,450 | 525,000 | 1,450 | 526,500 |
| Northwest | 315 | 50,590 | 315 | 50,850 |
| Bottom | 27 | 11,000 | 29 | 12,300 |
| Evaporation (pond) | (2,440) | (933,500) | (2,460) | (976,700) |
| Evaporation (aquifer) | 10,050 | 3,742,000 | 10,060 | 3,866,000 |
| **Total** (rounded) | 12,550 | 4,614,000 | 12,550 | 4,748,000 |
| Total net subsurface outflow | 2,400 | 844,700 | 2,390 | 855,100 |
| Total net loss to crystalline salt | | 974,800 | | 1,307,000 |

**Table 9.** Relation of fluid and solute components for calibrated simulation and sensitivity simulation when density of infiltrating fluid over carbonate mud was decreased from 1.17 to 1.15 grams per cubic centimeter

[-, indicates direction of movement is opposite of designated category; (), indicates value not added to total]

| Component | Calibrated simulation | | Sensitivity simulation | |
|---|---|---|---|---|
| | Acre-feet | Tons of solute | Acre-feet | Tons of solute |
| **Recharge** | | | | |
| West | 9 | -750 | 11 | -290 |
| North | 8 | 1,600 | 10 | 2,280 |
| East | 80 | 26,150 | 84 | 27,500 |
| Recharge (pond) | (2,440) | (938,300) | (2,430) | (929,400) |
| Recharge (aquifer) | 11,830 | 4,712,000 | 11,860 | 4,486,000 |
| **Total** (rounded) | 11,930 | 4,739,000 | 11,960 | 4,515,000 |
| **Discharge** | | | | |
| South | 705 | 285,100 | 700 | 281,300 |
| Ditch | 1,450 | 525,000 | 1,440 | 500,500 |
| Northwest | 315 | 50,590 | 312 | 49,550 |
| Bottom | 27 | 11,000 | 25 | 10,340 |
| Evaporation (pond) | (2,440) | (933,500) | (2,420) | (926,100) |
| Evaporation (aquifer) | 10,050 | 3,742,000 | 10,060 | 3,710,000 |
| **Total** (rounded) | 12,550 | 4,614,000 | 12,540 | 4,552,000 |
| Total net subsurface outflow | 2,400 | 844,700 | 2,370 | 812,200 |
| Total net loss to crystalline salt | | 974,800 | | 779,300 |

**Table 10.** Relation of fluid and solute components for calibrated simulation and sensitivity simulation when evaporation rates were increased by 20 percent of the calibrated rates

[-, indicates direction of movement is opposite of designated category; (), indicates value not added to total]

| Component | Calibrated simulation | | Sensitivity simulation | |
|---|---|---|---|---|
| | Acre-feet | Tons of solute | Acre-feet | Tons of solute |
| **Recharge** | | | | |
| West | 9 | -750 | 15 | 356 |
| North | 8 | 1,600 | 26 | 6,910 |
| East | 80 | 26,150 | 100 | 32,890 |
| Recharge (pond) | (2,440) | (938,300) | (1,310) | (501,400) |
| Recharge (aquifer) | 11,830 | 4,712,000 | 12,980 | 5,129,000 |
| **Total** (rounded) | 11,930 | 4,739,000 | 13,120 | 5,169,000 |
| **Discharge** | | | | |
| South | 705 | 285,100 | 653 | 267,100 |
| Ditch | 1,450 | 525,000 | 1,400 | 507,000 |
| Northwest | 315 | 50,590 | 300 | 48,360 |
| Bottom | 27 | 11,000 | 25 | 10,360 |
| Evaporation (pond) | (2,440) | (933,500) | (1,310) | (500,600) |
| Evaporation (aquifer) | 10,050 | 3,742,000 | 11,240 | 4,190,000 |
| **Total** (rounded) | 12,550 | 4,614,000 | 13,620 | 5,023,000 |
| Total net subsurface outflow | 2,400 | 844,700 | 2,240 | 792,700 |
| Total net loss to crystalline salt | | 974,800 | | 939,800 |

**Table 11.** Relation of fluid and solute components for calibrated simulation and sensitivity simulation when evaporation rates were decreased by 20 percent of the calibrated rates

[-, indicates direction of movement is opposite of designated category; (), indicates value not added to total]

| Component | Calibrated simulation | | Sensitivity simulation | |
|---|---|---|---|---|
| | Acre-feet | Tons of solute | Acre-feet | Tons of solute |
| **Recharge** | | | | |
| West | 9 | -750 | 3 | -2,150 |
| North | 8 | 1,600 | -13 | -4,520 |
| East | 80 | 26,150 | 54 | 17,450 |
| Recharge (pond) | (2,440) | (938,300) | (3,770) | (1,446,000) |
| Recharge (aquifer) | 11,830 | 4,712,000 | 10,520 | 4,184,000 |
| **Total** (rounded) | 11,930 | 4,739,000 | 10,560 | 4,195,000 |
| **Discharge** | | | | |
| South | 705 | 285,100 | 760 | 304,600 |
| Ditch | 1,450 | 525,000 | 1,510 | 546,500 |
| Northwest | 315 | 50,590 | 334 | 54,220 |
| Bottom | 27 | 11,000 | 29 | 11,760 |
| Evaporation (pond) | (2,440) | (933,500) | (3,770) | (1,422,000) |
| Evaporation (aquifer) | 10,050 | 3,742,000 | 8,600 | 3,212,000 |
| **Total** (rounded) | 12,550 | 4,614,000 | 11,230 | 4,129,000 |
| Total net subsurface outflow | 2,400 | 844,700 | 2,590 | 906,300 |
| Total net loss to crystalline salt | | 974,800 | | 996,000 |

### Porosity Values

The porosity value for each of the four zones was increased by 30 percent of the calibrated value. The water table at the end of the production season rose more than 0.1 ft in the pond area and the southeastern area and more than 0.2 ft in the vicinity of the brine-collection ditch along the southern boundary. At the end of the recovery season, the water table in the vicinity of the brine-collection ditch east of the salt crust and in the southeastern area was more than 0.2 ft lower than in the calibrated model. At the end of the recovery season, the water table was lower than the calibrated model by more than 0.2 ft for most of the region except near the brine-collection ditch east of the salt crust. Pond volume at the end of the recovery season decreased about 11 percent (table 12). Flow and solute-transport amounts through the southern boundary decreased about 1 percent. Solute production from the brine-collection ditch east of the salt crust increased 3 percent. Increasing the porosity increased the inventory of solute in the ground-water system from the beginning of the simulation. This increase persisted throughout the approach to periodic steady state and resulted in a 28-percent increase. The net annual loss of crystalline salt increased by 1 percent.

Porosity values were decreased by 30 percent of the calibrated values. Water levels at the end of the production season were more than 0.2 ft lower near the brine-collection ditch along the southern boundary and about 0.1 ft lower elsewhere except near the brine-collection ditch east of the salt crust, where levels were mostly unchanged. After the recovery season, water levels were more than 0.1 ft lower in the area of the pond and more than 0.4 ft higher in the southeastern area. At the brine-collection ditch east of the salt crust, water levels were about 0.5 ft higher than for the calibrated model. Pond volume at the end of the recovery season decreased about 15 percent (table 13). Flow and solute-transport amounts through the southern boundary increased 2 percent for the year. Production from the brine-collection ditch east of the salt crust decreased 4 percent. The inventory of solute in the ground-water system decreased 28 percent. The net annual loss of crystalline salt decreased by about 7 percent. Note that the water levels specified for the ditch along the southern boundary and the brine-collection ditch east of the salt crust are probably not realistic with this variation in porosity.

## Discussion

Total net subsurface outflow of solute from the shallow-brine aquifer for each sensitivity simulation and for the calibrated model is shown in figure 46. Because the solute content of the shallow-brine aquifer is assumed to be in periodic steady state, total subsurface outflow of solute is equal to total subsurface inflow of solute plus whatever amount of solute from the dissolution of crystalline salt is necessary to balance total subsurface outflow.

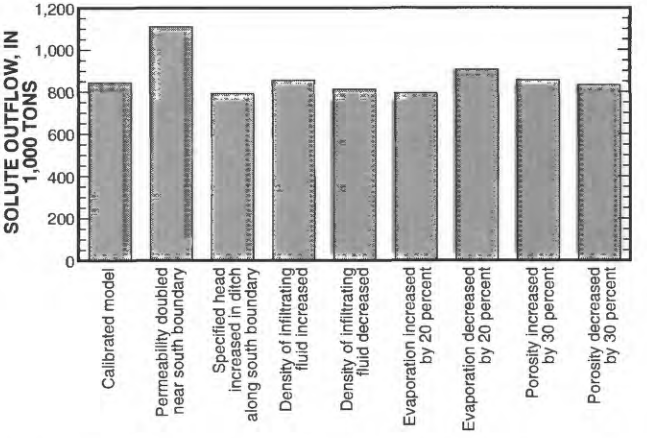


**Figure 46.** Total subsurface solute outflow for the calibrated model of the shallow-brine aquifer and for each sensitivity simulation, Bonneville Salt Flats, Utah.

Subsurface outflow of solute increased the most for the simulation where the permeability in the vicinity of the southern boundary was increased. It was moderately increased for the simulation of decreased evaporation. Moderate decreases in subsurface outflow of solute occurred in the simulations where water levels in the brine-collection ditch along the southern boundary were increased, evaporation flux was increased, and density of recharging fluid was decreased. The other sensitivity simulations resulted in little change in the amount of subsurface outflow of solute.

Subsurface outflow of brine and associated solute transport was most sensitive to the permeability in the vicinity of the southern boundary. This was caused mostly by the simulated low water levels maintained in the brine-collection ditch along that boundary. The annual loss of crystalline salt was most sensitive to the permeability in the vicinity of the southern boundary and to the density (solute concentration) of recharge infiltrating from the playa surface. Unfortunately, measurements of the density for this recharge could not be

**Table 12.** Relation of fluid and solute components for calibrated simulation and sensitivity simulation when effective porosity was increased by 30 percent of the calibrated distribution

[-, indicates direction of movement is opposite of designated category; (), indicates value not added to total]

| Component | Calibrated simulation | | Sensitivity simulation | |
|---|---|---|---|---|
| | Acre-feet | Tons of solute | Acre-feet | Tons of solute |
| **Recharge** | | | | |
| West | 9 | -750 | 10 | -490 |
| North | 8 | 1,600 | 8 | 1,890 |
| East | 80 | 26,150 | 82 | 26,980 |
| Recharge (pond) | (2,440) | (938,300) | (2,180) | (831,700) |
| Recharge (aquifer) | 11,830 | 4,712,000 | 12,110 | 4,801,000 |
| **Total** (rounded) | 11,930 | 4,739,000 | 12,210 | 4,829,000 |
| **Discharge** | | | | |
| South | 705 | 285,100 | 696 | 281,800 |
| Ditch | 1,450 | 525,000 | 1,500 | 541,000 |
| Northwest | 315 | 50,590 | 316 | 49,810 |
| Bottom | 27 | 11,000 | 27 | 10,840 |
| Evaporation (pond) | (2,440) | (933,500) | (2,180) | (833,000) |
| Evaporation (aquifer) | 10,050 | 3,742,000 | 10,300 | 3,815,000 |
| **Total** (rounded) | 12,550 | 4,614,000 | 12,840 | 4,698,000 |
| Total net subsurface outflow | 2,400 | 844,700 | 2,440 | 855,100 |
| Total net loss to crystalline salt | | 974,800 | | 984,700 |

**Table 13.** Relation of fluid and solute components for calibrated simulation and sensitivity simulation when effective porosity was decreased by 30 percent of the calibrated distribution

[-, indicates direction of movement is opposite of designated category; (), indicates value not added to total]

| Component | Calibrated simulation | | Sensitivity simulation | |
|---|---|---|---|---|
| | Acre-feet | Tons of solute | Acre-feet | Tons of solute |
| **Recharge** | | | | |
| West | 9 | -750 | 8 | -1,310 |
| North | 8 | 1,600 | 5 | 788 |
| East | 80 | 26,150 | 73 | 24,210 |
| Recharge (pond) | (2,440) | (938,300) | (2,800) | (1,083,000) |
| Recharge (aquifer) | 11,830 | 4,712,000 | 11,480 | 4,547,000 |
| **Total** (rounded) | 11,930 | 4,739,000 | 11,570 | 4,571,000 |
| **Discharge** | | | | |
| South | 705 | 285,100 | 717 | 290,100 |
| Ditch | 1,450 | 525,000 | 1,390 | 503,500 |
| Northwest | 315 | 50,590 | 318 | 53,870 |
| Bottom | 27 | 11,000 | 28 | 11,390 |
| Evaporation (pond) | (2,440) | (933,500) | (2,810) | (1,080,000) |
| Evaporation (aquifer) | 10,050 | 3,742,000 | 9,720 | 3,645,000 |
| **Total** (rounded) | 12,550 | 4,614,000 | 12,160 | 4,504,000 |
| Total net subsurface outflow | 2,400 | 844,700 | 2,370 | 835,200 |
| Total net loss to crystalline salt | | 974,800 | | 905,000 |

made. The inventory of solute in the shallow-brine aquifer was most sensitive to aquifer-porosity distribution. For a given configuration of boundary-condition water levels and a similar water table, the volume of brine and associated solute content varied directly with aquifer porosity.

All of the sensitivity simulations resulted in a total net loss of crystalline salt over the average year. This supports the hypothesis that the present configuration of average water levels in the brine-collection ditches east of the salt crust and along the southern boundary contribute substantially to the loss of crystalline salt from the Bonneville Salt Flats.

### Improved Calibration

It was possible, because of the sequential nature of the model-calibration procedure, that one or more of the sensitivity tests would produce a model that is more closely calibrated to the Bonneville Salt Flats system. Two of the above sensitivity simulations produced such a result: (1) the simulation with lower density for recharge through the carbonate-mud surface, and (2) the simulation with lower porosity values. The improvement obtained was a reduced rate of the gradual increase of solute in the shallow-brine aquifer during the simulations. The recovery of the water table in the carbonate-mud area east of the brine-collection ditch also was improved with the lower porosity values.

## Limitations of the Model

The hydrologic system of the Bonneville Salt Flats is complex and cannot be uniquely defined with the available data. In this respect, it is similar to most other basin-scale hydrologic systems. The model of the shallow-brine aquifer described in this report is based on the numerical solution of finite-difference approximations to the equations of flow and solute transport under variable-density conditions. As with every simulator, simplifying assumptions and approximations, as presented in the "Modeling approach" section of this report, mean that certain mechanisms are not realistically represented. Scarcity of data also means that any actual system will not be completely and accurately simulated in every feature.

Limitations of the present model of the shallow-brine aquifer in the Bonneville Salt Flats flow system include:

- Approximating the pond as a fixed areal region of very high permeability and 100-percent porosity, rather than as a surface-water feature coupled to the ground-water system;
- Having no mechanism for salt precipitation and dissolution at the land surface and above the water table;
- Representing the brine-collection ditches as a specified-pressure boundary rather than as a surface-water feature coupled to the ground-water system;
- Approximating flow in the fractured clay and salt media as equivalent porous media;
- Being constrained by the maximum horizontal mesh dimension to a longitudinal dispersivity of 500 ft;
- Accepting a 1.5-percent brine-flow and solute-transport balance error in the simulations;
- Approximating the simulation region as isothermal;
- Extrapolating and interpolating the distributions of porous-media properties, water levels, pressures, densities, and boundary-condition parameters from very sparse data in some areas; and
- Simplification of the transient system into two representative seasons, thus excluding system changes on a daily or monthly time scale.

The seasonal pond was approximated as a zone of the porous-media aquifer with 100-percent porosity and very high permeability within the simulation region. The development of a method for simulating the seasonal pond as a coupled, open body of water to the ground-water flow system was beyond the scope of this study. The approximation made the free surface of the pond vary more than about 0.2 ft throughout most of the pond area, with a decline of 0.3 ft in the southwestern and southeastern corners instead of being completely horizontal. However, it is believed that this inaccuracy does not significantly affect the overall balance results.

The HST3D simulator has no mechanism for concentration of solute in the fluid as evaporation takes place. Instead, the solute in the evaporating fluid is lost from the simulation region. This is essentially what happens when salt is precipitated to the solid phase at an evaporation surface, however, the actual system experiences a concentrating effect until saturation is reached. Data were not available to verify the forma-

tion of denser fluid in the vicinity of the evaporation surface; therefore, a solute-concentrating mechanism was not formulated for the HST3D simulator. Similarly, no data were available to quantify the salt-crust dissolution rates upon application of recharge from precipitation. Without these data, a dissolution mechanism could not be formulated accurately in the simulator. The primary effect of the lack of a solute-concentrating mechanism is that a layer of denser brine at the evaporating water-table surface does not form in the simulations. Because little vertical density variation was measured in the shallow-brine aquifer, and in view of the overall model objectives, lack of this mechanism is not a serious limitation to the model. The effect of a lack of a dissolution mechanism means that the densities of recharge from precipitation had to be estimated and specified as a model-boundary condition. In view of the sensitivity of the rate of net annual loss of crystalline salt to this parameter, it is unfortunate that definitive data could not be measured.

Simulation of brine-collection ditches as open bodies of water coupled to the ground-water flow system, similar to the pond, would have been more desirable. The consequence of representing the brine-collection ditches as specified-pressure boundaries was an instantaneous drawdown of the water table at each brine-collection ditch at the start of the production season. This approximation was of little consequence on the overall seasonal balances for the system because the response time for drawdown was estimated to be a few days, which is short relative to the 6-month production season.

Representing the fractured salt crust and carbonate mud that form the shallow-brine aquifer as equivalent porous media was necessary because data were not available to characterize the medium as a fractured system. Furthermore, no simulator of variable-density, ground-water flow was available that simulates fractured systems. Again, for the purposes of obtaining volumetric brine and solute-mass balances, this approximation is regarded as acceptable. However, for time of travel calculations and flow-path location, the potential for serious error is substantial.

The maximum horizontal mesh dimension of 1,000 ft constrained the minimum longitudinal dispersivity to 500 ft. Because the HST3D simulator treats dispersion as isotropic, this value of longitudinal dispersivity also applied to solute transport associated with vertical recharge flows. With an aquifer thickness of only 25 or 26 ft, this dispersivity value produced rapid mixing of any solute-concentration profiles over the aquifer thickness. Mixing occurs on the time scale of a few days; therefore, during a 6-month simulation season, the model does not sustain any vertical density gradients that might be present in the actual shallow-brine aquifer. However, as mentioned in the "Modeling approach" section of this report, numerous vertical fractures traverse the thickness of the shallow-brine aquifer, which probably produce a high degree of vertical mixing. Furthermore, field data show no significant gradients of density distribution with depth beneath the salt crust in the shallow-brine aquifer.

Having a global mass-balance error for flow and solute transport of about 1.5 percent for the production season and about 0.6 percent for the recovery season sets a limit on the accuracy of the simulations. Accuracy limitations mean that a periodic steady-state flow and solute transport could be achieved only to within about 2 percent. The development of more implicit algorithms for the evaporation and the water-table movement calculations for drying and rewetting of cells, which could have reduced this problem, was beyond the scope of the study. Simulation times would have become excessive if more stringent time-step controls had been applied to reduce the global mass-balance error.

Although temperature measurements were made when brine samples were withdrawn from the wells, insufficient spatial and temporal data on thermal properties and boundary conditions were available to simulate heat transport in the shallow-brine aquifer. A consequence of neglecting heat transport is that thermal-buoyancy effects were not represented in the model. No data were obtained to identify if this flow mechanism exists at the study site in the shallow-brine aquifer.

Because every model of a basin-scale aquifer system is based on insufficient data to some degree, data interpolation and extrapolation need to be done over large distances relative to the model dimensions. Some data must be estimated from offsite information. These limitations restrict the accuracy with which the model represents the actual system being studied. In the present study, no data were available to quantify the permeability of the lacustrine sediment beneath the shallow-brine aquifer. Permeability of the shallow-brine aquifer had to be estimated in the northwestern, northern, and northeastern parts of the simulation region. Measurement of water level and flow in the brine-collection ditch along the southern boundary,

which is on private property, was not possible. Because most of the precipitation and evaporation data obtained in the study area were collected during either an unusually cool, wet year or hot, dry year, evaporation rates were either less than or greater than normal. Estimates of typical conditions had to be made from short data records obtained near the end of the study period. These are examples of sparse data used to formulate the model of the shallow-brine aquifer.

Simplification of the transient system into two representative seasons with representative parameters for boundary conditions means that no historical period of record could be matched by the simulation. It was impractical to collect data on the time scales of days and weeks for this study. Lack of long-term data on the historical variability of the climatic environment during previous years also led to the average season approximation. However, this simplification is consistent with the goals of the simulations, which involved a time scale on the order of years to decades.

The set of boundary-condition types and parameters and the parameter distributions internal to the model are not a unique calibration, as is true for all field-scale ground-water models. A different combination of parameter values and boundary-condition types may yield similar results for calibration criteria, including production from brine-collection ditches and water-table configurations.

## NEED FOR ADDITIONAL STUDY

The hydrology of the playa and associated salt crust in the Bonneville Salt Flats is complex because of its transient nature. Estimation of fluid and solute fluxes in this type of transient system is difficult because the data represent only small segments of time. Monitoring of water levels in wells, brine chemistry, and evaporation needs to be continued over the long term in order to detect changes in the hydrologic system and to revise estimates of fluid flow and solute transport. Data collected and the interpretations made from them during this study have added to the understanding of the hydrologic system, but uncertainties remain.

Estimated and simulated subsurface flow to the south, which primarily seeps into a brine-collection ditch located on the southern boundary of the study area, was based on limited water-level data from wells and aquifer-test data prior to road construction. Estimated subsurface flow to the south was about three times more than the simulated amount. The water level and flow in this brine-collection ditch, located on private property, need to be monitored in order to quantify more accurately subsurface flow to the south.

The contradicting evidence for upward and downward leakage through the bottom of the shallow-brine aquifer needs to be resolved. Limited water-level data that were collected during wetter-than-normal conditions on the playa surface indicate downward movement, whereas, low $^{3}H$ values in brine from the shallow-brine aquifer at a few locations indicate upward movement. Additional nests of wells need to be completed in the shallow-brine aquifer and in the underlying lacustrine sediment of the upper part of the basin-fill aquifer and water levels need to be measured over a longer period of time in order to obtain a better spatial and temporal data distribution. Additional samples for $^{3}H$ analysis that are more spatially and temporally distributed need to be collected in order to define more accurately the extent of mixing with pre-bomb water. Samples should be collected for chlorofluorocarbon analysis to verify that low $^{3}H$ values are truly pre-bomb water.

More water is discharged by evaporation than by any other mechanism, yet data were collected at two weather stations for only two years each and represent atypical conditions. Monitoring at weather stations needs to be continued and data correlated with long-term records at the station in Wendover to establish long-term average evaporation and variation. An additional station needs to be located on the carbonate-mud surface where ground-water levels are closer to the playa surface and where winter ponding is unlikely. Formation of a thin salt crust might interfere with evaporation from the carbonate-mud surface.

Future modeling of the shallow-brine aquifer in the Bonneville Salt Flats needs to be based on removing the major limitations of the present model, most of which would require modifications to the simulator. Seasonal pond formation and brine-collection ditches need to be simulated as surface-water features coupled to ground-water flow. A mechanism for salt dissolution and precipitation at the playa surface and above the water table needs to be formulated. This would allow for a realistic simulation of the density of infiltrating fluid rather than specifying this density. In order to use realistic dispersivities on the order of 5 to 50 ft for the present mesh spacing, one of the newer numerical techniques such as flux-corrected-transport or total-variation-diminishing algorithms need to be implemented in

the simulator. Also, the simulator needs to be made more implicit with respect to the movement of the water-table surface in order to reduce mass-balance error. With a better understanding of vertical flow between the shallow-brine aquifer and the underlying lacustrine sediment, new simulations might result in a different mass balance.

## CONCLUSIONS

The Bonneville Salt Flats study area, located in northwestern Utah, contains a perennial salt crust surrounded by a mud playa. The combination of the salt-crust playa and the underlying ground water results in a complex and dynamic hydrologic system that is susceptible to ever-changing daily, seasonal, and yearly climatic conditions.

Objectives of this investigation were to identify the natural and anthropogenic processes causing salt loss from the crust and, where feasible, quantify these processes. Specific areas of study include transport of salt in solution by ground-water flow, and transport in solution by wind-driven ponds and the subsequent salt precipitation on the surface of the playa upon evaporation or seepage of brine into the subsurface. Data were collected to make conceptual estimates of these processes and to use in conjunction with variable-density, three-dimensional, solute-transport computer simulations. Because of the seasonal variability in salt transport within a given year and from one year to the next, any rigorous quantification was beyond the scope of this study. In addition, no continuous long-term data are available with which to assess trends in climate and mineral production. It was possible, however, to estimate relative quantities of salt being transported through different pathways. Uncertainties exist in estimates for advective flow and solute transport because they were made from spatially and temporally limited data.

The ground-water system in the Bonneville Salt Flats study area can be divided into three aquifers, the shallow-brine aquifer, alluvial-fan aquifer, and basin-fill aquifer. The shallow-brine aquifer in the Bonneville Salt Flats has the most immediate influence on the playa surface. Because of brine withdrawal for mineral production from the shallow-brine aquifer, this aquifer was studied in more detail.

The shallow-brine aquifer in the Bonneville Salt Flats appears to be in steady state with respect to long-term ground-water flow despite seasonal and yearly fluctuations. The potentiometric surface for the shallow-brine aquifer in September 1992 is virtually the same as the potentiometric surface shown by Lines (1979) for the fall of 1976. Recharge and discharge, therefore, must be approximately equal during a long-term period.

Recharge to the shallow-brine aquifer is primarily through infiltration of water from precipitation on the playa surface, subsurface flow from the east and north, and possibly through upward leakage. Infiltration of water dissolves salt from the crust, whereas subsurface flow the east and north along with upward leakage, if it occurs, transports salt into the shallow-brine aquifer. Recharge by infiltration for 1992 was estimated to range from 8,300 to 12,800 acre-ft. This estimate would be larger if a larger specific yield for the shallow-brine aquifer was assumed. Because of small horizontal gradients and low permeability values, subsurface flow from the east and north was estimated to be only 60 acre-ft. Although possible upward leakage could not be quantified, there is evidence, direct and indirect, to suggest that it occurs.

Discharge from the shallow-brine aquifer primarily occurs as evaporation from the playa surface, seepage to the brine-collection ditch east of the salt crust, subsurface flow to the south where it primarily seeps into another brine-collection ditch, subsurface flow to the northwestern margin of the playa, and downward leakage to the underlying lacustrine sediment. Salt is precipitated on the playa surface upon evaporation. Evaporation for 1992 was estimated to be 15,000 acre-ft, subsurface flow to the south ranged from 1,800 to 2,300 acre-ft, seepage to the brine-collection ditch east of the salt crust was 1,500 acre-ft, downward leakage ranged from 58 to 580 acre-ft, and subsurface flow to the northwestern margin was 40 acre-ft. Estimated net salt loss through subsurface flow out of the shallow-brine aquifer was more than 1.3 million tons. The estimated seepage to the brine-collection ditch east of the salt crust was considerably more than the 680 acre-ft estimated by Lines (1979).

Estimated total discharge is considerably larger than estimated recharge. This inequality contradicts the known fluid steady-state condition. Estimated subsurface flow to the south might be less than was estimated. This estimate was based on hydraulic gradient obtained from water-level data collected during this study and transmissivity values determined prior to construction of Interstate Highway 80. Removal of salt crust and compaction of underlying carbonate mud during con-

struction probably has constricted ground-water flow to the south.

Limited water-level data from 1993, which are representative of wetter-than-normal conditions on the playa surface, indicate that a small downward driving force existed between the shallow-brine aquifer and the underlying lacustrine sediment of the upper part of the basin-fill aquifer. Tritium values in brine from the shallow-brine aquifer ranged from 0 to 24 TU. Values of less than 10 TU, which are less than the value for recent precipitation, would indicate mixing with older pre-bomb water. The only possible source for such water is upward leakage from the underlying lacustrine sediment. Upward leakage, in the quantities necessary for mixing, is possible if water-level measurements in the shallow-brine aquifer were slightly lower than those measured in 1993 and if permeability values were four orders of magnitude larger than those assumed for the underlying sediment. If upward leakage is proven to be a substantial amount, then estimated net loss of salt from the shallow-brine aquifer would be less.

A comparison of long-term data indicate that dissolved-solids and potassium concentrations in brine from the shallow-brine aquifer have not changed appreciably since previous studies. Despite the net loss of salt by subsurface flow from the shallow-brine aquifer, the high dissolved-solids concentration is maintained mostly by dissolution of the salt crust and possibly upward leakage. Horizontal subsurface flow into the shallow-brine aquifer contributes only a small amount of salt.

The potassium concentration is unaffected by dissolution and precipitation of the salt crust. The potassium concentration decreases with infiltration of brine depleted with respect to potassium during the winter months but increases again during the summer months by the concentrating effect of evaporation. Possible sources for the replenishment of potassium that is lost through mineral production include diffusion from interstitial fluid and upward leakage.

Deuterium and oxygen-18 values for brine in the shallow-brine aquifer plot between the North American meteoric water line and the local evaporation line. This indicates that mixing occurs between highly evaporative and meteoric waters that have infiltrated into the shallow-brine aquifer.

Deuterium and oxygen-18 data from a line of nested wells perpendicular to the northwestern margin of the playa indicate that mixing occurs between brackish water from the alluvial-fan aquifer and brine from the shallow-brine aquifer or the underlying lacustrine sediment. A high dissolved-solids concentration and a more evaporative signature for D and $^{18}O$ in saline water from one well as compared to these values in water from the other two wells in a single nest would be indicative of induced mixing. Pumping from the alluvial-fan aquifer probably has induced the mixing.

Extensive flooding of the Bonneville Salt Flats during the winter of 1992-93 dramatically changed the salt surface. Much of the near-surface salt was dissolved and remained in solution into the summer of 1993, when the salt precipitated on the playa surface as the pond began to evaporate. A thin salt crust was deposited in areas beyond the extent of the crust mapped in 1992. An estimated 10 to 14 million tons was dissolved and subsequently redeposited on the playa surface or infiltrated into the shallow-brine aquifer. An unknown amount of surface salt might have been deposited beyond slight topographic divides where the salt might not be able to coalesce with the main salt body by subsequent dissolution and overland flow.

A three-dimensional ground-water flow and solute-transport model with variable density was developed for the shallow-brine aquifer in the Bonneville Salt Flats, Utah. The goals for the computer simulation of the shallow-brine aquifer in the Bonneville Salt Flats were: (1) to develop a fluid and solute balance, (2) to evaluate the effect on the salt crust of the brine production from the ditches, and (3) to identify the major and minor solute fluxes. The first two goals were met by computing (1) a flow balance on the shallow-brine aquifer beneath the Bonneville Salt Flats, (2) a solute balance for the simulation region, and (3) a mass balance for the total crystalline salt deposit. These quantitative balances help to understand how the brine production affects the gradual disappearance of the salt crust. The third goal is achieved by examination of the cumulative flow and transport amounts calculated for each boundary face.

Preliminary simulations indicated that the ground-water flow system does not reach steady state during production and recovery seasons because the response time is longer than the 6-month duration of each season. Because of the transient nature of the ground-water system, simulations were carried out to a periodic steady state with a repeated sequence of production and recovery seasons approximating a typical year rather than matching a specific period in time. Calibration criteria included matching the estimated

annual production from the brine-collection ditch, balancing volumetric fluid flows for periodic steady state, obtaining a reasonable match between simulated water-table contours and measured water-level data, and sufficient recharge to create a surface pond at the end of the recovery period. The overall mass-balance error for the brine was 1.5 percent during production seasons and 0.6 percent during recovery seasons. Similar errors were obtained for the solute balance. With these small mass-balance errors, the model adequately simulates the effects of brine withdrawal for mineral production on the solute and salt-crust balance of the shallow-brine aquifer and does not refute the conceptual understanding that brine withdrawal is a major cause for the loss of salt from the crust.

Simulation results indicate a net loss of salt of about 850,000 tons during a typical year through subsurface flow from the simulation region. This loss is primarily through seepage to the brine-collection ditch east of the salt crust and subsurface flow primarily to the brine-collection ditch along the southern boundary.

In order to reasonably match water levels along the southern part of the simulation region, permeabilities were reduced to one-sixth of previously estimated values. Simulated annual subsurface flow to the south, therefore, is 700 acre-ft of fluid and 285,000 tons of solute, about one-third of the estimated amount.

Simulated downward leakage from the shallow-brine aquifer was small. No upward leakage into the shallow-brine aquifer was simulated for the parameters used at this boundary.

Simulated fluxes through the playa surface were larger than at any other boundary. Simulated crystalline salt dissolution by infiltration at the playa surface was less than 5 million tons. Dissolution of crystalline salt occurs in the salt crust, in the thin salt overlying the carbonate mud, and in the crystalline salt in the carbonate-mud matrix. Simulated salt precipitation by evaporation was less than 4 million tons. The difference mostly can be attributed to the net loss of solute from the aquifer.

Sensitivity simulations were made to test the effect of uncertainties in spatially distributed data on the cumulative annual amounts for fluid and solute transport. Changes were made in permeability, specified water level in the brine-collection ditch along the southern boundary, density of infiltrating fluid from the playa surface, evaporation rate, and porosity. All sensitivity simulations resulted in a net loss of solute through subsurface flow from the shallow-brine aquifer. The model is most sensitive to an increase in permeability near the south boundary.

Limitations to the model include approximating surface ponding as a fixed region of very high permeability and 100-percent porosity, inability to simulate salt dissolution and precipitation, approximating flow in fractured clay and salt media as equivalent porous media, and being constrained to a longitudinal dispersivity of 500 feet.

## REFERENCES CITED


Anderson, M.P., 1979, Using models to simulate the movement of contaminants through groundwater flow systems: Critical Reviews in Environmental Control, v. 9, no. 2, p. 97-156.

Bear, Jacob, 1972, Dynamics of fluids in porous media: New York, American Elsevier, 764 p.

Bingham, C.P., 1980, Solar production of potash from brines of the Bonneville Salt Flats: *in* Gwynn, J.W., ed., Great Salt Lake, a Scientific, Historical and Economic Overview, Utah Geological and Mineral Survey Bulletin 16, p. 229-243.

Cheng, Xiangxue, and Anderson, M.P., 1993, Numerical simulation of ground-water interaction with lakes allowing for fluctuating lake levels: Groundwater, v. 31, no. 6, p. 929-933.

Cooley, R.L., 1974, Finite element solutions for the equations of ground-water flow: Technical Report Series H-W, Hydrology and Water Resources Publications No. 18, Reno, Nevada, Desert Research Institute, 134 p.

Cook, K.L., Halverson, M.D., Stepp, J.C., and Berg, Jr., J.W., 1964, Regional gravity survey of the northern Great Salt Lake Desert and adjacent areas in Utah, Nevada, and Idaho: Geological Society of America Bulletin, v. 75, no. 8, p. 715-740.

Coplen, T.B., 1993, Uses of environmental isotopes: *in* Alley, W.M., ed., Regional Ground-Water Quality, New York, Von Nostrand Reihold, p. 227-254.

Craig, Harmon, 1961, Standard for reporting concentrations of deuterium and oxygen-18 in natural water: Science, v. 133, p. 1702-1703.

Crittenden, M.D., 1963, New data on the isostatic deformation of Lake Bonneville: U.S. Geological Survey Professional Paper 454-E, 31 p.

Dansgaard, W., 1964, Stable isotopes in precipitation: Tallus, v. 16, p. 436-468.

Domenico, P.A., and Schwartz, F.W., 1990, Physical and chemical hydrogeology: New York, John Wiley and Sons, 824 p.

Drever, J.I., 1982, The geochemistry of natural waters: New Jersey, Prentice-Hall, 388 p.

Eardley, A.J., 1962, Gypsum dunes and evaporite history of the Great Salt Lake Desert: Utah Geological and Mineralogical Survey Special 2, 27 p.

Epstein, Samuel, and Mayeda, T.K., 1953, Variation of the O-18 content of water from natural sources: Geochemica et Cosmochimica Acta, v. 4, p. 213-224.

Fenneman, N.M., 1931, Physiography of the Western United States: New York, McGraw-Hill, 534 p.

Foley, J.D., van Dam, Andries, Feiner, S.K., and Hughes, J.F., 1990, Computer graphics, principles and practice, 2nd ed.: Reading, Mass., Addison-Wesley, 1175 p.

Freeze, R.A., and Cherry, J.A., 1979, Groundwater: New Jersey, Prentice-Hall, 604 p.

Gelhar, L.W., Welty, Claire, and Rehfeldt, K.R., 1992, A critical review of data on field-scale dispersion in aquifers: Water Resources Research, v. 28, no. 7, p. 1955-1974.

Gilbert, G.K., 1890, Lake Bonneville: U.S. Geological Survey Monograph 1, 438 p.

Gwynn, J.W., 1996, History of potash production from the Salduro Salt Marsh (Bonneville Salt Flats), Tooele County: Utah Geological Survey Notes, v. 28, no. 2, p. 1-3.

Harrill, J.R., Gates, J.S., and Thomas, J.M., 1988, Major ground-water flow systems in the Great Basin region of Nevada, Utah, and adjacent states: U.S. Geological Survey Hydrologic Investigations Atlas HA-694-C.

Hassanizadeh, S.M., and Leijnse, T., 1988, On the modeling of brine transport in porous media: Water Resources Research, v. 24, no. 3, p. 321-330.

Hubbert, M.K., 1953, Entrapment of petroleum under hydrodynamic conditions: Bulletin of the American Association of Petroleum Geologists, v. 37, no. 8, p. 1954-2026.

———1956, Darcy's Law and the field equations of the flow of underground fluids: AIME Petroleum Transactions, v. 207, p. 222-239.

Hunt, C.B., Robinson, T.W., Bowles, W.A., and Washburn, A.L., 1966, Hydrologic basin, Death Valley, California: U.S. Geological Survey Professional Paper 494-B, 138 p.

Kendall, Carol, and Coplen, T.B., 1985, Multisample conversion of water to hydrogen by zinc stable isotope determination: Analytical Chemistry, v. 57, p. 1437-1440.

Kipp, Jr., K.L., 1987, HST3D: A computer code for simulation of heat and solute transport in three-dimensional ground-water flow systems: U.S.Geological Survey Water-Resources Investigations Report 86-4095, 517 p.

———in press, Guide to the revised heat and solute transport simulator: HST3D—Version 2: U.S. Geological Survey Water-Resources Investigations Report 97–4157, 64 p.

Lines, G.C., 1978, Selected ground-water data, Bonneville Salt Flats and Pilot Valley, western Utah: U.S. Geological Survey Open-File Report, 14 p.

———1979, Hydrology and surface morphology of the Bonneville Salt Flats and Pilot Valley playa, Utah: U.S. Geological Survey Water-Supply Paper 2057, 107 p.

Malek, Esmaiel, Bingham, G.E., and McCurdy, G.D., 1990, Evapotranspiration from the margin and moist playa of a closed desert valley: Journal of Hydrology, v. 120, p. 15-34.

Mason, J.L., Brothers, W.C., Gerner, L.J., and Muir, P. S., 1995, Selected hydrologic data for the Bonneville Salt Flats and Pilot Valley, western Utah, 1991-93: U.S. Geological Survey Open-File Report 95-104, 56 p.

National Oceanic and Atmospheric Administration, 1971-1993, Climatological data annual summary 1970-1992, v. 72-94, no. 13.

———1993, Climatological data monthly summary, v. 95, no. 1-12.

———1994, Climatological data monthly summary, v. 96, no. 1-12.

Neuman, S.P., and Witherspoon, P.A., 1972, Field determination of the hydraulic properties of leaky multiple aquifer systems: Water Resources Research, v. 8, no. 5, p. 1284-1298.

Nield, D.A., and Bejan, Adrian, 1992, Convection in porous media: New York, Springer-Verlag, 408 p.

Nolan, T.B., 1928, Potash brines in the Great Salt Lake Desert, *in* Loughlin, G.F., and Mansfield, G.R., Contributions to economic geology, Part 1—Metals and nonmetals except fuels: U.S. Geological Survey Bulletin 795, p. 25-44.

Patankar, S.V., 1980, Numerical heat transfer and fluid flow: New York, Hemisphere Publishing Corporation, 278 p.

Post, R.C., 1992, The machines of nowhere: Invention and Technology, Spring 1992, p. 28-37.

Ripple, C.D., Rubin, Jacob, and van Hylckama, T.E.A., 1975, Estimating steady-state evaporation rates from bare soils under conditions of high water table: U.S. Geological Survey Water-Supply Paper 2019-A, 39 p.

Scheidegger, A.E., 1961, General theory of dispersion in porous media: Journal of Geophysical Research, v. 3, no. 2, p. 153-162.

Stephens, J.C., 1974, Hydrologic reconnaissance of the northern Great Salt Lake Desert and summary hydrologic reconnaissance of northwestern Utah: Utah Department of Natural Resources Technical Publication 42, 55 p.

Turk, L.J., 1969, Hydrology of the Bonneville Salt Flats, Utah: Unpublished Ph.D. dissertation, Stanford University, 307 p.

———1970, Evaporation of brine: A field study on the Bonneville Salt Flats, Utah: Water Resources Research, v. 6, no. 4, p. 1209-1215.

———1973, Hydrogeology of the Bonneville Salt Flats, Utah: Utah Geological and Mineralogical Survey Water-Resources Bulletin 19, 81 p.

———1978, Bonneville salt crust study: Kaiser Aluminum and Chemical Corporation (as of 1988, Reilly Industries), Wendover, Utah, 103 p.
Turk, L.J., Davis, S.N., and Bingham, C.P., 1973, Hydrogeology of lacustrine sediments, Bonneville Salt Flats, Utah: Economic Geology, v. 68, p. 65-78.
U.S. Department of Agriculture, 1936, Climatic summary, section 20—western Utah, 41 p.
[U.S.] Environmental Science Services Administration, 1967-1970, Climatological data annual summary 1966-1969, v. 68-71, no. 13.
[U.S.] Weather Bureau, 1957, Climatic summary of the United States—supplement for 1931 through 1952, 45 p.
———1962-1966, Climatological data annual summary 1961-1965, v. 63-67, no. 13.
Varga, R.S., 1962, Matrix iterative analysis: New Jersey, Prentice-Hall, 322 p.
Weast, R.C., Selpy, S.M., and Hodgman, C.D., 1964, Handbook of chemistry and physics (45th ed.): Ohio, Chemical Rubber Co., 1468 p.

# SELECTED SERIES OF U.S. GEOLOGICAL SURVEY PUBLICATIONS

## Periodical

**Preliminary Determination of Epicenters** (issued monthly).

## Technical Books and Reports

**Professional Papers** are mainly comprehensive scientific reports of wide and lasting interest and importance to professional scientists and engineers. Included are reports on the results of resource studies and of topographic, hydrologic, and geologic investigations. They also include collections of related papers addressing different aspects of a single scientific topic.

**Bulletins** contain significant data and interpretations that are of lasting scientific interest but are generally more limited in scope or geographic coverage than Professional Papers. They include the results of resource studies and of geologic and topographic investigations, as well as collections of short papers related to a specific topic.

**Water-Supply Papers** are comprehensive reports that present significant interpretive results of hydrologic investigations of wide interest to professional geologists, hydrologists, and engineers. The series covers investigations in all phases of hydrology, including hydrogeology, availability of water, quality of water, and use of water.

**Circulars** present administrative information or important scientific information of wide popular interest in a format designed for distribution at no cost to the public. Information is usually of short-term interest.

**Water-Resources Investigations Reports** are papers of an interpretive nature made available to the public outside the formal USGS publications series. Copies are reproduced on request unlike formal USGS publications, and they are also available for public inspection at depositories indicated in USGS catalogs.

**Open-File Reports** include unpublished manuscript reports, maps, and other material that are made available for public consultation at depositories. They are a nonpermanent form of publication that may be cited in other publications as sources of information.

## Maps

**Geologic Quadrangle Maps** are multicolor geologic maps on topographic bases in 7.5- or 15-minute quadrangle formats (scales mainly 1:24,000 or 1:62,500) showing bedrock, surficial, or engineering geology. Maps generally include brief texts; some maps include structure and columnar sections only.

**Geophysical Investigations Maps** are on topographic or planimetric bases at various scales; they show results of surveys using geophysical techniques, such as gravity, magnetic, seismic, or radioactivity, which reflect subsurface structures that are of economic or geologic significance. Many maps include correlations with the geology.

**Miscellaneous Investigations Series Maps** are on planimetric or topographic bases of regular and irregular areas at various scales; they present a wide variety of format and subject matter. The series also includes 7.5-minute quadrangle photogeologic maps on planimetric bases that show geology as interpreted from aerial photographs. Series also includes maps of Mars and the Moon.

**Coal Investigations Maps** are geologic maps on topographic or planimetric bases at various scales showing bedrock or surficial geology, stratigraphy, and structural relations in certain coal-resource areas.

**Oil and Gas Investigations Charts** show stratigraphic information for certain oil and gas fields and other areas having petroleum potential.

**Miscellaneous Field Studies Maps** are multicolor or black-and-white maps on topographic or planimetric bases for quadrangle or irregular areas at various scales. Pre-1971 maps show bedrock geology in relation to specific mining or mineral-deposit problems; post-1971 maps are primarily black-and-white maps on various subjects such as environmental studies or wilderness mineral investigations.

**Hydrologic Investigations Atlases** are multicolored or black-and-white maps on topographic or planimetric bases presenting a wide range of geohydrologic data of both regular and irregular areas; principal scale is 1:24,000, and regional studies are at 1:250,000 scale or smaller.

## Catalogs

Permanent catalogs, as well as some others, giving comprehensive listings of U.S. Geological Survey publications are available under the conditions indicated below from the U.S. Geological Survey, Information Services, Box 25286, Federal Center, Denver, CO 80225. (See latest Price and Availability List.)

**"Publications of the Geological Survey, 1879–1961"** may be purchased by mail and over the counter in paperback book form and as a set of microfiche.

**"Publications of the Geological Survey, 1962–1970"** may be purchased by mail and over the counter in paperback book form and as a set of microfiche.

**"Publications of the U.S. Geological Survey, 1971–1981"** may be purchased by mail and over the counter in paperback book form (two volumes, publications listing and index) and as a set of microfiche.

**Supplements** for 1982, 1983, 1984, 1985, 1986, and for subsequent years since the last permanent catalog may be purchased by mail and over the counter in paperback book form.

**State catalogs, "List of U.S. Geological Survey Geologic and Water-Supply Reports and Maps For (State),"** may be purchased by mail and over the counter in paperback booklet form only.

**"Price and Availability List of U.S. Geological Survey Publications,"** issued annually, is available free of charge in paperback booklet form only.

**Selected copies of a monthly catalog "New Publications of the U.S. Geological Survey"** are available free of charge by mail or may be obtained over the counter in paperback booklet form only. Those wishing a free subscription to the monthly catalog "New Publications of the U.S. Geological Survey" should write to the U.S. Geological Survey, 582 National Center, Reston, VA 20192.

**Note**—Prices of Government publications listed in older catalogs, announcements, and publications may be incorrect. Therefore, the prices charged may differ from the prices in catalogs, announcements, and publications.

ISBN 0-607-88306-5